COUNTRY-ROCK CONTAMINATION AND ASSIMILATION IN THE SOUTH MOUNTAIN BATHOLITH

by

Saskia Erdmann

Submitted in partial fulfillment of the requirements
for the degree of Doctor of Philosophy

at

Dalhousie University
Halifax, Nova Sctia
October 2006

Your file Votre référence
ISBN: 978-0-494-27177-3
Our file Notre référence
ISBN: 978-0-494-27177-3

DALHOUSIE UNIVERSITY

To comply with the Canadian Privacy Act the National Library of Canada has requested that the following pages be removed from this copy of the thesis:

Preliminary Pages

Examiners Signature Page (pii)

Dalhousie Library Copyright Agreement (piii)

Appendices

Copyright Releases (if applicable)

TABLE OF CONTENTS

LIST OF TABLES

LIST OF FIGURES

ABSTRACT

The South Mountain Batholith (SMB) of southern Nova Scotia is a large, peraluminous granitoid complex, intruded dominantly into rocks of the Meguma Group. Field and textural relations reveal evidence for contamination of the SMB by rocks of the Meguma Group in the form of xenoliths, xenocrysts, and former partial melt, and assimilation of the country-rock material through fracturing, dispersal, partial melting, dissolution, and ion exchange reactions. Assimilation of the metapsammitic rocks released xenocrystic quartz, biotite, and plagioclase, and ≤50 vol% of partial melt into the SMB magmas, whereas assimilation of the metapelitic rocks released xenocrystic garnet and cordierite, and ≤80 vol% of partial melt. In the SMB rocks remote from contacts with Meguma Group rocks, textural relations, chemical compositions, and zoning patterns permit the identification of xenocrystic garnet and cordierite with confidence. On the other hand, deciphering the origin of single quartz, biotite, and plagioclase crystals in the SMB has a considerable uncertainty, because textures and compositions of country rock-derived and small magmatic crystals are similar. Despite these difficulties, assuming that all suspect crystals are true xenocrysts, and that all xenocrysts are physically detectable, xenocrysts make up ≤4 vol% and ≤3 vol% in the marginal and more central rocks of the SMB. Using ratios of xenocrysts to partial melt determined in melting experiments employing rocks of the Meguma Group, the abundance of xenocrysts suggests that ≤10 vol% of physically invisible, complementary former country-rock partial melt is present in the SMB rocks. Together, ≤16 and ≤8 vol% of country-rock material appears to occur in the marginal and more central rocks of the SMB, respectively. However, existing whole-rock isotopic data indicate that at least the most evolved rocks of the SMB may have ≤56 vol% of additional former Meguma Group partial melt. Energy-constrained numerical modelling of the assimilation of Meguma Group rocks in the SMB magmas through partial melting shows that selective contamination of the exposed SMB rocks by Meguma Group-derived partial melt may explain the presence of the additional former partial melt, but cannot rule out that the partial melt was added to the SMB as part of the source.

ACKNOWLEDGEMENTS

I am grateful to Scott Paterson for unselfishly advising me to work on this project. I wish to thank Barrie Clarke for the chance to work with him, for his support, and many exciting, interesting, and ambitious discussions. For all their advice and their thoughts, most sincere thanks to the current and former members of my thesis committee, William Caley, Rebecca Jamieson, Michael MacDonald, Scott Paterson, and Ron Vernon. Thanks also to: Jean Bédard, Nicholas Culshaw, Barrie Clarke, Martin Gibling, and Rebecca Jamieson for their thoughts and comments on an earlier draft of my thesis; David London, George Morgan, and Antonio Acosta-Vigil at Oklahoma University for their collaboration and many vivid discussions; Patricia Stoffyn for technical assistance with the electron microprobe at Dalhousie University and for scientific discussions; Dan MacDonald and Michael Robertson for assistance with the SEM-CL microscopy; Marc Poujol for help with the color CL microscopy; Jiggs Diegor and Mike Tubrett for technical assistance with LA ICP-MS analyses, for carrying out a third of the trace element analysis in my absence, and for reduction of the ICP-MS raw data; Vaneeta Kaur Groover for introducing me to, and guiding me through the hierachical cluster analysis; Gordon Brown for preparing my thin sections; Sarah Carruzzo for discussions and help in preparing rock powder samples; Andrew Dunn for support in the field, and for preparing rock powder samples and mineral separates; and Aaron C. Seimers for his assistance in preparing some of my melting experiments. I have very much appreciated informal reviews on materials occurring in my thesis by William Caley, Barrie Clarke, Rebecca Jamieson, Jörn Kruhl, Jade Star Lackey, Michael MacDonald, and Ron Vernon, as well as formal reviews of submitted manuscripts by Trevor Green, Simon Harley, Robert Martin, Ron Vernon, and two anonymous reviewers. I would like to thank Nick Culshaw and Martin Gibling for their administrative support, and I like to acknowledge the support from an Izaak Walton Killam Pre-Doctoral Scholarship throughout this study, funding from GSA Student Research Grants in 2004 and 2005, and generous financial support through an NSERC Discovery grant to Barrie Clarke.

CHAPTER 1

Introduction

1.0 Statement of Problem

Deciphering the components and the significance of country-rock contamination in the genesis of igneous rocks is one of the most intractable problems in igneous petrology (e.g., Fournet 1846; Harker 1904; Bowen 1922a,b, 1928; Daly 1933; Kuno 1950; Wilcox 1954; Carter et al. 1978; Sparks 1986; Kelemen 1990; Bédard 1991; Fitton et al. 1991; Maury and Didier 1991; Clemens 2003; Beard et al. 2005; Davidson et al. 2005). Physical evidence for country-rock contamination may exist in the form of xenoliths or xenocrysts, but any approach to characterize country-rock contamination in igneous rocks based on xenoliths and xenocrysts only is likely to be incomplete, overlooking components and mass contributions from physically completely assimilated contaminants (Table 1.1) (Hoefs et al. 1980; Dungan and Davidson 2004; Beard et al. 2005). Chemical data may indicate the presence of country-rock components in igneous rocks in the form of major-element, trace-element, or isotopic variations (e.g., Doe 1967; Taylor et al. 1979; Taylor 1980), but any approach to characterize crustal contamination in igneous rocks based on chemical data alone cannot unequivocally determine the compositions or the origin of the contributing country-rock components (e.g., Woerner et al. 1992; Dungan et al. 2001; Ramos et al. 2005). Experimental data can indirectly constrain the compositions and fractions of solid and liquid contaminants, and provide information on the efficiency of assimilation reactions, but cannot constrain the amount of contamination or the extent of assimilation (e.g., Beard et al. 1993, 2004; Patiño Douce 1995; Edwards and Russell 1998; Castro 2001; Costa et al. 2002, 2004). Numerical modelling can simulate the geochemical evolution and constrain the potential of country-rock assimilation in igneous systems, and thereby provide a conceptual framework to make predictions for natural systems, but it cannot account for the complexity of the latter (e.g., DePaolo 1985; Aitcheson and Forrest 1994; Reiners et al. 1995; Spera and Bohrson 2001, 2004; Bohrson and Spera 2001). Consequently, no single approach to assess country rock contamination in igneous rocks is entirely adequate or unique, but an approach integrating field and textural observations, mineral and whole-rock geochemical data, as well as experimental results and numerical

modelling, permits the characterization of country-rock contamination in igneous rocks to the currently best possible level.

Table 1.1: Employed key definitions.

Term	Definition	Reference
Assimilation	Process of rendering one material impure by another material, where the nature of the incorporated material is changed into the nature of the host material.	Clarke in press
Contamination	Process of rendering one material impure by another material, where the nature of the incorporated material may, or may not, be preserved.	Clarke in press
Contaminant	Foreign material incorporated into magmas. Contaminants may occur in the form of xenoliths, xenocryst, former partial melt, and former fluids.	e.g., Clarke in press
Country rocks (CR)	Rocks that surround the ascending and emplaced magmas.	*
Country-rock assimilation	Process of physical and/or chemical conversion of country-rock material into the nature of the magmatic host.	Clarke in press; this thesis
Country-rock contamination	Process of incorporation of country rocks into a magma.	Clarke in press; this thesis
Hybridization	Process of mixing two magmas or melts of differing composition.	*
Hybrid magma	Mixture of two compositionally different magmas/melts. The hybrid magmas/melts I refer to in my thesis are, if not otherwise stated, mixtures of main SMB magmas/melts and country-rock derived partial melts.	*
Orthoxenocryst (OXC)	Xenocrysts of the original, subsolidus assemblage derived from *in situ* country rocks, source rocks, or xenoliths.	Erdmann and Clarke 2005
Paraxenocryst (PXC)	Crystals that formed in a peritectic melting reaction between contaminants and host magma.	Erdmann and Clarke 2005
RAFC processes	Magma recharge (R), assimilation (A), and fractional crystallization (FC) processes	e.g., DePaolo 1985
Source rocks (SR)	Rocks that generated most of the magma. Dominantly liquid components segregate from the source rocks, whereas most of the solid components remain in the source area.	e.g., Clemens 2003; Vernon in press
Xenocryst	Monomineralic solids of foreign origin. Xenocrysts may be derived from country rocks, source rocks, or from magmas differing in composition from the main magma.	*
Xenolith (XLTH)	Inclusion of polymineralic solids of foreign origin. Most xenoliths are of country-rock origin, but they may also be of source-rock origin.	*

* Definitions, for example, by Hughes (1982), Best (1982), Shelley (1983), Hess (1989), McBirney (1993), and Winter (2001).

1.1 State of Knowledge

1.1.1 Country-rock Contamination and Assimilation

Magmas ascending through, and intruding into, the crust are in thermal and chemical disequilibrium with their surroundings (e.g., Spera et al. 1982, 1985; Sparks 1986; Ghiorso and Kelemen 1987; Huppert and Sparks 1988; Marsh 1989; Kelemen 1990; Reiners et al 1995; Barboza and Bergantz 1997, 1998; Raia and Spera 1997; Spera and Bohrson 2001, 2004; Bohrson and Spera 2001; Fowler et al. 2004), and they need space (e.g., Goodchild 1892; Daly 1903; Myers 1975; Hutton 1996; McNulty et al. 1996; Paterson et al. 1996; O'Hara 1998; Okubo and Martel 1998; Miller and Paterson 1999; Culshaw and Bhatnagar 2001; Coleman et al.2004; Hawkins and Wiebe 2004; Dumond et al. 2005; Zak and Paterson 2005). As a result, magmas thermally, chemically, and physically interact with their country rocks to various degrees, releasing heat and fluids into the country rocks, and displacing and incorporating country-rock material. Evidence for the incorporation of country-rock material into former magmas, or in other terms, evidence for the contamination of magmas by country-rock material, is present in igneous rocks of most compositions and from practically all tectonic settings and ages (Sparks 1986 and references therein).

Country-rock contaminants may be incorporated into the magmas in the form of xenoliths, xenocrysts, partial melt, and fluids. Country rocks may contaminate magmas in bulk, if whole rocks are entrained in the magma system, or they may selectively contaminate magmas, if only partial melt or fluids are included. Once incorporated in a magma, country-rock material may undergo assimilation through fracturing, partial melting, dissolution, thermal decomposition, and ion exchange reactions, in combination with segregation and dispersal (e.g., Bowen 1922a,b; Daly 1933; Marsh 1982; Furlong and Myers 1985; Castro 1987; Clarke et al. 1998; Green 1994; Bédard and Hébert 1996; Dungan and Davidson 2004; Beard et al. 2005). The degree of assimilation of country-rock material through fracturing is dominantly constrained by rock strength, the amount and rate of strain, country-rock temperature, temperature contrast between magma and country rocks, and the presence or absence of volatiles (Glenn et al. 1986; Spence and Turcotte 1985; Grady and Kipp 1987; Rubin 1993). On the other hand, the degree of assimilation of country-rock material through partial melting, dissolution, thermal decomposition, and ion exchange reactions is dominantly constrained by the mineralogy and composition of country rocks, the absence or presence of volatiles, the initial

country-rock temperature, as well as the sensible and latent heat of the magma (e.g., Campbell and Turner 1987; Bergantz 1992; Spera and Bohrson 2001).

Country-rock contamination in the form of xenoliths is easily detectable, but the more efficient country-rock assimilation in a magma was, the worse are the chances to physically identify the presence and the amount of all country-rock contaminants (Fig. 1.1). The scarcity of xenoliths and other obvious country-rock contaminants in many igneous rocks may be evidence for a minor country-rock contribution to the magmas (e.g., Brown and Pressley 1999; Clemens 2003), but may also be the result of efficient assimilation (Green 1994; Reiners et al. 1995; Bohrson and Spera 2001; Dungan and Davidson 2004; Davidson et al. 2005). Important to appreciate is that our estimates on the significance of country-rock material in a given igneous rock at least partly reflect our ability to recognize (or not recognize) all foreign components present, and thus the methods employed (e.g., field versus geochemical studies).

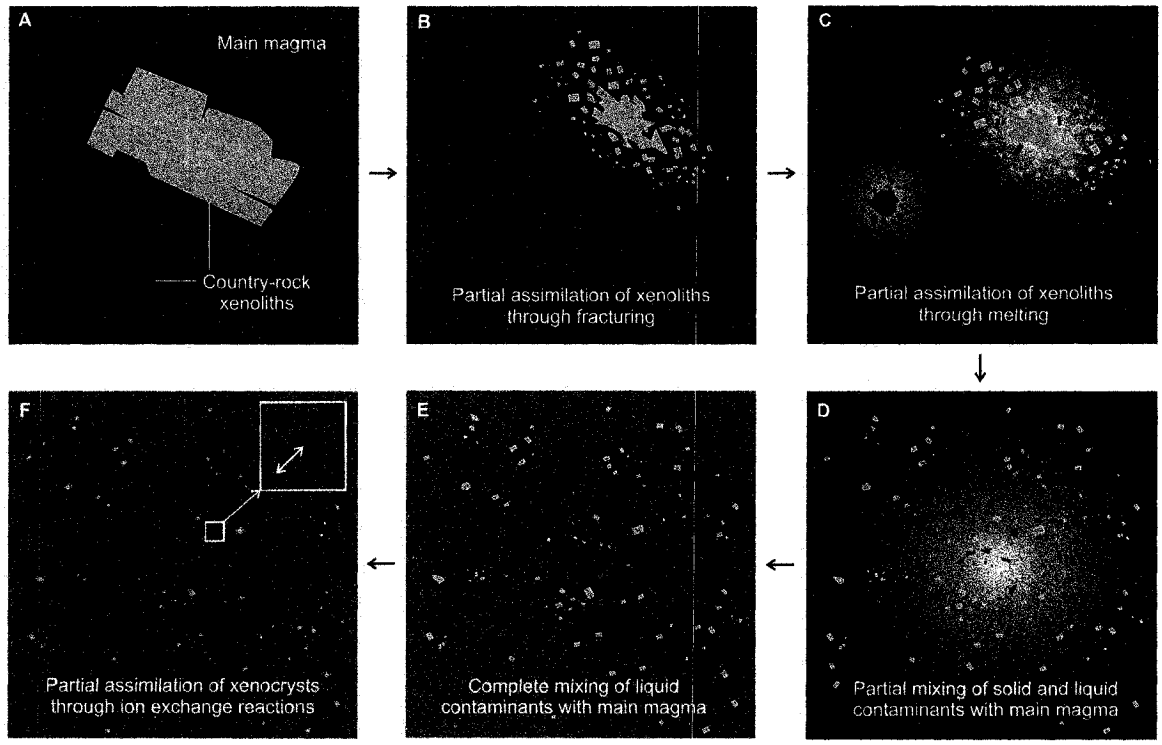

Figure 1.1: Sketches illustrating country-rock assimilation by a magma, with increasing assimilation from A to F. The presence and amount of country-rock contaminants in A to C can be easily estimated based on physical evidence. Red = cognate magma; green = xenoliths and orthoxenocrysts; yellow = country-rock-derived partial melt; orange = hybrid magma; blue = paraxenocrysts. For D to F, whole-rock geochemical analysis may detect the presence, but cannot reliably determine the amount, the composition, or the origin of the foreign material.

To test the significance of country-rock contamination in igneous rocks of various compositions and from various tectonic settings, it is critical to study country-rock contamination and assimilation in igneous bodies case-by-case. With recent advances in microanalytical techniques, the recognition of some highly assimilated country-rock components has become more common in various types of igneous rocks, and made country-rock contamination and assimilation an active field of research in igneous petrology and geochemistry over the past few years (e.g., Davidson et al. 1990, 2001; Simonetti and Bell 1993; Cox et al. 1996; Davidson and Tepley 1997; Knesel et al. 1999; Waight et al. 2000; Ginibre et al. 2002; Thomas et al. 2002; Müller et al. 2003; Tepley and Davidson 2003; Dungan and Davidson 2004; Gagnevin et al. 2005; Beard et al. 2005; Costa and Dungan 2005; Ramos et al. 2005).

1.1.2 The South Mountain Batholith

The late-Devonian, ca. 380-390 Ma, South Mountain Batholith (SMB) of southern Nova Scotia, Canada, is a petrologically and geochemically exceptionally well characterized, composite granite complex. Therefore, the batholith is ideal for a case study to advance our knowledge on the role, the nature, and the significance of country-rock contamination and assimilation relative to source variations and other magma chamber processes in the evolution of granitic and other plutonic rocks. However, most rock-forming minerals of the SMB are similar to the rock-forming minerals of the country rocks, and the identification of country-rock xenocrysts in the SMB rocks is not a trivial problem.

The SMB is part of the Meguma terrane, the most outboard terrane in the Appalachian orogen (Williams and Hatcher 1982) (Fig. 1.2A). The batholith is the largest of more than 25 individual granitic intrusions of the terrane, consisting dominantly of peraluminous granodiorite (10 vol%), biotite monzogranite (52 vol%), biotite-muscovite monzogranite (9 vol%), coarse-grained leucomonzogranite (21 vol%), fine-grained leucomonzo-granites (7 vol%), and leucogranite (1 vol%). Mafic porphyries are rare (≤0.07 vol%), characterized by abundant biotite and feldspar phenocrysts, and in cases by abundant garnet and andalusite, and they range in composition from tonalites to monzogranites (MacDonald 2001). Mafic porphyries occur dominantly in the marginal regions of granodiorites and biotite monzogranites of the SMB. They have the highest concentrations of xenoliths of any rocks of the SMB, with the exception of some SMB rocks along the immediate country-rock contact. Contacts between granodiorites,

monzogranites, and leucomonzogranites are mostly gradational, whereas contacts with the leucogranites are exclusively sharp (MacDonald 2001). Contacts between the mafic porphyries and all other granitic rocks are gradational to sharp.

The SMB rocks are exposed in 260 mappable granite bodies and 13 plutons (e.g., MacDonald et al. 1992; Clarke et al. 1997; MacDonald 2001). The plutons are grouped into Stage 1 and Stage 2 plutons, where Stage 1 plutons dominantly consist of granodiorite and biotite monzogranite, and minor fine-grained leucomonzogranites, and Stage 2 plutons dominantly consist biotite-muscovite monzogranite, coarse- and fine-grained leucomonzogranite, and minor biotite granodiorite, biotite monzogranite, and leucogranite. Contacts between Stage 1 and Stage 2 plutons are rarely exposed, but Stage 1 plutons appear invariably intruded by Stage 2 plutons. The plutons show normal mineralogical and chemical zoning from more primitive (more mafic) to more evolved (more felsic) granitic facies, reverse, normal and reverse, or no mineralogical and chemical zoning. Also, the most primitive SMB rocks, the mafic porphyries and granodiorites, have the highest concentrations of Sr+Zr, whereas the lowest concentrations of these two trace elements occur in the late, evolved muscovite-bearing leucogranites.

Various Rb-Sr whole-rock ages for the SMB granites give a mean age of ca. 370 Ma, ranging between 380 and 240 Ma, where young ages (≤ca. 364 Ma) are the result of isotopic resetting (Clarke and Halliday 1980; Cormier et al. 1988; Harper 1988; Chatterjee and Cormier 1991; Hill 1991). The oldest cooling ages obtained for the SMB rocks are U-Pb zircon and monazite ages, ranging between ca. 385 and 368 Ma (Harper 1988; Hill 1991; Keppie et al. 1993; Currie et al. 1998; Keppie and Krogh 1999;Clarke et al. 2000). The oldest Re-Os and Ar-Ar mica and K-feldspar ages are ca. 378 Ma, and thus similar to the U-Pb crystallization ages, suggesting rapid cooling of the SMB to temperatures below 350 ±50 °C (Carruzzo 2003). Emplacement of the SMB occurred ~10 to 15 Ma after ca. 390 Ma main deformation phase recorded in the Meguma Terrane (Reynolds and Muecke 1978; Keppie and Dallmeyer 1979; Hicks et al. 1999); exhumation of the batholith occurred prior to 360 Ma (Martel et al. 1993; Martel and Gibling 1996).

At the present level of erosion, the >500 km perimeter of the batholith is in contact with greenschist to amphibolite facies metasedimentary and metavolcanic rocks of the Cambrian-Ordovician Meguma Group (>90 %) and the overlying Silurian-Devonian Annapolis Group (≤ 10%)(Fig. 1.2B; e.g., McKenzie and Clarke 1975; Keppie and

Muecke 1979; Schenk 1971, 1991, 1995; MacDonald and Clarke 1985; Clarke et al. 1997, Waldron et al. 1992, Hicks et al. 1999; MacDonald 2001). The lowest metamorphic grades occur in the central part of the Meguma terrane, with metamorphic grades increasing towards the south and northeast (Keppie and Muecke 1979). Exposed Meguma Group rocks of amphibolite facies grade are present only in southern Nova Scotia (Fig. 1.2B), and may be related to contact metamorphism of unexposed, underlying granitic or mafic intrusions (Hope et al. 1986).

The average thickness of the SMB is 5 to 10 km; the maximum thickness is 25 km in two root zones (Clarke and Muecke 1985; Clarke and Chatterjee 1988). Exposed contacts between SMB and country rocks seem to represent the near-roof level of the batholith (Halter et al. 1994; Horne 1994; MacDonald et al. 1992), whereas the floor of the batholith is inferred to be located at or near the transition between Meguma Group rocks and high-grade gneissic rocks, similar to those exposed in the Liscomb Complex of central Nova Scotia (Benn et al. 1997; Culshaw and Lee 2006). In the late Devonian, prior to the intrusion of the SMB, the Meguma Group may have been up to 20 km thick (Schenk 1997; Richardson 2000), where the currently exposed rocks occurred at a depth of ca. 10 km (Raeside and Mahoney 1996; Culshaw and Lee 2006, and references therein). Pelitic and metavolcanic gneisses, similar to the rocks of the Liscomb Complex of central Nova Scotia, probably underlay the Meguma Group between a depth of ca. 20-30 km (Clarke et al. 1993; Kontak and Reynolds 1994). Felsic to mafic metaigneous and metasedimentary granulites, similar to xenoliths exposed in the Tangier mafic dykes northeast of the SMB, and hereafter referred to as Tangier basement rocks, occurred between depths of ca. 30 to ≥55km (Owen et al. 1988; Eberz et al. 1991; Keen et al. 1991; Clarke et al. 1993; Greenough et al. 1999).

The Meguma Group comprises the Halifax Formation, dominated by metapelitic rocks, and the underlying Goldenville Formation, dominated by metapsammitic rocks (Schenk 1971, 1991, 1997; Waldron and Jensen 1985; Krogh and Keppie 1990). The Goldenville Formation, ca. 5500 to 7000 m thick (Schenk 1971; Henderson et al. 1986; Krogh and Keppie 1990), is overlain by the Halifax Formation, with inferred thicknesses varying between ca. 500-4000 m (Krogh and Keppie 1990) and up to 8000 m (Schenk 1991). Exposed is the folded transition between Halifax and Goldenville Formation, where rocks of the Halifax and Goldenville formations share a contact of similar length scale with the SMB. However, at deeper, unexposed levels of the batholith, SMB magmas were dominantly in contact with rocks of the metapsammite-dominated Goldenville Formation.

The metapsammitic rocks of the Goldenville and Halifax formations are quartzites and greywackes. Calc-silicate lenses of decimetre to metre size occur locally. The metapelitic rocks of the Halifax and Goldenville formations are rich in muscovite, have locally abundant graphite, and Fe±Cu-sulphides. The transition zone between Halifax and Goldenville formations is rich in Mn, Au, Mn, Pb, Sn, Cu, and Fe, and minerals such as spessartine-rich garnet and Fe±Cu-sulphides (e.g., Chatterjee et al. 1992; Cameron and Zentilli 1997).

The relationship between Meguma terrane, composed of Meguma Group rocks and Liscomb Gneisses, and the underlying rocks of the Tangier basement is unresolved. One hypothesis is that the Meguma terrane and the underlying Tangier basement rocks were unrelated prior to the Devonian collision with Laurentia (Schenk 1991). A second hypothesis is that the Meguma terrane and the underlying rocks of the Tangier basement were separate until Ordovician times (Murphy et al. 2004). A third hypothesis is that that the Meguma Group and Liscomb rocks overlay the Tangier basement rocks throughout their history (Keppie and Krogh 2000; Murphy et al. 2004). The SMB and other late Devonian granitic plutons of southern Nova Scotia may thus have intruded into a normal, or a thickened crust. The injection of mafic magmas into the lower crust underlying the Meguma terrane provided the heat for high-grade metamorphism at ca. 369-378 Ma, generating the voluminous granitic magmas (Tate 1995; Gibbons et al. 1996; Clarke et al. 1997; Greenough et al. 1998; Keppie and Krogh 1999). Physical and chemical evidence ($\delta^{18}0$, $\delta^{34}S$, εNd, and trace element data) for mixing between the mafic and granitic magmas exists for several of the peripheral late-Devonian granite intrusions of the southern and northeastern Meguma terrane (Clarke et al. 1997; Tate and Clarke 1997), but not for the central intrusions, including the SMB (e.g., Clarke et al. 1997; Tate and Clarke 1997; MacDonald 2001; Murphy et al. 2004). Sr and Nd isotopic data suggest that the felsic rocks of the Tangier basement are the volumetrically most important source of the SMB magmas (Eberz et al. 1991), but potential source-contributions from rocks similar to the Liscomb gneisses and/or Meguma Group metasedimentary rocks may have occurred (Eberz et al. 1991; Clarke et al. 1993; MacDonald 2001).

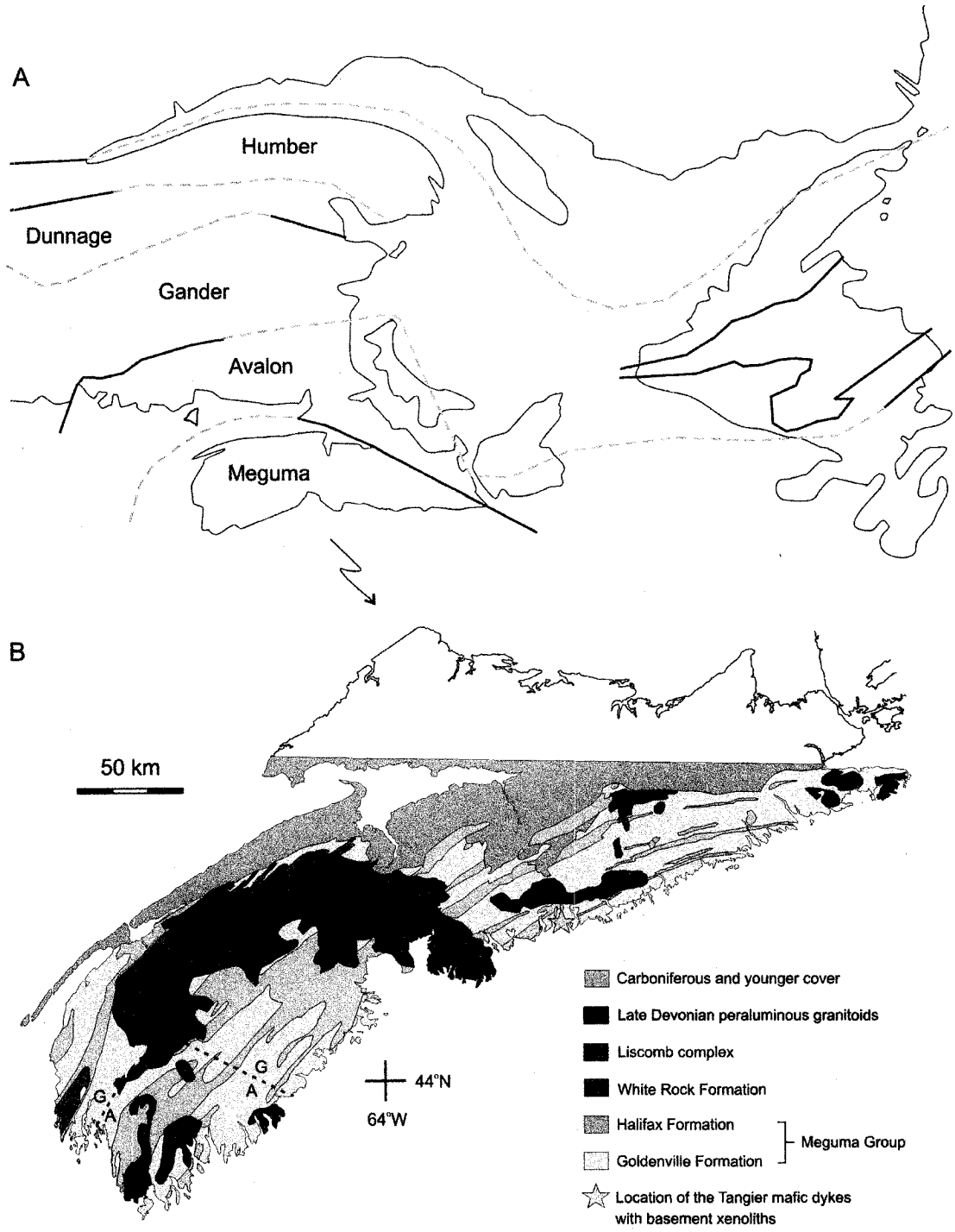

Figure 1.2: A) The Meguma Zone within the Appalachian orogen (after Williams and Hatcher 1982). B) Geology of the Meguma terrane, showing the South Mountain Batholith (SMB) and its host rocks, as well as exposed Liscomb gneisses, and the location of the mafic Tangier dykes with basement xenoliths (modified after Tate 1995). Stippled lines mark transition between greenschist (G) and amphibolite (A) facies grade of exposed Meguma Group rocks.

1.1.3 Country-rock Contamination and Assimilation in the SMB

The most important country-rock contaminants in the SMB are metapsammitic and metapelitic rocks of Meguma Group origin, whereas country-rock contaminants originating from the Liscomb gneisses are rare to absent (Jamieson 1974; Kubilius 1983; MacDonald and Horne 1988; Kontak 1990, 1993; Poulson et al. 1991; MacDonald 2001; Clarke and Erdmann 2005), and only one xenolith of Tangier basement origin has been reported (Corey and Chatterjee 1990). At least at the current level of exposure, bulk contamination of SMB magmas by country rocks was the dominant style of contamination (e.g., Jamieson 1974; Tate 1994; MacDonald 2001; Clarke and Erdmann 2005). Assimilation of country rocks occurred dominantly through a combination of fracturing and partial melting (Jamieson 1974; Clarke et al. 1998; Clarke and Erdmann 2005), releasing xenoliths, xenocrysts, and partial melt into the SMB magmas (Clarke et al. 1998; Erdmann and Clarke 2005).

Xenoliths and obvious xenocrysts, such as coarse-grained chiastolite, coarse-grained vein quartz, and subidioblastic garnet, are most common in the more primitive rocks of the SMB, but occur sporadically throughout most exposed parts of the batholith (Jamieson 1974; MacDonald 2001; Clarke and Erdmann 2005; Erdmann and Clarke 2005). In the more primitive rocks of the SMB, xenocrystic and magmatic ilmenite crystals occur, showing evidence for reequilibration through ion exchange with their former host magma (Clarke and Carruzzo in press). Xenocrystic rutile is rare in the more primitive SMB rocks, probably reflecting the assimilation of most rutile xenocrysts through dissolution (Carruzzo et al. 2006; Clarke and Carruzzo in press). In the intermediate SMB rocks, both xenocrystic and magmatic ilmenite and rutile occur, where crystals of magmatic origin are more common than xenocrysts. In the most evolved SMB rocks, ilmenite is absent, where xenocrystic ilmenite may have been consumed through partial melting and/or dissolution, whereas rutile xenocrysts occur. Many Fe-sulphides in the SMB, particularly near the external margin of the batholith, are derived from Meguma Group country rocks, occurring as former xenocrysts and/or sulphide partial melts (Poulson et al. 1991; Clarke and Erdmann 2005; Samson 2005; Samson and Clarke 2005). Locally, the Fe-sulphides, mostly pyrite and chalcopyrite, may make up ≤5 vol%, but their overall abundance in the batholith is «1 vol% (Clarke and Erdmann 2005). Zircons of Meguma Group origin, as well as of Tangier Basement origin, are present (Keppie and Krogh 1999). Cordierite-rich, as well as biotite-rich zones of the SMB may represent highly contaminated parts of the batholith (Clarke and Erdmann 2005).

Assuming that only bulk contamination of average Meguma Group metasedimentary rocks took place, and that the SMB granodiorites are uncontaminated, Clarke et al. (2004) estimated the importance of country-rock contamination and assimilation versus fractional crystallization in the SMB, using $^{87}Sr/^{86}Sr_i$ and $^{143}Nd/^{144}Nd_i$ isotopic compositions (Clarke and Halliday 1980, 1985; Clarke et al. 1988), as well as whole-rock A/CNK data. They calculated that the leucogranites of the SMB can contain as much as 36 % of bulk Meguma Group material, if contamination was followed by fractional crystallization, or 7 % of bulk Meguma Group material, if fractional crystallization was followed by contamination. On the other hand, $\delta^{34}S$ signatures of some marginal granodiorites indicate a mixture of up to 70 % of Meguma-Group-derived and only 30 % of cognate magmatic sulfur, but seem to be best explained by selective assimilation (Poulson and Ohmoto 1989; Whitney 1989; Poulson et al. 1991; Samson 2005; Samson and Clarke 2005).

The abundance of physically detectable country-rock contaminants in the SMB (xenoliths and large xenocrysts) and $\delta^{34}S$ signatures suggest a higher degree of contamination for the marginal rocks of the batholith, and a lower degree of contamination for the more central rocks of the intrusion (e.g., Jamieson 1974; Poulson et al. 1991; MacDonald 2001; Clarke and Erdmann 2005). On the other hand, the Sr-Nd whole-rock geochemical data indicate a higher degree of contamination by Meguma Group country rocks for the most evolved and typically more central rocks of the batholith than for the more primitive and typically more marginal rocks of the SMB (Clarke et al. 2004). One hypothesis to explain these apparently contradictory results is that country rocks of the Meguma Group were progressively more strongly assimilated from the margin toward the center of the SMB, leaving little physical evidence for contamination in the most evolved rocks, but a whole-rock chemical signature indicating a high degree of contamination.

1.2 Objectives and Motivation

Field, textural, mineral chemical, and whole-rock isotopic studies have shown that the mineralogical, textural, and chemical variation of the SMB rocks is the result of a combination of source variations, closed-system fractional crystallization, country-rock contamination, and fluid interaction. However, the significance of the individual processes and their effect on the evolution and characteristic properties of the batholith is only partly constrained, and physical and Sr-Nd whole-rock data are apparently

contradictory. To take a first step towards quantitatively better understanding the plethora of components and processes recorded in the exposed rocks of the batholith, the objective for my PhD study was to characterize *all* country-rock components and to assess their volumetric significance. To achieve this objective, my endeavour was:

(1) to texturally and chemically characterize all major components of country-rock contamination;

(2) to determine the dominant style (selective/bulk), mechanisms, and the efficiency of country-rock assimilation in the former SMB magmas; and

(3) to estimate the distribution and abundance of country-rock contaminants throughout the various units of the batholith.

The main motivation for my study was, besides the immediate motivation to better understand the evolution of the SMB, to provide a more comprehensive and more sophisticated means of characterizing country-rock contamination in igneous rocks in general, and thereby contributing to a better understanding of (i) the degree to which magmatic rocks carry information from their source; (ii) the importance of intra-crustal recycling ("crustal cannibalism") and the creation of space for magmas during ascent and emplacement; as well as (iii) the origin of some mineral resources.

1.3 Methods

To fulfill the above objectives, I have carried out a combination of field studies, textural and mineral chemical analyses, high-T, low-P experiments, and numerical modelling, as outlined below:

(i) Field studies. In my field studies, I characterized types, distribution, and abundance of all macroscopically visible country-rock contaminants in SMB rocks, in order to constrain their nature and their significance. I studied mineralogically and/or texturally distinct zones in the batholith, in order to evaluate if they are the result of country-rock contamination. My mapping focused on the northeastern margin of the SMB and the Halifax Pluton, where the exposure is better than elsewhere in the batholith. Given the limitations in both vertical as well as horizontal exposure of the SMB, and the limits of my study area, the results of my study are *sensu stricto* only applicable to the Halifax pluton and adjacent parts of the northeastern exposure of the SMB. Sampling included country rocks of the Meguma Group, Meguma Group xenoliths, SMB rocks of various

compositions and textures from locations close to, and remote from, the external contact of the SMB, and potential source rocks of the Tangier basement.

(ii) Textural and mineral chemical analysis. I carried out transmitted light, back-scattered electron, and cathodoluminescence microscopy (i) to characterize the known country-rock contaminants (obvious xenoliths, xenocrysts, and minerals crystallized from former country-rock partial melt), and (ii) to identify and characterize potential contaminants (e.g., fine-grained crystals that resemble the texture of crystals typical for the Meguma Group rocks). Subsequent to the textural analysis, I determined major-element and trace-element compositions for crystals of obviously and potentially xenocrystic and magmatic origins, using electron microprobe analysis and laser ablation inductively coupled mass spectrometry.

(iii) High-T, low-P experiments. I performed melting experiments using cores or powders of Meguma Group country rocks and granites of variable composition, to study melting reactions, fractions of solid and liquid contaminants, and their compositions, as well reaction relations between the country-rock and the granitic materials.

(iv) Numerical modelling. I calculated the assimilation of Meguma Group country-rocks through partial melting in SMB magmas, using the energy-constrained AFC model of Spera and Bohrson (2001). The rationale for the numerical modelling was to overcome the limitations in studying country-rock contamination and assimilation in the SMB inflicted by the limited vertical exposure of the batholith.

1.4 Thesis Organization

Chapters 2 to 4 are modified versions of manuscripts published, in press, and submitted to peer-reviewed journals. Chapters 5 and 6 are prepared for submission for publication. Chapter 2 is a "pilot study" to decipher the origin of cordierite, one of the characteristic rock-forming minerals in the SMB, using a combination of textural criteria and major-element compositions. Chapter 3 presents my experimental studies, which played a key role in estimating the significance and the nature of country-rock contaminants in the exposed rocks of the SMB. Chapter 4 is a compilation of all field and textural evidence for the nature and the significance of metapsammitic and metapelitic Meguma Group contaminants in the SMB. In combination with my experimental results and existing geochemical data, this study permitted an estimate of country-rock contamination at the exposed level of the batholith. Chapter 5 summarizes my attempt to detect crystals of

foreign origin chemically in the SMB, and describes and discusses magma chamber processes recorded in the chemical signatures of rock-forming magmatic minerals in the SMB. Chapter 6 presents energy-constrained numerical model results for the assimilation of Meguma Group country rocks in SMB magmas. Chapter 7 summarizes the conclusions of my study and gives recommendations for future work. All mineral chemical analyses are included in EXCEL spreadsheet format in Appendix 2, but are also available from the author upon request.

The order of the chapters reflects the chronology of my studies. Manuscripts already published or in press occur at the beginning of my thesis; chapters building on the conclusions from these studies are presented subsequently. Another possible order of the materials outlined could have been: i) Introduction (Chapter 1), ii) field and textural observations (Chapter 4), iii) chemistry of rock-forming minerals (Chapter 5), iv) cordierite case-study (Chapter 2), v) experimental study (Chapter 3), vi) energy-constrained modelling (Chapter 6), and vii) summary and conclusions. The reader is free to follow the chapters in either order. Given the organization of my thesis with published manuscripts or manuscripts intended for publication as chapters, I acknowledge repetitions in the introductory sections throughout Chapters 2 to 6. But despite their repetitive character, I consider the introductory paragraphs important to guide the reader through every single chapter of my thesis, pointing out the relevant concepts and important aspects of our knowledge for all subsequent observations and interpretations. In Chapters 2, 3, 4, and 6, which are multi-author manuscripts, statements and observations refer to "we", but in my thesis, I take exclusive responsibility for all the material.

CHAPTER 2

Origin of Chemically Zoned and Unzoned Cordierites from the South Mountain and Musquodoboit Batholiths, Nova Scotia

2.0 Preamble

This chapter has been published by S. Erdmann, D.B. Clarke, and M.A. MacDonald in the *Transactions of the Royal Society of Edinburgh, Earth Sciences 95*, 99-110 (2004). I acquired the quantitative data, designed all Figures and Tables, and drafted all but paragraph 2.4.4 of the manuscript. D.B. Clarke acquired the qualitative data, helped drafting, and critically revising the text. M.A. MacDonald contributed with his regional geological knowledge and experience, and had many helpful suggestions for revising the manuscript. Observations and interpretations in this chapter are presented in the form of the original manuscript, although the most favourable interpretations of some of the cordierite types have changed in the light of further data. The refined interpretations appear as parenthetical comments in the text.

The scope of this study was to establish and evaluate criteria for distinguishing between cordierite of various origins in igneous rocks, and specifically to interpret the crystallization history and underlying magma chamber processes recorded in zoning patterns of cordierite from the South Mountain and Musquodoboit batholiths.

2.1 Abstract

Textural relations and chemical zoning of cordierites in granites act as sensitive recorders of the conditions of their crystallization history and underlying magma chamber processes. In this contribution, we present new data on texturally distinct and variably zoned cordierites from the late-Devonian, granitic South Mountain and Musquodoboit batholiths, and infer the conditions of their formation. Using a combined textural (grain size, grain shape, inclusion relationships) and chemical (major-element composition, compositional zoning) classification, we recognize the following six cordierite types (CG = chemical group; TT = textural type): CG1/TT1 - anhedral to subhedral macrocrysts with random inclusions and patchy normal zoning; CG2a/TT2 - euhedral to subhedral macrocrysts with random inclusions and normal zoning; CG2b/TT2 - euhedral to subhedral macrocrysts with random or oriented inclusions and oscillatory zoning; CG3a/TT3 - subhedral to euhedral microcrysts with no inclusions and reverse zoning;

CG3b/TT4 - euhedral macrocrysts with no inclusions and no zoning; and CG4/TT5 - anhedral macrocrysts with random inclusions and normal zoning. The textural criteria suggest that these cordierites formed as a primary magmatic phase, or as the result of a peritectic reaction involving country-rock material. The combined chemical and textural criteria suggest that: (i) normal zoning results from crystallization during cooling, epitactic overgrowths on grains formed in a peritectic reaction with country-rock material, or cation exchange with a fluid; (ii) oscillatory zoning results from crystallization during variations in X_{Mg} of the silicate melt following magma replenishment; (iii) reverse zoning results from crystallization during pressure quenching; and (iv) the unzoned cordierite results from magmatic crystallization under constant T-P-X conditions.

2.2 Introduction

The late-Devonian South Mountain and Musquodoboit batholiths (Fig. 2.1) intruded dominantly into metasedimentary rocks of the Cambro-Ordovician Meguma Group (e.g., McKenzie and Clarke 1975; MacDonald and Clarke 1985). Both batholiths are connected at a depth of ~5 km (O'Reilly 1975; McKenzie 1976; Douma 1978), and the South Mountain Batholith (SMB) consists of several plutons with distinct compositions (MacDonald et al. 1992; MacDonald 2001). The Halifax Pluton (Fig. 2.1B) is one of the larger plutons in the South Mountain Batholith, exhibiting normal compositional zoning from more primitive to more evolved rocks inward from the margin, and reverse zoning in the core (MacDonald and Horne 1988). The temporal succession is biotite granodiorite, biotite monzogranite, leucomonzogranite, and muscovite-biotite monzogranite, where all units are locally intruded by aplites and pegmatites. Cordierite is present in all rock types of the pluton in traces to ≤1 modal%, including aplites and pegmatites, but is most prominent in the muscovite-biotite monzogranites and in the coarse-grained leucomonzogranites, where it constitutes up to 5 modal%. The Musquodoboit Batholith (MB), located northeast of the SMB (Fig. 2.1A,C), consists mainly of muscovite-biotite monzogranite, and minor leucomonzogranite. Cordierite is present typically in amounts ranging from traces to ≤1 modal% throughout the batholith, but occurs locally with up to 4-10 % of the mode (MacDonald and Clarke 1985; Ham 1999).

All granitoid rocks in the South Mountain Batholith and in the Musquodoboit Batholith are peraluminous (A/CNK >1) and, thus, permit a primary magmatic origin for minerals such as biotite, muscovite, garnet, cordierite, and andalusite, all of which occur as zoned and

unzoned varieties in different units of the Halifax Pluton (Ding 1995) and in the Musquodoboit Batholith (MacDonald and Clarke 1985). However, these minerals may also have a foreign origin; they may be xenocrystic (crystals derived from country rocks that did not form as a result of a chemical reaction with the main magma), or they may have formed in a peritectic reaction, involving country-rock material and main magma (e.g., Bt + Qtz + Pl + L1→ Crd ± other minerals + L2; L1 = main magma, L2 = hybrid magma consisting of country-rock partial melt and main magma) (abbreviations after Kretz 1983). In other words: the origin of each mineral in the granites has to be questioned, and the peraluminous nature of the granitoid rocks may reflect the peraluminosity of the primary magma, as well as the peraluminosity of a random mixture of primary magma and country-rock material. Hence, only a detailed microstructural and microchemical study of the mineral assemblage may permit a correct determination of the origin of the grains of an igneous rock, and may, moreover, lead to a better constrained interpretation of whole-rock geochemical data (explaining, for example, variations in peraluminosity dominantly as a result of fractional crystallization, or as a result of fractional crystallization combined with contamination by country-rock material).

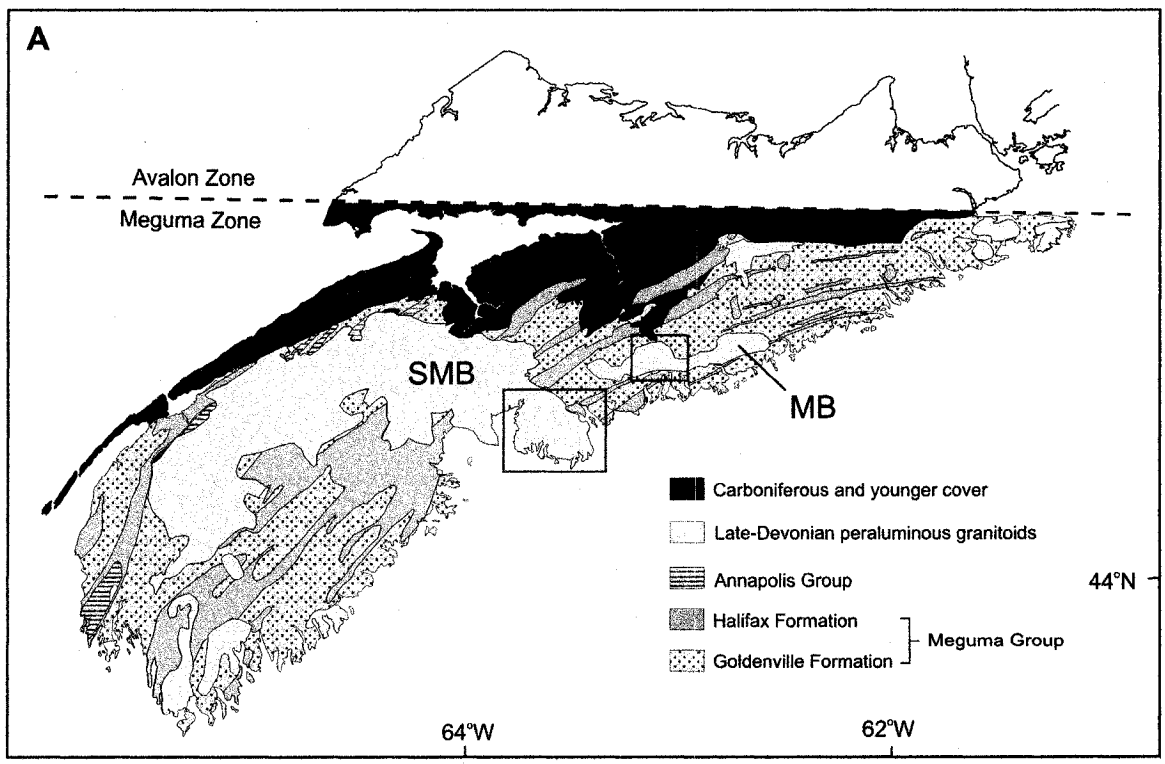

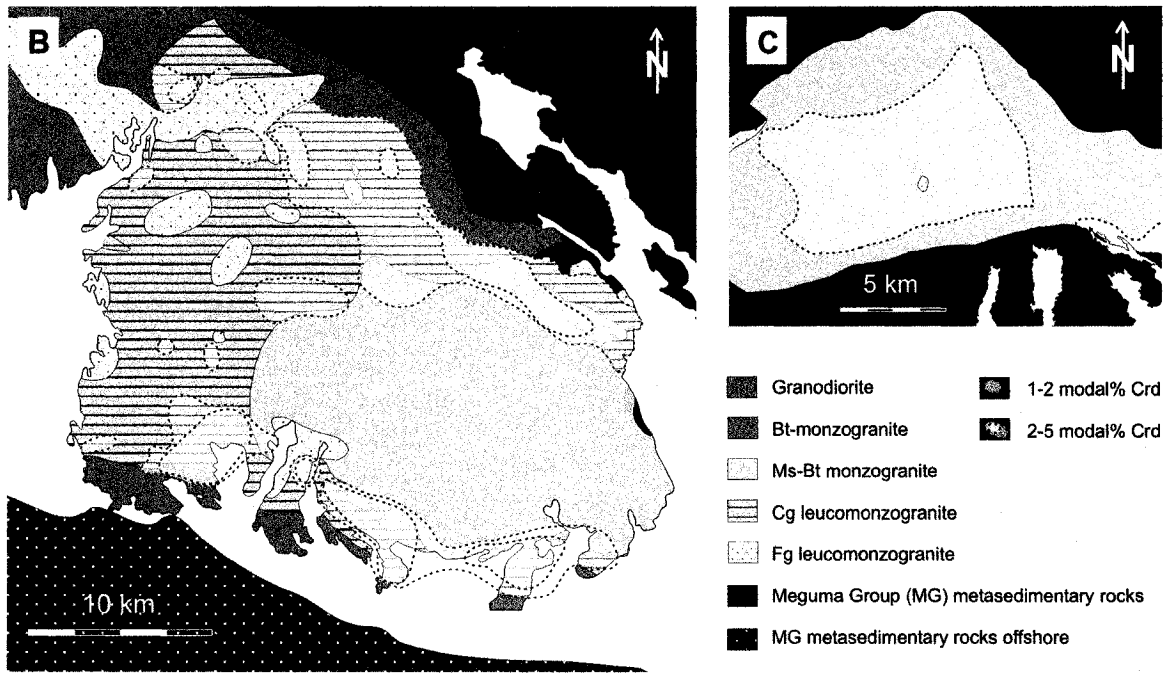

Figure 2.1: A) Geological map of Nova Scotia, showing the location of the South Mountain and Musquodoboit batholiths (SMB and MB) (modified after Tate 1995). The blue box marks Fig. 2.1B, the red box marks Fig. 2.1C. B) Detailed map of the Halifax Pluton. Cordierite is most abundant in zones subparallel, but away from the external margin of the SMB (modified after MacDonald 2001)(The spatial distribution is only approximate. The crosscutting relationship between cordierite-rich zones and the various monzogranites types may not be correct (personal communication, M.A. MacDonald, Department of Natural Resources Nova Scotia, 2006). C) Detailed map of the centre of the Musquodoboit Batholith. In contrast to the Halifax Pluton, cordierite is most abundant in one major, and in several smaller zones showing no spatial relationship to the margin of the batholith (modified after Ham 1999). Cg = coarse-grained, Fg = fine-grained, Crd = cordierite.

Of all minerals in the South Mountain Batholith and the Musquodoboit batholith, cordierite has the most striking textural and chemical variability (Maillet and Clarke 1985). Therefore, cordierite appears to be most amenable to search for grains of different origins, and to reveal key information about magma chamber processes and conditions of crystallization at various stages of the chemical evolution of these batholiths. In this paper, we (i) evaluate potential criteria for distinguishing between primary magmatic (L $\rightarrow$ Crd + other minerals), peritectic magmatic (country rock (Bt + Qtz + Pl) + magma (L1) $\rightarrow$ Crd $\pm$ other minerals + L2), and xenocrystic (derived from the country rocks) cordierite; (ii) discuss the driving forces for the normal, oscillatory, and reverse zoning in the cordierites studied; and (iii) make inferences about the origin and the growth history of the various cordierite types investigated.

2.3 Cordierite-bearing Rocks of the SMB and MB

The samples investigated are muscovite-biotite monzogranites and aplites from the Halifax Pluton and the Musquodoboit Batholith, and a pegmatite dyke from the Halifax Pluton. The monzogranites of the Halifax Pluton are coarse-grained. They contain quartz, plagioclase, K-feldspar, biotite, muscovite, ± cordierite, ± garnet, ± rutile, and traces of apatite, zircon, monazite, xenotime, and ilmenite. X_{Mg} of the monzogranites varies between 0.26 and 0.39, and MnO ranges from 0.04 to 0.08 (Table 2.1; Ham 1989, 1990). The aplites of the Halifax Pluton are fine-grained. They are characterized by the assemblage of quartz, K-feldspar, plagioclase, muscovite, biotite, ± cordierite, ± garnet, ± andalusite, and traces apatite, zircon, monazite, xenotime, and ilmenite. X_{Mg} of the aplites varies between 0.24 and 0.27, and MnO lies between 0.04 and 0.09 (MacDonald 2001). Pegmatites have a similar mineralogy to the aplites, but contain in addition tourmaline, fluorite, and various disseminated sulphides (e.g., MacDonald 2001). Whole-rock geochemical analyses for the pegmatite samples are not available.

Table 2.1: Average whole-rock chemical compositions for monzogranites and aplites from the Halifax Pluton (HP) and the Musquodoboit Batholith (MB).

	Monzogranites				Aplites		
	HP (n=26)*		MB (n=7)**		HP (n=8)***		MB (n=1)**
	wt%	1σ	wt%	1σ	wt%	1σ	wt%
Crd textural type	TT1, TT2		TT1, TT2		TT3		TT5
Crd chemical group	CG1, CG2		CG1, CG2		CG3		CG4
SiO_2	71.11	1.04	71.92	1.11	72.00	1.19	72.56
TiO_2	0.39	0.07	0.28	0.09	0.26	0.08	0.04
Al_2O_3	14.63	0.38	14.58	0.16	14.55	0.15	15.21
FeO^T	2.52	0.39	1.72	0.40	1.67	0.41	0.51
MnO	0.06	0.01	0.06	0.02	0.06	0.02	0.17
MgO	1.23	0.18	0.53	0.22	0.59	0.16	0.08
CaO	1.02	0.29	0.86	0.20	0.80	0.12	0.28
Na_2O	3.57	0.42	3.60	0.11	3.63	0.10	3.82
K_2O	4.47	0.25	4.60	0.23	4.60	0.25	4.8
P_2O_5	0.25	0.03	0.25	0.09	0.28	0.04	0.9
F	0.07	0.01	-	-	-	-	
LOI	0.64	0.15	1.14	0.27	1.20	0.24	0.44
Total	99.89	0.39	99.68	0.64	99.80	0.61	98.81
X_{Mg}	0.33	0.04	0.23	0.07	0.26	0.01	0.14

n = number of samples analyzed by XRF. Sources of data: * Ham et al. 1989, 1990, ** MacDonald and Clarke 1985, and *** MacDonald 2001; FeO^T = Fe total as FeO.

The monzogranites of the Musquodoboit Batholith are medium- to coarse-grained. They are characterized by the assemblage of quartz, K-feldspar, plagioclase, biotite, muscovite, ± cordierite, ± andalusite, ± garnet, ± rutile, and traces of apatite, zircon, monazite, ilmenite. The X_{Mg} of the monzogranites ranges from 0.31 to 0.46, and MnO varies between 0.04 and 0.07 (Table 2.1; MacDonald and Clarke 1985). The aplites of the Musquodoboit Batholith are fine-grained. They comprise an assemblage of quartz, K-feldspar, plagioclase, muscovite, ± biotite, ± garnet, ± andalusite, ± tourmaline ± cordierite, and traces of apatite, zircon, monazite, xenotime, and ilmenite. Whole-rock geochemical analysis for the aplite sample studied is not available, but several aplites of the Musquodoboit Batholith have low X_{Mg} (~0.14) and are high in MnO (~0.17) (MacDonald and Clarke 1985).

2.4 Cordierite in the SMB and MB

2.4.1 Textural-chemical Classification

Cordierite in peraluminous granites may have various origins, and two or more origins may be valid for cordierites even from a single rock sample (Clarke 1995). Correctly inferring the origin of a given cordierite crystal may involves applying a combination of the following textural and chemical criteria:

(i) *Grain shape.* Metamorphic and xenocrystic cordierite (formed via a subsolidus or a peritectic reaction) is typically subhedral to anhedral (e.g., Phillips et al. 1981; Bouloton 1992; Pereira and Bea 1994; Barbey et al. 1999; Cenki et al. 2002). In contrast, primary magmatic cordierite is commonly subhedral to euhedral (e.g., Phillips et al. 1981; Bouloton 1992; Pereira and Bea 1994; Villaseca and Barbero 1994), but may be subhedral to anhedral in the case of grain interference during magmatic growth, or in the case of subsequent reaction.

(ii) *Inclusions.* If cordierite contains inclusions, the sizes, shapes, and compositions of the inclusions, and the inclusion patterns, may help to constrain its crystallization history, and thus its origin. If cordierite contains inclusions of former partial melt (now in the form of solids that crystallized from the melt), its origin is probably magmatic (either cotectic or peritectic). In contrast, inclusions that do not belong to the mineral assemblage of the igneous rock otherwise, most likely suggest a metamorphic xenocrystic, or a peritectic magmatic origin. However, even primary magmatic cordierite can contain inclusions of 'foreign' minerals, if it overgrew xenocrysts present in the melt.

(iii) *Grain size.* Dimensional compatibility of a crystal of unknown origin with other, generally accepted igneous rock-forming minerals in the sample may suggest that the mineral in question also has a magmatic origin. Dimensional incompatibility, on the other hand, may point to, but does not necessarily require, different origins. The grain sizes of the various igneous minerals in any rock, and also the grain size of a certain mineral, can vary by orders of magnitude.

(iv) *Mineral composition.* Major-element compositions may indicate different populations of a single mineral. Metamorphic cordierites, for example, tend to have an X_{Mg} of ~0.50-0.95, whereas magmatic cordierites commonly have lower values (Deer et al. 1997). Other components, such as Na_2O, as well as H_2O and CO_2, are less useful for determining the origin of an unknown cordierite, because their concentrations depend strongly on the cooling history (e.g., Schreyer and Yoder 1964; Johannes and Schreyer 1981; Harley et al. 2002).

(iiv) *Chemical zoning.* Normal and reversely zoned, as well as unzoned cordierite occurs in metamorphic and magmatic rocks (e.g., review by Deer et al. 1997), and those zoning patterns do thus not necessarily reflect a distinct origin of a grain in question. Oscillatory zoning in cordierite, on the other hand, is known exclusively from igneous rocks (Hiroi et al. 2002), and although the origin of the oscillatory zoned cordierite may be metamorphic, such an origin seems rather improbable, except if episodic growth of the cordierite took place in the presence of a compositionally variable fluid.

For the present textural and chemical study, we have examined the textures of more than 70 cordierite grains from 15 samples, and selected 21 grains from the various rock units. To classify the selected grains, we used the following textural variables: size (macrocrysts >1 mm, microcrysts <1 mm); shape (euhedral, subhedral, anhedral); and inclusions (absence, presence – mineral types, assemblages – random, oriented). The chemical variables for the classification are X_{Mg} = [Mg/(Mg+Mn+Fe)] and MnO, and chemical zoning (normal, reverse, oscillatory, unzoned), in which normal zoning indicates a core to rim decrease in X_{Mg} and increase in MnO.

2.4.2 Cordierite Textures

Using grain size, grain shape, and inclusions, we recognize five main textural types of cordierite (TT1-5; Fig. 2.2, Table 2.2) in the granitic rocks of the South Mountain and Musquodoboit batholiths. TT1 crystals are <25 mm in size, and anhedral to subhedral, showing randomly oriented quartz and biotite inclusions (Fig. 2.2A). The quartz and

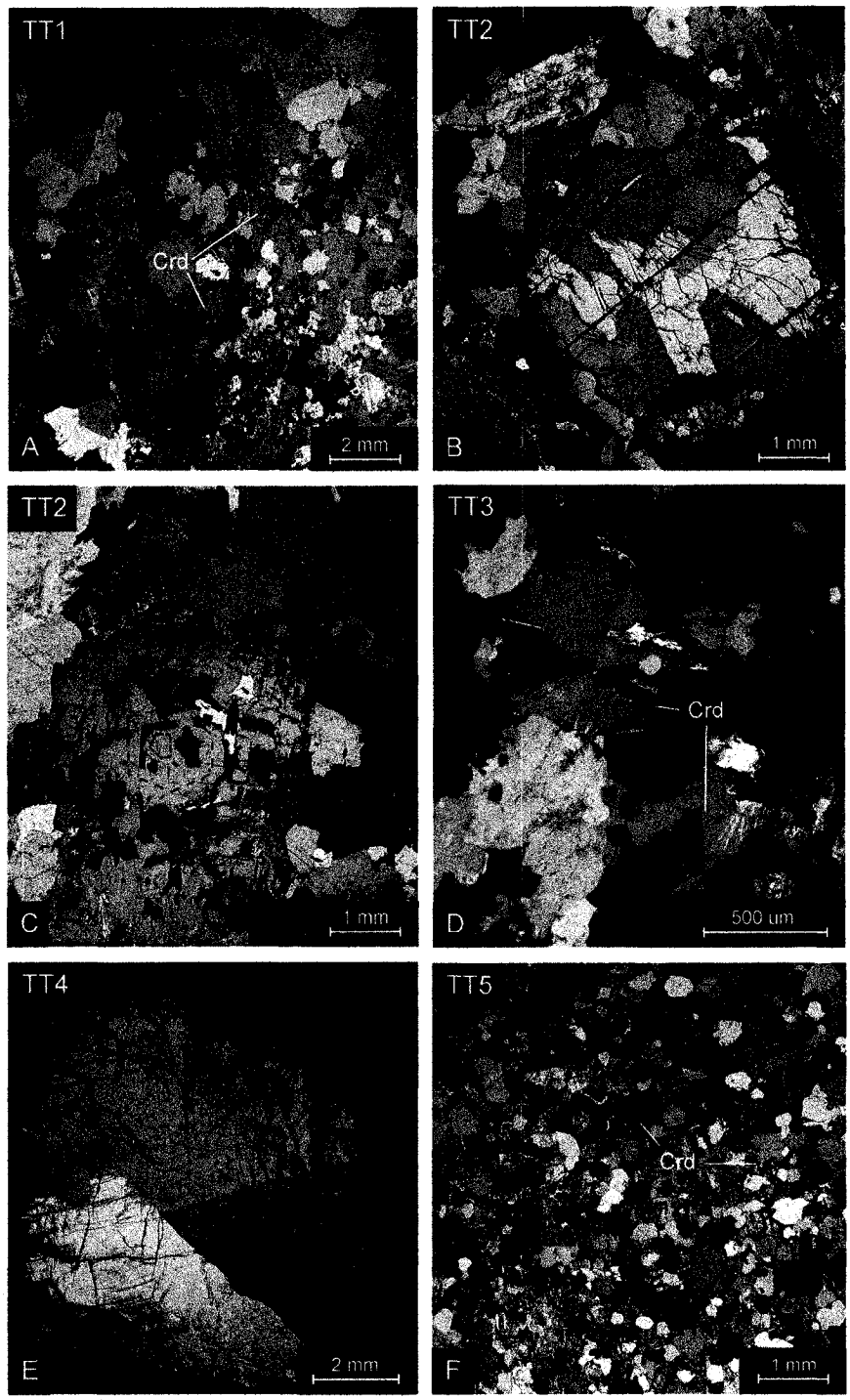

Figure 2.2: Photomicrographs (crossed-polarized light) of the five main textural cordierite types. A) TT1: Part of a subhedral cordierite macrocryst with random inclusions of biotite and quartz (Sample 306-X). B) TT2: Euhedral cordierite macrocryst with few randomly oriented biotite and quartz inclusions (Sample 304i). C) TT2: Euhedral cordierite macrocryst, showing a concentric zoned texture (marked by the broken red lines) (Sample 306-2). D) TT3: Cluster of subhedral cordierite microcrysts with no inclusions (Sample 103A5iiiA). E) TT4: Euhedral cordierite macrocryst with no inclusions (grain separate) (Sample L83-Z). F) TT5: Large, anhedral cordierite macrocrysts with abundant random quartz inclusions (Sample MD79-0085).

biotite inclusions consist of rounded single grains or monomineralic aggregates. Although lobate cordierite grain boundaries dominate, subhedral parts of the macrocrysts with few inclusions do occur. TT2 consists of large (~3-10 mm), subhedral to euhedral, single and multiple macrocrysts, occurring as isolated grains, or in grain clusters (Fig. 2.2B). Inclusions are randomly oriented, and relatively rare, except in one grain, where there is a concentric pattern of euhedral to rounded biotite, and anhedral quartz inclusions, separating three growth shells of cordierite (core, intermediate and rim zone; Fig. 2.2C). TT3 microcrysts have a grain size of ~0.2-1.0 mm, and occur as single or multiple, subhedral to euhedral, inclusion-free grains (Fig. 2.2D). TT4 crystals are large (≤10 mm), euhedral, and inclusion-free (Fig. 2.2E). TT5 crystals are up to 10 mm in diameter, and anhedral (Fig. 2.2F). This type of macrocryst shows abundant inclusions of small quartz crystals similar in shape and slightly smaller than quartz of the surrounding matrix; other inclusions are lacking.

Table 2.2: Textural-chemical classification of cordierite in the SMB and MB.

Textural type	TT1	TT2	TT3	TT4	TT5
Chemical group	CG1	CG2	CG3	CG3	CG4
Rock type	Mng	Mng	Apl	Peg	Apl
n	1	11	5	1	3
Size	> 1 mm	> 1 mm	< 1 mm	>> 1 mm	> 1 mm
Shape	ah-sh	sh - eh	sh - eh	sh - eh	ah
Inclusion type	Bt, Qtz, Acc	Bt, Qtz, Acc	-	-	Qtz
Inclusion orientation	r	r/o	-	-	r
X_{Mg}	0.45-0.64	0.37-0.50	0.20-0.32	0.24-0.25	0.35-0.36
Mn (apfu)	0.01-0.06	0.04-0.09	0.10-0.12	0.13-0.14	0.20-0.25
Zoning	nz	nz/oz	rz	uz	nz

Mng = monzogranite, Apl = aplite, and Peg = pegmatite. n = number of crystals investigated by electron microprobe; Acc = accesories; ah = anhedral, sh = subhedral, eh = euhedral; r = random, o = oriented; nz = normally zoned; oz = oscillatory zoned; rz = reversely zoned, uz = unzoned.

2.4.3. Cordierite Mineral Compositions and Chemical Zoning

Based on X_{Mg} and Mn apfu, determined by microprobe analysis, we recognize four main chemical groups of cordierite (CG1-4) in the granitic rocks of the South Mountain and Musquodoboit batholiths (Fig. 2.3; Table 2.3). Three of these groups define a linear trend from high X_{Mg}-low Mn to low X_{Mg}-high Mn, and the fourth group lies well off this trend.

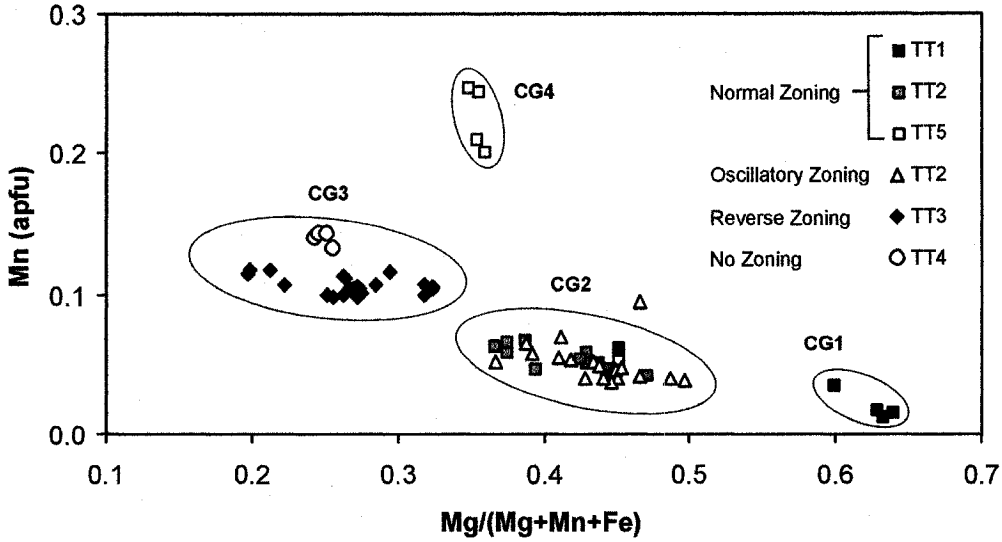

Figure 2.3: X_{Mg} versus Mn (apfu) plot showing the four main chemical groups. The analyses represent the 21 cordierite grains selected, including: (i) core and rim compositions for the normally and reversely zoned grains; and (ii) minimum and maximum values for the oscillatory zoned grains. Although the four main chemical groups are distinct based on the present data, the major-element composition of some groups may eventually overlap for an enlarged data set.

Furthermore, the style of chemical zoning (normal, reverse, oscillatory, unzoned) enables us to subdivide some of these groups. Chemical Group CG1 has the highest X_{Mg} (0.64) and lowest Mn values (0.01-0.06 apfu). Cordierite belonging to this chemical group is characterized by patchy normal zoning, where X_{Mg} decreases towards grain boundaries and towards micro-cracks (Fig. 2.4A). Chemical Group CG2 has intermediate X_{Mg} (0.37-0.50) and Mn values (0.04-0.09 apfu), and consists of grains showing either normal or oscillatory zoning. The normally zoned grains (CG2a) have high-X_{Mg}, low-Mn cores (~0.47, 0.04 apfu), and low-X_{Mg}-, high-Mn rims (~0.37, 0.07 apfu), where the lowest X_{Mg} and highest Mn values occur along grain boundaries and micro-cracks (Fig. 2.4B). The oscillatory zoned grains (CG2b) are characterized by sharp to diffuse, asymmetric, large-scale oscillations (0.1-1.0 mm) in Fe-Mg-Mn (Fig. 2.4C, 2.5A,C) with a maximum X_{Mg}-amplitude of 0.02, and a maximum Mn-amplitude of 0.001. The width of the oscillating growth layers varies between crystallographically non-equivalent faces, but resorption features are absent. Normal zoning is superimposed on the oscillatory zoning along grain boundaries and cracks. Chemical Group CG3 shows the lowest X_{Mg} (0.20-0.32), and higher Mn values (0.10-0.14 apfu). Cordierite from this chemical group is either unzoned (CG3a) or is reversely zoned (CG3b). The reverse zoning consists of monotonic increases in X_{Mg} from core to rim (Fig. 2.4D, 2.5B,D), in which the maximum

compositional range within a single grain is 0.07 for X_{Mg}, and 0.003 apfu for Mn. CG4 has intermediate X_{Mg} (0.35-0.36) and the highest Mn-concentration (0.20-0.25). Cordierite belonging to this group has weak normal zoning along grain boundaries and towards micro-cracks.

Table 2.3: Characteristic core-rim EMP analyses of the four main chemical cordierite groups.

	Cordierite								Garnet		Biotite	
Type	CG1		CG2		CG3		CG4		Grt		Bt*	
	core	rim	core	rim	core	rim	core	rim	core	rim	core	rim
Rock type	Mng		Mng		Apl		Apl		Apl		Apl	
SiO_2	46.43	47.30	47.07	46.29	45.71	46.03	46.89	47.05	36.74	36.74	33.52	33.61
TiO_2	0.01	-	0.03	0.02	-	0.01	-	-	0.07	0.02	3.27	3.27
Al_2O_3	31.42	31.76	31.47	31.33	30.61	30.61	31.39	31.13	20.58	20.64	19.12	19.33
FeO	7.96	10.25	10.42	12.16	14.71	13.74	10.52	9.95	3.88	3.88	24.02	23.81
MnO	0.18	0.67	0.57	0.68	1.22	1.20	2.21	2.71	9.67	8.56	0.39	0.41
MgO	7.73	5.06	5.11	4.18	2.20	3.02	4.04	3.81	0.83	0.97	3.66	3.68
CaO	0.01	0.01	0.03	0.00	0.03	-	0.01	-	0.29	0.40	-	-
Na_2O	0.78	1.49	1.50	1.30	1.05	0.96	1.77	1.88	-	-	0.13	0.09
K_2O	-	-	-	-	-	-	-	-	-	-	9.33	9.16
Cl	-	-	0.00	0.00	0.01	0.01	-	-	-	-	-	-
Total	94.51	96.54	96.20	95.96	95.56	95.58	96.83	96.52	100.27	99.44	93.44	93.36
Si	4.989	5.041	5.039	5.012	5.040	5.048	5.033	5.064	5.971	5.994	4.381	4.384
Ti	0.001	-	0.002	0.002	-	0.001	-	-	0.008	0.002	0.321	0.321
Al	3.979	3.990	3.972	3.999	3.979	3.956	3.971	3.949	3.942	3.969	2.945	2.972
Fe^{2+}	0.715	0.914	0.933	1.101	1.357	1.260	0.944	0.895	3.834	3.851	2.626	2.598
Fe^{3+}	-	-	-	-	-	-	-	-	0.475	0.477	-	-
Mn	0.017	0.061	0.052	0.062	0.114	0.111	0.201	0.247	1.331	1.183	0.043	0.045
Mg	1.238	0.803	0.815	0.674	0.361	0.494	0.646	0.611	0.202	0.235	0.714	0.715
Ca	0.001	0.001	0.003	0.000	0.004	-	0.002	-	0.051	0.069	-	-
Na	0.163	0.308	0.311	0.273	0.226	0.204	0.369	0.392	-	-	0.033	0.022
K	-	-	-	-	-	-	-	-	-	-	1.556	1.525
Cl	-	-	0.001	0.000	0.003	0.001	-	-	-	-	-	-
Total	11.10	11.12	11.13	11.12	11.08	11.08	11.17	11.16	15.81	15.78	12.62	12.58
A	0.66	0.66	0.66	0.65	0.63	0.63	0.65	0.65	0.59	0.61	-0.46	-0.44
F	0.37	0.55	0.55	0.63	0.80	0.73	0.64	0.65	0.97	0.96	0.79	0.79
M	0.63	0.45	0.45	0.37	0.20	0.27	0.36	0.35	0.03	0.04	0.21	0.21

Microprobe operating conditions were: 15 kV, 15 nA, 10 µm spot size, and 40-second counting times. * Analysis given for the most common, unzoned Bt-type. Mng = monzogranite, Apl = aplite. The rather low totals for cordierite may be the result of submicroscopic decomposition.

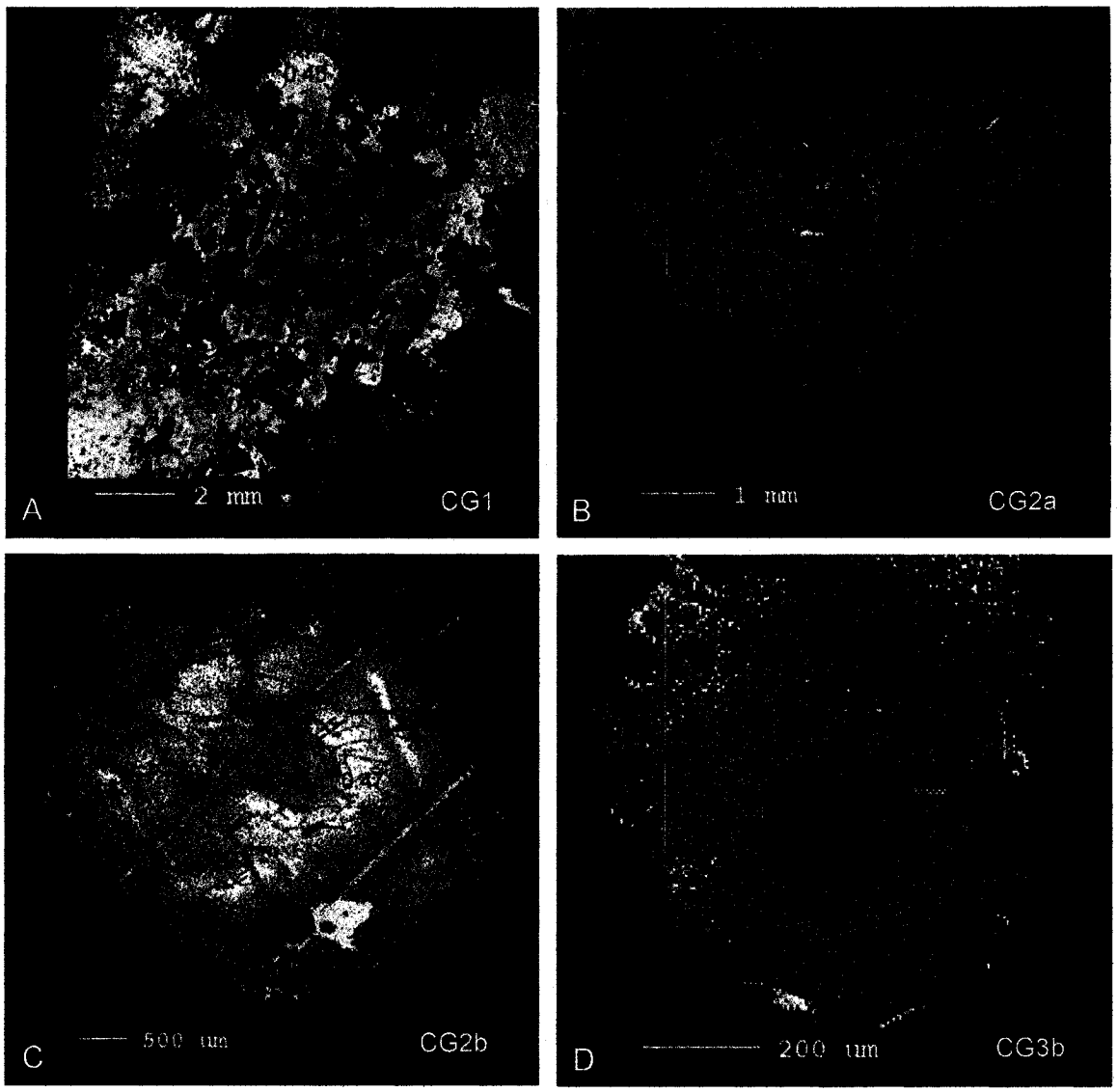

Figure 2.4: X-ray maps showing compositional zoning in Mg. Microprobe operating conditions were: 15 kV, 200 nA, 500 ms/pixel, 10 μm/pixel. Warm colours represent higher Mg values, but the colours are not standardized to fixed Mg-concentrations; the numbers represent X_{Mg} values of certain parts of the grains. A) Patchy normal zoning in CG1/TT1 (Sample 306-X). Note that the green and blue colours represent pinite. B) Normally zoned CG2a/TT2, where Mg decreases along grain boundaries and micro-cracks (Sample 304iiii). The dark blue colours represent pinite. C) Oscillatory zoned CG2b/TT2 grain, showing sharp to diffuse, roughly concentric growth shells (Sample 304i). The blue colour marks pinite. D) Reversely zoned CG3a/TT3 (Sample 103A5iiiA).

2.4.4 Combined Textural-chemical Classification

We have identified five textural types and four main chemical groups of cordierite in the granitic rocks of the South Mountain and Musquodoboit batholiths. The symbols on Figure 2.3 illustrate the close relationship between the textural types and chemical

groups. The large, anhedral to subhedral, inclusion-ridden cordierite (TT1) is chemically most primitive (CG1). The subhedral single and multiple macrocrysts (TT2) with few inclusions have intermediate chemical compositions (CG2); normal and oscillatory zoning patterns permit a chemical subdivision of these cordierites. The large inclusion-free cordierite (TT4) falls in the most evolved chemical group (CG3), and is unzoned. The large, normally zoned grain of cordierite with abundant random inclusions of quartz (TT5) has a composition off the chemical trend (CG4). The high MnO composition of CG4 probably reflects a high bulk MnO of the host aplite. The more primitive composition of cordierite CG1 and CG2, compared to cordierite CG3 and CG4, can be explained by their occurrence within the monzogranites and the relatively more evolved aplites, respectively. However, the compositional difference between CG1 and CG2 cannot be explained by variation in the whole-rock geochemistry, given that the CG1 cordierite occurs in the same sample as crystals classified as CG2. The grain size of the cordierites does generally correlate with the grain size of the host rock (e.g., small cordierite crystals (TT3) in some aplites, and large cordierite crystals (TT4) in the pegmatite), but exceptions occur (e.g., TT5 in the aplites).

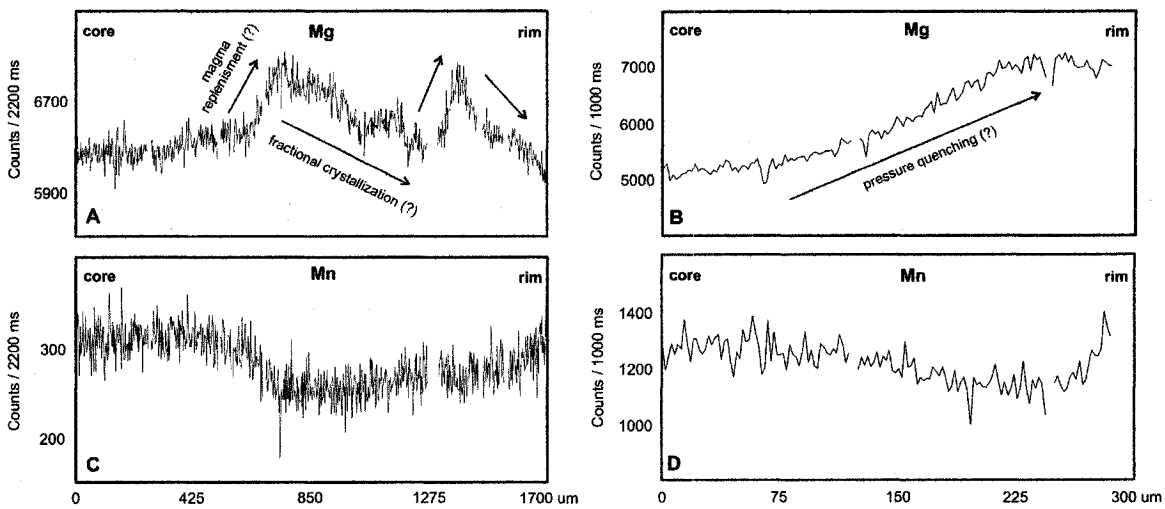

Figure 2.5: Plot of Mg (A,B) and Mn (C,D) concentrations versus radius for CG2b/TT2 (A,C), and CG3a/TT3 (B,D), with the suggested processes responsible. Figure 2.4 shows the locations of the profiles. Microprobe operating conditions were: 200 nA, 500 ms/pixel, and 2 μm/pixel for CG2b/TT2 (A,C); and 200 nA, 1000 ms/pixel, and 2 μm/pixel for CG3a/TT3 (B,D).

2.4.5 Spatial Occurrence

Categories CG1/TT1 and CG2/TT2 predominate in the monzogranites of the Halifax Pluton and Musquodoboit Batholith. Category CG2/TT2 dominates in abundance; however, the relative abundance of CG2a/TT2 and CG2b/TT2 is unclear. In the samples investigated, CG2a/TT2 and CG2b/TT2 are equally abundant, but too few samples were studied to be representative. Detailed mapping has revealed that cordierite (CG1/TT1 and CG2/TT2) in the Halifax Pluton is most abundant in zones that occur 1-5 km away from the granite/metasediment contact, roughly parallel to the margin of the pluton, and apparently oriented independently of internal lithological boundaries (Fig. 2.1B; MacDonald and Horne 1988; MacDonald 2001) (The spatial distribution is only approximate. The crosscutting relationship between cordierite-rich zones and the various monzogranites types may not be correct (personal communication, M.A. MacDonald, Department of Natural Resources Nova Scotia, 2006)). In contrast, CG1/TT1 and CG2/TT2 in the Musquodoboit Batholith are dominant in one major, and in several smaller zones, showing no regular spatial relationship to the margin of the batholith (Fig. 2.1C). CG4/TT5 and CG3/TT3 occur in aplites, and CG3/TT4 in a pegmatite.

2.5 Other Zoned Minerals

Plagioclase macrocrysts from the monzogranites of the Halifax Pluton and the Musquodoboit Batholith show complex oscillatory zoning. Some have rounded, resorbed cores, and euhedral to subhedral epitaxial rims, in which the dissolution surface marks a major drop in X_{Ca}; other crystals lack a core-rim texture. The composition ranges between X_{An} = 1 and X_{An} = 36, showing complex large- and small-scale oscillations. The large-scale oscillations are characterized by a mostly saw-tooth like pattern, consisting of reverse and normally zoned, <50 to 500 μm wide layers; superimposed are small scale oscillations with a width of < 20 μm, and an An-amplitude of ≤0.01. Zoning patterns of different plagioclase macrocrysts, or zoning patterns of spatially related cordierite macrocrysts do not correlate.

Garnet crystals from the aplites are small to large, euhedral in outline, showing fine-grained quartz inclusions. The composition is almandine-spessartine-dominated (X_{Alm} = 0.73-0.75, X_{Sps} 0.20-0.23), in which the spessartine component decreases, and the grossular and pyrope components increase from core to rim (Fig. 2.6). As for cordierite

type CG3a/TT3 from the same samples, the reverse zoning pattern of garnet is monotonic.

Biotite crystals from the aplites are small, and subhedral. X_{Mg} varies between 0.21 and 0.25. Most biotite crystals are unzoned, however, a few have normal zoning (Ding 1995), and some show weak reverse zoning. The origin of the various biotite zoning patterns is not yet clear.

2.6 Causes of Zoning

Normally and reversely zoned cordierite has been reported from magmatic and metamorphic environments (e.g., review by Deer et al. 1997). Normal zoning may result from epitactic overgrowths on crystals formed in a peritectic reaction (Flood and Shaw 1975). Reverse zoning has been suggested to result from processes such as a decrease in H_2O (Birch and Gleadow 1974), an increase in temperature and the degree of partial melting (e.g., Holtz and Johannes 1991; Pereira and Bea 1994), or solid-state diffusion during cooling (Ashworth and Chinner 1978). Hiroi et al. (2002) described, but did not explain the origin of oscillatory zoning from cordierite in granites.

2.6.1. Normal Zoning

Normal zoning in the cordierites investigated may be the result of magmatic growth, diffusion, or both, involving the following mechanisms:

(i) *Fractional crystallization.* Closed-system fractional crystallization should result in the formation of normally zoned cordierite with a high-X_{Mg}, low-MnO core, and a low-X_{Mg}, high-MnO rim. Fractional crystallization may account for the normal zoning in CG2a/TT2, but the evidence is not clear, whereas this mechanism probably played an important role in the formation of the oscillatory zoning of CG2b/TT2 (see below).

(ii) *Epitactic crystallization.* Epitactic overgrowths on Mg-rich xenocrystic or peritectic cordierite may result in normal zoning, with a core of high X_{Mg}, and a rim of low X_{Mg}, with or without hiatus or resorption features. Normal zoning without hiatus or resorption features in CG1/TT1 may be the result of this mechanism. The absence of any hiatus or resorption features may support a peritectic origin of the cordierite core (compositional disequilibrium with the main magma is more likely for xenocrystic cordierite than for a peritectic cordierite), resulting from the reaction between country-rock material and main magma, whereas the rim may have crystallized mostly from the main magma, involving little or no country-rock material.

(iii) *Decreasing* fO_2. Falling oxygen fugacity may cause normal zoning in Fe-Mg in cordierite, because at a lower fO_2, more Fe^{2+} becomes available for the crystallization of cordierite. However, evidence for a falling oxygen fugacity during the crystallization of the various rock types of the SMB and MB is lacking; instead, the phase assemblages of the more evolved rocks of the two intrusions are indicative of a rising, and not a falling oxygen fugacity with progressive chemical evolution (MacDonald 2001).

(iv) *Diffusive exchange.* Diffusive exchange between cordierite and other Fe-Mg-Mn-bearing phases during cooling may also produce normal zoning, and will be most efficient along grain boundaries and along micro-cracks. All of the cordierites investigated show, to varying degrees, irregular to patchy normal zoning along grain boundaries and micro-cracks, suggesting that diffusive exchange was the dominant mechanism for the formation of normal zoning in our sample set.

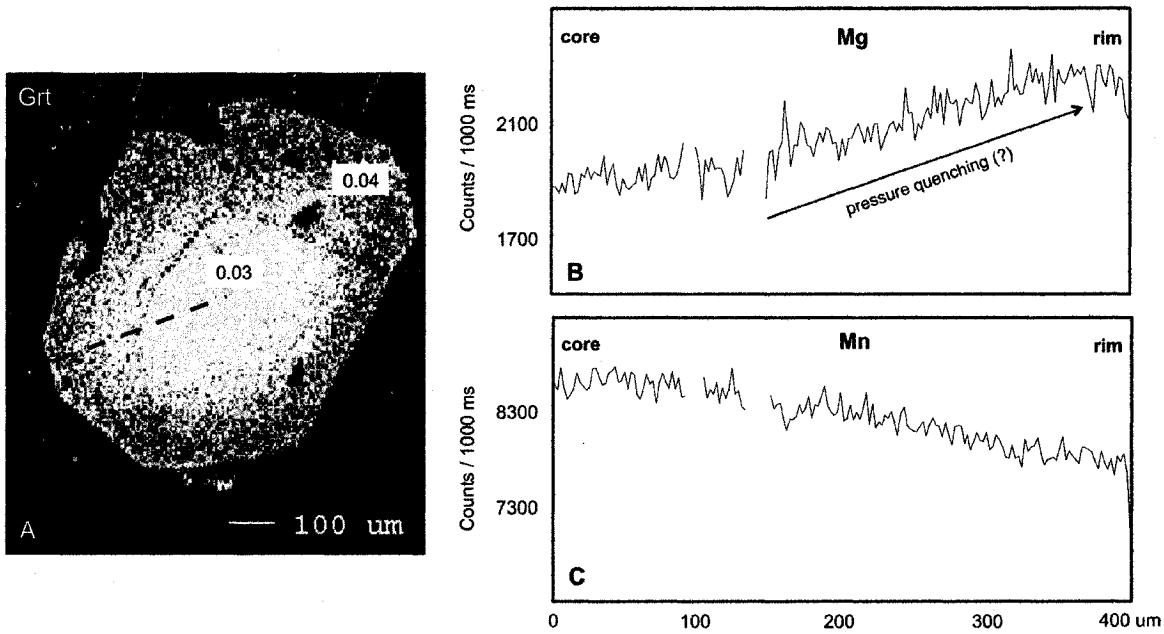

Figure 2.6: A) X-ray map showing reverse zoning in Mg for garnet from an aplite (Sample 103A5iiiA). Microprobe operating conditions were: 15 kV, 200 nA, 500 ms/pixel, and 10 μm/pixel. The numbers represent X_{Mg} of quantitative core and rim analysis. Plot of qualitative Mg (B) and Mn (C) concentrations versus radius for the profile marked in (A), and the suggested process responsible. Microprobe operating conditions were: 200 nA, 1000 ms/pixel, and 2 μm/pixel.

2.6.2 Oscillatory Zoning

Oscillatory-zoned cordierite may, at least theoretically, form in magmatic and metamorphic environments, in an open system, with repeated changes in T, P, and/or X, or as a result of local fluctuations in the composition of a boundary layer of melt around

the growing crystal (e.g., Shore and Fowler 1996), where the following processes are the most likely driving forces to cause oscillatory zoning in igneous crystals:

(i) *Advection of crystals.* Magmatic convection, and therefore advection of minerals through different T-P-X environments within the magma chamber, as first suggested by Bowen (1928), may be a mechanism for producing oscillatory zoning (the classic example is plagioclase) (e.g., Singer et al. 1995). Though physically possible, we cannot test the importance of this mechanism, but advection appears to be rather unlikely to produce the characteristic asymmetrical sawtooth-like oscillation patterns in the compositional profiles of the cordierites studied (Fig. 2.5A,C).

(ii) *Chemical assimilation of xenolithic material.* Minerals crystallizing and growing adjacent to xenoliths may record chemical changes caused by assimilation (Edwards and Russell 1996), but the formation of oscillatory zoning as a result of assimilation is unlikely in the samples studied, because it would require periodically repeated chemical contamination close to the same cordierite crystal.

(iii) *Degassing processes.* Changes in fluid pressure and fluid composition may account for changes in the composition of cordierite. Based on our data set, we cannot test the importance of fluid pressure and/or composition for the oscillatory zoning observed, but CG2b/TT2 appears to have crystallized during an early stage of the magmatic evolution, when degassing and/or fluid flux variation were probably less important than other processes (In Chapter 5 (page 141) fluid degassing or magma eruption are considered as mechanisms that caused the oscillatory zoning patterns in CG2b/TT2).

(iv) *Diffusion-controlled growth.* Diffusion-controlled growth may generate heterogeneous, oscillating compositional patterns (e.g., L'Heureux and Fowler 1996), if the growth rate of a crystal increases with the concentration of certain components in the surrounding melt layer, and if the partition relationship favours a higher concentration of certain species in the crystal than in the silicate melt. Although possible, we think that this mechanism is unlikely to explain the observed oscillatory zoning, because the zone thicknesses in cordierite are relatively large and highly variable compared to the zone thicknesses that are usually ascribed to diffusion-controlled growth (e.g., L'Heureux and Fowler 1996; Ginibre et al. 2002).

(iiv) *Magma replenishment.* Magma replenishment results in increasing T, followed by compositional changes if mixing is sufficient. Repeated mass flux into, or through, the region in which the crystal growth takes place will produce periodic changes in the T-X-a_{H2O} conditions, and may thus produce oscillatory zoning. Evidence for repeated magma

recharge in the Halifax Pluton includes the occurrence of several types of microgranitoid enclaves (Tate 1994), and the occurrence of inverse zoning of the Halifax Pluton itself (MacDonald and Horne 1988; MacDonald 2001). Thus, magma replenishment appears most likely to be the cause of the reversely zoned segments of the oscillatory zoning in CG2b/TT2, whereas the normally zoned segments probably result from fractional crystallization (Fig. 2.5A,C) (In Chapter 5 (page 141) fluid degassing or magma eruption are considered as mechanisms that caused the oscillatory zoning patterns in CG2b/TT2).

2.6.3 Reverse Zoning

Possible mechanisms to explain reverse zoning in the cordierites from the aplite samples investigated involve:

(i) *Magma recharge and increasing T.* Evidence for the influx of more primitive (high X_{Mg}), and thus hotter magma, is absent, and unlikely in the aplites studied. Garnet-cordierite thermometry (Perchuck et al. 1985) suggests cordierite and garnet growth during cooling (T_{core} = 780 °C, T_{rim}= 700 °C, calculations are for P = 200 MPa; garnet-cordierite core and garnet-cordierite rim compositions from Table 2.3). Garnet-biotite thermometry (Ganguly and Saxena 1984), on the other hand, suggests growth during rising T (T_{core} = 710 °C, T_{rim}= 760 °C, calculations are for P = 200 MPa; garnet-cordierite core and garnet-cordierite rim compositions from Table 2.3), a condition unlikely in the aplites investigated, indicating that biotite may have crystallized early, followed by cordierite and garnet.

(ii) *Increasing fO_2.* Rising oxygen fugacity, caused by the dissociation of exsolved magmatic H_2O, may account for gradual reverse zoning in AFM minerals by oxidizing Fe^{2+} of the melt to Fe^{3+}. Because Fe^{3+} becomes preferentially partitioned into Fe-oxides, this change increases the X_{Mg} of the melt, and silicates such as cordierite, garnet and biotite would incorporate more Mg towards the rim (Czmanske and Wones 1973; Lalonde and Martin 1983). Although this mechanism is consistent with reverse zoning observed in cordierite and garnet, it does not seem to apply because of the paucity of Fe-oxides in the aplite samples studied.

(iv) *Metasomatic reaction.* Reaction of cordierite and garnet with fluids of changing composition may have caused the reverse zoning observed. However, the 'freshness' of coexisting plagioclase and K-feldspar suggests that hydrothermal alteration at temperatures below the feldspar stability was not important for the samples studied. A

reaction at a temperature above the stability of feldspar alteration minerals is theoretically possible, but unlikely because the aplite dykes hosting the reversely zoned garnet and cordierite crystals are thin, and they would have cooled too quickly to have permitted diffusive exchange over the ≥150 μm wide the rim zones.

(v) *Pressure quenching.* Under equilibrium conditions, a decrease in P may lead to the breakdown of biotite, and the formation of reversely zoned cordierite and garnet (L + Bt + Qtz → Grt + Crd + Kfs + H_2O) (J.D. Clemens, pers. comm. 2004). Biotite may have crystallized prior to the rapid ascent of the aplite magma; during decompression, biotite may have partly decomposed to cordierite and garnet. With progressive decompression, the divariant reaction would result in the crystallization of continuously more Mg-rich cordierite and garnet, producing the zoning patterns observed. Although a possible explanation, we do not see textural evidence for the consumption of biotite. Under disequilibrium conditions, on the other hand, biotite may have remained metastable, or may have undergone metastable growth, whereas cordierite and garnet may have crystallized directly from the melt (L → Crd + Grt + other phases). The reverse zoning may have developed, if diffusivities of Fe in the melt were high compared to diffusivities of Mg towards the growing cordierite and garnet crystals.

2.7 Origin of Cordierites in the SMB and MB

(i) CG1/TT1. Most likely, CG1/TT1 (Fig. 2.2A, 2.4A) crystallized as a result of the reaction between xenolithic material and the main magma, as suggested by its abundant small, rounded biotite and quartz inclusions, which show no textural relationship to the magmatic biotite of the surrounding granitic matrix, and may thus have a 'foreign' origin. A xenocrystic origin is unlikely, given that cordierite crystals from the country rocks is smaller and shows different inclusion relations. The high-X_{Mg} composition of CG1/TT1 (compared to all other cordierite types studied) probably reflects the consumption of Mg-rich biotite, either in a dehydration reaction, or in a melting reaction, whereas the low-X_{Mg} margins of the cordierite grain may represent epitactic magmatic overgrowths (Fig. 2.4A). Superimposed on the potential magmatic normal zoning is a second normal zoning resulting from of diffusive exchange along grain boundaries and micro-cracks.

(ii) CG2/TT2. The alternating, concentrically zoned, texture of the unusual CG2b/TT2 grain (Fig. 2.2C), and the subhedral to euhedral shape, as well as the chemical oscillatory zoning of all other CG2b/TT2 grains (Fig. 2.2B, 2.4C), strongly supports a primary magmatic origin, whereas the origin of the normally zoned CG2a/TT2 grains is

less clear, and may be peritectic, primary magmatic, or a combination (with epitactic overgrowths on peritectic grains). However, both types of cordierite show similar compositions and occur moreover in single rock samples. A possible explanation is that some initially (maybe weakly) oscillatory zoned grains have lost their zoning by diffusion, but we do not see a range of oscillatory-zoned cordierites with high- and low-amplitude oscillations. Another possible explanation is that magma mixing events were localized, and that the compositional changes were recorded only by few crystals, namely CG2b/TT2 grains. If so, the different cordierite types must have been spatially homogenized after growth, during ascent or final emplacement of the magma, because evidence for compositional variation caused by magma mixing or mingling on the scale of a hand specimen is lacking. A third possible explanation may be that only CG2b/TT2 cordierite has been affected by magma recharge events, potentially in deeper parts of the magma chamber, whereas CG2a/TT2 grains may have crystallized near or at the emplacement level in zones that did not experience significant magma replenishment, but contamination by country-rock material. Although a true xenocrystic nature for CG2a/TT2 is unlikely, as cordierite of the country rocks has usually small to intermediate sizes, is anhedral and commonly inclusion-rich (Maillet and Clarke 1985; MacDonald 2001), CG2a/TT2 may be the result of a reaction relationship between xenoliths and the magma, and may thus have a 'foreign', peritectic origin (country rock (Bt + Qtz + Plag) ± L1→ Crd ± other minerals + L2), as suggested by abundant peritectic cordierite along the margin of wall rocks and xenoliths, and in the surrounding granodiorite, respectively (Fig. 2.7). Such a 'xenocrystic birth' of CG2a/TT2 is further suggested by the spatial distribution of cordierite in the Halifax Pluton in zones that roughly parallel the margin of the pluton, independent of the rock unit (Fig. 2.1B) (In subsequent Chapters 3,4, and 5, I suggest that CG2a/TT2 is primary magmatic (pages 61, 88, and 140). The results of my experimental study (Chapter 3) show that CG2a/TT2 in the SMB may be of partially foreign origin, with cordierite components partially derived from metapelitic country rocks). However, most of the CG2a/TT2 cordierites appear to have crystallized from the SMB magmas with little or no contribution from exposed country-rock material (Chapter 4). Strikingly, these zones occur 1-5 kilometres away from the metasedimentary contact, in rocks with lower percentages of xenoliths (MacDonald 2001), but perhaps with higher percentages of xenocrystic/peritectic crystals than the marginal units. In the Musquodoboit Batholith, however, cordierite shows no obvious relationship to the margin of the batholith, but is most abundant in several irregular zones (MacDonald and Clarke

1985), which may either represent zones or layers of a relatively cordierite-rich magma, or contaminated near-roof zones of the granite (Fig. 2.1C).

(iii) CG3a/TT3. The hypidiomorphic to idiomorphic grain shapes of CG3a/TT3, and comparable grain sizes to the other rock-forming minerals of the aplites, suggest former equilibrium with the melt, and thus most likely, a primary magmatic origin. The reverse zoning of cordierite and coexisting garnet are probably a result of growth during pressure quenching, but the details of the reaction mechanism are not yet clear.

(iv) CG3b/TT4. Textural relationships and the grain shape of CG3b/TT4 indicate a primary magmatic origin. The lack of compositional zoning indicates crystallization from a homogeneous reservoir.

(v) CG4/TT5. The anhedral grain shape of CG4/TT5 and its abundant quartz inclusions, which have similar grain shapes but slightly smaller grain sizes than the quartz grains of the surrounding granitic matrix, may be explained if cordierite consumed all phases except quartz (e.g., Bt ± Kfs ± Pl± L + Qtz → Crd + Qtz), but we do not see evidence for a reaction between cordierite and the other phases. The most likely explanation is thus that cordierite crystallized from a melt, where quartz was already present. Biotite, and in cases K-feldspar, show similar anhedral textures to cordierite, indicating that these phases may have crystallized together with cordierite, whereas the large grain size of cordierite and biotite (±K-feldspar) suggests the production or growth of only few nuclei.

The analysis of additional samples from the various units, and the analysis of trace elements such as Be, Cs, Li, B, as well as H_2O and CO_2,or isotopic analysis, were beyond the scope of this study, but may help to further constrain the crystallization conditions of the various cordierites investigated (e.g., Harley et al. 2002; Evenson and London 2003).

2.8 Summary and Conclusions

We have considered several textural (grain size, grain shape, inclusion relations) and chemical (chemical composition, chemical zoning) criteria for classifying and determining the origin of cordierite in a given rock, and have examined in detail zoning patterns and possible explanations for normal, oscillatory, and reverse zoning in cordierite from various units of two related peraluminous batholiths. We believe that grain shape and inclusion relationships are the most useful criteria with which to determine the origin of cordierite; however, chemical zoning appears (at least in our sample set) to be the most reliable criterion with which to discriminate different cordierite populations, and to detect

the crystallization, and post-crystallization history, of the cordierite, and the underlying magma chamber processes in detail.

Using a combination of key characteristics, we tentatively conclude that (i) type CG1/TT1 and CG2a/TT2 cordierite grew in a peritectic reaction between country rocks and melt; and (ii) type CG2b/TT2, CG3a/TT3, CG3b/TT4, and CG4/TT5 cordierite crystallized from the main magma. Because cordierite grains in granites may have multiple origins, only a detailed examination of combined textural and chemical criteria can lead to a correct determination of their origin and crystallization history; apparent magmatic grains may be foreign, and thus contamination of the granite by country rocks may be greater than expected. A more refined and combined consideration of all zoned and unzoned minerals from the batholiths is required to put better constraints on the suggested magma chamber processes, and their importance and timing in the evolution of the batholiths.

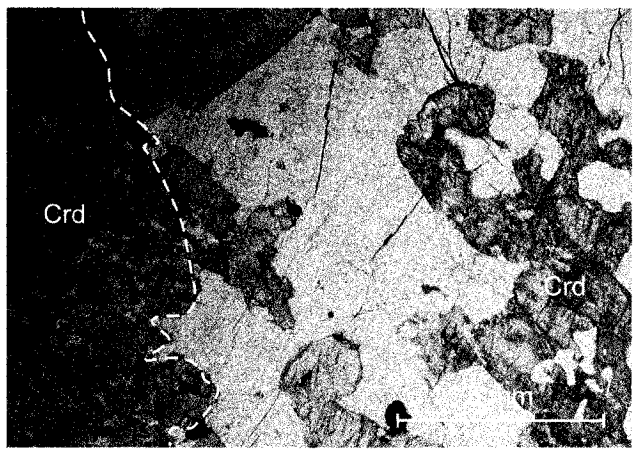

Figure 2.7: Photomicrograph (plane polarized light), showing the contact (stippled line) between fine-grained country rocks of the Meguma Group (left) and coarse-grained biotite granodiorite (right) (Sample E 433). Cordierite (now highly pinitized) in the granites may have formed in a peritectic reaction along the boundary between country rock and the surrounding magma (In subsequent Chapters 3,4, and 5, I suggest that CG2a/TT2 is primary magmatic (pages 61, 88, and 140). The results of my experimental study (Chapter 3) show that CG2a/TT2 in the SMB may be of partially foreign origin, with cordierite components partially derived from metapelitic country rocks. However, most of the CG2a/TT2 cordierites appear to have crystallized from the SMB magmas with little or no contribution from exposed country-rock material (Chapter 4)). The crystals within the granodiorite show features similar to CG2a/TT2, and may indicate how a significant proportion of cordierite from the South Mountain and Musquodoboit batholiths may have formed. The highly altered nature of the country-rock and adjacent cordierite prohibited their chemical analysis.

2.9 Acknowledgements

D.B. Clarke acknowledges the support of an NSERC research grant that made this study possible; Saskia Erdmann acknowledges the support of a Killam Scholarship at Dalhousie University. We thank John Clemens for generously sharing his view on the origin of the reversely zoned cordierite, Ron Vernon for his many helpful comments on an earlier draft of this manuscript, and Simon Harley and an anonymous reviewer for their many constructive contributions towards improving the manuscript. We also thank Gordon Brown for the polished thin sections and Robert MacKay and Patricia Stoffyn for assistance at the Dalhousie Regional Electron Microprobe Laboratory.

CHAPTER 3

Contamination of Granitic Magma by Metasedimentary Country-rock Material: an Experimental Study

3.0 Preamble

The study presented in this chapter has been accepted for publication in a special volume of *The Canadian Mineralogist*, and is the result of a collaboration between S. Erdmann, D. London, G.B. Morgan VI, and D.B. Clarke. I have designed the study, carried out 22 of the 26 experiments, contributed to all mineral chemical analyses, prepared all Figures and Tables, and wrote the manuscript. D. London G.B. Morgan VI supervised me during the experiments, carried out the additional four experiments, actively discussed the results with me during and subsequent to my stay at Oklahoma University, and commented on the manuscript. G.B. Morgan also technically assisted all the imaging and the quantitative microprobe analyses. D.B. Clarke contributed to discussions throughout the course of this study and thoroughly revised the manuscript.
The textural-chemical study of various cordierite types from the South Mountain and Musquodoboit batholiths presented in the previous chapter has shown that various crystals of one mineral type in the granites may have different origins. Moreover, the investigation revealed that cordierite occurring in the granites may have formed through partial melting of metapelitic Meguma Group rocks in contact with SMB magmas. This experimental study helps to characterize the reaction relations between country rocks and SMB magmas and, more importantly, permits the estimation of country-rock melt fractions and the determination of country-rock melt compositions, neither of which has survived in the natural record.

3.1 Abstract

Melting experiments involving metasediments and granitic rocks provide an opportunity to study reactions and products of granite contamination by assimilation of metasedimentary material. The main products of melting metasedimentary rocks from the Meguma Group for 4-26 days, at 700 or 800 °C, 200 MPa, at water-undersaturated or water-saturated conditions, are new magmatic solids such as cordierite and magnetite, and a highly peraluminous partial melt. Quartz, biotite, and plagioclase are the dominant relict phases. Melting of metasedimentary rocks from the Meguma Group

under similar conditions, but juxtaposed against a granodiorite from the South Mountain Batholith (SMB), or a synthetic haplogranite glass, have run products similar to the experiments melting metasedimentary rocks or the SMB granodiorite only, except for a zone along the contact of the two materials, where melt fractions are higher, and magmatic cordierite or K-feldspar may be more abundant than in the rest of the charge. The experiments at 800 °C produce melt fractions of >50 vol% with the highest melt fractions occurring along the contact between metasedimentary and granitic material, whereas in the 700 °C experiments, only the metapelitic rocks of the Meguma Group in contact with the haplogranite generate a significant fraction of partial melt (~50 vol%). These results suggest that at temperatures of ≥800 °C, assimilation of Meguma Group country-rock material through partial melting may have been an important process in the SMB. At temperatures of ≤700 °C, minor partial melting may have caused disintegration of Meguma Group country-rocks rather than their assimilation. At both temperatures, new magmatic phases, partly composed of country-rock material, and partly composed of magmatic material, may have formed along the contact between metasedimentary rocks and SMB host magmas.

3.2 Introduction

Contamination of magmas by country-rock material is recorded in many igneous bodies, but no single approach to assess the significance of country-rock contamination is entirely adequate or unique. Field data may give estimates of the abundance of country-rock contaminants in the form of visible xenoliths, and possibly in the form of distinctive foreign minerals, but most likely overlooks the presence of former country-rock partial melt, if the compositions of the country-rock partial melt and the main magma were similar (e.g., Allan and Clarke 1981; Maillet and Clarke 1985; Bouloton 1992; Barbey et al. 1999; Tepley and Davidson 2003; Erdmann et al. 2004; Gottesmann and Förster 2004; Clarke et al. 2005; Clarke in press). Whole-rock geochemical data can constrain minimum and maximum amounts of country-rock contamination (e.g., DePaolo 1981; Bohrson and Spera 2003; Clarke et al. 2004), but the number of assumptions in such modelling is large, and the uncertainty of the estimates is high (e.g., not knowing the original composition of the magma or the contaminant). Experimental data cannot directly constrain the amount of contamination in magmatic rocks, but may provide information on the efficiency of melting and dissolution in specific systems, as well as

mode, texture, and composition of various contaminants (e.g., xenocrysts and partial melt).

In this contribution, we describe experiments designed to better understand the extent of country-rock contamination in the granitic South Mountain Batholith (SMB) of southern Nova Scotia, as well as the nature of the country-rock contaminants. The experiments were carried out at 700 and 800 °C, using a SMB granodiorite and a synthetic haplogranite as host magmas, and metapelitic and metapsammitic rocks of the adjoining Meguma Group as contaminants.

3.3 The South Mountain Batholith

The South Mountain Batholith (SMB) consists of peraluminous granodiorite, monzogranite, leucomonzogranite, and leucogranite (e.g., McKenzie and Clarke 1975; MacDonald 2001), intruding metapelitic to metapsammitic rocks of the Meguma Group (Schenk 1970, 1997; Clarke et al. 1988; Hicks et al. 1999). Chemical, isotopic, and textural evidence for contamination of the SMB by metasedimentary country rocks exists, but a detailed and unequivocal characterization of all country-rock contaminants and their relative and absolute significance in the SMB rocks is still pending (e.g., Jamieson 1974; Clarke and Halliday 1980; Allan and Clarke 1981; Maillet and Clarke 1985; Clarke and Chatterjee 1988; Clarke et al. 1988, 2004; Tate 1994; MacDonald 2001; Erdmann et al. 2004; Carruzzo and Clarke 2005; Clarke and Erdmann 2005; Samson and Clarke 2005). The abundances of xenoliths in the SMB suggest a higher degree of contamination for the marginal rocks of the batholith, and a lower degree of contamination for the more central rocks of the intrusion (e.g., Jamieson 1974; MacDonald 2001; Clarke and Erdmann 2005). On the other hand, whole-rock Sr-Nd isotopic geochemical data suggest a higher degree of contamination by Meguma Group country-rocks for the most evolved and typically more central rocks of the batholith (leucogranites) than for the more primitive and typically more marginal rocks (granodiorites) of the SMB (Clarke et al. 2004). One possible explanation for these apparently contradictory results is that country rocks of the Meguma Group are progressively more strongly assimilated from the margin toward the center of the SMB, leaving little macroscopically visible evidence for contamination in the most evolved rocks, but a whole-rock chemical signature indicating a high degree of contamination.

3.4 *Starting Materials and Methods*

3.4.1 Starting Materials

The starting materials were cores and powders of metapelitic and metapsammitic rocks (Meguma Group, Nova Scotia), powders of a granodiorite (SMB, Nova Scotia) and a synthetic, anhydrous haplogranitic glass (Corning Lab Services, New York, USA). The Meguma Group samples are of hornfels facies metamorphic grade from outcrops within of the SMB contact aureole (Samples E 430-Exp and E 450); the granodiorite is from the Five Mile Lake pluton of the SMB (Sample E 430-Exp2). Table 3.1 records their mineralogy as well as bulk chemical compositions.

Table 3.1: Mineralogy (vol%) and composition (wt%) of starting materials

Material	Metapelite	Metapsammite	Granodiorite	Haplogranite*
Quartz	12	50	28	32**
Plagioclase	10	25	40	38**
K-feldspar	-	10	20	30**
Biotite	10	12	12	-
Cordierite$	20	1	-	-
Muscovite	40	2	-	-
Chlorite	5	-	-	-
Andalusite	3	-	-	-
SiO_2	58.51	74.67	67.73	77.69
TiO_2	1.04	0.55	0.87	0.01
Al_2O_3	23.72	11.70	15.47	13.02
FeO#	4.62	3.82	5.04	0.02
MnO	0.07	0.05	0.08	0.00
MgO	1.68	1.38	1.68	0.01
CaO	0.27	1.32	2.62	0.01
Na_2O	1.26	2.40	3.36	4.60
K_2O	3.89	2.06	2.98	4.78
P_2O_5	0.08	0.12	0.25	n.d.
L.O.I.	4.74	0.74	0.50	0.00
Total	99.87	98.81	100.57	100.14
ASI##	3.50	1.36	1.14	1.00
X_{Mg}@	0.27	0.27	0.25	-
K/(K+Na)	0.76	0.46	0.47	0.51

Reported mineralogy denotes major mineral assemblage; * data from Acosta-Vigil et al. 2002; ** normative assemblage; $ altered in metapelitic starting material; # total Fe as FeO; ## ASI = molar $[Al_2O_3/(CaO+NaO+K_2O)]$; @ X_{Mg} = Mg/(Mg+Fe).

The rock powders were crushed in a jaw crusher, and then pulverized in a tungsten carbide swing mill to a grain-size of typically <20 μm, but several grains of ≥100 μm remained. The haplogranitic glass was ground in an agate mortar with distilled water. Rock cores, ca. 1.7 mm in diameter and ca. 3-4 mm in length, were drilled normal to the foliation plane of the metapelitic and metapsammitic rocks, using a diamond core bit.

3.4.2 Experimental Methods

In one set of experiments (Table 3.2), hereafter referred to as melting experiments, gold capsules were loaded with deionized, ultrafiltered H_2O, and (i) granodiorite (GD), metapelite (PEL), or metapsammite (PSA) powder, or (ii) with metapelite or metapsammite cores. In a second set of experiments (Table 3.3), hereafter referred to as contamination experiments, gold capsules were loaded with deionized, ultrafiltered H_2O, (i) granodiorite or haplogranite powder, as well as (ii) metapelite or metapsammite cores. We added H_2O in excess to most of our experiments to facilitate melting, and therefore, to form melt pockets large enough to meaningful analyze by EMPA, ideally using a spot size of 20 μm (Morgan and London 1996, 2005). To prevent loss of added water during preparation, the capsules were frozen during welding; weighing before and after welding ensured that volatilization of the added H_2O did not take place. The melting experiments were heated to ~185 °C after welding for >1 h to check for leaks, and to distribute H_2O throughout the capsule. The contamination experiments were not heated prior to the experiment, because we wanted to avoid redistribution of cores and powders within the capsules.

The experiments were performed at the University of Oklahoma in cold-seal vessels at 700 and 800 °C, 200 MPa, and for ~4 to 23 days (Table 3.2, 3.3). The gold capsules were pressurized at room temperature. Once pressurized, the temperature was raised to the experimental temperature within ~30 min. The temperature was measured internally using chromel-alumel thermocouples; the pressure was monitored with a Heise Bourdon gauge. Measured variations in temperature and pressure were <2 °C, and ≤2 MPa; uncertainties are <10 °C, and <10 MPa. The oxygen fugacity imparted by the composition of the NIMONIC105® vessels is 0.5 log units below the Ni-NiO buffer (Wolf et al. 1994), but internal reactions involving carbon (graphite) resulted in more reduced conditions at least early in the duration of these experiments.

The experiments were quenched isobarically in air to <400 °C at a rate of ~200 °C/min; cooling to room temperature took ~30 min. Capsules were then weighed to test for leaks

or weight gain (all capsules gained weight as a result of Ni-diffusion from the vessels into the Au capsule), and were punctured to check for H_2O saturation. Capsules were sliced in half longitudinally, perpendicular to the foliation of the metapelite or metapsammite cores, using a Buehler IsoMet slow-speed saw, and then half the charge was mounted in Buehler EpoThin epoxy. Samples were ground under water using Al_2O_3-impregnated lapping films with grit sizes from 60 to 3 μm, and finally polished to a grit size of 0.25 μm using alumina suspended in water.

Table 3.2: Characteristic properties and origins of the mineral assemblage of the melting and contamination experiments

Mineral	Grain size	Grain shape	Inclusions	Origin
Bt	~ 30-200 μm	ah-sh	Mgt, Zrn, Mnz,	CR crystal
Crd1	~ 50-200 μm	sh	-	CR crystal
Crd2	< 100 μm	sh-eh	Mgt, Sil or Crn	new magmatic phase
Sil or Crn	< 5 μm	ah	-	new magmatic phase
Kfs1	~ 50-200 μm	sh	Qtz	CR crystal
Kfs2	< 200 μm	skeletal to eh	glass, Mgt, Sil or Crn	new magmatic phase
Mgt	< 30 μm	sh-eh	-	new magmatic phase
Opx	< 100 μm	sh-eh	-	new magmatic phase
Pl1	~ 50-300 μm	sh	-	CR crystal
Pl2	< 300 μm	spongy to skeletal	-	new magmatic phase
Qtz	~ 50-300 μm	sh	-	CR crystal

Mineral abbreviations after Kretz (1983); ah = anhedral; sh = subhedral; eh = euhedral; CR = country rock

Table 3.3: Starting materials (100 wt%), temperature (T [°C]), duration (D [days]), and run-products (vol%) of the melting experiments

Run no.	Starting materials*	T (°C)	D (d)	L	Qtz	Bt	Pl1	Pl2	Crd1	Crd2	Mgt	Sil or Cm	Kfs1	Kfs2	Opx	Ms
GD-5	88.9 GD powder + 11.1 H_2O	800	4	70	2	6	3	15	-	1	2	<1	-	-	-	-
GD-3	96.3 GD powder + 3.7 H_2O	800	14	50	12	10	15	10	-	1	2	<1	-	-	-	-
GD-4	89.3 GD powder + 10.7 H_2O	800	14	70	2	6	3	15	-	1	2	<1	-	-	-	-
PEL-2	99.5 PEL powder + 0.5 H_2O	800	4	55	5	3	1	<1	-	20	2	14	-	-	-	-
PEL-1	89.1 PEL powder + 10.9 H_2O	800	4	70	2	1	1	<1	-	20	2	4	-	-	-	-
PEL-4	99.5 PEL powder + 0.5 H_2O	800	14	55	5	3	1	<1	-	20	2	14	-	-	-	-
PEL-3	89.3 PEL powder + 10.7 H_2O	800	14	70	2	1	1	<1	-	20	2	4	-	-	-	-
PEL-18	99.5 PEL powder + 0.5 H_2O	700	23	-	30	-	-	-	30	-	3	-	37	-	-	-
PEL-19	89.9 PEL powder + 10.1 H_2O	700	23	50	3	1	1	1	-	30	1	5	-	8	-	-
PEL-14	92.6 PEL core + 7.4 H_2O	800	14	70	2	1	1	<1	-	20	2	4	-	-	-	-
PSA-1	99.5 PSA powder + 0.5 H_2O	800	4	3	50	12	20	2	1	<1	1	-	10	-	-	-
PSA-2	89.2 PSA powder + 10.8 H_2O	800	4	75	8	3	1	1	1	6	2	-	-	-	3	-
PSA-4	88.8 PSA powder + 11.2 H_2O	800	17	75	8	3	1	1	1	6	2	-	-	-	3	-
PSA-3	99.5 PSA powder + 0.5 H_2O	800	17	3	50	12	20	2	1	<1	1	-	10	-	-	-
PSA-13	99.5 PSA powder + 0.5 H_2O	700	23	-	50	12	25	-	1	-	-	-	10	-	-	2
PSA-14	90.2 PSA powder + 9.8 H_2O	700	23	30	40	12	15	2	-	-	1	-	-	-	-	-
PSA-7	92.7 PSA core + 7.3 H_2O	800	14	50	28	8	2	2	1	5	2	-	-	-	2	-

All experiments were run at P = 200 MPa. * Starting materials do not appear in the order they were loaded into the gold capsules. Total H_2O is H_2O added, and H_2O adsorbed to the starting materials. The amount of adsorbed H_2O was determined for granodiorite powder (~ 0.5 wt%), haplogranite powder (~ 0.2 wt%), metapelite powder (~ 0.5 wt%), and metapsammite powder (~ 0.5 wt%). H_2O was always loaded first, then rock powder or rock core. T= temperature (in °C); D = duration (in days); L = liquid; GD = granodiorite; PEL = metpelitic material; PSA = metapsammitic material. Mineral abbreviations after Kretz (1983).

3.4.3 Experimental Rationale

Our rationale for the melting experiments was to determine the amount and composition of the solid products of reaction and especially of partial melt in the pure granodiorite, metapelite, and metapsammite systems. The objective of the contamination experiments was to specifically determine the melting reactions and reaction products, where contaminants and magma are in contact. The melting experiments using powders permit the characterization of compositions of partial melt of average granodiorite, metapelitic and metapsammitic rocks, whereas melting and contamination experiments employing metasedimentary cores in contact with granitic powders permitted the observation of textural and spatial relations that mimic those of a xenolith immersed in magma.

We have chosen the metapelitic and metapsammitic rocks as starting materials for the contaminants because they are potentially the most important country-rock contaminants in the SMB. The granodiorite was used as a starting material for the magma, because we have field evidence for the interaction between former SMB magmas and the metapsammitic and metapelitic country-rocks, and we wanted to mimic the reactions of the natural examples. The synthetic haplogranitic glass was used as a granitic starting material, because we wanted to explore if, or how, reaction relations between metasedimentary rocks and a granitic magma are affected by a lower ASI value (molar $[Al_2O_3/(CaO+NaO+K_2O)]$) than that of the granodiorite.

3.4.4 Analytical Methods

Back-scattered electron (BSE) imaging, energy-dispersion X-ray analysis (EDXA), and wavelength-dispersion spectroscopy (WDS) were performed with a Cameca SX50 electron microprobe at the University of Oklahoma. Petrographic study was accomplished by BSE imaging, coupled with EDXA using an accelerating voltage of 20 kV and a beam current of 5 nA. Although BSE imaging was performed mostly prior to quantitative analysis, care was taken not to irradiate the sample for extended periods, nor at high magnification (raster were > 100 x 100 μm), to prevent migration of alkalis in glass. Glass and crystals were analyzed by WDS. Natural and synthetic crystalline materials were used as primary standards, and data reduction employed the PAP procedure (Pouchou and Pichoir 1985). To minimize alkali migration and attendant changes to the count rates, glass domains were analyzed using two beam conditions (Morgan and London 1996, 2005). An initial 20 kV, 2 nA beam was used for determining concentrations of Na, Al, Si, K, and Ca (concentrations of Na and Al were determined

first and concurrently); counting times were 30 s on the peak. A subsequent analysis with a 20 kV, 20 nA beam was used for determining the concentrations of all other elements, also using 30 s counting times. For the melting experiments, glass compositions were acquired on random spots across the sample. For the contamination experiments, glass compositions were determined along a point profile perpendicular to the contact between metasedimentary and the granitic material, across the whole length of the sample. If possible, a 20 μm defocused spot was used for analysis, but small pods of melt in a few experiments (PEL-1,2,6,13,14,18,19) required the use of a 5 μm spot, where SiO_2, Al_2O_3, and Na_2O concentrations were corrected by reference to a hydrated glass (~ 6.6 wt% H_2O; Acosta-Vigil et al. 2003; Morgan and London 2005). Glass pods in the metapelite melting experiments PEL-3 and PEL-4 were too small for quantitative analysis, even at a 5 μm spot size. Crystals were analyzed using a 20 kV, 20 nA beam with 3 μm spot size, and counting times of 30 s for all elements.

3.5 Results

3.5.1 Run Products

3.5.1.1 Melting of Starting Materials

Important products of the melting experiments involving granodiorite powder, or powder or cores of metapelitic or metapsammitic rocks, are partial melt, quartz, plagioclase (Pl1, Pl2), biotite, cordierite (Crd1, Crd2), magnetite, ± K-feldspar (Kfs1, Kfs2), ± ortho-pyroxene, and ± sillimanite or corundum. Figure 3.1 shows the characteristic run products, Table 3.2 summarizes the characteristic properties of the run products, and Table 3.4 gives the run products and their modal proportions (Table 3.1 gives the mineralogy of the starting materials).

Melting experiments at 800 °C with ~11 wt% H_2O added (PSA-2,4; PEL-1,3; GD-4,5) result in a high degree of partial melting (≥70 vol% melt; Fig. 3.2). Melting of granodiorite powder at 800 °C with ~4 wt% H_2O added (GD-3), melting of metapelite powder at 800 °C with no H_2O added (PEL-2,4), and melting of metapelite powder at 700 °C with ~10 wt% H_2O added (PEL-19), yields intermediate fractions of melt (~50 vol%). Melting of metapsammite powder at 700 °C and ~10 wt% H_2O added (PSA-14) produces intermediate to low amounts of partial melt (~30 vol%), and melting of metapsammite powder at 800 °C with no H_2O added (PSA-1,3), results in a low degree of melting (~3 vol%). Experiments at 700 °C with no H_2O added (PEL-18,13) remain unmelted.

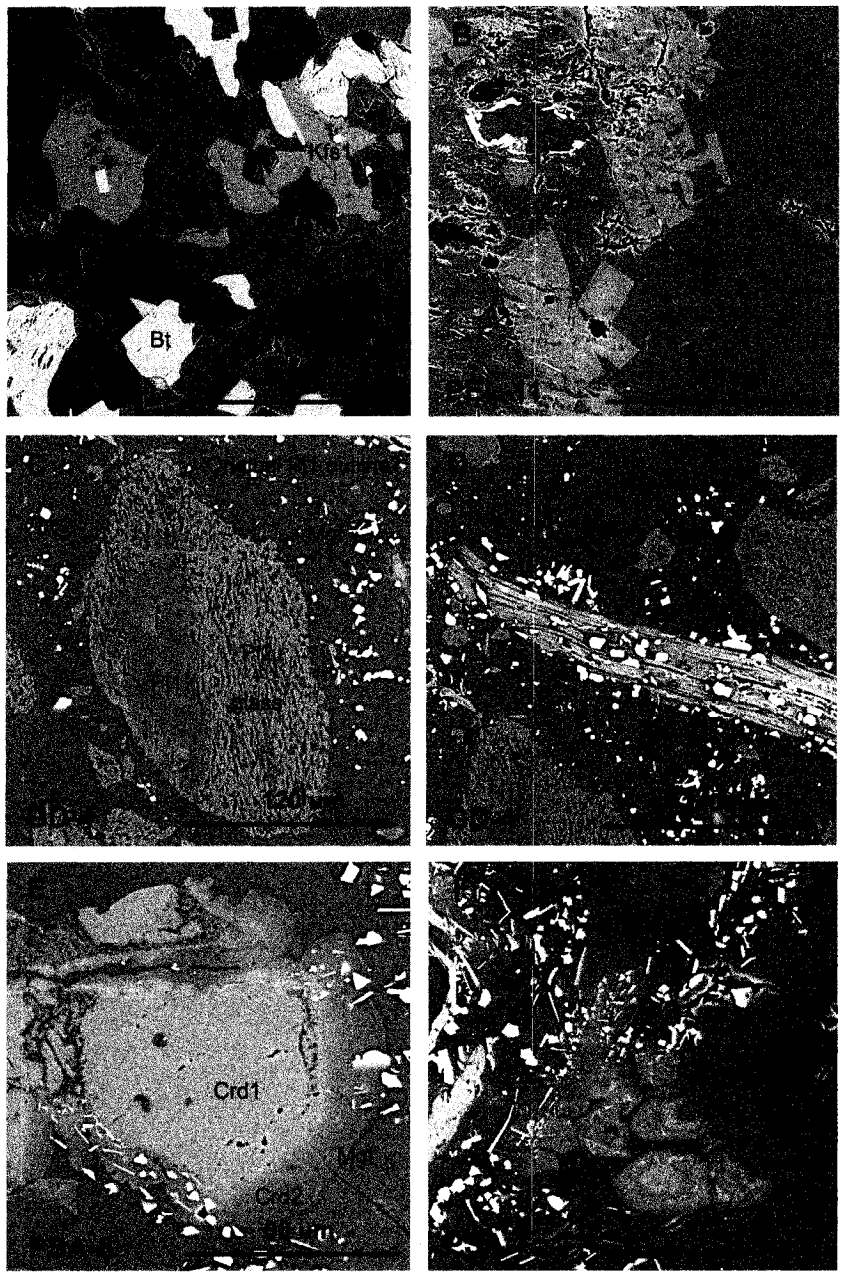

Figure 3.1: BSE images showing characteristic mineral textures. Pl1, Kfs1, Qtz, Bt, and Crd1 are crystals of the original country-rock assemblage. Sil or Crn, Kfs 2, Pl2, Mgt, and Crd2 are newly formed magmatic crystals. Their characteristic properties are in Table 3.2. A) Subhedral, inclusion-poor, unzoned Kfs1, Pl1, quartz, and biotite. Photomicrograph of unmelted metapsammite starting material. B) Skeletal, inclusion-rich, zoned Kfs2. Inclusions are glass, magnetite, and sillimanite or corundum (Sil or Crn). PEL-11 = 700 °C melting experiment. C) Pl1 grain (core), rimmed by spongy Pl2. GD-4 = 800 °C melting experiment. D) Anhedral to subhedral biotite with abundant magnetite and glass along cleavage planes. E) Subhedral grain of inclusion-poor, unzoned Crd1 (core) with a thin overgrowth of Crd2. Marginal inclusions are magnetite. PSA-8 = 800 °C contamination experiment. F) Euhedral to subhedral, oscillatory zoned Crd2 in a matrix of glass and magnetite. PSA-7 = 800 °C melting experiment.

Table 3.4: Starting materials (100 wt%), temperature (T [°C]), duration (D [days]), and run-products (vol%) from the contact zones of the contamination experiments

Run no.	Starting materials*	T (°C)	D (d)	CZ	L	Qtz	Bt	Pl1	Pl2	Crd1	Crd2	Mgt	Sil or Cm	Kfs1	Kfs2	Opx	Ms
PEL-8	49.2 PEL core + 45.6 GD powder + 5.2 H_2O	800	16	PEL	75	2	1	1	<1	-	17	2	1	-	-	-	-
				GD	94	-	-	-	-	-	5	1	-	-	-	-	-
PEL-9	45.7 PEL core + 46.8 GD powder + 7.5 H_2O	800	16	PEL	75	2	1	1	<1	-	17	2	1	-	-	-	-
				GD	94	-	-	-	-	-	5	1	-	-	-	-	-
PEL-12	46.2 PEL core + 46.0 GD powder + 7.8 H_2O	700	16	PEL	60	5	5	1	<1	-	25	2	5	-	-	-	2
				GD	40	15	15	15	12	-	1	2	<1	-	-	-	-
PEL-10	46.1 PEL core + 46.1 HG powder + 7.8 H_2O	800	14	PEL	60	5	2	1	<1	-	20	2	10	-	-	-	-
				HG	100	-	-	-	-	-	-	-	-	-	-	-	-
PEL-11	46.4 PEL core + 46.5 HG powder + 7.1 H_2O	700	14	PEL	50	5	3	1	<1	-	5	2	15	-	20	-	-
				HG	100	-	-	-	-	-	-	-	-	-	-	-	-
PSA-8	46.0 PSA core + 46.0 GD powder + 8.0 H_2O	800	14	PSA	75	8	3	1	1	1	6	2	-	-	-	3	-
				GD	96	-	2	-	1	-	-	1	-	-	-	-	-
PSA-9	46.2 PSA core + 46.0 GD powder + 7.8 H_2O	700	14	PSA	10	45	12	19	3	1	<1	1	-	8	-	-	-
				GD	30	20	15	15	10	-	1	1	<1	1	-	-	-
PSA-10	47.1 PSA core + 45.7 HG powder + 7.2 H_2O	800	14	PSA	60	15	5	3	4	1	6	2	-	3	-	1	-
				HG	100	-	-	-	-	-	-	-	-	-	-	-	-
PSA-12	45.5 PSA core + 45.1 HG powder + 9.4 H_2O	700	14	PSA	10	48	12	18	2	1	<1	1	-	8	-	-	-
				HG	100	-	-	-	-	-	-	-	-	-	-	-	-

All experiments were run at P = 200 MPa. * Starting materials do not appear in the order they were loaded into the gold capsules. Total H_2O is H_2O added, and H_2O adsorbed to the starting materials. H_2O was always loaded first, then the rock powder, and finally the rock core. The amount of adsorbed H_2O was determined for granodiorite powder (~ 0.5 wt%), haplogranite powder (~ 0.2 wt%), metapelite powder (~ 0.5 wt%), and metapsammite powder (~ 0.5 wt%). T= temperature (in °C); D = duration (in days); CZ = contact zone; L = liquid; PEL = metpelitic material; GD = granodiorite; HG = haplogranite; PSA = metapsammitic material. Mineral abbreviations after Kretz (1983).

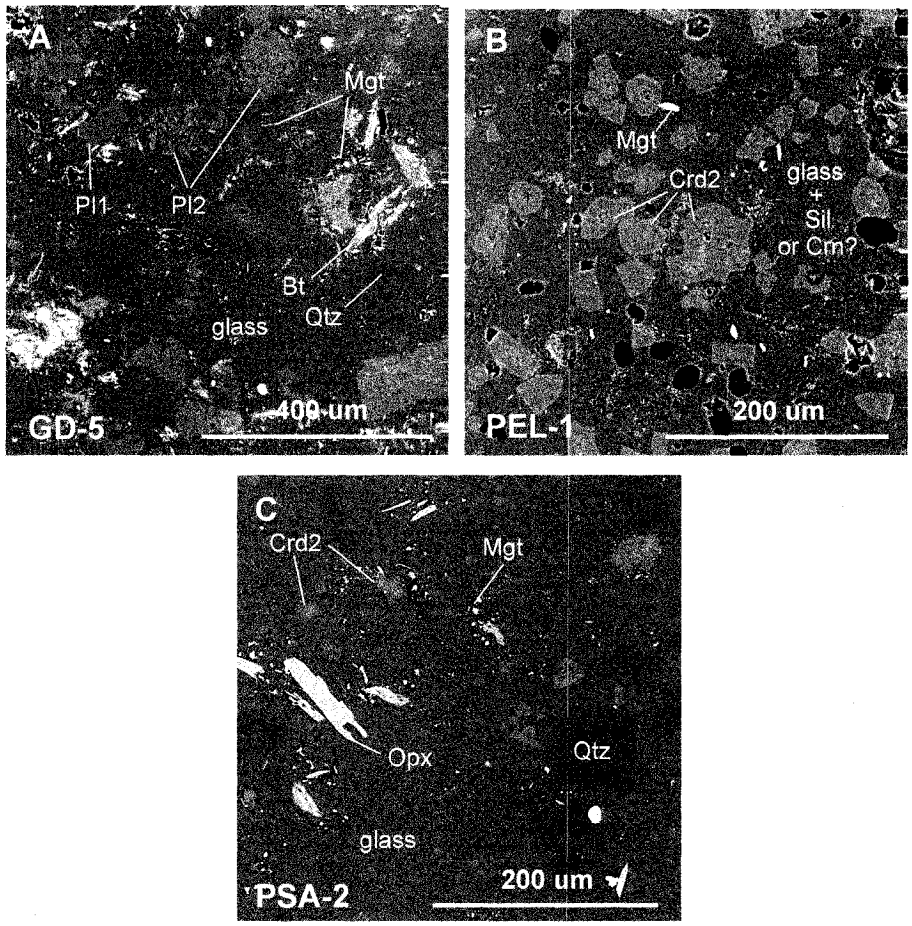

Figure 3.2: BSE images showing run products of powder melting experiments with the highest melt fractions (800 °C). A) Melting of granodiorite powder (GD-5) with 11.1 wt% H_2O added produces ~70 vol% glass. B) Melting of metapelite powder (PEL-1) with 10.9 wt% H_2O added produces ~70 vol% glass. C) Melting of metapsammite powder (PSA-2) with 10.8 wt% H_2O added produces ~75 vol% glass. GD = granodiorite, PEL = metapelite, PSA = metapsammite. Mineral abbreviations after Kretz (1983).

Melting of metapelite or metapsammite cores at 800 °C (PEL-6,14; PSA-6,7) results in similar run products and similar or lower fractions of melt than the equivalent metapelite or metapsammite powder melting experiments.

Chlorite, muscovite, K-feldspar (Kfs1), plagioclase (Pl1), quartz, and biotite are the phases that are dominantly consumed in the melting reactions. New cordierite (Crd2), plagioclase (Pl2), magnetite, ± orthopyroxene, and ± sillimanite or corundum form in the melting experiments at 800 °C, whereas cordierite (Crd2), plagioclase (Pl2), magnetite, ± K-feldspar (Kfs2), and ± sillimanite or corundum form in the melting experiments at 700 °C. Ellipsoidal vesicles are abundant in the melting experiments involving

metapelites, but rare in the melting experiments involving granodiorites or metapsammites.

3.5.1.2 Contamination Experiments

Contamination experiments with metasedimentary cores in contact with either granodiorite or haplogranite powder have run products similar to those of the melting experiments using powders or cores only, except for a ≤900 μm wide zone along the contact of the two materials, where melt-fractions, mineral assemblages, or modal abundances are different from the rest of the charge. In this section, our descriptions focus on the characteristics of these contact zones, whereas Table 3.4 summarizes the run products and their modal proportions.

Melting of a metapelite core in contact with granodiorite powder produces a zone of high melt-fraction along the original contact of the two materials that is asymmetrical, extending further into the granodiorite than into the metapelitic material (PEL-8,9,12; Fig. 3.3 A,B). In the 800 °C experiment, the contact zone is ~900 μm wide (Fig. 3.3A), and in the 700 °C experiment, the contact zone is ~400 μm wide (Fig. 3.3B). In the experiment at 800 °C, the metapelite part of the contact zone is characterized by a low abundance of sillimanite or corundum, whereas the granodiorite part of the contact zone is characterized by abundant Crd2. In the experiment at 700 °C, abundant Crd2 occurs in the metapelite part of the contact zone, whereas the mineralogy of the granodiorite part of the contact zone is similar to the mineralogy of the granodiorite elsewhere in the charge.

Melting of a metapelite core in contact with haplogranite powder at 800 °C (PEL-10; Fig. 3.3C) produces a sharp (in BSE images), and cuspate-lobate contact between the two materials, but a contact zone characterized by an increased melt fraction is not evident. Melting of a metapelite core in contact with haplogranite powder at 700 °C (PEL-11; Fig. 3.3D) results in a ~800 μm wide contact zone with an increased fraction of melt within the metapelitic material, and the occurrence of abundant Crd2 and Kfs2 along the contact between the metapelitic and haplogranitic material.

Melting of a metapsammite core in contact with granodiorite powder at 800 °C produces a ~500 μm wide zone of high melt-fraction along the original contact of the two materials that is asymmetric, extending further into the metapsammitic material than into the granodiorite (PSA-8; Fig. 3.4A). In the 700 °C experiment, employing a metapsammite core and granodiorite powder, no distinct contact zone developed (PSA-9; Fig. 3.4B).

Melting of a metapsammite core in contact with haplogranite powder at 800 °C results in a ~300 μm wide zone of high fraction of melt within the metapsammitic material (PSA-10; Fig. 3.4C). In the 700 °C experiment of a metapsammite core in contact with haplogranite powder, no characteristic contact zone developed in either the metapsammitic or the haplogranite materials (PSA-12; Fig. 3.4D).

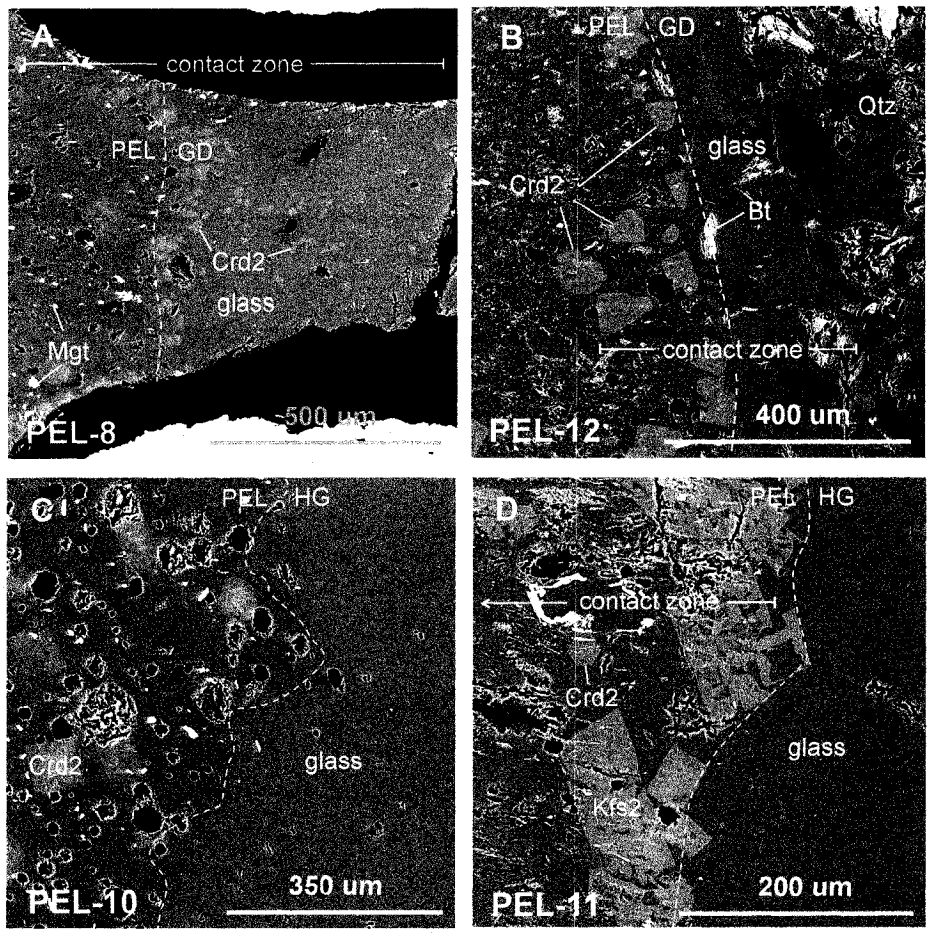

Figure 3.3: BSE images showing the contact zones of the metapelite contamination experiments. A) PEL-8, 800 °C. Contact zone in the metapelitic material is ~300 μm wide, contact zone in the granodiorite is ~600 μm wide. B) PEL-12, 700 °C. Contact zone in both materials is ~200 μm wide. C) PEL-10, 800 °C. No contact zone is visible, and the contact is cuspate-lobate. D) PEL-11, 700 °C. Contact zone in the metapelitic material is ~800 μm wide. GD = granodiorite, PEL = metapelite, HG = haplogranite. Mineral abbreviations after Kretz (1983).

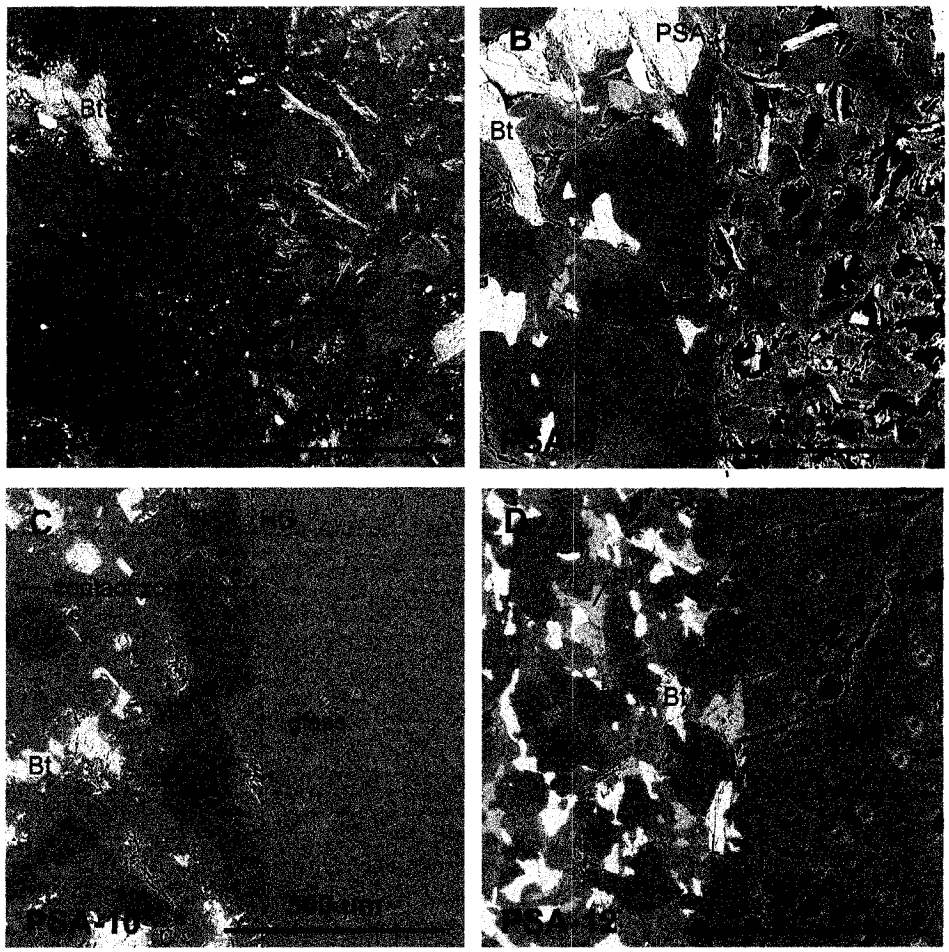

Figure 3.4: BSE images showing the contact zones of the metapsammite contamination experiments. A) PSA-8, 800 °C. Contact zone in the metapsammite material is ~300 μm wide, contact zone in the granodiorite is ~250 μm wide. B) PSA-9, 700 °C. No contact zone is visible. C) PSA-10, 800 °C. Contact zone in the metapelitic material is ~500 μm wide. D) PSA-12, 700 °C. No contact zone is visible. GD = granodiorite, PSA = metapsammite, HG = haplogranite. Mineral abbreviations after Kretz (1983).

3.5.2 Melt Compositions

3.5.2.1 Melting Experiments

Table 3.5 lists the mean compositions of silicate glass from the partial melting of granodiorite, metapelite, and metapsammite powders. Low standard deviations in the mineral chemical analyses suggest relatively homogeneous compositions, but compositionally variable boundary-layers may occur adjacent to the various solid phases, which may not have been detected given the 20 μm analytical spot size. Analyzed glasses are peraluminous, and granitic to granodioritic. Average ASI values (molar $[Al_2O_3/(CaO+NaO+K_2O])$ vary between 1.18 and 1.45, where a high ASI value for

the glass correlates with a high H_2O content, and the H_2O concentration of glass also correlates with the amounts of H_2O added to the experiments. For glass with the highest ASI values (from the metapelitic starting material), inclusions of small sillimanite or corundum crystals may have interfered with the analysis of glass, thereby increasing the measured Al-content and ASI values.

3.5.2.2 Contamination Experiments

In the metapelite-granodiorite contamination experiments, melt in the metapelitic material has a higher concentration of K, a lower concentration of Mn, Mg, and Ca, and similar concentrations of Si, Ti, Al, Fe, Mn, Na, P, and F, compared with melt in the granodiorite (PEL-9; Fig. 3.5A). The ASI and K/(K+Na) values of melts derived from the metapelitic material are higher than those of the melts derived from the granodiorite. In the metapelite-haplogranite contamination experiments, melt in the metapelitic material has higher concentrations of Ti, Al, Fe, Mn, Mg, and Ca, lower concentrations of Si, and similar concentrations of Na, K, P, and F, relative to the haplogranitic melt (PEL-10; Fig. 3.5B). The ASI value of the melt derived from the metapelitic material is higher, but molar K/(K+Na) is similar to those of the haplogranitic melt.

In the metapsammite-granodiorite contamination experiments, melt in the metapsammitic material has higher concentrations of Si and Fe, lower concentrations of Al, Mn, Mg, and Ca, and similar concentrations of Ti, Na, K, P, and F, compared to melt in the granodiorite (PSA-8; Fig. 3.5C). The ASI values and molar K/(K+Na) are approximately constant throughout the melt in both metapsammitic material and granodiorite. In the metapsammite-haplogranite contamination experiments, melt formed in the metapsammitic material has higher concentrations of Ti, Fe, Mn, Mg, Ca, P, lower concentrations of Na and K, and similar concentrations of Si, Al, and F, relative to the haplogranitic melt (PSA-10; Fig. 3.5D). The molar K/(K+Na) of the melt derived from the metapsammitic material is higher, and the ASI value is similar to that of the haplogranitic melt. The described contact zones with compositions intermediate between the two materials in mutual contact are ≤1000 μm wide for all elements except for K, which varies over the whole length of the analyzed profiles (Fig. 3.5).

Table 3.5: Compositions of silicate glasses from granodiorite, metapelite, and metapsammite melting experiments

Run	GD-3		GD-4		GD-5		PEL-1		PEL-2	PEL-14		PSA-2		PSA-4		PSA-7		PEL-19		PSA-14	
Material	Powder		Powder		Powder		Powder		Powder	Core		Powder		Powder		Core		Powder		Powder	
T (°C)	800		800		800		800		800	800		800		800		800		700		700	
H_2O (wt%)	3.7		10.7		11.1		10.9		0.5	7.4		10.8		11.2		7.3		10.1			
n	20	SD	20	SD	20	SD	4	SD	1*	15	SD	20	SD	23	SD	12	SD	9	SD	10	SD
SiO_2	72.68	0.54	69.62	0.45	69.78	1.12	67.59	0.22	72.40	71.22	0.54	72.27	0.39	73.94	0.36	73.26	0.86	70.18	0.51	71.14	0.61
TiO_2	0.15	0.03	0.16	0.02	0.14	0.03	0.24	0.04	0.23	0.24	0.05	0.17	0.02	0.16	0.03	0.16	0.02	0.11	0.02	0.09	0.01
Al_2O_3	12.56	0.18	13.40	0.19	13.13	0.34	13.43	0.14	12.72	12.09	0.20	11.62	0.20	11.37	0.11	12.13	0.46	13.13	1.15	12.02	0.18
FeO	0.61	0.07	0.61	0.04	0.58	0.04	1.41	0.05	1.03	1.31	0.06	1.50	0.07	1.23	0.03	0.88	0.07	0.68	0.07	0.55	0.07
MnO	0.06	0.01	0.06	0.01	0.06	0.01	0.04	0.02	0.02	0.03	0.01	0.02	0.01	0.03	0.01	0.03	0.01	0.02	0.01	0.03	0.01
MgO	0.42	0.03	0.64	0.02	0.66	0.04	0.15	0.01	0.33	0.13	0.03	0.47	0.01	1.23	0.05	0.52	0.03	0.05	0.01	0.16	0.01
CaO	0.88	0.07	1.53	0.06	1.43	0.11	0.32	0.05	0.08	0.33	0.04	1.20	0.09	0.41	0.02	1.34	0.10	0.38	0.04	0.80	0.03
Na_2O	2.86	0.12	3.11	0.13	2.96	0.12	1.65	0.08	1.92	1.58	0.11	2.59	0.15	2.78	0.15	3.32	0.13	1.78	0.13	2.14	0.18
K_2O	3.90	0.08	2.92	0.08	2.84	0.11	5.73	0.16	6.05	5.24	0.16	2.69	0.08	2.60	0.08	2.23	0.07	5.02	0.15	4.03	0.08
P_2O_5	0.16	0.04	0.15	0.02	0.11	0.03	0.06	0.01	0.03	0.10	0.14	0.08	0.02	0.09	0.03	0.07	0.02	0.06	0.03	0.11	0.02
F	0.13	0.09	0.09	0.06	0.11	0.07	0.19	0.09	0.15	0.13	0.06	0.14	0.09	0.15	0.09	0.16	0.08	0.25	0.08	0.13	0.09
Cl	0.03	0.01	0.02	0.01	0.01	0.01	0.00	0.00	0.02	0.02	0.02	0.01	0.01	0.01	0.01	-	-	0.01	0.01	0.01	0.01
Total	94.37	0.56	92.26	0.47	91.77	0.93	90.75	0.21	94.91	92.35	0.51	92.72	0.49	93.94	0.46	94.04	0.44	91.58	0.98	91.16	0.67
ASI	1.19		1.21		1.25		1.41		1.25	1.38		1.24		1.18		1.18		1.45		1.29	
K/(K+Na)	0.47		0.38		0.39		0.70		0.67	0.77		0.41		0.38		0.31		0.65		0.55	
H_2O	5.63		7.74		8.23		9.25		5.09	7.65		7.28		6.06		5.96		8.15		8.84	
X_{Mg}	0.02		0.02		0.02		0.06		0.04	0.09		0.06		0.05		0.03		0.13		0.33	

T = temperature; n = number of analysis; SD = standard deviation; ASI = molar $Al_2O_3/(CaO+NaO+K_2O)$; X_{Mg} = Mg/(Mg+Fe). * Glass analysis for PEL-2 was only feasible on one spot, owing to minute inclusions of Sil or Crn in the glass. The analysis has been accepted, given that the composition seems to be reasonable, compared to glass compositions of PEL-1 and PEL-14. GD = granodiorite; PEL = metpelitic material; PSA = metapsammitic material. GD = granodiorite, PEL = metapelite, PSA = metapsammite. Mineral abbreviations after Kretz (1983).

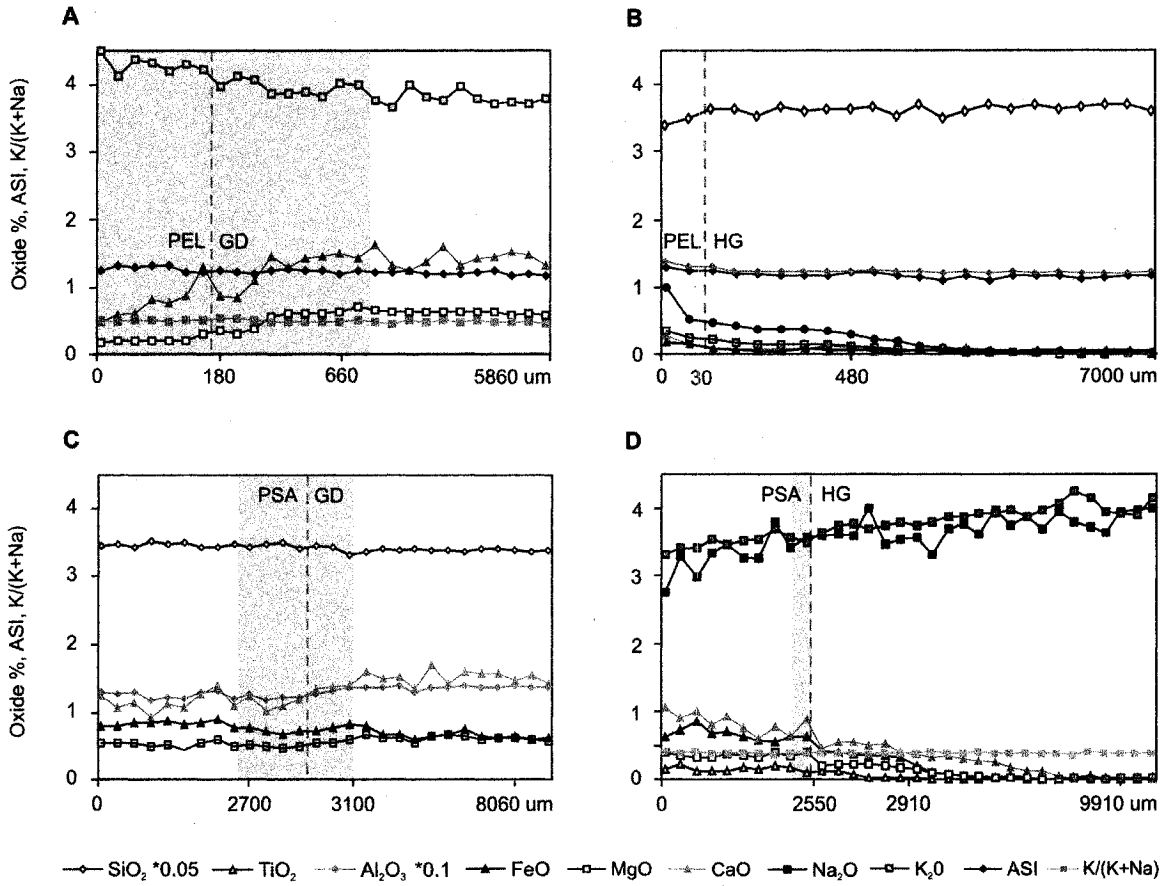

Figure 3.5: Plot of oxide concentrations, ASI, and modal K/(K+Na) versus distance for four 800 °C contamination experiments. Oxide concentrations, ASI, and modal K/(K+Na) are shown only if variable; MnO, P_2O_5, and F are not shown. A) PEL-9, metapelite – granodiorite. B) PEL-10, metapelite – haplogranite. C) PSA-8, metapsammite – granodiorite. D) PSA-10, metapsammite – haplogranite. The broken gray lines indicate the original contact between the two materials; the shaded area marks the contact zone visible in BSE mode.

3.5.3 Mineral Compositions

In Table 3.6, we list selected compositions of Pl1, Pl2, Kfs1, Kfs2, biotite, and orthopyroxene, as well as average X_{An}, X_{Or}, and X_{Mg} values. Pl1 has oligoclase to andesine compositions, whereas Pl2 is andesine. Both plagioclase types are largely unzoned. Kfs1 has an X_{Or} composition of ~0.73-0.87. Kfs2 rims are sodic relative to Kfs1, with X_{Or} of ~0.66-0.71, but core compositions could not be determined. Biotite from the unmelted starting material is rich in annite component, whereas biotite from the partially melted material is relatively rich in phlogopite component. Cordierite1 is relatively rich in Mn. Cordierite2 shows grains of cordierite and sekaninaite compositions, and relatively low Mn concentrations. Most Crd2 crystals are zoned, with a high-Mg core zone, a low-

Mg intermediate or rim zone, and a high-Mg, <2 μm wide rim. Orthopyroxene is enstatite-dominated.

Table 3.6: Selected mineral compositions and compositional variations in X_{An}, X_{Or}, or X_{Mg}

Label	Pl1	Pl2	Kfs1	Kfs2	Bt1*	Bt2**	Crd1	Crd2	Opx
Run	GD-4	GD-5	PSA-5	PEL-11		GD-5	PSA-5	PSA-2	PSA-2
SiO_2	59.49	58.02	64.38	66.51	34.49	36.37	48.24	48.80	49.76
TiO_2	0.02	0.02	0.04	0.01	3.68	3.84	0.01	0.00	0.27
Al_2O_3	25.64	26.23	18.76	18.41	20.01	19.55	32.35	32.83	4.81
FeO	0.11	0.22	0.04	0.04	20.66	15.80	9.92	6.12	24.55
MnO	0.01	0.00	0.02	0.00	0.22	0.18	0.59	0.10	0.49
MgO	0.00	0.03	0.01	0.02	7.52	11.30	7.39	9.86	20.43
CaO	7.20	8.44	0.03	0.05	0.01	0.02	0.02	0.32	0.24
BaO	0.02	0.40	0.80	0.73	0.09	0.04	0.00	0.00	0.00
Na_2O	7.30	6.06	1.79	3.08	0.05	0.30	0.17	0.41	0.00
K_2O	0.23	0.55	13.86	11.48	9.54	9.66	0.02	0.20	0.02
F	0.00	0.23	0.05	0.13	0.27	0.43	0.01	0.01	0.00
Total	100.03	100.10	99.78	100.40	96.54	97.48	98.72	98.64	100.58
n	40	15	24	9	13	44	21	125	18
X_{An}	0.19-0.34	0.40-0.47	-	-	-	-	-	-	-
X_{Or}	-	-	0.73-0.87	0.66-0.71	-	-	-	-	-
X_{Mg}	-	-	-	-	-	0.40-0.81	0.36-0.59	0.41-0.94	0.52-0.63

*Bt1 = Biotite from the unmelted starting material; n = number of analysis. X_{An}, X_{Or}, and X_{Mg} give the compositional range for all analyses performed.

3.6 Discussion

3.6.1 Interpretation of Run Products and Reaction Relations

3.6.1.1 Crystalline Reaction Products

The crystalline run products of our experiments are relict phases and new solid phases. To determine the origin of the various crystalline run products, we compared the mineral assemblages of the starting materials with the mineral assemblages of the experiments, examined textural criteria such as grain size, grain shape, and inclusion relationships, and used chemical criteria such as composition and compositional zoning. Using the decision tree of Figure 3.6, we interpret quartz, Pl1, Crd1, and biotite as relict phases, and Crd2, Pl2, orthopyroxene, sillimanite or corundum, Kfs2, and magnetite, as new magmatic phases.

Cordierite1 from the metapsammitic material develops a ≤40 μm thick magmatic overgrowth of Crd2 in the experiments, preventing melting or dissolution of the Crd1 core; if the same relationships developed under natural conditions, Crd1 probably survived the incorporation into SMB magma. Cordierite1 from the metapelite starting

material is not preserved in the run products, because it is largely altered in the original assemblage, and thus not stable in the experiments. However, in nature, these cordierite grains may have been preserved in a similar way as Crd1 from the metapsammitic rocks, if the alteration occurred subsequent to the intrusion of the SMB. Plagioclase2 typically rims Pl1, and seems to mimic the original outline of Pl1 grains. The textural relation and the high-An composition of Pl2 compared to Pl1 suggests that Pl2 is a melting product of Pl1. Similar textural and chemical relations of plagioclase have been described from other melting experiments (e.g., Johannes 1989; Johannes and Köppke 2001), as well as from natural examples (e.g., Kaczor et al. 1988; Green 1994), where the plagioclase skeletons are interpreted to be relics of melting or dissolution reactions (Pl1 → Pl2 + L). The modal abundance of Pl2 in our experiments appears to be constant with time, but this relation may reflect metastable survival of Pl2 under local disequilibrium rather than the stability of Pl2. Biotite1 partially decomposes to melt and magnetite. The composition of the partially decomposed biotite (Bt2) is enriched in Ti and Mg compared to Bt1 of the starting materials, suggesting that the Bt2 is a reequilibrated product of the melting reaction.

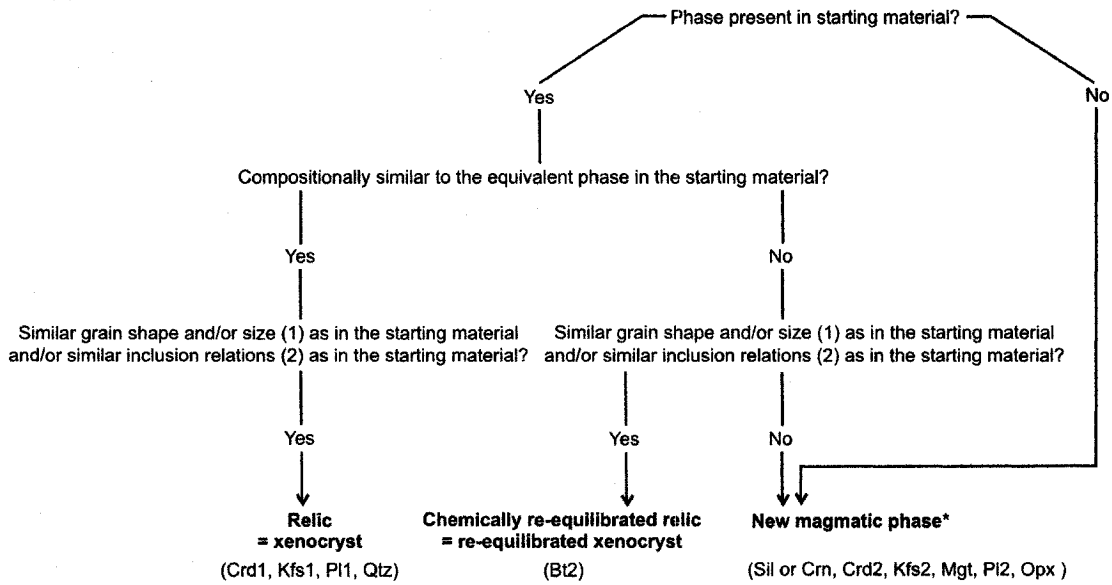

Figure 3.6: Decision matrix for interpreting the origin of crystalline reaction products derived from the metapelite and metapsammite starting materials. (1) Similar grain shape and/or size may change as a result of melting, dissolution, or crystallization. Hence, grain shape and grain size are not distinct criteria, but may help, in combination with other criteria, to determine the origin of a grain in question. (2) Inclusion relations such as mineralogy and textures of inclusions may be characteristic for different versions of the same mineral. The mineralogy of the inclusions may change as a result of reaction, but the pattern of the inclusions is likely to be preserved, if the host phase remains stable. * New magmatic phases include peritectic and cotectic phases produced during incongruent melting of country rock material.

3.6.1.2 Non-crystalline Reaction Products

The non-crystalline reaction products of our experiments are partial melt, quenched to glass, and vapour, represented by ellipsoidal cavities within the glass. The inferred melting reaction for the metapelitic material is Ms + Chl + Qtz + And + Bt + Crd1 + Kfs1 + Pl1 + V1→ Pl2 + Crd2 + Mgt + Sil or Crn ± Kfs2 + V2 + L (V = vapour; L = liquid). The inferred melting reaction for the metapsammitic material is Qtz + Pl1 + Kfs1 + Bt + Ms + V1→ Pl2 + Opx + Crd2 + Mgt + L ± V2. The abundant ellipsoidal cavities in the metapelite run products probably represent a dominantly CO_2-rich vapour, resulting from the oxidation of graphite. In the run products of experiments involving metapsammitic material and granodiorite, ellipsoidal cavities are small and rare, suggesting that the amount of free vapour was only minor. Given the scarcity or absence of graphite in the metapsammitic and granodiorite starting materials, the vapour phase in these experiments was probably N_2- (representing trapped air in the capsule) and H_2O-rich.

The analyses of the glasses show that the melt derived from the granodiorite starting material became depleted in Mn, Mg, and Ca in contact with partially molten metapelitic and metapsammitic contaminants, and enriched in K in contact with partially molten metapelitic contaminants (Fig. 3.5A,C; Table 3.5). The haplogranite in contact with metapelitic and metapsammitic contaminants became dominantly enriched in Ti, Fe, Mn, Mg, and Ca, and depleted in Na and K. As a result, the ASI and K/(K+Na) values of the granodiorite increase, if contaminated by partial melt derived from the metapelitic material, but remain similar, if contaminated by partial melt derived from the metapsammitic material of the Meguma Group. The ASI and K/(K+Na) values of the haplogranite increase, if contaminated by partial melt derived from metapelitic material, whereas the ASI value increases and the K/(K+Na) value remains similar, if contaminated by partial melt derived from the metapsammitic rocks.

The amount of partial melt produced varies with the composition of the system (e.g., metapelite alone, metapelite in contact with granodiorite or haplogranite), and with the amount of H_2O added to the experiments. At 800 °C and H_2O-saturated conditions, melting of the metapsammitic rocks produces a higher amount of melt than melting of the metapelitic rocks, because the composition of the metapsammitic rocks ($Ab_{63}Or_{37}$) is closer to the composition of the granite minimum at 200 MPa ($Ab_{56}Or_{43}$) than the composition of the metapelitic rocks ($Ab_{32}Or_{68}$). At 700 °C and H_2O-saturated conditions, melting of the metapelitic material yields approximately twice as much partial melt as the equivalent metapsammite material (PEL-19, PSA-14), because a larger percentage of

the assemblage of the metapelitic rock melts at a lower temperature (PEL is rich in white mica, PSA is poor in white mica). At 800 and 700 °C, melting of metapsammitic or metapelitic rocks in contact with granodiorite or haplogranite, yields the highest melt-fractions along the contact between the two materials, owing to the diffusion of Na out of the granites into the relatively Na-poor metasedimentary melt phases, which lowers the solidus within the contact zones (Table 3.1, 3.6).

3.6.2 Limitations of the Experimental Results

Before proceeding to the applications of these results, we must assess the potential limitations of our work.

(i) Disequilibrium conditions. Equilibrium was not attained in our experiments, as indicated by compositional gradients across the charge in the contamination experiments, and the presence of Pl2 in the melting and contamination experiments. However, we suggest that equilibrium in the melting experiments was approached, as experiments of variable duration (e.g., GD-4 and GD-5; Table 3.3) show no significant variation in run products and their compositions. The disequilibrium conditions of the contamination experiments were intended, in order to permit the identification of reaction relations and reaction textures to facilitate the interpretation of the natural examples (following Sections 3.6.3.1-3).

(ii) *Amount of H_2O added.* The concentration of H_2O in the former SMB magmas is unknown. Silicic to intermediate magmas have typically <1 wt% to ~7 wt% H_2O at the source (e.g., Clemens 1984), but become more enriched in H_2O during their evolution. We added H_2O of ~7 wt% and ~10 wt% to several of our experiments (Table 3.3, 3.4), and acknowledge that the water concentrations of the experiments may have been too high compared to the natural conditions during most of the evolution of the SMB magmas. If the SMB magmas had H_2O contents of ≥4 wt%, the experimentally determined melt fractions may be on the order of ~20 vol% higher than under natural conditions (e.g., comparing melt fractions in GD-3 and GD-4 with 3.7 and 10.7 wt% H_2O added and 50 and 70% partial melt produced).

(iii) *Constant rate of heat supply and heat capacity.* Given the constant rate of heat supply in our experiments, the degree of reaction (e.g., amount of partial melt produced) is dominantly a function of time and the composition of the components of the system (country-rock composition and composition of the host melt), whereas in natural systems, the amount and the rate of heat available is critical to the amount of material

that can be assimilated (e.g., Reiners et al. 1995; Bohrson and Spera 2003). For this reason, the experiments can show the direction of reaction upon assimilation, but not the extent of assimilation.

(iv) *Pressure limit.* The pressure limit of the cold-seal system used is 200 MPa and therefore restricts the ferromagnesian mineral assemblage to the field of cordierite, rather than garnet, whereas in the SMB, emplaced at ≥200-400 MPa (Raeside and Mahoney 1996), garnet in addition to cordierite is an important product of the disintegration of pelitic xenoliths (Clarke and Erdmann 2005). The disparity in pressure also has a moderate effect on the solubility of H_2O in the melt, a minor effect on the X_{Mg} of the silicate phases including melt, and a small effect on the solidus temperature.

(v) *Maximum temperature of SMB magmas.* The maximum temperature of the SMB magmas is unknown. Orthopyroxene, present in the melting experiments using metapsammitic rocks, does not occur in the SMB, possibly indicating that the biotite-out temperature of ~780 °C at 400 MPa (Vielzeuf and Holloway 1988) was not overstepped. However, orthopyroxene may have also been present in the SMB magmas, and temperatures may have been ≥780 °C, if orthopyroxene disappeared in hydration reactions during cooling (Beard et al. 2004, 2005). With no evidence to the contrary, we hypothesize that the SMB magmas may have had initial temperatures of ≥800 °C, and that our high-temperature experiments are thus reasonable for the natural conditions of country-rock assimilation during the early evolution of the SMB magmas and in the center of the batholith.

(vi) *$f(O_2)$.* The conditions during the emplacement of the SMB were more reduced than in our experiments. In them, magnetite is the most abundant Fe-bearing oxide, whereas in the granodiorites of the SMB, magnetite is absent and ilmenite is the most abundant Fe-bearing oxide. In the SMB, ilmenite instead of magnetite may be an important contaminant, and as a result, coexisting biotite, cordierite, garnet, and melt should have a lower X_{Mg} than in the experiments.

(vii) *Length scale.* The length scales of the experiments are on the order of μm to cm. The reactions resulting from diffusive exchange between country-rock and granite melt phase are thus only comparable to reactions near the contact between both materials. However, thermal equilibration is more efficient than diffusive exchange of chemical species in a melt phase (e.g., Clarke in press), and partial melting of country rocks under natural conditions (and probably longer time-scales) may have thus occurred over larger length-scales than in our experiments.

(viii) *Low-temperature alteration of the mineral assemblage.* Although we took care to sample the freshest material available, the mineral assemblage of our starting material is partly altered, and thus not equivalent to the material that contaminated the SMB. The alteration affected cordierite from the metapelitic rocks, and to a minor degree biotite, K-feldspar, and plagioclase. The products of the low-temperature alteration reacted at a temperature lower than the original assemblage would have reacted, but the low-temperature alteration products make up <3 vol% in the samples, and the effect on the reaction relations of our experiments is thus only minor.

3.6.3 Applications of the Experimental Results

3.6.3.1 Interpreting Textures

Some xenoliths in the SMB have a rim that is mineralogically, texturally, or compositionally different from the granite host (e.g., a biotite-, cordierite-, or feldspar-rich rim). Such rims may: (i) be the result of the preferential nucleation of magmatic minerals on the surface of the xenoliths; (ii) reflect a temperature gradient between the rim and the core of a xenolith that permitted partial melting or other reactions only along the xenolith rim (at near-solidus conditions, where the consumption of heat in melting reactions freezes the system); or (iii) result from partial melting of country rocks in combination with diffusive exchange of melt species between country-rock material and host magma. Cordierite- and feldspar-rich zones at the contacts between metasedimentary and granitic material in our experiments, which arise from melting of the metapelitic rock and diffusive mass-transport between the two compositions, resemble cordierite- and feldspar-mantled xenoliths in the SMB (Fig. 3.3A,D, 3.7). Therefore, we suggest that the cordierite- and feldspar-rich rims on naturally occurring xenoliths are probably also a result of partial melting of metasedimentary rocks and diffusive exchange between the partial melt of the metasedimentary rock and the melt fraction of the former host magma. At higher temperatures of the host magma, the cordierite-rich rims may have formed; at lower temperatures, the feldspar-rich rims may have formed.

3.6.3.2 Assessing Country-rock Assimilation

Our results suggest that at relatively high temperatures (≥800 °C), the assimilation of country rocks of the Meguma Group through partial melting may have been an important

mechanism in the SMB, with peritectic magmatic crystals composed entirely or largely of foreign components (e.g., cordierite, garnet, ilmenite), quartz and possibly biotite xenocrysts, and partial melt derived from xenoliths, as the major contaminants. At relatively low temperatures (~700 °C), partial melting may have still played a role, but should have caused disintegration rather than assimilation of Meguma Group country rocks in the SMB, with xenocrysts, released through loss of cohesion along melt-wetted grain boundaries, as the major contaminants. For country rocks that have a higher solidus temperature than the rocks used in our experiments, for example, quartzitic rocks of the Meguma Group, disintegration and assimilation through partial melting may have been less significant, but diffusive exchange with the host magma may have permitted minor partial melting even in these xenoliths, and thereby their disintegration and partial assimilation.

According to our experiments, chances of survival of xenocrystic muscovite, chlorite, K-feldspar, and plagioclase in the SMB magmas were low, whereas those of xenocrystic quartz, cordierite, and biotite were much higher. Chances of survival of peritectic magmatic crystals formed as a result of partial melting of country-rock material, cannot be assessed using our experimental results, but the peritectic phases may: (i) have remained unreacted; (ii) have partly or completely dissolved, if they came into contact with the SMB magmas (as a result of dispersal or diffusive exchange that reequilibrated the composition of the country-rock partial melt with the large reservoir of the SMB magma); or (iii) partly or completely reacted during cooling, where, for example, garnet and cordierite may have been consumed by biotite (Allan and Clarke 1981), and andalusite or sillimanite may have been consumed by muscovite (Clarke et al. 2005).

Our experiments also show that evidence for dispersed former partial melt derived from Meguma Group country rocks may be indirectly preserved in zoning patterns of magmatic crystals (e.g., Edwards and Russell 1996; Tepley and Davidson 2003), or in whole-rock geochemical signatures of the SMB rocks, given that compositions of melt fractions derived from Meguma Group country rocks and SMB granodiorites are different. Compositional differences between the melt phases derived from country rocks and granites, such as ASI value and molar K/(K+Na), are almost completely eliminated in our experiments, whereas differences in concentration of elements such as Na, Ca, Si, Fe, Mg, and Ti remain. Under natural conditions, with much longer reaction times, compositions of country-rock partial melt will have largely re-equilibrated with SMB magmas for all components, but the SMB host may still have been preferentially

contaminated by certain elements (e.g., diffusion of K over a longer distance than the other elements). The diffusive exchange of elements and isotopes may have been recorded in growing primary and peritectic magmatic minerals (e.g., Ginibre et al. 2002).

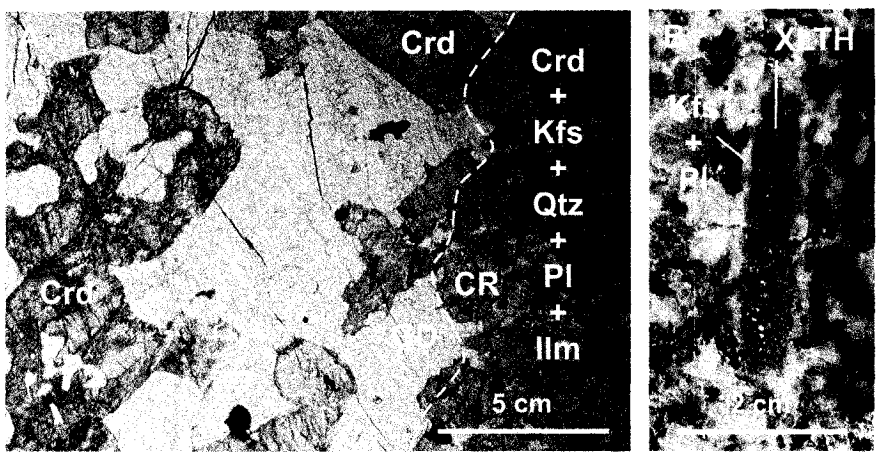

Figure 3.7: A) Photomicrograph (plane polarized light), showing the contact (stippled line) between fine-grained country rocks of the Meguma Group (right), and coarse-grained granodiorite (left). Cordierite (highly altered) formed as a result of partial melting of the country rock (within the country rock, CR) and through diffusive exchange between the country-rock melt phase and the host SMB magma (within the granodiorite, GD). B) K-feldspar and plagioclase-rich rim around a metapelitic xenolith (XLTH) enclosed in a granodiorite of the SMB.

3.6.3.3 Estimating Contamination

In our melting experiments, partial melting of metapelitic and metapsammitic country rocks at 800 °C yields ≤10 vol% relict phases (= xenocrysts), ~15-30 vol% new magmatic phases (= composed entirely or largely of foreign components), and ~70-75 vol% partial melt. The xenocrysts as well as peritectic and cotectic crystals of foreign origin are likely to be physically detectable in contaminated granites, whereas dispersed partial melt may only be indirectly apparent in zoning patterns of magmatic crystals, or the geochemical signature of a rock. The amount of foreign material present in granites should thus be generally greater than the amount of physically detectable foreign material, if assimilation of country rocks occurred through partial melting, but simple extrapolations such as "1 vol% xenocrysts in the SMB represent ~8 vol% foreign material" (using the volume fractions of the experiments for calculation, corrected for the fact that experimental melt fractions that may be ~ 20 vol% too high) are not permissible. In addition to the problem of not knowing the bulk composition of the contaminant (e.g., the ratio of metapelitic versus metapsammitic contaminants in the SMB), further

complications arise from: (i) the simultaneous or subsequent operation of various processes of assimilation, such as physical disintegration and partial melting of xenoliths (e.g., in the case of xenolith partial melting, 1 vol% xenocrysts in a granite may represent a significant amount of foreign material, but only a minor amount in the case of physical disintegration, where xenocrysts are the major or only product of disintegration); (ii) phases of a hybrid origin, such as cordierite, that may have incorporated material derived from the country rocks, and material derived from the main magma (atoms of the cordierite may be 100% foreign, 100% cognate magmatic, or a mixture of the two); and (iii) spatial separation of various products of disintegration through flow or gravity settling (e.g., separation of xenocrysts and xenolithic partial melt).

Nevertheless, the presence of physically recognizable contaminants (xenoliths, xenocrysts, magmatic minerals of foreign origin) can at least indicate that contamination by country-rock material occurred in a sample, pluton, or batholith under consideration. Experiments can help to constrain under which conditions it is likely that certain country rocks were assimilated through partial melting, and how much physically "invisible" foreign material may be expected.

3.7 Conclusions

The results from this experimental study suggest that:

(i) Meguma Group xenoliths incorporated into SMB magmas at high temperatures (≥800 °C) may have been assimilated through partial melting, whereas at lower temperatures (≤700 °C), minor partial melting may have caused disintegration of xenolithic material rather than chemical assimilation.

(ii) If melting takes place at high-H_2O concentrations, the metapsammitic rocks of the Meguma Group are a better source of melt than the metapelitic rocks, because their bulk composition more closely approaches the composition of the granite minimum.

(iii) The highest degree of partial melting in the metapelitic and metapsammitic rocks occurs in contact with the melt of granodiorite or haplogranite, owing to the diffusion of Na out of the granites into the relatively Na-poor metasedimentary melt phases, lowering the solidus of the latter.

(iv) Quartz, biotite, and cordierite derived from the Meguma Group have relatively high chances to survive incorporation into the SMB magma.

(v) Abundant cordierite may crystallize at the contact between metapelitic xenoliths and SMB granodioritic magma, whereas abundant K-feldspar may crystallize at the contact between metapelitic xenoliths and a metaluminous or only slightly peraluminous magma.
(vi) Diffusive exchange of elements between country-rock derived partial melt and the host magma occurs at geologically extremely rapid rates, with K and Na exchanging at the highest rates, and thus preferentially contaminated the SMB magmas (e.g., changing the ASI composition of the magma and rocks, but not their X_{Mg}).
(vii) Estimates for the degree of country-rock contamination in igneous rocks based on the abundance of xenoliths, xenocrysts, as well as peritectic and cotectic magmatic crystals composed entirely or largely of foreign components underestimate the amount of foreign material present, given that physically "invisible" contaminants of former partial melt must also occur.

3.8 Acknowledgements

An NSERC Discovery Grant to D.B. Clarke, a GSA Student Research Grant (No. 7655-04), and an Izaak Walton Killam Memorial scholarship to Saskia Erdmann, as well as support by NSF grant EAR-0124179 to David London, made this study possible. The electron microprobe laboratory at Oklahoma University was established by grant DE-FG22-87FE1146 from the U.S. Department of Energy to David London, and is supported annually by the Office of the Vice President of Research at Oklahoma University. We thank Antonio Acosta-Vigil for help with the experiments and initial discussions, Sarah Carruzzo for help with preparing the metapelite, metapsammite, and granodiorite powders, Jörn H. Kruhl for comments on an early draft of the manuscript, and Aaron C. Seimers for his assistance in preparing some of the experiments. Helpful and very constructive comments by Trevor Green and an anonymous reviewer and by editors Robert Martin and Ron Vernon are very much appreciated.

CHAPTER 4

Nature and Significance of Metapsammitic and Metapelitic Contaminants in the Peraluminous South Mountain Batholith

4.0 Preamble

This chapter will be submitted as manuscript to a peer-reviewed journal by S. Erdmann and D.B. Clarke. I am responsible for all observations, as well as their interpretation, have written the manuscript, and prepared all Figures and Tables. D.B. Clarke joined me on observations, significantly contributed to this study in ongoing discussions over the years, and provided critical comments which greatly improved the manuscript.

The aim of the study presented in this chapter was to characterize all physically detectable country-rock contaminants and to estimate their significance in the SMB at an unprecedented level of detail. We did not expect to quantitatively recognize the presence of all country-rock contaminants in the SMB rocks, given that assimilation of Meguma Group rocks through partial melting by SMB magmas played a role, and that some xenocrysts may be assimilated to a degree where they are no longer recognizable (e.g., Jamieson 1974; Clarke and Erdmann 2005; Erdmann and Clarke 2005). However, with a detailed knowledge of the nature and the significance of all physically detectable country-rock contaminants in the SMB at hand, we expected to be in the position to at least semi-quantitatively estimate the significance of country-rock contamination and assimilation in the exposed SMB rocks, using the results from this study in combination with the experimental data presented in Chapter 3.

4.1 Abstract

The South Mountain Batholith (SMB) of southern Nova Scotia, Canada, intruded metapsammitic and metapelitic rocks of the Meguma Group, and consists of peraluminous granodiorite, monzogranite, leucomonzogranite, and leucogranite. Field observations, as well as observations from optical and cathodoluminescence microscopy, reveal evidence for country-rock contamination in the form of xenoliths, orthoxenocrysts (xenocrysts of the original, subsolidus assemblage of the country rocks), paraxenocrysts (xenocrysts that formed in a peritectic melting reaction between contaminants and host magma), and former partial melt. The assimilation of country-rock material occurred through a combination of fracturing and partial melting, and

subsequent dispersal. The assimilation of the metapelitic country rocks dominantly released paraxenocrystic garnet or cordierite, and a silicate partial melt into the SMB magmas. The assimilation of the metapsammitic country rocks dominantly released orthoxenocrysts of quartz, biotite, and plagioclase, and a silicate partial melt into the SMB magmas. In SMB rocks remote from contacts with Meguma Group rocks, textural relations permit the identification of paraxenocrystic garnet and cordierite with confidence, but the detection of quartz, biotite, and plagioclase orthoxenocrysts has a considerable uncertainty, and former partial melt is physically largely undetectable. Nevertheless, assuming that all texturally suspect minerals are xenocrysts, and that we detected all xenocrysts present in the rocks studied, xenocrysts make up ~4 vol% in the marginal and <3 vol% in the more central rocks of the SMB. Assuming ratios of orthoxenocrysts and paraxenocrysts to partial melt determined in melting experiments simulating the assimilation of metapelitic and metapsammitic rocks of the Meguma Group in SMB magmas, the abundance of orthoxenocrysts and paraxenocrysts in the SMB rocks suggests that up to 10 vol% of complementary, former country-rock partial melt may be present. Together, xenoliths, xenocrysts, and complementary former country-rock partial melt make up a maximum of ~16 and ~8 vol% of Meguma Group country-rock material in the marginal and more central rocks of the SMB, respectively. Country-rock contamination has thus played a role in the evolution of the SMB, but the combined effects of source variations, fractional crystallization, and/or fluid interaction appear more important in explaining the observed mineralogical, textural, and chemical variation between the various rock types of the exposed batholith, unless the selective contamination of the exposed SMB rocks by country-rock derived partial melt from unexposed Meguma Group rocks was volumetrically important.

4.2 Introduction

Country rocks in contact with a magma, or country rocks entrained in a magma, may fracture and/or partially melt, resulting in the formation of xenoliths, xenocrysts, and/or partial melt (e.g., Furlong and Myers 1985; Bédard 1991; Maury and Didier 1991; Green 1994; Clarke et al. 1998; Connolly et al. 1997; Dungan and Davidson 2004; Beard et al. 2005). Furthermore, minerals of the country rocks *in situ*, or minerals of the country rocks released as xenocrysts, may undergo hydration, dehydration, decomposition, melting, or ion exchange reactions (e.g., Maury and Didier 1991; Bédard and Hébert 1996; Costa and Dungan 2005; Beard et al. 2005; Clarke in press). The probability that magmas and

country rocks have the same composition for all chemical elements is zero, and therefore the probability of reaction would be close to one (except in cases where mantling or quenching prevents it). Hence, all igneous rocks must be contaminated (rendered impure) by country-rock, but the amount and nature of that contamination, and the degree and nature of assimilation determine how the mineralogical, textural, and chemical characteristics of the igneous rocks are affected.

The South Mountain Batholith (SMB) of southern Nova Scotia intruded greenschist to amphibolite facies metapsammitic and metapelitic rocks of the Meguma Group, and consists of peraluminous granodiorite, monzogranite, leucomonzogranite, and leucogranite (McKenzie and Clarke 1975; MacDonald et al. 1992; Clarke et al. 1993, 1998; MacDonald 2001) (Fig. 4.1). The mineralogical, textural, and chemical variation in the SMB resulted from a combination of closed-system fractional crystallization, open-system contamination, and fluid interaction, but the importance of the various processes and their effect on the evolution and characteristic properties of the batholith is only partly understood (e.g., Jamieson 1974; McKenzie and Clarke 1975; Clarke and Chatterjee 1988; Clarke et al. 1993; Clarke et al. 1998; MacDonald 2001; Clarke et al. 2004; Clarke and Erdmann 2005). Field observations reveal a greater abundance of xenoliths in the marginal than in the more central rocks of the SMB (e.g., Jamieson 1974; MacDonald 2001), whereas whole-rock Sr-Nd isotopic data shows that the most evolved rocks of the SMB have a higher amount of components derived from rocks of the Meguma Group than the more primitive rocks of the batholith (Clarke et al. 2004). A previously proposed explanation for these apparently contradictory observations is that country rocks of the Meguma Group are progressively more strongly assimilated from the margin toward the center of the SMB, leaving little macroscopically visible evidence for contamination in the most evolved rocks, but a whole-rock chemical signature indicating a high degree of contamination (Clarke et al. 1988; Clarke et al. 2004; Clarke and Erdmann 2005).

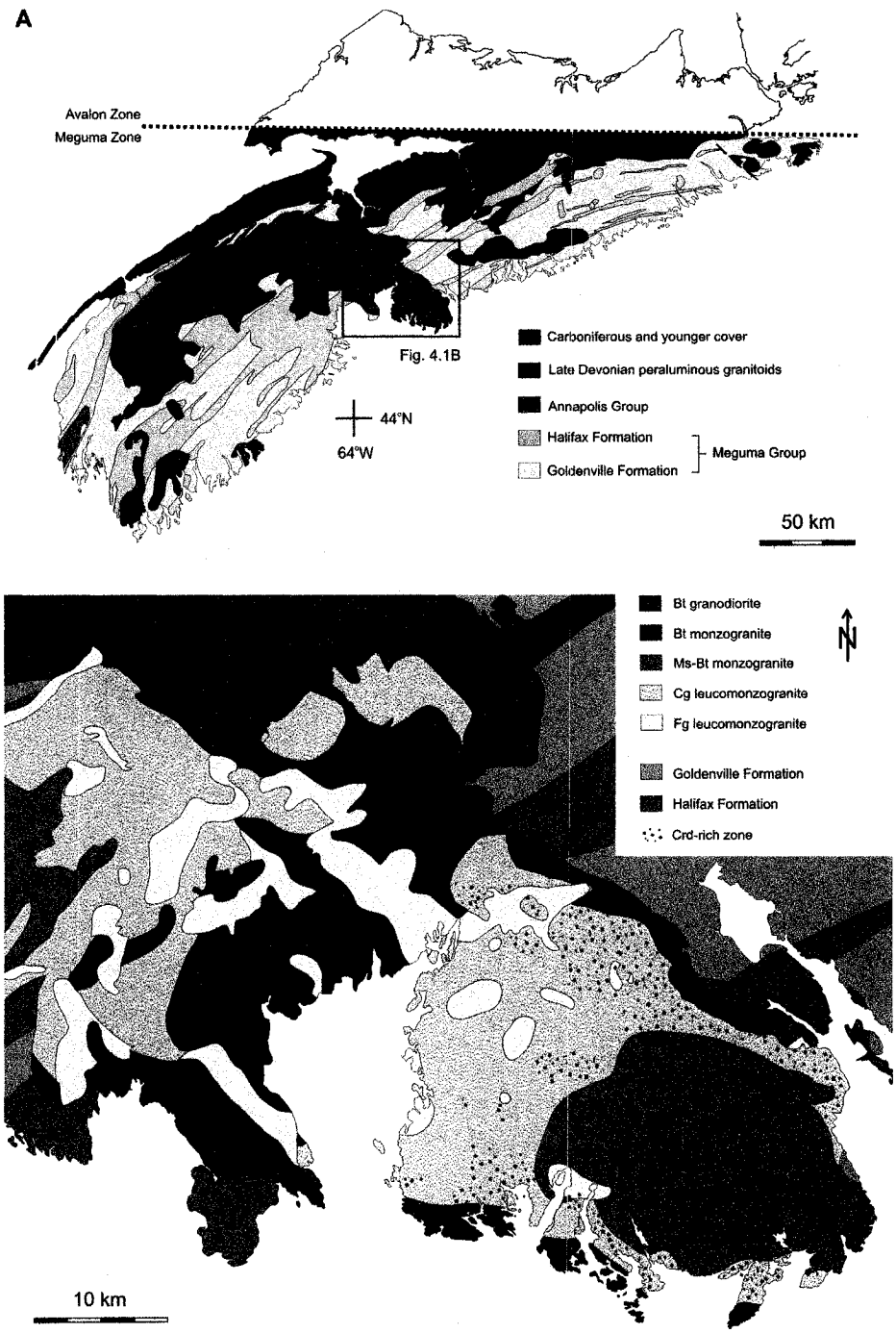

Figure 4.1: A) Geological map of southern Nova Scotia (after Tate 1995). The South Mountain Batholith (SMB) intruded dominantly rocks of the Meguma Group. Contacts between the SMB and the metapsammite-dominated Goldenville Formation and the metapelite-dominated Halifax Formation of the Meguma Group and SMB have subequal lengths. B) Detailed geological map of the study area (after MacDonald 2001). Xenoliths in the SMB are most abundant near the exposed contact with the Meguma Group country rocks, whereas cordierite-rich zones occur away from the contact with the metasedimentary country rocks. HP = Halifax Pluton; Cg = coarse-grained; Fg = fine-grained.

In this paper, we present field and textural observations to characterize and estimate the importance of metapsammitic and metapelitic contaminants of the Meguma Group in the marginal and more central rocks of the eastern part of the SMB. This work represents a first step toward a more quantitative analysis of the plethora of components and processes recorded in the SMB rocks, and tries to explain the apparently contradictory field observations and whole-rock Sr-Nd isotopic data in regard to the role of country-rock contamination in the evolution of the SMB. Clarke and Carruzzo (in press) evaluated the importance of Fe-Ti-oxides derived from the metasedimentary rocks of the Meguma Group in the SMB, and Samson (2005) and Samson and Clarke (2005) evaluated the significance of Meguma Group Fe±Cu-sulphides in the former SMB magmas. Our description and discussion focuses on the volumetrically more important silicate country-rock components and their respective contaminants.

4.3 Methods

Observations in this paper are the result of field studies and microscopic textural examination. Our field studies focused on the northeastern margin and the Halifax Pluton of the SMB (Fig. 4.1), where the exposure is better than elsewhere in the batholith. Rocks of the Meguma Group have been studied close to, but several metres away from the exposed contact with the SMB. The abundance of xenoliths, mineralogically and texturally distinct contact zones, garnet-rich layers and schlieren, and coarse-grained suspect xenocrysts were estimated in the field. The abundances of fine-grained suspect xenocrysts was estimated, again visually, from >150 thin sections of the mineralogically and texturally variable rocks of the study area. Our textural observations and our interpretation of the origin of various crystals from the SMB rocks are based on transmitted, back-scattered electron, and cathodoluminescence (CL) microscopy. Color CL microscopy was carried out at Memorial University, using a Nuclide luminoscope ELM-2B. To permit determination of low-contrast cathodoluminescence textures, CL images were collected using a JEOL JSM-5900CS scanning electron microscope (SEM) at Acadia University. To determine the origin of various crystals of the rock-forming minerals in the SMB, we texturally compared the minerals of the Meguma Group country rocks with the minerals of the SMB rocks, examining grain size, grain shape, inclusion relationships, twinning and deformation features, and mineral assemblages.

4.4 Results

4.4.1 Field Relations

4.4.1.1 Metapsammitic and Metapelitic Rocks of the Meguma Group

At the level of exposure in the area studied, metapsammitic and metapelitic *in situ* rocks of the Meguma Group have similar abundances (Fig. 4.1). The metapsammitic rocks are massive or layered on a mm- to cm-scale. The metapelitic rocks are commonly layered on a mm-scale. Both rock types are variably interlayered. The metapsammitic rocks have abundant quartz, plagioclase, biotite, and K-feldspar, and minor cordierite as well as Fe±Cu-sulphides. The metapelitic rocks dominantly consist of muscovite, cordierite, andalusite, biotite, quartz, plagioclase, and ± Fe±Cu-sulphides, and may have minor garnet and sillimanite. The metapelitic rocks are dominantly very fine-grained, whereas the metapsammitic rocks are dominantly fine-grained, but biotite, cordierite, andalusite, and Fe±Cu-sulphides may form porphyroblasts of up to 1 cm in size. Iron-copper-sulphides also form mm- to cm-thick lenses or irregular layers. Contact relations between *in situ* country rocks and SMB rocks are similar to the contact relations between xenoliths and SMB rocks (Section 4.4.1.3).

4.4.1.2 Metapsammitic and Metapelitic Xenoliths in the SMB

Despite the similar abundances of metapsammitic and metapelitic country rocks, at least at the currently exposed level, xenoliths in the SMB are dominantly metapsammitic (~95 %), whereas metapelitic xenoliths are rare (~4 %). In addition, <1 % calc-silicate xenoliths occur. The xenoliths range from micrometres to several metres in length, and have shapes that are subangular to highly irregular (Fig. 4.2). They occur throughout all map units of the South Mountain Batholith, but are absent from many outcrops. Close to the contacts with the *in situ* Meguma Group country rocks, xenoliths may occur with up to ~30 vol% in an outcrop, but in SMB rocks > 200 m away from exposed contacts between the batholith and country rocks, xenoliths make up ≤2 vol%. Close to the margin of the batholith, xenoliths of all sizes occur, away from the margin, xenoliths are on the mm- to dm-scale.

The mineral assemblages and textures of most of the metapsammitic and metapelitic xenoliths are similar to those of the metapsammitic and metapelitic *in situ* country rocks of the Meguma Group. Other *in situ* country rocks and xenoliths may have texturally

and/or mineralogically distinct contact zones that are ≤10 cm wide. These contact zones are described in Sections 4.4.1.3 and 4.4.1.4.

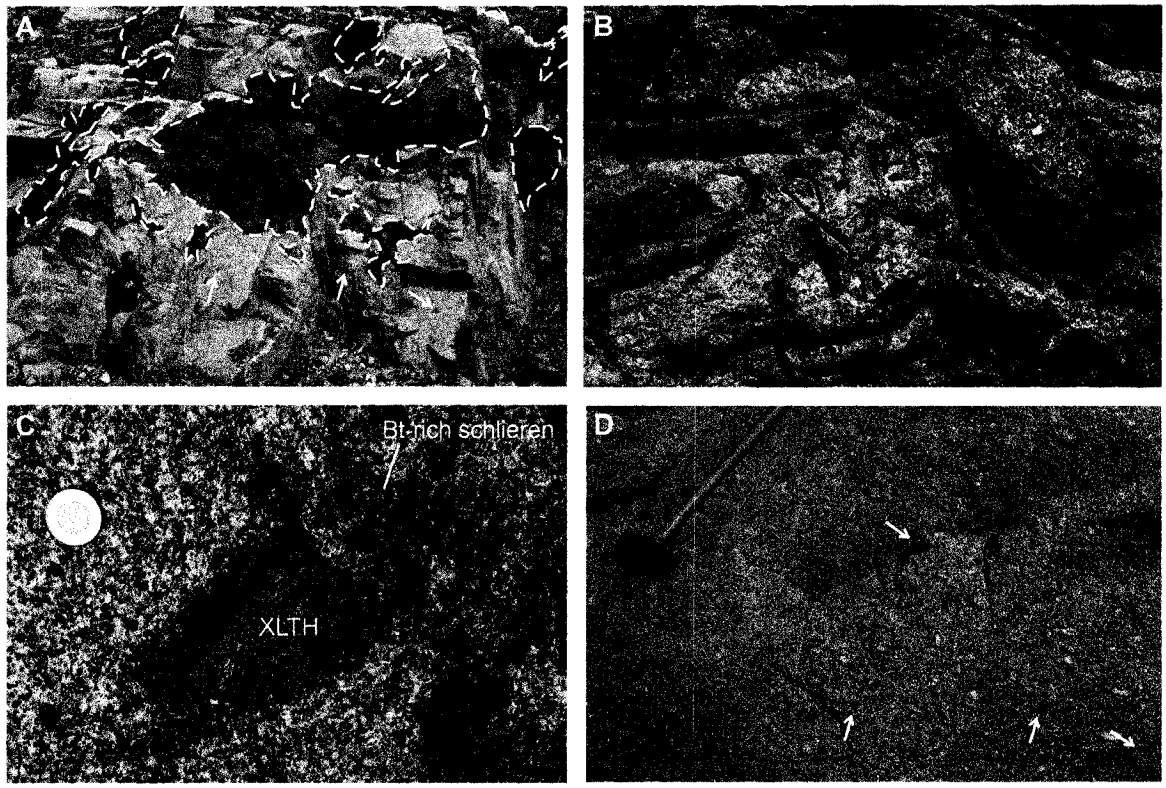

Figure 4.2: Xenoliths of various sizes and shapes in the SMB. A) Irregular metapsammitic xenoliths in biotite granodiorites <20 m from the exposed contact between Meguma Group country rocks and SMB. Dashed lines mark the larger xenoliths; arrows mark some smaller xenoliths. Location E 430. B) Angular xenoliths from a large disintegrating xenolith ("exploding elephant"; Clarke et al. 1998) in a monzogranite host. Location Stop 1.6. C) Metapsammitic xenolith (XLTH) and biotite(Bt)-rich schlieren. Location E 430. D) Abundant xenoliths in leucomonzogranite. Arrows mark some xenoliths. Location E 484.

4.4.1.3 Contacts between Metasedimentary Rocks and SMB

Contacts between metasedimentary rocks and SMB rocks are sharp to gradational, and Meguma Group rocks as well as SMB rocks along the contacts may be texturally and/or mineralogically distinct (Fig. 4.3). In the following section, we first describe contact zones of the metapsammitic and metapelitic rocks against the SMB, dominated by obviously metasedimentary material. Second, we describe SMB rocks in contact with metasedimentary rocks that are mineralogically and/or texturally distinct from the common SMB host. Third, we characterize garnet-rich layers from contacts between metasedimentary rocks of the Meguma Group and the SMB.

Contact Zones of Metapsammitic Rocks

Contacts between the metapsammitic rocks and the SMB are irregular on the μm- to m-scale, and sharp to gradational (Fig. 4.4). Approximately 80 % of the studied contacts involving metapsammitic rocks are texturally and mineralogically similar to the metapsammitic rocks of the Meguma Group remote from contacts with the SMB (Fig. 4.4A). Approximately 18 % of the contacts have a fine-grained to coarse-grained assemblage with dominantly small crystals, and ca. 2 % of the contacts show a fine-grained to coarse-grained assemblage with dominantly large crystals (Fig. 4.4B,C). Contact zones showing small to large crystals are typically <10 cm wide.

Contact Zones of Metapelitic Rocks

Contacts between the metapelitic rocks and the SMB are irregular on a micrometre to metre scale, and sharp to gradational (Fig. 4.5). Few, ca. 2 % of the studied metapelitic rocks have contact zones that are mineralogically similar to, but coarser grained than, the metapelitic rocks away from the contact (Fig. 4.5A). Most (~98 %) of all studied metapelite-SMB contacts, are rich in medium-grained cordierite ± K-feldspar (Fig. 4.5B). These contact zones are up to ~20 cm wide.

4.4.1.4 Contact Zones of SMB Rocks

Texturally and/or mineralogically distinct contact zones in the granitic rocks are sharp to gradational against the metasedimentary rocks of the Meguma Group, and gradational against the common SMB rocks (Fig. 4.6). Biotite-rich contact zones occur along ~10 % of all studied contacts. They may have up to ~80 vol% large and clotty biotite, and are typically <10 cm wide (Fig. 4.6A, Fig. 4.2C). Approximately 5 % of the granitic rocks in contact with cordierite- and ± K-feldspar-rich contact zones of the metapelitic rocks have abundant large, euhedral to subhedral cordierite crystals, where most of the cordierite crystals occur within a ~5 cm wide zone (Fig. 4.6B). A <0.5 cm wide plagioclase- and K-feldspar-rich SMB contact zone is present along <1% of all studied contacts, occurring only where granitic rocks are juxtaposed against metapelitic rocks that are mineralogically similar to metapelitic rocks away from the contact (Fig. 4.5A).

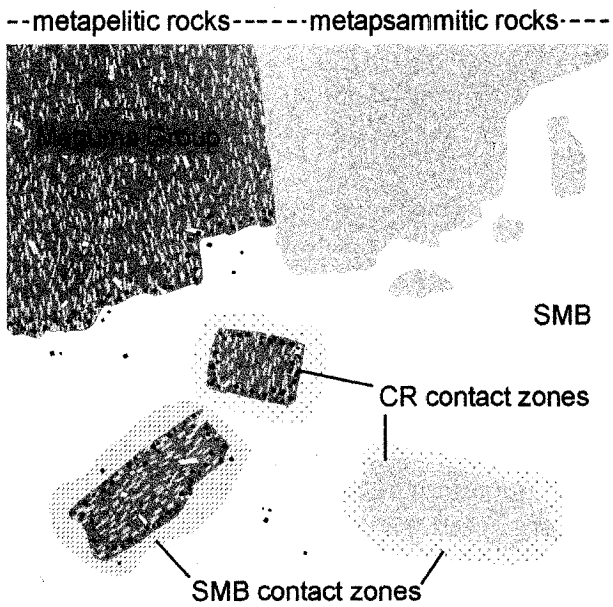

Figure 4.3: Contact relations between metapelitic and metapsammitic rocks of the Meguma Group and the South Mountain Batholith (SMB). Country-rock (CR) contact zones are texturally and/or mineralogically different from the SMB host rocks. SMB contact zones as zones are mineralogically and/or texturally distinct from the common SMB host.

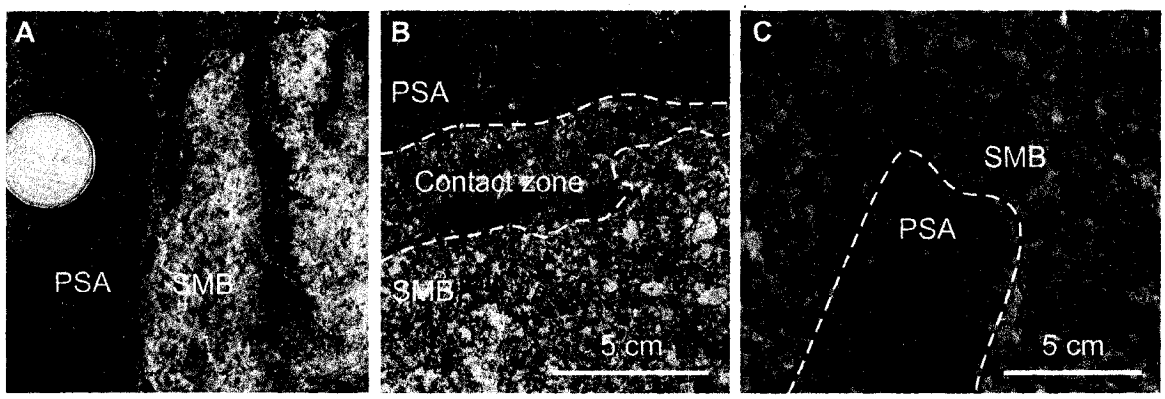

Figure 4.4: Contact relations between metapsammitic rocks of the Meguma Group (PSA) and the SMB. Location E 430. A) Sharp contact between metapsammitic rocks and biotite monzogranite. B) Gradational contact between metapsammitic rocks and granodiorite, with a metasedimentary contact zone showing small to large crystals (XLs) of quartz, plagioclase, and biotite. Location E 430. C) Contact between metapsammitic rocks and biotite granodiorite. The metapsammitic xenolith is dominated by crystals that are medium to large in size, but compared to its host, has more small crystals and shows a preferred orientation of biotite. Location Stop 1.2.

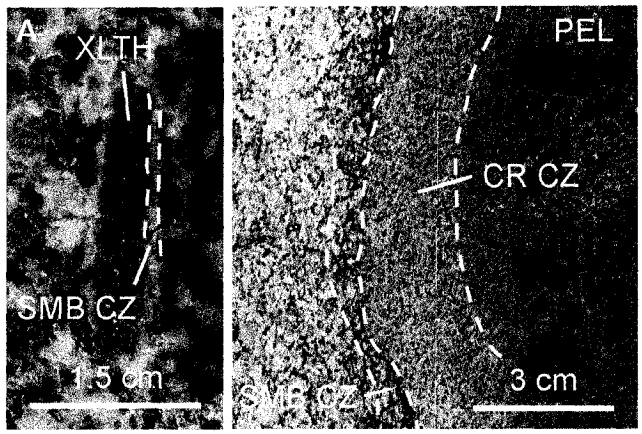

Figure 4.5: Contact relations between metapelitic rocks of the Meguma Group (PEL) and the SMB. A) Sharp contact between a metapelitic xenolith (XLTH) and biotite granodiorite. The host granodiorite shows a thin plagioclase- and K-feldspar-rich contact zone (CZ) against the xenolith. Location E 436. B) Metapelitic xenolith with a cordierite-rich, relatively coarse-grained contact zone (CR CZ), and a biotite-rich SMB contact zone. Location E 428.

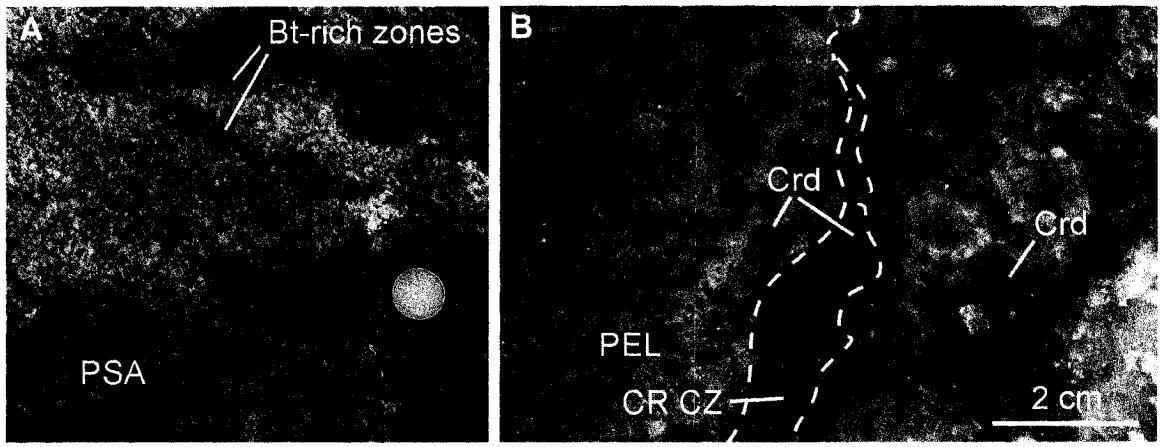

Figure 4.6: Mineralogically and/or texturally distinct SMB contact zones. A) Biotite-rich contact zones and schlieren in a granodiorite in contact with metapsammitic rocks of the Meguma Group (PSA). Location E 430. B) Cordierite-rich SMB contact zone (CR CZ) between cordierite-rich metapelitic rocks (PEL) that also show a cordierite-rich contact zone, and muscovite-biotite leucomonzo-granites of the SMB. Location E 433.

4.4.1.5 Garnet-rich Layers

Garnet-rich layers are present along <1 % of the contacts between SMB rocks and Meguma Group rocks, most commonly in contact with the metapelite-dominated Halifax Formation. The layers consist of medium to large garnet, cordierite, Fe±Cu-sulphides, Fe-Ti-oxides, biotite, quartz, plagioclase, and K-feldspar (Fig. 4.7). They show an abrupt change in mineralogy and texture against both the metasedimentary and the SMB rocks. Thicknesses of these layers are ≤50 cm, and exposed length-scales are ≤3 m.

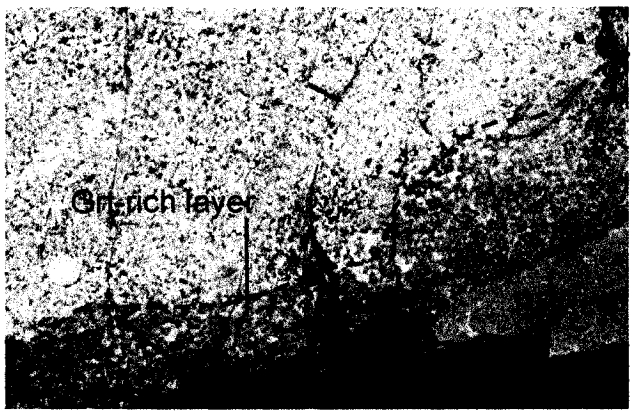

Figure 4.7: Garnet(Grt)-rich layer in contact with metapsammitic rocks (PSA) of the Meguma Group and SMB granodiorites. The garnet-rich layers are typically <1m thick, but may be several metres in length. Location E 430.

4.4.2 Mineralogy and Textures

4.4.2.1 Metapsammitic and Metapelitic Rocks of the Meguma Group

The metapsammitic rocks of the Meguma Group dominantly consist of small quartz, plagioclase, K-feldspar, and biotite crystals (Fig. 4.8A). Biotite is subhedral and stubby. Most quartz, plagioclase, and K-feldspar crystals are subhedral and equant. Inclusions in quartz, plagioclase, and K-feldspar are rare; common inclusions in biotite are zircon, monazite, apatite, and Fe-Ti-oxides. Cordierite and garnet may occur as subhedral, typically equant, inclusion-poor to inclusion-rich crystals. Iron-copper-sulphides occur typically as small and subhedral crystals, and in accessory amounts, but they may also form large porphyroblasts or irregular bands.

In the metapelitic rocks of the Meguma Group, muscovite, biotite, quartz, plagioclase, K-feldspar, and cordierite form commonly small crystals (Fig. 4.8B). Muscovite and biotite are subhedral and stubby; quartz, plagioclase, K-feldspar, and cordierite are subhedral and equant. Cordierite is also present as large, ellipsoidal, and typically inclusion-rich porphyroblasts. Garnet may form subhedral, inclusion-rich crystals, or euhedral, inclusion-rich to inclusion-poor crystals. Andalusite forms small, subhedral to euhedral crystals, or large, euhedral chiastolite crystals. Iron-copper-sulphides occur as large, ellipsoidal, inclusion-poor to poikilitic single grains or as multi grains in irregular bands. Sillimanite is typically fibrous. Iron-titanium oxides, Fe±Cu-sulphides, zircon, monazite, and apatite occur as inclusions in quartz, plagioclase, cordierite, and biotite more than they do in the equivalent minerals of the metapsammitic rocks.

In both metapsammitic and metapelitic rocks, plagioclase has common polysynthetic or simple growth twins, and cordierite typically shows sector twinning. Small crystals of quartz, plagioclase, K-feldspar, and cordierite may exhibit weak undulose extinction. Large quartz crystals may show subgrain patterns, and plagioclase may have deformation twins. The CL color of quartz is a stable dark blue, plagioclase shows a turquoise color, and K-feldspar shows a light blue (Fig. 4.8C). Cathodoluminescence patterns of quartz, plagioclase, and K-feldspar are typically patchy, showing abundant healed micro-fractures (Fig. 4.8D). Plagioclase and K-feldspar may also show zoning with dark CL cores and bright CL rims.

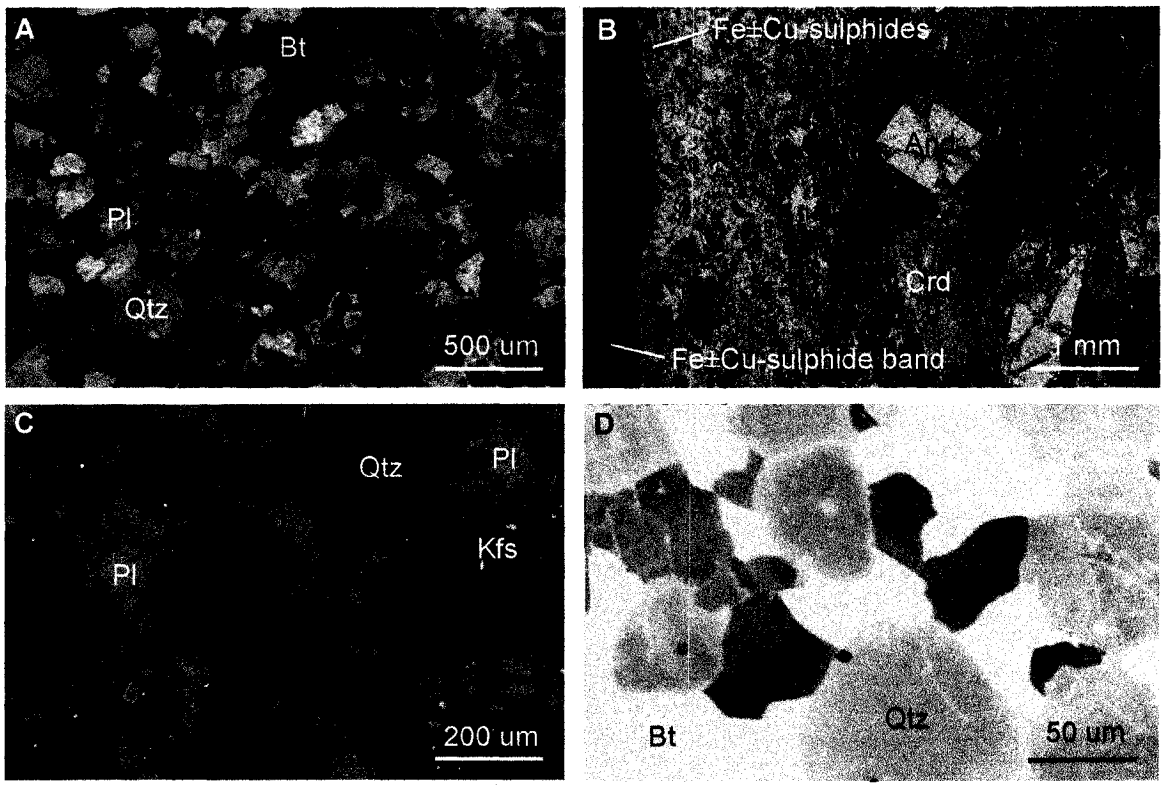

Figure 4.8: Photomicrographs of characteristic metapsammitic and metapelitic rocks of the Meguma Group. A) Metapsammitic rock, dominated by small, subhedral quartz and plagioclase, and stubby biotite. Photo with crossed polarizers. Sample E 430V. B) Metapelitic rock, consisting of a matrix of muscovite, biotite, quartz, plagioclase, K-feldspar, and cordierite, and porphyroblasts of andalusite, cordierite, and Fe±Cu-sulphides. Photo with plane polarized light. Sample H-03. C) Color CL image of a metapsammitic rock of the Meguma Group. Quartz shows a dark blue color, plagioclase is turquoise, and K-feldspar has a light blue color. Orange colors mark accessory minerals. Sample E 430V. D) SEM-CL image of a metapsammitic rock of the Meguma Group. Quartz and plagioclase show a patchy pattern and abundant healed microfractures. Mineral abbreviations after Kretz (1983). Sample E 430-Exp.

4.4.2.2 Metapsammitic and Metapelitic Xenoliths in the SMB

The mineralogy and textures of most metapsammitic xenoliths and the finer-grained metapelitic xenoliths are similar to those of the equivalent metasedimentary rocks of the Meguma Group away from the contact with the SMB. However, they are coarser-grained, and <1 m away from the contact with the SMB, anhedral K-feldspar, plagioclase, or quartz crystals commonly occur around the assemblage of equant grains.

4.4.2.3 Contacts between Metasedimentary Rocks and SMB

Contact Zones of Metapsammitic Rocks

Metapsammitic rocks with sharp contacts against the SMB are irregular on the grain-scale, and may be embayed along grain boundaries of the country-rock assemblage (Fig. 4.9A). Metapsammitic rocks with a fine-grained (≤50 μm) to coarse-grained (≤2 mm) assemblage have small as well as large crystals of quartz, plagioclase, K-feldspar, and biotite (Fig. 4.9B,C). Minor cordierite and garnet crystals that are texturally similar to the equivalent minerals in the metasedimentary rocks away from the contact zone may also be present. The small crystals of these contact zones typically occur as grain clusters, as inclusions in the large crystals, or as single grains. The large crystals within the contact zone show subhedral to euhedral outlines, and are texturally similar to the equivalent crystals in the SMB.

Contact Zones of Metapelitic Rocks

The metapelitic rocks that are mineralogically similar to the metapelitic rocks away from the contact show a sharp contact with the SMB, inclusions of grains common to the metapelitic rocks being abundant in the adjacent magmatic crystals (Fig. 4.10A). Metapelitic rocks with texturally and mineralogically distinct contact zones consist of medium to large, subhedral, inclusion-rich cordierite and K-feldspar, quartz, plagioclase, ± Fe±Cu-sulphides, ± andalusite, ± biotite, ± muscovite, ± Fe-Ti-oxides, and ± garnet (Fig. 4.10B). In these zones, biotite and muscovite are rare relative to the metapelitic rocks away from the contact with the SMB, and quartz and plagioclase of small to medium size occur interstitially, where quartz is subhedral and plagioclase subhedral to euhedral (Fig. 4.10C).

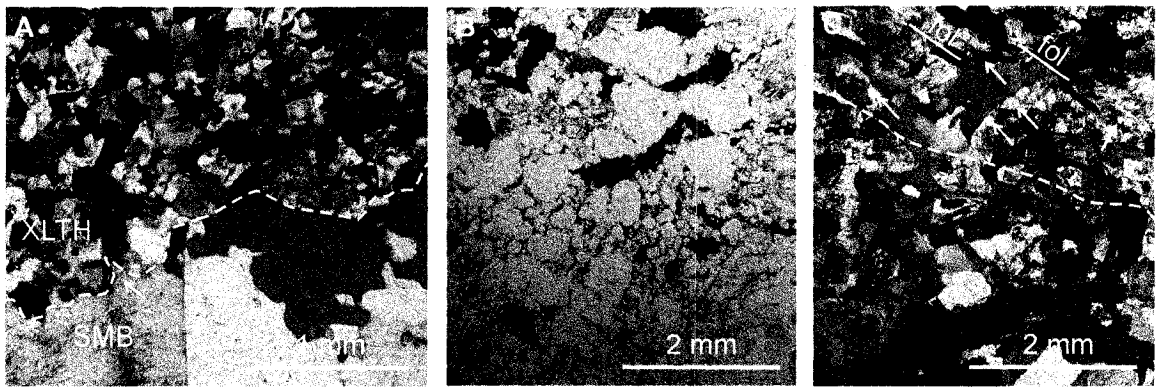

Figure 4.9: Photomicrographs of contacts between metapsammitic rocks and SMB. A) Sharp contact, marked by stippled line. Arrows mark embayment along grain boundaries of the country-rock assemblage. Photo with crossed polarizers. Sample E 430W. B) Gradational contact zone within a metapsammitic rock, consisting of small to large crystals, dominated by small crystals. Photo with plane polarized light. Sample E 429. C) Gradational contact dominantly consisting of a coarse-grained assemblage. Dashed line marks the contact approximately. Arrows mark some of the small crystals within the metasedimentary material, which are more common in the metapsammitic rock than in the SMB. Biotite of the metasedimentary rock shows a preferred orientation (fol = foliation), whereas biotite in the host is largely randomly oriented. Photo with crossed polarizers and gypsum plate. Sample Stop 1.2.

4.4.2.4 Contact Zones of SMB Rocks

Biotite-rich SMB contact zones against metapsammitic and metapelitic rocks have randomly oriented biotite (Fig. 4.11). The biotite normally forms clusters of up to 1 cm in size, the grains of which have abundant inclusions of apatite, zircon, monazite, ± Fe-Ti-oxides, ± quartz, ± plagioclase, and ± Fe±Cu-sulphides. Plagioclase- and K-feldspar-rich SMB contact zones have abundant medium-grained, subhedral to euhedral, inclusion-rich crystals (Fig. 4.10A). Cordierite-rich SMB contact zones involve subhedral to euhedral, medium to large, inclusion-poor cordierite crystals, but subhedral, inclusion-rich cordierite and K-feldspar crystals as well as large andalusite crystals, similar to those of the metapelitic rocks, may also occur in these contact zones (Fig. 4.10B,C).

Twins, deformation textures, and CL patterns of quartz (undulose extinction, dark blue CL color, patchy CL pattern), plagioclase (polysynthetic twins, undulose extinction, turquoise CL color, patchy CL pattern), K-feldspar (undulose extinction, light blue CL color, patchy CL pattern), and cordierite (sector twins) in the country rocks, country-rock and SMB contact zones, and SMB host rocks are similar.

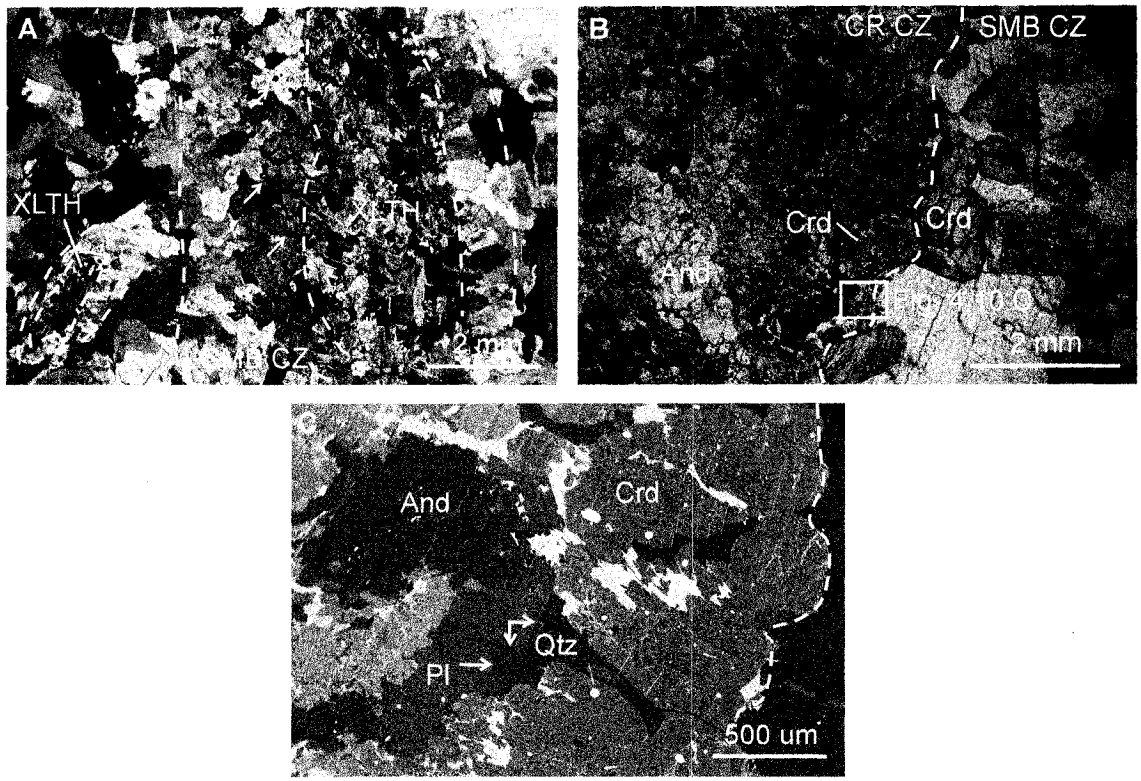

Figure 4.10: Photomicrographs of contacts between metapelitic rocks and SMB. A) Sharp contacts between two micro-xenoliths and granodiorite. The contact between common SMB granodiorite and metapelitic xenoliths is plagioclase- and K-feldspar-rich. Arrows mark some plagioclase and K-feldspar crystals with abundant small inclusions. Photo with crossed polarizers and gypsum plate. Sample E 436B. B) Cordierite- and K-feldspar-rich country-rock contact zone (CR CZ) with a cordierite-rich SMB contact zone (SMB CZ). Cordierite is highly pinitized. Photo with plane polarized light. Sample E 433. C) BSE image of cordierite- and K-feldspar-rich contact zone from the location shown in Fig. 4.10B. Quartz and plagioclase occur interstitial to cordierite and andalusite; plagioclase has subhedral to euhedral outlines. Sample E 433.

4.4.2.5 Garnet-rich Layers

Garnet-rich layers have abundant large, subhedral garnet crystals. The garnet crystals are typically intergrown with small biotite crystals, and may be rimmed by medium to large biotite grains (Fig. 4.12). Common inclusions in the garnet and biotite are Fe-Ti-oxides and apatite, and rarely Fe±Cu-sulphides. Cordierite occurs as medium to large, subhedral crystals, with inclusions of biotite, minor quartz, or Fe-Ti-oxides. Andalusite is rare, forming anhedral crystals that are typically rimmed by muscovite or K-feldspar.

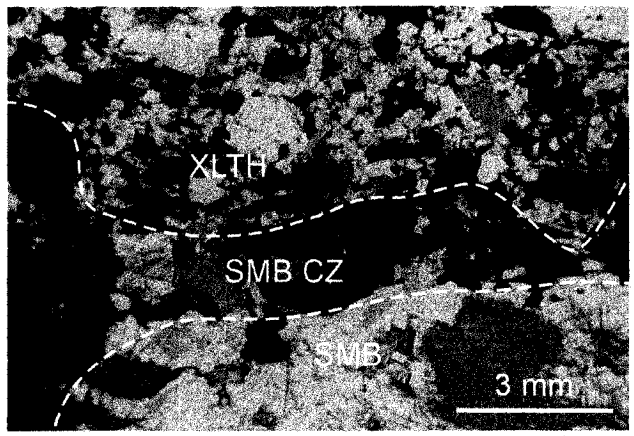

Figure 4.11: Biotite-rich SMB contact zone. Biotite in the contact zone (SMB CZ) is significantly larger in size than biotite in the metasedimentary xenolith (XLTH), and randomly oriented. Photo with plane polarized light. Sample E 430-II.

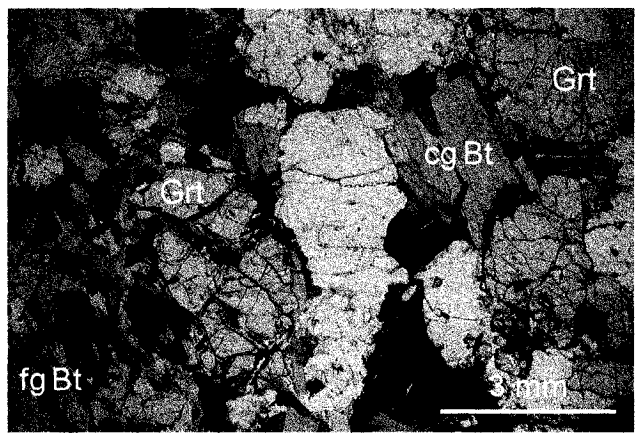

Figure 4.12: Photomicrograph of a garnet-rich layer. Garnet (Grt) is subhedral, and intergrown with small biotite crystals (fg Bt). Large biotite crystals (cg Bt) form typically clusters, and is commonly in contact with garnet crystals. Photo with plane polarized light. Sample E 465A.

4.5 Discussion

4.5.1 Metapsammitic and Metapelitic Xenoliths in the SMB

The fine-grained metapsammitic and metapelitic xenoliths in the SMB are rocks of Meguma Group origin that experienced little or no partial melting, and only minor grain-coarsening compared to the *in situ* Meguma Group rocks near the SMB contact. Sharp contacts of most *in situ* country rocks and xenoliths against the SMB show that incorporation of country rocks largely occurred through fracturing, where the xenoliths occur dominantly close to the external margin of the batholith (Fig. 4.1). Moreover, the xenoliths appear to occur near their site of formation (e.g., metapelitic near the exposed

contact with metapelitic *in situ* country rocks), suggesting that country-rock contamination at the exposed level of the batholith played at least some role in the evolution of the SMB magmas.

4.5.2 Contacts between Metasedimentary Rocks and SMB

Contact zones between the rocks of the Meguma Group and the SMB rocks reveal potential contaminants and evidence for assimilation reactions and their mechanisms. The garnet-rich layers, and texturally and/or mineralogically distinct zones in the SMB, may contain products of country-rock assimilation, but these zones may also represent accumulations of primary magmatic crystals. Xenocrysts within the SMB rocks may consist of two populations, "old" and "new" solids, which we define as "orthoxenocrysts" (original, subsolidus assemblage of rocks of the Meguma Group), and "paraxenocrysts" (crystals that formed from Meguma Group material in a peritectic melting reaction), respectively (Erdmann and Clarke 2005). Primary magmatic crystals from the contact zones between the metasedimentary and magmatic rocks, but also elsewhere in the batholith, may have a cognate, a hybrid, or a foreign magmatic origin. Below, we discuss our observations on the various contact zones studied, suggest mechanisms for their formation, and infer the products of country-rock contamination and assimilation. Table 4.1 summarizes the disintegration and assimilation mechanisms we infer, and the origin of minerals in the country-rock contact zones as well as in the garnet-rich layers.

4.5.2.1 Contact Zones of Metapsammitic Rocks

The sharp contacts between metapsammitic and SMB rocks represent fracture surfaces, potentially modified by minor partial melting or dissolution, resulting in the embayment of some of the grain boundaries of the country-rock assemblage (Fig. 4.13A). The contact may mark the original fracture surface, along which the xenolith detached from the *in situ* metasedimentary country-rocks of the SMB, or it may mark a modified fracture surface that stabilized after smaller xenolithic fragments or orthoxenocrysts separated from the main xenolith through fracturing, or through loss of cohesion along melt-wetted grain boundaries.

The contact zones between metapsammitic rocks and SMB rocks showing small to large crystals, but dominantly small crystals, are the result of disintegration of the metasedimentary rocks through fracturing, partial melting, or a combination of both processes, and subsequent mixing of the disintegrated country rock material and host

magma (Fig. 4.13B). We interpret the fine-grained assemblage as country-rock crystals, forming either small xenoliths or orthoxenocrysts, and the medium- to coarse-grained assemblage as magmatic, as suggested by the euhdreal grain shapes of plagioclase, and other textural features such as oscillatory zoning. Embayments (Fig. 4.9A), as well as anhedral crystals of K-feldspar, plagioclase, or quartz around the small, equant crystals are evidence for minor partial melting or dissolution of country-rock crystals (e.g., Rosenberg and Riller 2000; Sawyer 2001; Marchildon and Brown 2002). The breakdown of muscovite, which is present in minor amounts in most metapsammitic rocks (except in the contact zones), and minor partial melting of the assemblage of K-feldspar, plagioclase, and quartz, most likely facilitated the disintegration of the country rocks along melt-wetted grain boundaries. In addition, disintegration of the country rocks may have been driven by reaction-induced fracturing (Connolly et al. 1997; Rushmer 2001), or by the injection of SMB melts along grain boundaries of the country-rock assemblage. Unequivocal evidence for these processes is not preserved.

The contact zones between metapsammitic rocks and SMB rocks showing small to large crystals, but dominantly large crystals, may represent metapsammitic material that experienced partial melting of several volume percent (Fig. 4.13C). As with the contact zones that have dominantly small crystals, we interpret the small minerals as the residual metamorphic assemblage. We suggest that the medium to large crystals of quartz, plagioclase, and K-feldspar represent former melt, because they show characteristic magmatic textures (e.g., euhedral crystal faces). Medium to large biotite occurs typically parallel to the layering, and we therefore suggest that the medium-grained biotite crystals are not new magmatic crystals, but that they are metamorphic grains that have increased in grain size. Small inclusions of plagioclase, quartz, and K-feldspar in the magmatic assemblage, and the lack of prograde muscovite, peritectic garnet or peritectic cordierite, suggest that partial melting occurred through the consumption of K-feldspar, plagioclase, quartz, and ±muscovite. Some of the xenoliths show evidence for the presence of up to ~30 vol% melt, probably representing partial melt derived from the xenolith as well as injected SMB melt.

4.5.2.2 Contact Zones of Metapelitic Rocks

All contacts between metapelitic rocks of the Meguma Group and the SMB (Fig. 4.13D) show a reaction relationship involving former partial melting. The metapelitic contact zones that are mineralogically similar to the metapelitic rocks away from the contact with

the SMB, but coarser-grained, are zones of minor partial melting (Fig. 4.13E). Inclusion-rich K-feldspar and rare sillimanite in these metapelitic contact zones are consistent with partial melting through minor muscovite-dehydration melting, sillimanite having been largely replaced by muscovite during cooling.

Metapelitic contact zones that have inclusion-rich cordierite and K-feldspar, with interstitial subhedral quartz and euhedral plagioclase are inferred to be the result of partial melting, the euhedral shapes of plagioclase and interstitial quartz indicating crystallization from a melt (Fig. 4.13F). The scarcity of biotite within the contact zone, and the abundance of Fe-Ti-oxides suggest that the melting reaction involved biotite, forming peritectic cordierite, K-feldspar, and Fe-Ti-oxides. The inclusion-rich cordierite and K-feldspar crystals, as well as Fe-Ti-oxides, occur not only within the country-rock contact zone, but also within the surrounding granite. Disintegration or dispersal of the metapelitic assemblage thus occurred through reaction-induced fracturing (Connolly et al. 1997; Rushmer 2001), along melt-wetted grain boundaries, or as a result of the injection of SMB melts along grain boundaries of the country-rock assemblage. The products of the partial assimilation of the cordierite-rich metapelitic rocks are dominantly orthoxenocrysts of andalusite (Clarke et al. 2005), quartz, and plagioclase, paraxenocrysts of inclusion-rich cordierite and K-feldspar, as well as a silicate partial melt.

4.5.2.3 Contact Zones of SMB Rocks

The biotite-rich SMB contact zones (Fig. 4.14A) can have two probable origins. They may be the relics of partial assimilation of country rocks, or they may be the result of preferential nucleation or adhesion of cognate magmatic biotite on, or near, the surface of country rocks. If these rims result from country-rock assimilation, the biotite would have a completely or partially foreign origin (orthoxenocryst or paraxenocryst), but concerns about this explanation are: (i) the scarcity (<1 vol%) of orthoxenocrystic quartz or plagioclase in most of the biotite-rich contact zones (melting of the felsic country-rock assemblage would have to be nearly complete); (ii) that the biotite-rich zones occur along the various characteristic contacts with metapsammitic and metapelitic rocks, including contacts that show little or no evidence for former partial melting (Fig. 4.14A); and (iii) the high modal abundance of biotite of up to ~80 vol% in some of the contact zones (former country-rock partial melt must have been largely removed).

Table 4.1: Mechanisms of disintegration and assimilation, and the origin of minerals within country-rock contact zones and garnet layers

Characteristics	Figure	Mechanism of assimilation	Inferred melting reaction	Orthoxenocrysts	Paraxenocrysts	Former partial melt
Metapsammitic rocks						
Sharp contact	4.13A	fracturing	no reaction apparent	± fg Qtz, Pl, Bt, Kfs, Crd	-	-
Contact with fg to cg XLs, dominated by fg XLs	4.13B	fracturing, minor partial melting	Pl + Kfs + Ms + Qtz = L ± Kfs	fg Qtz, Pl, Bt, ± Kfs, ± Crd	± incl-rich Kfs (± Sil)	mg and cg Qtz, Pl, Bt, Kfs
Contact with fg to cg XLs, dominated by cg XLs	4.13C	significant partial melting	Pl + Kfs + Ms + Qtz = L ± Kfs	fg Qtz, Pl, ± Kfs, ± Crd, fg to cg Bt	± incl-rich Kfs (± Sil)	mg and cg Qtz, Pl, Kfs
Metapelitic rocks						
Contact with fg to mg XLs, Ms and incl-rich Kfs	4.13E	fracturing, minor partial melting	Ms + Pl + Kfs + Qtz = L ± Kfs	fg Qtz, Pl, Bt, ± Kfs, ± Grt, ± Crd	± incl-rich Kfs (± Sil)	mg and cg Qtz, Pl, Bt, Kfs
Contact with fg to mg XLs, abundant incl-rich Crd and Kfs	4.13F	significant partial melting	Ms + Bt + Qtz + Pl = Crd + Kfs + Fe-Ti-oxides + L	fg Qtz, Pl, Bt, ± Kfs	incl-rich Crd, Kfs	mg and cg Qtz, Pl, Bt, Kfs
Grt-rich layers						
Diffuse	4.13H,I	significant partial melting	Bt + And /Sil + Pl + Ms + Qtz = Grt + L	fg Qtz, Bt, ± Pl, fg-mg Crd	Grt	mg and cg Qtz, Pl, Bt, Kfs

XL = crystal; mineral abbreviations after Kretz (1983); fg, mg, cg = fine-, medium, and coarse-grained.

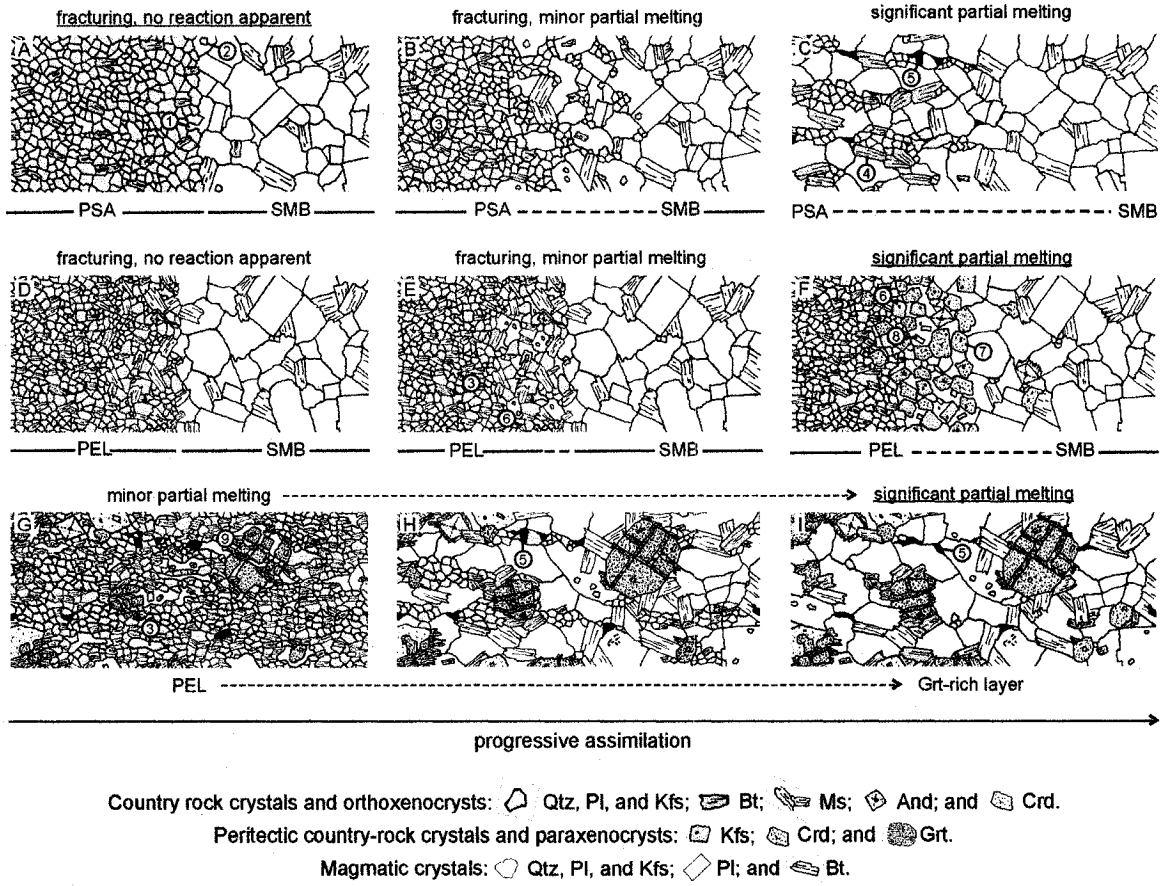

Figure 4.13: Interpretation of textural and mineralogical characteristics of the contact zones between metasedimentary rocks of the Meguma Group and SMB rocks. A-C) Contact relations between metapsammitic rocks of the Meguma Group and SMB. D-F) Contact relations between metapelitic rocks of the Meguma Group and SMB. Contact relations similar to D do not exist. G-I) Suggested formation of the garnet-rich layers. Relations sketched in G and H have not been observed. 1 = Embayment in the country-rock assemblage, indicating minor partial melting or dissolution. 2 = Orthoxenocrysts. 3 = Crystals formed from country-rock partial melt, marking sites of minor partial melting. 4 = Large biotite resulting from grain-coarsening. 5 = Fe±Cu-sulphides. 6 = Peritectic cordierite. 7 = Peritectic K-feldspar. 8 = New magmatic plagioclase, formed from a country-rock partial melt. 9 = Peritectic garnet.

If the biotite rims on xenoliths result from preferential nucleation and growth of primary magmatic biotite on the surface or in the vicinity of country rocks, xenoliths, and xenocrysts, they may have grown as a result of local under-cooling, possibly in combination with minor partial melting or dissolution of the country-rock assemblage. Similar textural relationships, such as monomineralic or polymineralic contact zones around xenoliths or enclaves consisting of minerals common to the magmatic host, or quartz-biotite ocelli, have been interpreted as a result of adherence by surface tension or as a phenomenon of local under-cooling in combination with minor dissolution (e.g.,

Vernon 1991; Barbarin and Didier 1991; Hibbard 1991). Alternatively, biotite may have adhered to the surface of xenoliths and xenocrysts while these traveled through the magma chamber.

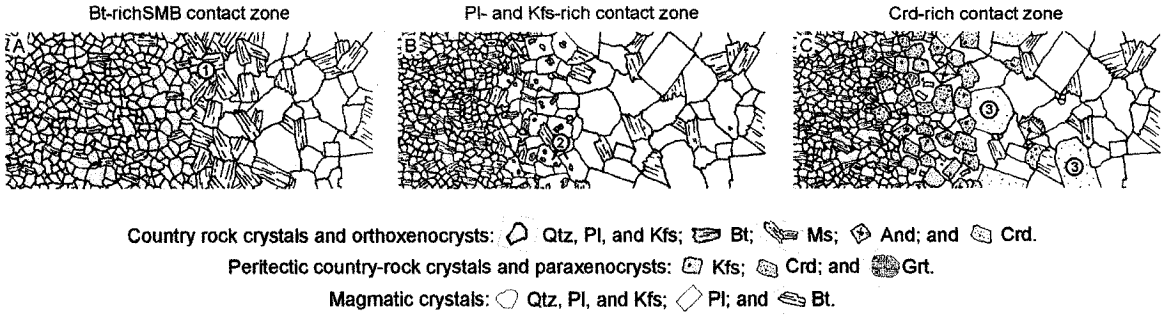

Figure 4.14: Characteristic SMB contact zones. A) Biotite-rich contact zone between metasedimentary rocks and SMB. B) Plagioclase- and K-feldspar-rich contact zone, characteristic of contacts between metapelitic rocks and SMB. C) Cordierite-rich contact zone, characteristic for contacts between metapelitic rocks and SMB. 1 = Large biotite. 2 = Medium-grained, inclusion-rich plagioclase and K-feldspar. 3 = Magmatic cordierite. We currently conclude that the biotite-rich contact zones are a result of under-cooling and preferential nucleation of biotite on the surface or near country-rock material, whereas the plagioclase- and K-feldspar-rich as well as the cordierite-rich contact zones are probably a result of partial melting of the country-rock material and diffusive elemental exchange between the country-rock partial melt and the host magma.

The plagioclase- and K-feldspar-rich contact zones around some xenoliths (Fig. 4.14B) probably reflect minor partial melting of the country-rock material, and preferential crystallization of plagioclase and K-feldspar in the mixing zone between country-rock partial melt and main magma as a result of migration of chemical species from the country-rock partial melt into the main magma. Small mineral inclusions of biotite, quartz, and plagioclase indicate the partial consumption of the metamorphic assemblage, whereas the subhedral to euhedral outlines of the plagioclase and K-feldspar crystal suggest a magmatic origin. Experiments involving the melting of metapelitic rocks of the Meguma Group in contact with a haplogranite at 700 °C produce abundant K-feldspar crystals along the contact between the materials, mimicking the observed feldspar-rich SMB contacts of the natural examples (Chapter 3). In agreement with the melting experiments, we infer that the feldspar-rich SMB contact zones formed as a result of diffusive elemental exchange between a country-rock and the SMB melt phase at relatively low magmatic temperatures, and thus during a late stage of the magmatic evolution of the SMB.

The cordierite-rich SMB contact zones contain dominantly inclusion-poor cordierite crystals that are texturally distinct from the inclusion-rich paraxenocrystic cordierite (Fig. 4.14C). We infer that contamination of the SMB magmas by components derived from a highly peraluminous country-rock partial melt of the metapelitic rocks permitted the crystallization of the cordierite crystals, and thus have a similar origin as the plagioclase- and K-feldspar-rich SMB contact zones. Melting experiments, which were designed to mimic the contamination of SMB magmas by metapelitic rocks of the Meguma Group, support this interpretation (Chapter 3). The experiments produce new magmatic cordierite in the melt fraction of the SMB material only near the contact with the metapelitic contaminants, where glass analyses of the run products signify diffusive exchange of elements between the melt phase derived from the metapelitic material and the melt phase derived from the SMB material, resulting in a hybrid melt with a composition that is apparently favorable for the crystallization of cordierite.

4.5.2.4 Garnet-rich Layers

We interpret the garnet-rich layers as the result of the assimilation of metapelitic country rocks with ≥70 vol% partial melting (Fig. 4.13G-I). The subhedral, large garnet crystals, characteristic of these zones, do not occur in Meguma Group country-rocks without evidence of partial melting, and we therefore infer that the garnet formed in a peritectic melting reaction. Small biotite crystals, dominantly intergrown with garnet, and small quartz and plagioclase crystals within the diffuse, garnet-bearing contact zones, are inferred to be the relics of the country rock assemblage. Aluminosilicates are ubiquitous in the metapelitic country-rocks, but rare in the garnet-rich layers. Their scarcity may suggest consumption during melting, as well as during cooling (retrograde consumption by muscovite). Inclusion-rich cordierite of country-rock origin is abundant in the garnet layers, where grain shapes do not indicate partial consumption. Medium-grained quartz, plagioclase, K-feldspar, and biotite are inferred to be of primary magmatic origin, and to have crystallized from a melt consisting of country rock and SMB components.

The garnet-rich layers most likely represent former layers of metapelitic rocks that were compositionally different from the metapelitic rocks that formed the cordierite-rich contact zones (e.g., relatively rich in Fe and possibly rich in Mn). The assimilation of these layers must have been more efficient than the assimilation of most metapelitic Meguma Group rocks, because intermediate stages of assimilation, such as those shown for

metapsammitic and metapelitic Meguma Group rocks in Figures 4.13G and H, have not been observed.

4.5.3 Importance of Metapsammitic and Metapelitic Contaminants in the SMB

4.5.3.1 Metapsammitic and Metapelitic Xenoliths

Xenoliths have an overall abundance of ~2 vol% in the marginal rocks of the SMB (<200 m away from the exposed contact), and <1 vol% in the more central SMB rocks. Metapsammitic xenoliths dominate over metapelitic xenoliths with ~10:1, compared to a ratio of ~1:1 for metapsammitic and metapelitic *in situ* country rocks. This relation may reflect the larger volume of metapsammitic to metapelitic rocks in contact with the SMB below the exposed surface (e.g., Culshaw and Bhatnagar 2001; Culshaw and Lee 2006), the preferential incorporation of metapsammitic rocks into the SMB, and/or the preferential assimilation of the metapelitic contaminants. The dominant occurrence of metapsammitic xenoliths in the vicinity of the *in situ* metapsammitic rocks, and the dominant occurrence of metapelitic xenoliths in the vicinity of the in situ metapelitic rocks suggests that a large amount of the exposed xenoliths were trapped near their site of formation. The abundance of the metapsammitic and metapelitic xenoliths should thus reflect the abundance of the exposed *in situ* metapelitic and metapsammitic rocks, ruling out that the incorporation of larger volumes of metapsammitic xenoliths at depth dominantly determined the high ratio of metapsammitic to metapelitic xenoliths. The dominance of the metapsammitic over the metapelitic xenoliths may instead be the result of preferential incorporation of metapsammitic xenoliths, or the preferential assimilation of the metapelitic xenoliths.

4.5.3.2 Potential Orthoxenocrysts

Schlieren of fine-grained country-rock material, representing country-rock xenoliths in an early stage of disintegration, are rare throughout the batholith («1 vol%); the length and the width of the observed schlieren are typically <1 dm. Single grains in the SMB rocks that may have an orthoxenocrystic origin are also rare, but they vary in abundance between the various rock types and spatially within the different rock units. Granodiorites exposed along the northern contact of the SMB have ≤2 vol% crystals of potentially orthoxenocrystic origin (Fig. 4.15A). Alternatively, some monzogranites and leucogranites, which usually occur further away from the external contact of the SMB,

have up to ~30 vol% of small crystals that are texturally similar to grains of the Meguma Group rocks (Fig. 4.15B). However, the small crystals of the monzogranites and leucogranites are dominated by K-feldspar, and given that K-feldspar is rare in the Meguma Group country rocks as well as in the source rocks of the SMB, they are unlikely of orthoxenocrystic origin. Therefore, we suggest that most of the small crystals of the monzogranites and leucogranites represent primary magmatic crystals, and not country-rock material. Alternatively, potential orthoxenocrysts in the granodiorites consist dominantly of quartz and plagioclase, as well as some of the cordierite, garnet, and andalusite, which are common rock-forming minerals of the Meguma Group country rocks.

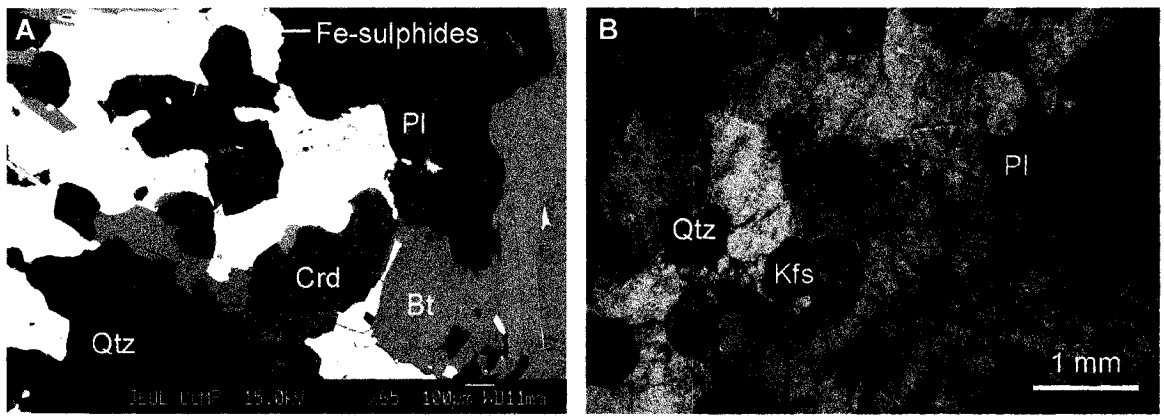

Figure 4.15: Texturally similar crystals of various origins. A) Small crystals in a Meguma Group xenolith. BSE image. Sample H-03. B) Small magmatic crystals in a leucomonzogranite of the SMB. Photo with crossed polarizers. Sample E 943.

Despite the uncertainties in identifying all orthoxenocrysts in the SMB rocks, assuming that all suspect minerals are orthoxenocrysts, and that no orthoxenocrysts were overlooked with the methods used, we infer that the marginal units of the SMB comprise ~2 vol% of orthoxenocrysts. Evidence for contamination in the form of xenoliths, paraxenocrysts (as outlined below), and unequivocally detectable orthoxenocrysts, such as cordierite and garnet is less common in the monzogranites and leucogranites of the SMB than in the marginal and more primitive SMB rocks. We therefore suggest that orthoxenocrysts are probably also less common (≤2 vol%) in the monzogranites and leucogranites than in the marginal rocks of the batholith.

4.5.3.3 Potential Paraxenocrysts

Schlieren comprising abundant paraxenocrystic garnet, and single paraxenocrystic garnet crystals throughout the SMB rocks, account for <1 vol%, of the studied rocks, but in the marginal units of the SMB, garnet schlieren may make up ~2 vol%. The garnet schlieren are several cm to <5 m in length, with widths varying between a few cm and <2 m. The orientation of the garnet-rich schlieren is random, but they are more common near the exposed SMB contacts against the metapelite-dominated Halifax Formation of the Meguma Group than against the metapsammite-dominated Goldenville Formation.

The cordierite-rich zones, with >1 vol% to ~5 vol% cordierite, which were suggested to possibly mark zones with a high degree of country-rock contamination, occur throughout the SMB, but are most common in the Halifax Pluton of the SMB, where they make up ~30 % of the mapped area (Fig. 4.1; MacDonald 2001). They are several km in length and several hundred metres wide. Given the poor outcrop situation away from road cuts and the coast, their spatial distribution can only be considered as approximate, and apparent crosscutting relations, as outlined in Figure 4.1, may not be correct (personal communication M.A. MacDonald, Department of Natural Resources, Nova Scotia, 2005). The cordierite grains of the cordierite-rich zones are dominantly euhedral and inclusion-poor (≥98 %), and are probably of primary magmatic origin (Erdmann et al. 2004). Based on textural analysis alone, we cannot unequivocally determine whether the magmatic cordierite grains are dominantly of foreign or dominantly of cognate magmatic origin, but we suggest that most of the euhedral cordierite crystals are primary magmatic, and that they do not represent evidence for the *in situ* assimilation of Meguma Group rocks in these zones. Evidence against significant amounts of foreign material in the cordierite-rich zones, and therefore in the cordierite grains themselves, is the spatial occurrence of the schlieren, as well as the scarcity of xenoliths, orthoxenocrysts, or paraxenocrystic cordierite in the schlieren. If the cordierite-rich zones represent xenoliths or largely assimilated septa of Meguma Group rocks, they should be spatially related to the metapelite-dominated Halifax Formation of the Meguma Group country rocks, similar to the relationship that exists between garnet schlieren and the metapelitic *in situ* rocks of the Meguma Group. Moreover, the scarcity of xenoliths, orthoxenocrysts, and paraxenocrysts in the cordierite-rich zones would require more or less complete physical and chemical assimilation of the country-rock contaminants through melting, dissolution, or spatial separation of physically "visible" solid contaminants and physically "invisible" former liquid contaminants, and although all these processes may have played a role,

they are unlikely to have erased the mineralogical evidence for country-rock contamination. The observation that assimilation of metapelitic Meguma Group country rocks through partial melting along the exposed contact with the batholith occurred only over zones of less than a few metres suggests that the heat that would have been required to melt Meguma Group contaminants, resulting in the formation of up to several kilometre thick cordierite-rich zones, was not available in the system. The most likely interpretation of the cordierite-rich zones is that they formed as a result of fractional crystallization of cognate magmatic material, with little or no contribution from exposed Meguma Group country-rock material (MacDonald and Horne 1988; MacDonald 2001). The high abundance of K-feldspar megacrysts in these zones may be further evidence for the physical concentration of the large cordierite crystals.

Paraxenocrystic K-feldspar and sillimanite are rare to absent in the SMB rocks studied («1 %). We infer that peritectic K-feldspar and sillimanite formed at relatively low magmatic temperatures, when the consumption of heat in the melting reactions may have caused final crystallization of the host magma, effectively freezing the system and the assimilation reactions, and permitting little or no dispersal of peritectic K-feldspar or cordierite.

4.5.3.4 Country-rock Silicate Partial Melt

The most difficult parameter to estimate is the importance of former silicate partial melt in the SMB derived from Meguma Group country-rock contaminants, because (i) the most important minerals that may have crystallized from a silicate partial melt derived from the Meguma Group country rocks are also ubiquitous to the granites, and (ii) because diffusive exchange between a country-rock-derived partial melt and the melt fraction of the main magma would have erased compositional differences that may have originally existed (Chapter 3). With our current knowledge, we can determine the amount of former partial melt derived from the Meguma Group country rocks only indirectly through the occurrence of orthoxenocrysts and paraxenocrysts. Orthoxenocrysts in the SMB are dominantly the products of the disintegration of metapsammitic Meguma Group rocks, formed through fracturing and/or partial melting in combination with loss of cohesion along melt-wetted grain boundaries. Orthoxenocrysts make up ~2 vol% of the marginal rocks, and we may have overlooked up to ~2 vol% of complementary silicate partial melt, assuming maximum liquid to solid ratios as determined in melting experiments at 800 °C and ~7 wt% H_2O, employing metapsammitic rocks of the Meguma Group (Chapter 3).

Paraxenocrysts in the SMB are dominantly the product metapelitic Meguma Group rocks, formed as a result of partial melting and subsequent dispersal. If it is correct that paraxenocrysts make up ~2 vol% of the marginal rocks, it is possible that we have overlooked up to ~8 vol% of complementary silicate partial melt, assuming maximum liquid to solid ratios as determined in melting experiments at 800 °C and ~7 wt% H_2O, employing metapelitic rocks of the Meguma Group, and also assuming a similar ratio of partial melt versus paraxenocrysts in the garnet and cordierite-forming melting reactions (Chapter 3).

4.5.3.5 All Contaminants

Unless selective contamination with a physically invisible partial melt occurred, the exposed marginal <200 m of the SMB may overall comprise a maximum of ~16 vol% of Meguma Group material, may contain of ~2 vol% xenoliths, ~2 vol% orthoxenocrysts, ~2 vol% paraxenocrysts, and up to ~10 vol% of a former silicate melt of Meguma Group origin. The more central rocks of the SMB probably contain a maximum of ≤8 vol% of Meguma Group material, consisting of ≤1 vol% xenoliths, ≤2 vol% orthoxenocrysts, ≤1 vol% paraxenocrysts, and ≤4 vol% of a former silicate melt of Meguma Group origin. However, xenoliths of various sizes, schlieren of fine-grained country-rock material, and garnet-schlieren can be easily identified in the field, and the amount of country-rock material disintegrated or assimilated to a degree to which it is macroscopically no longer evident, and likely to be unwittingly included in whole-rock geochemical analysis, is less than the estimated amount of country-rock contamination, on the order of ≤10 vol% for the marginal and ≤5 vol% for the central SMB rocks studied.

The amount of partially assimilated metapelitic material is higher than the amount of partially assimilated metapsammitic material, and the dominance of metapsammitic over metapelitic xenoliths in the SMB may thus at least partly be explained by a more efficient assimilation of the metapelitic rocks relative to the metapsammitic rocks. In all studied examples, assimilation of Meguma Group country rocks in the SMB involved at least minor partial melting, facilitating disintegration and dispersal of the country-rock material in the former host magmas. Assimilation of Meguma Group material through fracturing alone has certainly occurred to some degree, given that fracturing is a fractal process, which should have produced xenoliths of various sizes, as well as xenocrysts. However, fracturing of xenoliths down to the grain-scale (e.g., further disintegration of xenoliths

shown in Fig. 4.2B), driven by thermal stress fracturing as suggested by Clarke et al. 1998, has not been observed.

4.5.4 Physical versus Chemical Evidence for Contamination in the SMB

Our results agree with previous field observations (e.g., Jamieson 1974; MacDonald 2001) that country-rock contaminants are more abundant near the margin of the SMB, but apparently contradict with the possible interpretation of whole-rock Sr-Nd isotopic data that suggest that the most evolved rocks and typically more central units of the SMB contain more Meguma Group country-rock contaminants than the most primitive, and typically marginal rocks of the batholith (Clarke et al. 1988; Clarke et al. 2004; Clarke and Erdmann 2005). The hypothesis that country rocks of the Meguma Group are progressively more strongly assimilated from the margin toward the center of the SMB, leaving little macroscopically visible evidence for contamination in the most evolved rocks, but a whole-rock chemical signature indicating a high degree of contamination is impossible to rule out on physical evidence, but arguments against this hypothesis are strong. Our detailed study demonstrates that assimilation of Meguma Group country-rock material in the SMB is only partial, and that physical evidence for contamination by Meguma Group rocks remains in the form of refractory xenoliths and/or xenocrysts. If country-rock contamination and assimilation occurred dominantly at the exposed level of the batholith, less direct evidence, but a higher degree of contamination in the more evolved than in the more primitive rocks of the SMB can thus only be explained if xenocrysts dissolved more readily, or if spatial separation of xenoliths and xenocrysts on one hand, and country-rock partial melt on the other hand, were more efficient for the contaminants in the more evolved magmas than in the more primitive magmas of the SMB. More efficient dissolution of xenocrysts in the more evolved magmas is unlikely, because potential products of peritectic dissolution reactions, for example biotite (replacing garnet or cordierite), are rare to absent in the most evolved SMB rocks (e.g., <2 vol% biotite in leucogranites), but common in the marginal rocks. Spatial separation of solid and former liquid contaminants in the SMB magmas is theoretically possible, and may have been more efficient in the more evolved and more central than in the more primitive and marginal magmas of the SMB. However, solid contaminants such as quartz and plagioclase, as well as small crystals of biotite, garnet, and cordierite xenocrysts, should have separated less efficiently from the liquid contaminants than xenoliths, large biotite, garnet, or cordierite crystals, and should thus be abundant in the

central rocks of the SMB, if country-rock contamination were volumetrically significantly more important in the more evolved than in the more primitive rocks of the SMB.

Although uncertainties remain regarding the absolute amount of contamination, estimates of the relative importance of the contamination of SMB magmas by bulk Meguma Group rocks based on physical evidence are reliable. We therefore conclude that the isotopic signature of the more evolved SMB rocks either reflects selective contamination by Meguma-Group-derived partial melt at unexposed levels of the batholith, or variations in the source (Fig. 4.16).

Contributions from a Meguma Group source and selective contamination of SMB magmas by Meguma Group rocks may have had very similar effects on the exposed part of the batholith. However, if rocks of the Meguma Group became part of the source, refractory and peritectic phases mostly remained in the source (Vernon in press), and only partial melt and possibly minor solid phases would have become part of the SMB, whereas country-rock contamination would have contributed all solid and liquid phases to the SMB. Moreover, in the case of a Meguma Group source contribution, the heat for melting of Meguma Group rocks will have originated from mafic intrusions (e.g., Tate 1995; Clarke et al. 1997; Keppie and Krogh 1999), whereas in the case of country-rock contamination, the heat for melting of Meguma Group rocks will have originated from the SMB magma itself. Distinguishing between the two possible evolutionary scenarios is thus important in regard to better understand the mechanisms and the relative importance of emplacement mechanisms, as well as the thermal evolution of the SMB and its host and source rocks.

4.6 Conclusions

The findings of our study show that an approach combining field, textural, mineral chemical, and experimental data has the potential to characterize all country-rock contaminants in a given igneous rock. Although characteristic textural criteria to unequivocally determine the origin of every foreign crystal in the SMB have not been identified, using optical, backscattered-electron, and cathodoluminescence microscopy, we were able to estimate the importance of orthoxenocrysts and paraxenocrysts versus cognate magmatic minerals in the assemblages of the studied rocks. Field and textural relations have revealed evidence for contamination of the SMB by rocks of the Meguma Group in the form of xenoliths, orthoxenocrysts, paraxenocrysts, and former partial melt, and assimilation of the country-rock material through a combination of fracturing,

dispersal, partial melting, dissolution, and ion exchange reactions. Important country-rock contaminants derived from the metapelitic rocks of the Meguma Group in the SMB are paraxenocrystic garnet or cordierite, and former country-rock-derived partial melt. Important silicate country-rock contaminants derived from the metapsammitic rocks of the Meguma Group are orthoxenocrystic quartz, biotite, and plagioclase, as well as former partial melt.

Assuming that only bulk contamination occurred, and that spatial separation of the various country-rock contaminants was minimal, we estimate that country-rock contaminants of Meguma Group origin in the SMB amount to a maximum of ~16 and ~8 vol% in the marginal and more central rocks of the SMB, respectively. If so, country-rock contamination has played a role in the evolution of the SMB, but source variations, fractional crystallization, and/or fluid interaction are more important for explaining the mineralogical, textural, and chemical variation between the various rock types of the exposed batholith. However, if selective contamination of the exposed SMB rocks by country-rock partial melt was important, the amount of Meguma Group material occurring in the studied SMB rocks may be higher than estimated based only on physical evidence.

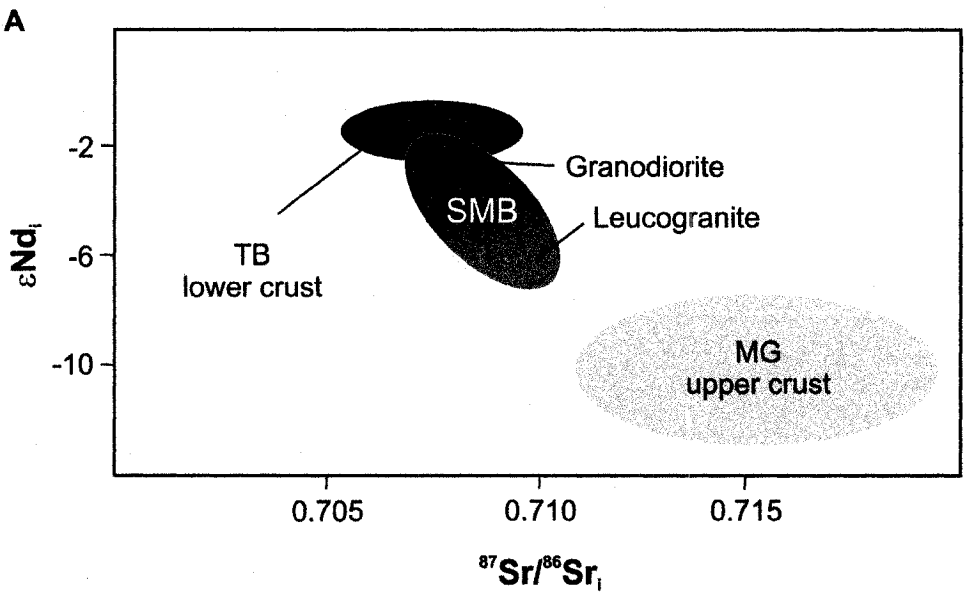

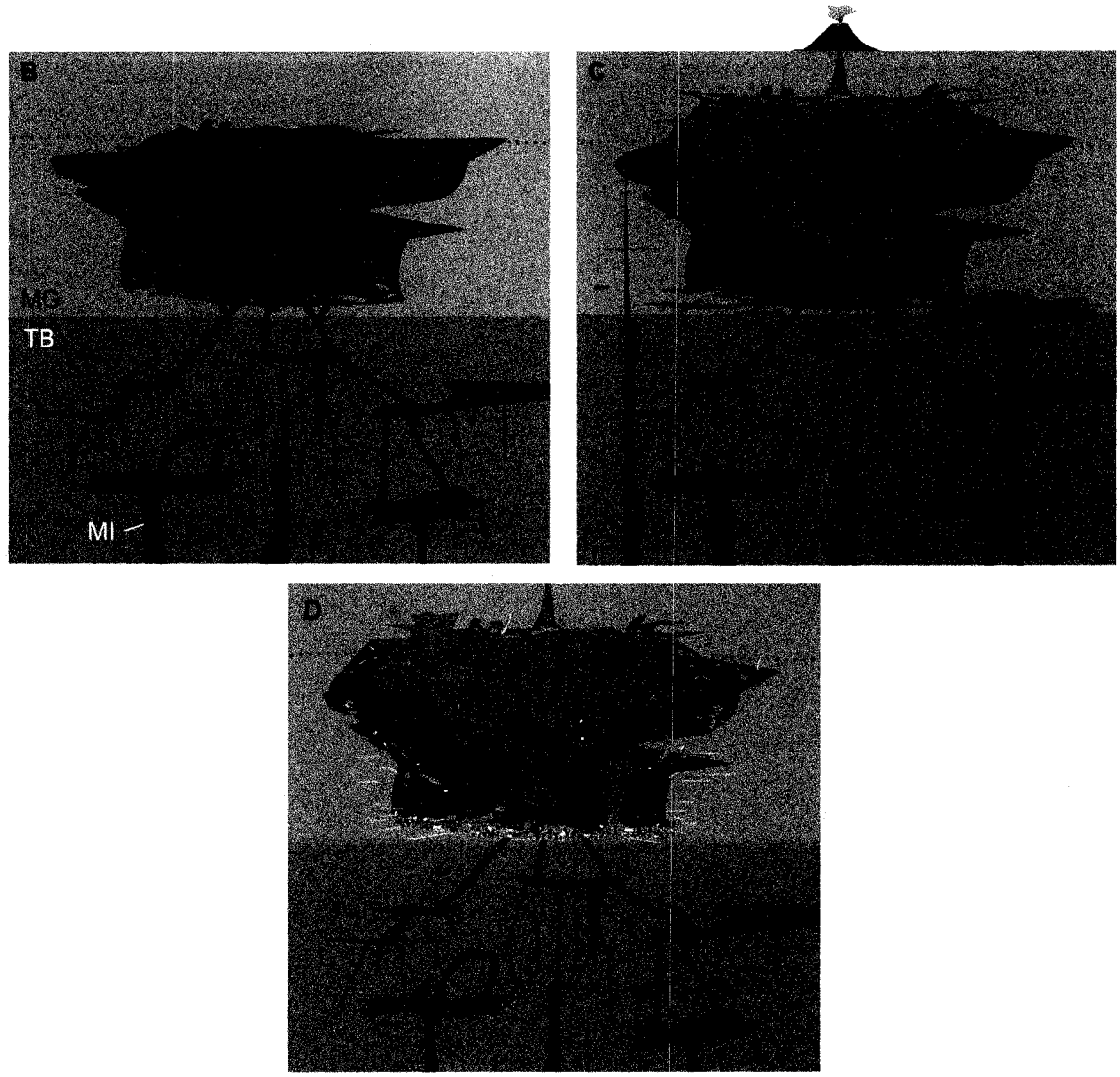

Figure 4.16: A) Nd and Sr isotopic compositions for rocks of the South Mountain Batholith (SMB), for rocks of the Tangier basement (TB), and for rocks of the Meguma Group (MG). Felsic rocks of the Tangier basement are the volumetrically most important source rocks of the SMB (Clarke et al. 1988; Owen et al. 1988; Eberz et al. 1991; Greenough et al. 1999). However, the isotopic composition of the leucogranite rocks relative to the granodiorites of the SMB suggest the presence of a higher degree of Meguma Group components in the more evolved than in the more primitive rocks, which may have become part of the SMB rocks as a result of a Meguma Group contribution to the source, or as a result of selective contamination of the evolving SMB magmas at unexposed levels of the batholith. B) Inferred petrogenetic evolution during the formation of the early, most primitive rocks of the SMB. Crustal thickening and mafic intrusions (MI) result in partial melting of lower crustal rocks, where the TB is the important, and possibly only source for the granodiorite SMB magmas. C) Source variations as an explanation for the isotopic signature of primitive versus evolved SMB rocks and the scarcity of physically detectable country-rock contaminants in evolved SMB rocks, where rocks of the Meguma Group became part of the SMB magma source during the late-stage evolution of the batholith. D) Country-rock contamination and assimilation, in combination with selective contamination of evolving SMB magmas by country-rock-derived partial melt at unexposed levels of the SMB.

4.7 Acknowledgements

An Izaak Walton Killam Memorial scholarship to S. Erdmann, and an NSERC Discovery Grant to D.B. Clarke made this study possible. We benefitted from numerous stimulating discussions with W.F. Caley, S. Carruzzo, R.A. Jamieson, J.H. Kruhl, M.A. MacDonald, S.R. Paterson, and R.H. Vernon on country-rock contamination and assimilation. We thank A. Dunn for support in the field, G. Brown for the polished thin sections, D. MacDonald and M. Robertson for assistance with the SEM-CL microscopy, and M. Poujol for help with the color CL microscopy. Informal reviews by J.S. Lackey and R.H. Vernon are greatly appreciated.

CHAPTER 5

Magma Chamber Processes Recorded in Compositions of Rock-forming Minerals: an Example from the Granitic South Mountain Batholith, Nova Scotia, Canada

5.0 Preamble

This chapter has been prepared for submission for publication in the *Journal of Geology* by S. Erdmann and D.B. Clarke. In this study, I have carried out all mineral chemical analyses, except for one set of trace-element analyses. I am responsible for the cluster analysis, wrote the manuscript, and prepared all Figures and Tables. D.B. Clarke discussed analytical approach and results with me, and provided productive comments which greatly improved the outcome of this study.

The main purpose of the mineral chemical investigation presented in this chapter was to test whether the textural classification of orthoxenocrystic, paraxenocrystic, and primary magmatic grains from the SMB rocks presented in Chapter 4 is valid, and to explore what other information can be discerned from the compositions and compositional zoning of the rock-forming minerals of the SMB. The overall objective was to deduce if, and how, mineral chemical analyses and textural analyses can be best combined to understand the causes of small- to large-scale compositional variations in igneous rocks.

5.1 Abstract

Major- and trace-element, and isotopic compositions of mineral phases in igneous rocks have the potential to provide detailed insights into magma chamber processes and to identify magma- and country-rock-derived components even in well mixed plutonic systems, in which evidence on a larger scale may be obscured. In this study, we present major-element compositions and trace-element compositions (V, Cr, Co, Ni, Zn, Ga, Ge, Rb, Sr, Y, Nb, Cs, Ba, La, Ce, Pr, Nd Sm, and Eu) of plagioclase, biotite, garnet, and cordierite from the South Mountain Batholith, from Meguma Group country rocks, and Tangier basement source rocks, determined by electron microprobe analysis and laser ablation inductively coupled mass spectrometry. In the SMB rocks, plagioclase, biotite, garnet, and cordierite have more than one origin. Plagioclase and biotite occur as orthoxenocrysts (crystals of the original country-rock assemblage) and primary magmatic crystals. Garnet and cordierite occur as orthoxenocrysts, paraxenocrysts (crystals formed in a reaction between country-rock material and host magma), and

(crystals formed in a reaction between country-rock material and host magma), and primary magmatic crystals. The analyzed major- and/or trace-element compositions of country-rock plagioclase, biotite, garnet, and cordierite are largely distinct from those of the equivalent primary magmatic mineral phases, whereas the compositional differences between xenolithic and primary magmatic crystals are minor to negligible, indicating diffusive reequilibration between country-rock material and SMB host magmas. Small plagioclase, biotite, and garnet orthoxenocrysts crystals were largely chemically assimilated by the SMB magmas through solid-liquid ion exchange reactions, whereas large garnet and cordierite paraxenocrysts have largely retained their original compositional signature. Major- and trace-element compositions of primary magmatic plagioclase record fractional crystallization, whereas biotite lost its compositional evidence for magma chamber processes as a result of diffusive reequilibration. We suggest that major- and trace-element zoning with a core, an intermediate, and a rim zone in garnet indicates magma recharge and possibly source variations, whereas oscillatory zoning in major element concentrations, but apparently not in trace element concentrations, in primary magmatic cordierite alludes to recurring events of magma eruption or fluid degassing during an intermediate stage of the chemical evolution of the SMB. Major-element and trace-element data for source-rock crystals show that restitic material inherited from the SMB source is absent or rare in the rocks studied. These results underline that mineral chemical evidence for the origin of small crystals, and minerals with diffusivities similar to plagioclase and biotite of the studied compositions, may be readily lost in plutonic magma systems. Therefore, it seems most important to determine the nature of the various components of an igneous rock based on textural criteria in combination with the compositional analysis of refractory and/or large crystals, as well as in combination with the analysis of major- and trace-element zoning patterns of the various crystal populations.

5.2 Introduction

Major-element, trace-element, and isotopic variations of igneous rocks may result from a combination of source variations, fractional crystallization, country-rock assimilation, and fluid flux. However, the relative and absolute importance of these various processes are largely unresolved for most igneous systems (e.g., Clemens 2003; Beard et al. 2005; Coleman et al. 2004; Davidson et al. 2005). Classically, field and textural data, whole-rock geochemical, and major-element mineral chemical analyses are the basis for

assessing the significance of the different system components and underlying processes, but rapid advances in microanalytical techniques permit increasingly more detailed insights into the extent and the timing of open-system magma chamber processes and the origin of the various rock components (e.g., Davidson et al. 1990, 2001; Simonetti and Bell 1993; Davidson and Tepley 1997; Cox et al. 1999; Knesel et al. 1999; Thomas 2000; Waight et al. 2000; Tepley and Davidson 2003; Dungan and Davidson 2004; Gagnevin et al. 2005; Beard et al. 2005; Costa and Dungan 2005; Ramos et al. 2005). To date, mineral-scale chemical analyses, performed to better understand the causes of compositional variations within igneous systems, have focused on minerals from volcanic systems (e.g., Davidson and Tepley 1997; Tepley et al. 1999, 2000; Knesel et al. 1999; Costa and Dungan 2005; Christiansen 2005; Lukacs et al. 2005; Wolff et al. 2005), and refractory and/or large crystals from plutonic systems (e.g., Bindeman and Valley 2003; Blundy and Shimizu 1991; Cox et al. 1996; Nelson et al. 2000; Waight et al. 2000; Erdmann et al. 2004; Gagnevin et al. 2005; van Breeman et al. 2005). The original chemical signature, and thus the origin of reactive and/or small crystals is more likely lost or obscured by diffusive reequilibration than the chemical signature of equivalent crystals in volcanic systems, or larger crystals of the same minerals. Hence, opportunities to unequivocally decipher the details of the genesis of various crystal populations, and therefore the genesis of the plutonic rocks, are far fewer.

The South Mountain Batholith (SMB) of southern Nova Scotia is a composite granitoid complex showing physical and chemical evidence for fractional crystallization, country-rock contamination and assimilation, fluid influx and loss, and possibly source variations (McKenzie and Clarke 1975; Muecke and Clarke 1981; Clarke and Halliday 1980, 1985; Clarke and Chatterjee 1988; Kontak et al. 1988; MacDonald et al. 1988; Horne et al. 1989; Ham et al. 1990; Poulson et al. 1991; Corey and Chatterjee 1992; Clarke et al. 1993; Clarke et al. 1997, Tate and Clarke 1997; MacDonald 2001; Clarke and Bogutyn 2003; Clarke et al. 2004). The batholith consists dominantly of granodiorite, monzogranite, leucomonzogranite, and leucogranite, all of which contain one or more of the common characteristic minerals of peraluminous granites (Clarke 1981; Allan and Clarke 1981; Maillet and Clarke 1985; Ding 1995; Clarke and Bogutyn 2003; Erdmann and Clarke 2004). The volumetrically most important source rocks of the SMB are felsic rocks of the Tangier basement (Eberz et al. 1991), but may possibly include pelitic and metavolcanic gneisses similar to those of the Liscomb Complex of central Nova Scotia

(Clarke et al. 1993; Kontak and Reynolds 1994), as well as metasedimentary rocks of the Meguma Group (Clarke et al. 1993; MacDonald 2001; Clarke et al. 2004; Chapter 4) (Fig. 5.1). Solid material, inherited from the source rocks, has been identified only in the form of rare zircons (Keppie and Krogh 1999), but other crystals may theoretically occur in the SMB, and their presence or absence needs to be evaluated. The metasedimentary Meguma Group rocks are the most important country-rock contaminants, contributing xenoliths, orthoxenocrysts (OXC), paraxenocrysts (PXC), and partial melt (PM) to the SMB magmas. Minerals occurring in the SMB rocks may thus be of orthoxenocrystic and paraxenocrystic origin (derived from Meguma Group rocks), foreign primary magmatic (country-rock melt dominated), cognate primary magmatic (source-melt dominated), or source-rock origin (derived from Tangier Basement rocks). The challenge in identifying these various crystal types is that the major rock-forming minerals, plagioclase, quartz, and biotite, are similar for granites, country rocks, as well as source rocks (Clarke and Erdmann 2005; Erdmann and Clarke 2005; Chapter 4).

Crystal types of various origins in the SMB have been previously classified on the basis of textural criteria (grain size, grain shape, inclusion relationships, cathodoluminescence patterns, and mineral assemblage), and for garnet, cordierite, ilmenite, rutile, and Fe±Cu-sulphides based major-element compositions, but uncertainties in their classification remain (Fig. 5.2) (Jamieson 1974, Allan and Clarke 1981; Maillet and Clarke 1985, Poulson et al. 1991, Clarke and Bogutyn 2003; Erdmann et al. 2004; Clarke and Erdmann 2005; Samson 2005; Carruzzo and Clarke in press, Clarke and Carruzzo in press, Chapter 4). In the study presented here, we seek to further constrain the origin of the previously studied crystal types, and to decipher their magma chamber history, using electron microprobe (EMP) analysis and laser ablation inductively coupled mass spectrometry (LAM ICP-MS). The overall aim of our analyses was to explore the confidence in characterizing the details of magma chamber processes from mineral chemical data of rock-forming minerals in peraluminous granites. We chose to focus on the analysis of plagioclase, biotite, garnet, and cordierite, because they are modally important minerals of many such granites. We did not include K-feldspar in our analyses, because of complications arising from exsolution features, and we excluded quartz because a pilot study showed that no characteristic compositional variations exist for quartz crystals from the Meguma Group country rocks, the SMB, as well as the Tangier basement source rocks. We inspected the acquired mineral chemical data in two-

element plots as well as in multi-element cluster analysis to test for chemical groups that might be similar to, or distinct from, the texturally defined crystal types in our data set.

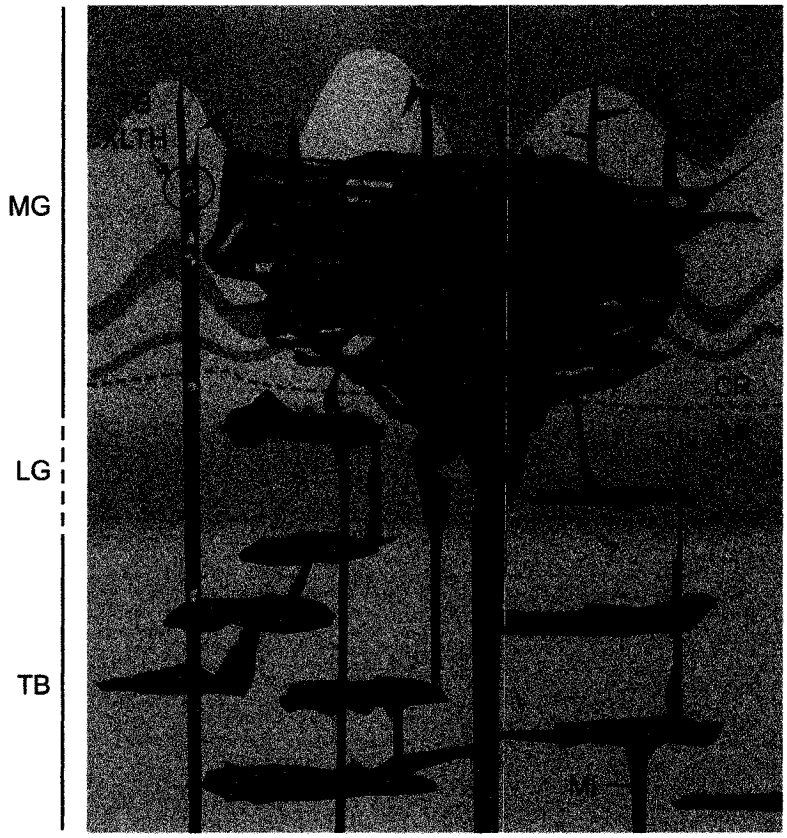

Figure 5.1: Schematic cross section showing the magma chamber of the South Mountain Batholith, intruded into rocks of the Meguma Group (MG) and possibly into gneisses similar to those of the Liscomb Complex (LG) (see text for references). Mafic intrusions (MI) in combination with crustal thickening generated the heat for the formation of the SMB magmas. Felsic rocks of the Tangier basement (TB) are the volumetrically most important source rocks (SR) of the SMB, but *in situ* Liscomb gneisses and Meguma Group rocks may have also contributed to the evolving magmas. Material derived from the source is dominated by partial melt (PM), but may contain minor amounts of xenoliths (XLTH) and source-rock crystals (SR XL). The stippled line schematically marks the transition between country rocks (CR) and source rocks (SR) of the SMB. Country rocks encompass those rocks that may have contributed to the SMB rocks as a bulk addition, whereas source rocks encompass those rocks that selectively contributed partial melt to the SMB magmas, and little or no solid material.

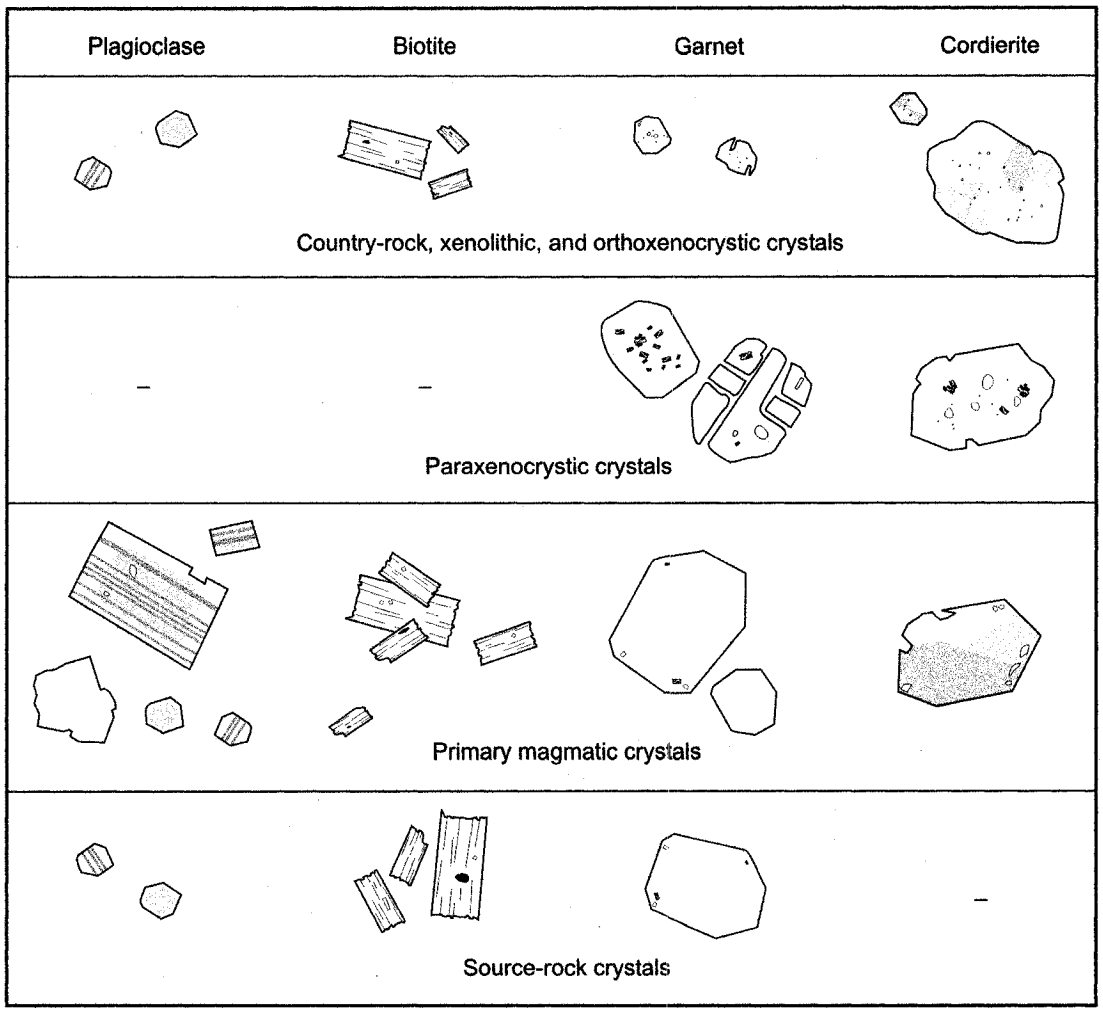

Figure 5.2: Sketch showing textural characteristics of plagioclase, biotite, garnet, and cordierite of various origins. Country-rock, xenolithic, orthoxenocrystic, and paraxenocrystic crystals are of Meguma Group origin, primary magmatic crystals may have crystallized from a cognate magmatic SMB melt phase, or from a hybrid melt phase with country-rock-derived and cognate magmatic components, and source-rock crystals are restitic crystals from felsic rocks of the Tangier basement (Clarke and Erdmann 2005; Erdmann and Clarke 2005; Chapter 2). Based on textural criteria alone, orthoxenocrystic, small crystals of primary magmatic, and source rock plagioclase cannot be distinguished from each other, whereas biotite of all possible origins is texturally largely indistinct, except that country-rock, xenolithic, and orthoxenocrystic biotite crystals have on average a smaller grain size than the primary magmatic crystals. Garnet crystals of various origins are typically texturally distinct, but some of the large, inclusion poor crystals of the SMB are texturally similar to garnet from the felsic Tangier basement source rocks, and chemical data are thus necessary to unequivocally determine their origin.

5.3 Studied Samples

The Meguma Group country-rock samples were collected within <100 m of the northeastern margin of the batholith (Fig. 5.3), but additional data for country-rock samples (Betts-Robertson 1998; Hart 2006; Tobey 2006) from across the thermal aureole are given for reference. The country-rock mineral chemical data most relevant in comparison to, and for identifying xenolithic and orthoxenocrystic crystals, are data from country rocks at the immediate contact with the SMB, and those are the only samples that were used for trace-element analysis.

The SMB samples studied are from the Five Mile Lake pluton and the Halifax Pluton of the SMB, where country-rock contamination and assimilation were previously characterized and quantified based on field observations and textural evidence (Clarke and Erdmann 2005; Chapter 4). Samples from the SMB are granodiorites and biotite monzogranites, and muscovite-biotite monzogranites, which variably include xenoliths of Meguma Group origin, texturally defined orthoxenocrysts and paraxenocrysts, and one garnet-rich magmatic enclave. The studied source rock samples of the Tangier basement occur as xenoliths in a mafic dyke swarm northeast of the SMB (Fig. 5.1), which have been previously described elsewhere (Owen et al. 1988; Eberz et al. 1991; Keen et al. 1991; Clarke et al. 1993; Greenough et al. 1999). To classify the origin of the various grains from our sample set, we used the textural characteristics summarized in Figure 5.2.

Subsequent to texturally classifying grains of various origins, we examined major-element compositions of >1200 crystals from 60 samples, and trace-element compositions of >250 crystals from 30 samples. Analyses presented for primary magmatic crystals are of unquestionably primary magmatic origin (e.g., euhedral oscillatory zoned plagioclase grains), with the exception of biotite crystals, for which textural criteria do not permit a confident determination of the origin of a grain in question (Chapter 4). On the other hand, analyses presented for orthoxenocrysts include grains of unquestionably orthoxenocrystic origin (Fig. 5.4A), as well as grains that may have an orthoxenocrystic, primary, or source-rock origin (plagioclase in Fig. 5.2, 5.4B). Analyses of magmatic plagioclase and biotite include crystals that formed from a melt phase of the main magma, as well as crystals that clearly formed from a melt with a Meguma Group contribution (Clarke and Erdmann 2005; Chapter 4) (Fig. 5.5).

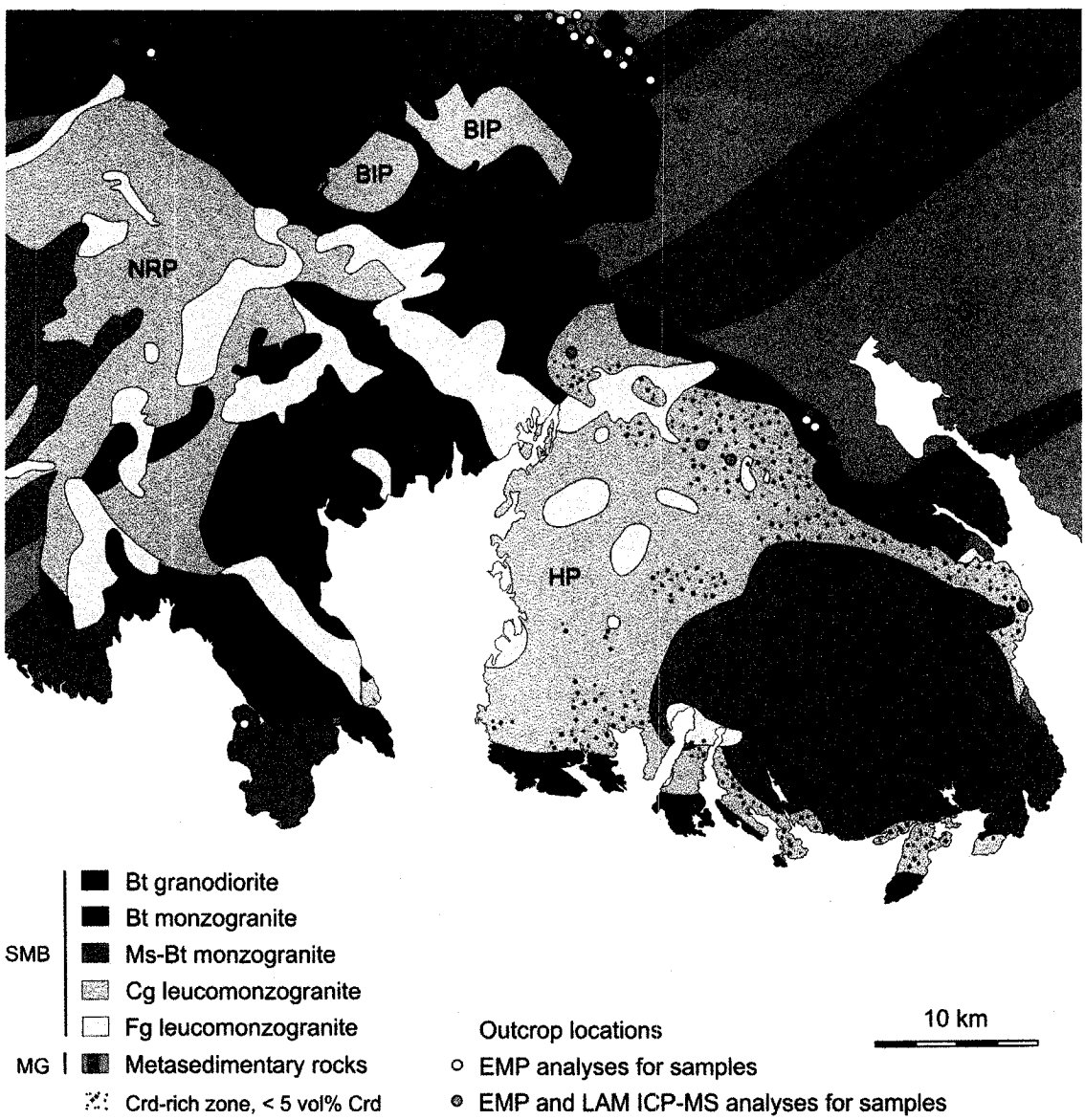

Figure 5.3: Geological map of the northeastern margin of the SMB in contact with rocks of the Meguma Group (MG). Mineral chemical analyses presented in this study are from samples from outcrops within the Five Mile Lake pluton (FMP), the Halifax Pluton (HP), Meguma Group country rocks, and xenoliths from the Tangier basement occurring in a mafic dyke northeast of the SMB (Fig. 1). Open circles denote outcrops from which samples have been analyzed by EMP only, whereas filled circles mark outcrop locations from which samples which have been analyzed by EMP as well as LA ICP-MS. For most outcrops, minerals have been analyzed from more than one sample. Bt = biotite, Ms = muscovite, Cg = coarse-grained, Fg = fine-grained, NRP = New Ross Pluton, STP = Salmontail Lake Pluton, BIP = Big Indian Lake pluton, HF = Halifax Formation (metapelite-dominated), and GF = Goldenville Formation (metapsammite-dominated).

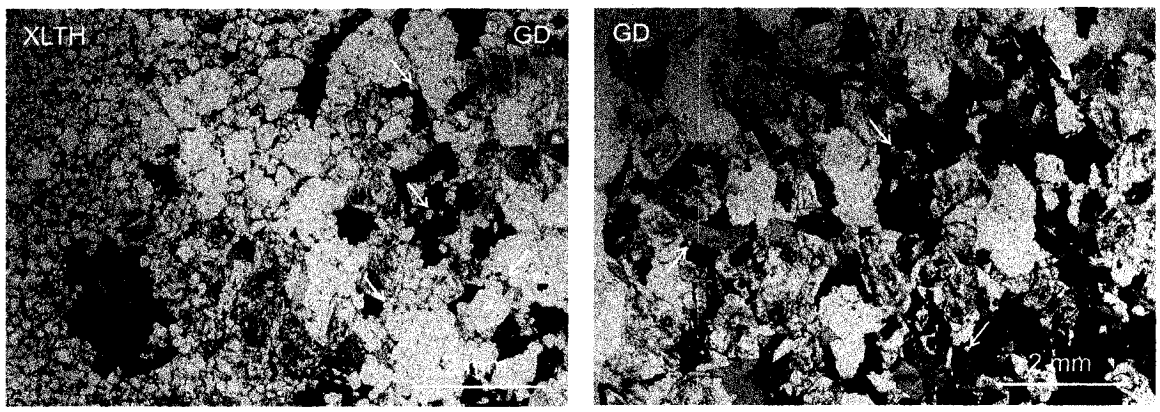

Figure 5.4: Photomicrograph (plane polarized light) showing grains of certain and potential orthoxenocrystic origin, marked by arrows. A) Xenolith (XLTH) in contact with granodiorite (GD). Along the contact, small xenoliths and orthoxenocrysts occur, some of which are marked by arrows. Sample E 429. B) Granodiorite that has grains of potentially orthoxenocrystic origin, marked by arrows. Sample E 471.

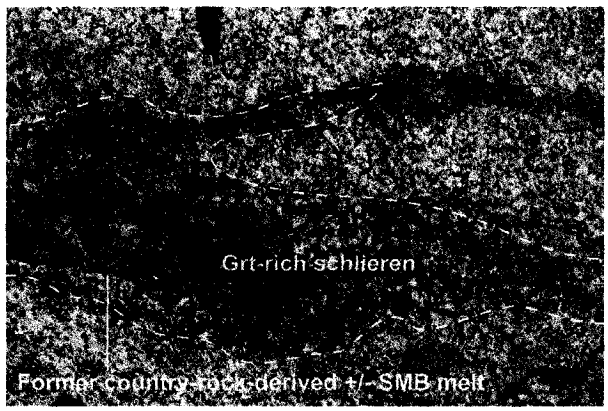

Figure 5.5: Garnet-rich schlieren in SMB granodiorite. Garnet-rich schlieren in the SMB result from the assimilation of metapelitic rocks of the Meguma Group by former SMB magmas through partial melting (Jamieson 1974; Clarke and Erdmann 2005; Chapter 4). Quartz, plagioclase, K-feldspar, and biotite within the schlieren crystallized from a melt phase consisting of country-rock and SMB-derived melt components. Location E 430.

5.4 Methods

We determined major-element compositions using a JEOL 8200 electron microprobe at Dalhousie University, operating at 15 keV and 15 nA, with a 3-15 μm spot size, and 40-s counting times. We refer to normal zoning in cordierite as a core to rim decrease in X_{Mg} and an increase in the Mn concentration; for garnet, we define normal zoning as a core to rim decrease in X_{Py} and an increase in the X_{Sps} concentration. Trace-element concentrations were characterized by inductively coupled plasma mass spectrometry (LAM ICP-MS) at Memorial University, using a NUWAVE 213 nm NdYAG laser system attached to a Hewlett-Packard 4500plus quadrupole mass spectrometer. For a laser spot size of 40 μm diameter, we operated the laser at 10 Hz with an energy output of approximately 12 J/cm^2, but we used spot sizes of up to 100 μm for larger grains, and

spot sizes of ≥20 μm for smaller grains. All measurements at the ICP-MS were performed in time resolved analyses utilizing peak jumping mode with 1 point per mass peak. The integration time was 10 ms per mass, with a quadrupole settling time of about 2 ms per mass. Total acquisition time per analysis was about 90 s, with a 30 s measurement of the gas blank, followed by 60 s of measurement of the ablated material. We used NIST glass NBS612 and BCR-2G as reference materials; SiO_2 was used as an internal standard. Trace elements analyzed for all crystals are V, Cr, Co, Ni, Zn, Ga, Ge, Rb, Sr, Y, Nb, Cs, Ba, La, Ce, Pr, Nd Sm, and Eu. In a pilot study on five samples, Cu, Sn, Gd, Ho, Tm, Yb, Lu, and Ta were also analyzed, but subsequently removed from the analytical file, given that they showed no characteristic variation for any of the studied mineral phases.

Cluster analysis was performed for selected major- and trace-element of plagioclase, biotite, cordierite, and garnet, in order to test for chemical groups that might be similar to, or distinct from, the texturally defined crystal types in our data set, using the program SPSS (Version 14.0, www.spss.com). Cluster analysis arranges data of similar characteristics into groups, separating cases that have different properties (e.g., Aldendorfer and Blashfield 1984; Everitt 1993). In our study, we performed cluster analysis to reveal groupings within the chemical data acquired, using major- and trace-element compositions, with the main task to evaluate our textural classification of the subsequently chemically analyzed grains, and to possibly suggest other useful solutions for grouping the various crystals that may not be apparent from the textural data or on two-element plots. We present cluster analysis for those elements that show compositional variations for the analyzed cases, but we also explored the effects of using other trace element combinations as independent variables and performed cluster analysis with variable clusters. The results for the cluster analysis varied with the different independent variables used, but the implications of the results were in all cases similar, as discussed in Section 5.6.1.

To define the chemical clusters, we applied the Ward's method, which creates clusters with the smallest possible within-cluster variance. Given that the concentrations of various trace elements used for the cluster analysis are highly variable (e.g., Sr on average ca. 410 ppm, La on average ca. 5 ppm plagioclase), we standardized all variables to a mean of zero and a standard deviation of 1 (using z scores), to avoid having the trace elements with the highest concentration dominate the cluster analysis. We recognize that some data groups (e.g., source-rock plagioclase) contain only few

analyses, and that the results may not be representative as addressed in our discussion of the results.

5.5 Results

5.5.1 Mineral Chemistry

5.5.1.1 Plagioclase

Plagioclase crystals of various origins overlap compositionally in X_{An} and X_{Or}, except for (i) primary magmatic plagioclase grains from the leucomonzogranites of the batholith which have X_{Or} concentrations of >0.02, (ii) country-rock plagioclase grains occurring in the distant contact aureole of the SMB which have X_{Or} compositions of <0.01, and (iii) source-rock plagioclase crystals, which have high-X_{An} (0.75-0.84) or high-X_{Or} compositions (0.05-0.08) (Fig. 5.6A; Table 5.1). Analyzed country-rock plagioclase has X_{An} compositions of ~0.01 to 0.25, and X_{Or} concentrations of less than ~0.02. Xenolithic and texturally orthoxenocrystic plagioclase in our data set show higher X_{An} values, dominantly between ~0.15 and 0.4, but a similar variation in X_{Or} as the country-rock plagioclase crystals analyzed. Primary magmatic plagioclase exhibits the largest compositional variation, with X_{An} varying between ca. 0.01 and 0.45, and X_{Or} concentrations of up to 0.03. Xenolithic and associated texturally orthoxenocrystic plagioclase from single samples tend to have a relatively low variation in X_{An} and a relatively high variation in X_{Or}, up to twice as high as the range of X_{Or} of plagioclase in spatially associated country rocks. Primary magmatic plagioclase from the same samples tends to have a high variation in X_{An} and a relatively low variation in X_{Or}. Source-rock plagioclase is high in X_{Or} (0.054-0.0081) and low in X_{An} (0.24-0.33), or low in X_{Or} (~0.006) and high in X_{An} (0.75-0.84). Plagioclase crystals of all textural types may exhibit core-rim zoning with X_{An}-rich ($\pm X_{Or}$-rich) cores and X_{An}-poor ($\pm X_{Or}$-poor) rims, and primary magmatic plagioclase may show superimposed large-scale (<500 μm wide) and small-scale (<20 μm wide) oscillatory growth zoning in X_{An}.

Trace-element concentrations in all plagioclase types are high for Sr (~20-680 ppm; on average ~410 ppm) and high for Ba (~5-300 ppm; on average ~150 ppm), and on the order of 5 ppm or more for Ga, Ce, Nd, and La (Table 5.2). Concentrations of Sr, Ce, Pr, Nd, Ba, Eu, and La increase with X_{An}, whereas Ga, Nb, and other trace elements show no characteristic variation with respect to X_{An} (Fig. 5.6B,C). For a given X_{An}, country-rock plagioclase has on average a higher Sr concentration, a similar Nb concentration, and a

lower Ga, Ba, La, Ce, Pr, Nd, and Eu concentration than primary magmatic plagioclase from SMB biotite granodiorites and monzogranites. Xenolithic plagioclase has Ga, Ba, La, Ce, Pr, and Nd concentrations between, as well as Sr and Eu concentrations below, those of country-rock plagioclase and primary magmatic plagioclase from SMB biotite granodiorites and monzogranites. Texturally orthoxenocrystic plagioclase grains have Sr, Ba, and Eu compositions between xenolithic and primary magmatic plagioclase, and Ga, La, Ce, Pr, and Nd compositions similar to primary magmatic plagioclase crystals from SMB biotite granodiorites and monzogranites. Primary magmatic plagioclase grains from SMB biotite granodiorites and monzogranites have higher concentrations in all trace elements, except for Ga, than all primary magmatic plagioclase crystals from the leucomonzogranites, with the exception of two core analyses. Trends for Sr and Eu versus X_{An} are subparallel for primary magmatic plagioclase grains from SMB biotite granodiorites and monzogranites and leucomonzogranites, whereas trends for all other trace elements analyzed are variable for primary magmatic plagioclase grains from the SMB biotite granodiorites and monzogranites and those of SMB leucogranites (Fig. 5.6B,C). Source-rock plagioclase grains have Ga, Sr, Nb, Ba, and Eu concentrations similar, and La, Ce, Pr, Nd, concentrations lower than the primary magmatic plagioclase crystals from the SMB biotite granodiorites and monzogranites, whereas concentrations in Ga and Ba are higher and concentrations in Sr are lower than those of country-rock plagioclase. Core-rim compositional trends, tested only for primary magmatic plagioclase, appear to decrease for Ga, Sr, and Eu, whereas core-rim trace-element variations for all other elements analyzed are non-systematic.

A

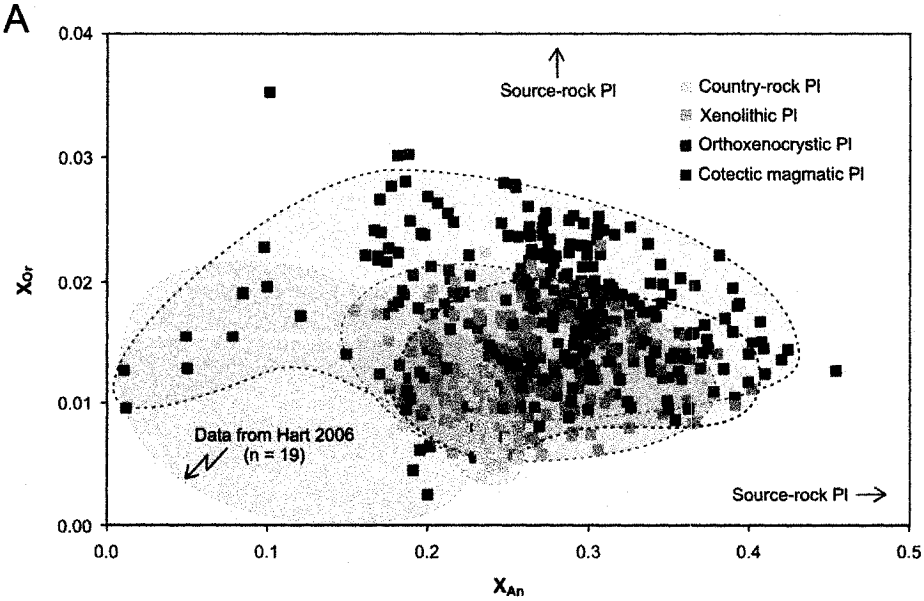

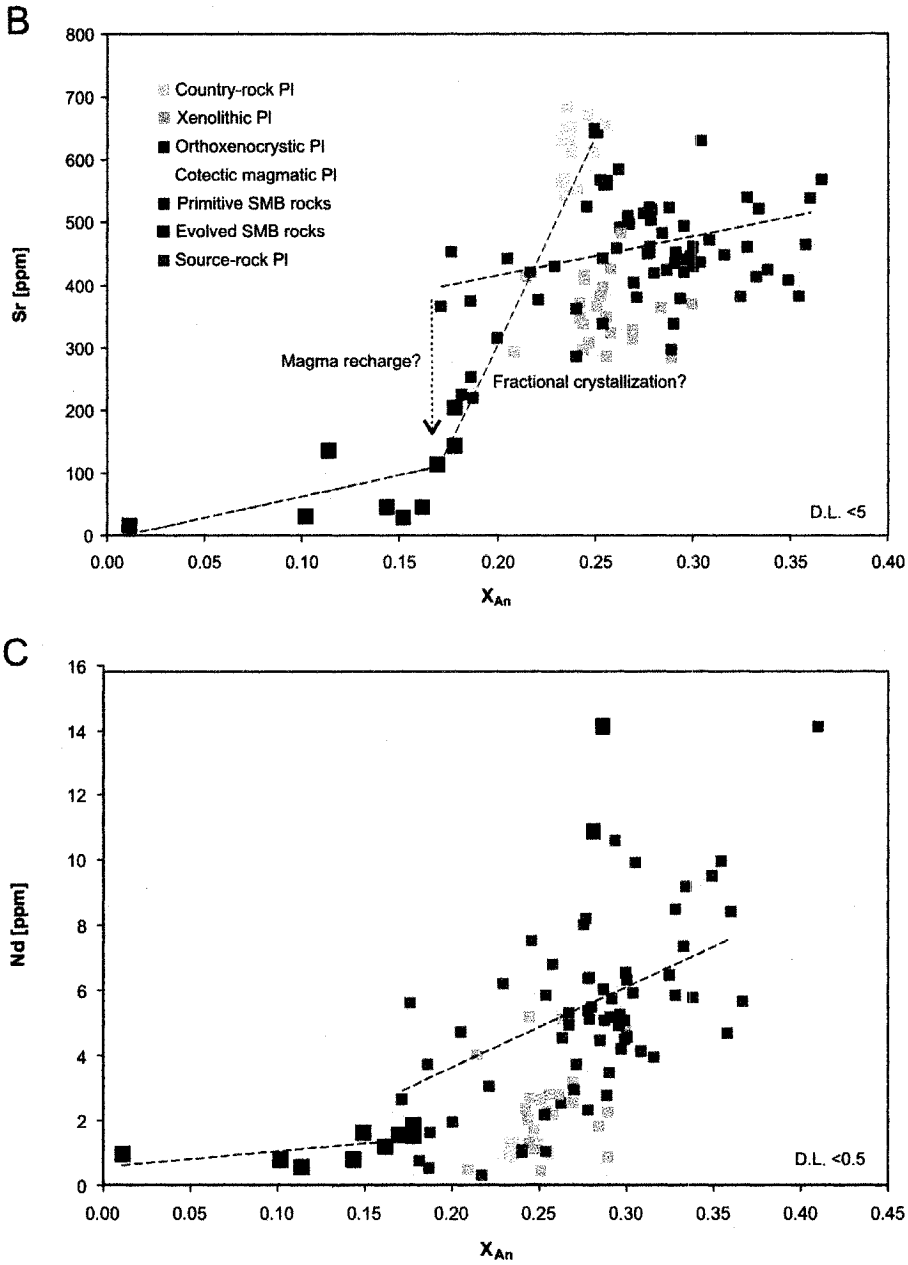

Figure 5.6: Compositions of the various textural plagioclase (Pl) types. A) Concentrations of X_{Or} versus X_{An} for country-rock, xenolithic, texturally orthoxenocrystic, and primary magmatic plagioclase. Colored fields outline the compositional fields for country-rock (yellow), xenolithic (orange), orthoxenocrystic (red), and primary magmatic plagioclase (blue). The yellow field with no data points marks the compositional field for country-rock plagioclase across the thermal aureole of the SMB (Hart 2006). B) Sr (ppm) and C) Nd (ppm) concentrations of the various textural plagioclase types as a function of X_{An}. Trend lines in B) and C) are for cognate magmatic plagioclase.

Table 5.1: Plagioclase (Pl) major-element concentrations (determined by EMP) for the various textural groups.

	CR Pl			XLTH Pl			OXC Pl			ME Pl			PM Pl (pSMB)			SR Pl (Or-rich)			SR Pl (An-rich)		
n	38			189			78			15			260			11			9		
	Av	Max	Min	Av	Max	Min	Av	Max	Min	Av	Max	Min	Av	Max	Min	Av	Max	Min	Av	Max	Min
SiO_2	62.43	64.73	61.59	61.54	69.37	57.07	60.49	63.81	56.95	61.95	63.71	59.30	60.89	67.57	55.05	62.37	63.88	61.68	48.44	49.87	47.43
TiO_2	0.01	0.04	0.00	0.01	0.24	0.00	0.01	0.18	0.00	0.00	0.01	0.00	0.02	0.26	0.00	0.00	0.01	0.00	0.00	0.00	0.00
Al_2O_3	23.59	24.31	22.13	23.90	26.55	18.18	24.43	26.40	22.71	23.33	24.85	22.09	24.16	27.47	18.25	24.46	24.83	23.59	34.27	35.18	33.28
FeO	0.08	0.71	0.00	0.06	2.01	0.00	0.14	2.06	0.00	0.04	0.11	0.00	0.03	0.22	0.00	0.04	0.08	0.02	0.11	0.21	0.06
MnO	0.00	0.03	0.00	0.01	0.06	0.00	0.01	0.04	0.00	0.02	0.06	0.00	0.01	0.11	0.00	0.01	0.03	0.00	0.01	0.02	0.00
MgO	0.01	0.25	0.00	0.01	0.61	0.00	0.01	0.58	0.00	0.00	0.01	0.00	0.00	0.07	0.00	0.01	0.02	0.00	0.01	0.02	0.00
CaO	4.97	5.48	3.79	5.38	8.89	0.00	5.93	8.83	3.89	5.34	7.43	3.95	5.76	9.45	0.00	5.26	5.64	4.49	16.79	17.51	15.78
Na_2O	8.95	9.37	8.43	8.59	12.66	1.08	8.24	9.81	6.80	8.61	10.06	7.15	8.25	11.69	1.23	7.83	8.09	7.59	2.21	2.77	1.75
K_2O	0.15	0.39	0.07	0.55	15.87	0.01	0.25	0.93	0.10	0.25	0.33	0.16	0.44	15.59	0.04	1.14	1.40	1.00	0.09	0.12	0.07
Cl	0.00	0.00	0.00	0.00	0.00	0.00	0.00	0.00	0.00	0.00	0.00	0.00	0.00	0.00	0.00	0.00	0.00	0.00	0.00	0.00	0.00
F	0.02	0.12	0.00	0.01	0.10	0.00	0.01	0.10	0.00	0.00	0.00	0.00	0.02	0.28	0.00	0.00	0.00	0.00	0.00	0.00	0.00
Cr_2O_3	0.06	0.16	0.00	0.03	0.18	0.00	0.04	0.12	0.00	0.00	0.02	0.00	0.03	0.16	0.00	0.10	0.13	0.04	0.11	0.14	0.06
BaO	0.01	0.06	0.00	0.01	0.63	0.00	0.01	0.08	0.00	0.00	0.00	0.00	0.02	0.43	0.00	0.00	0.00	0.00	0.00	0.00	0.00
P_2O_5	0.00	0.02	0.00	0.00	0.06	0.00	0.00	0.00	0.00	0.00	0.00	0.00	0.00	0.01	0.00	0.00	0.00	0.00	0.00	0.00	0.00
Total	100.25	101.53	99.16	100.10	102.30	97.96	99.57	101.93	97.01	99.54	101.62	98.53	99.62	101.91	98.01	101.21	101.61	100.71	102.03	102.52	101.50
X_{An}	0.23	0.26	0.18	0.25	0.40	0.00	0.28	0.40	0.18	0.25	0.36	0.19	0.27	0.45	0.00	0.25	0.27	0.22	0.80	0.84	0.75
X_{Or}	0.01	0.02	0.00	0.04	0.98	0.00	0.01	0.05	0.01	0.01	0.02	0.01	0.02	0.89	0.00	0.07	0.08	0.06	0.00	0.01	0.00

Complete data set available from authors upon request. CR = country-rock, XLTH =xenolithic, OXC = orthoxenocrystic, ME = magmatic enclave, PM = primary magmatic, pSMB = from primitive SMB rocks, and eSMB = from evolved SMB rocks. Av = average, Max = maximum, and Min = minimum.

Table 5.2: Plagioclase (Pl) trace-element concentrations (determined by LAM ICP-MS) for the various textural groups.

	D.L.	CR Pl			XLTH Pl			OXC Pl			PM Pl (pSMB)			CM Pl (eSMB)			SR Pl		
n		15			24			32			11			30			3		
	Max	Av	Max	Min	Av	Max	Min	Av	Max	Min	Av	Max	Min	Av	Max	Min	Av	Max	Min
Li	4	81	375	2	5	13	1	84	304	0	2	4	1	70	271	1	3	7	1
Be	19	0	0	0	-	-	-	-	-	-	5	10	0	0	0	0	-	-	-
B	106	4	28	15	-	-	-	-	-	-	26	53	2	0	0	0	-	-	-
V	1	4	14	0	5	18	0	5	16	0	1	4	0	4	17	0	1	3	0
Cr	8	22	64	2	4	10	0	25	72	0	1	3	1	19	65	0	1	2	1
Zn	5	15	57	2	11	30	1	143	3037	2	5	5	5	10	50	0	7	14	1
Ga	1	13	17	9	17	25	3	22	33	14	56	27	19	24	29	17	27	39	18
Ge	2	11	33	1	1	2	0	11	30	1	18	9	1	7	28	1	1	1	1
Rb	0.4	1	4	0	11	30	0	4	27	0	1	3	0	2	17	0	2	4	1
Sr	3	619	684	542	285	395	48	416	583	218	195	486	16	468	631	364	502	602	420
Y	0.2	0.6	1.2	0.2	0.8	1.8	0.0	1.0	2.9	0.2	0.1	0.4	0.1	0.8	1.6	0.6	0.4	0.5	0.4
Nb	0.2	0.5	1.5	0.0	0.9	4.3	0.0	0.5	1.8	0.0	0.1	0.3	0.0	0.5	1.9	0.0	0.2	0.2	0.1
Cs	0.1	0.3	1.3	0.0	0.3	0.8	0.0	0.3	0.7	0.0	0.1	0.1	0.0	0.3	3.1	0.0	0.1	0.3	0.0
Ba	1	108	138	66	140	230	50	158	287	52	131	339	2	215	306	92	115	187	23
La	0.1	3	4	2	5	14	1	10	28	2	6	13	2	10	17	1	2	5	0
Ce	0.1	4	5	2	9	23	2	17	45	2	6	22	3	18	31	2	4	8	1
Pr	0.0	0.4	0.7	0.2	0.8	2.2	0.1	1.6	4.6	0.2	0.6	1.9	0.2	1.7	2.9	0.2	0.4	0.9	0.1
Nd	0.2	1	4	1	2	7	0	5	14	1	2	6	1	6	10	0	1	3	0
Sm	0.2	0.9	4.4	0.0	0.6	1.4	0.1	0.9	2.4	0.2	0.3	1.2	0.0	1.0	1.6	0.4	0.1	0.4	0.1
Eu	0.1	2.3	2.6	1.8	1.7	2.8	0.2	2.6	4.6	1.2	0.8	3.1	0.0	3.1	4.2	2.2	1.7	2.2	1.0

Complete data set available from authors upon request. CR = country-rock, XLTH =xenolithic, OXC = orthoxenocrystic, PM = primary magmatic, pSMB = from primitive SMB rocks (biotite granodiorite and monzogranite), eSMB = from evolved SMB rocks (leucomonzogranites), and SR = source-rock. D.L. = detection limit, Av = average, Max = maximum, and Min = minimum.

5.5.1.2 Biotite

Analyzed biotite grains of the various textural groups are chemically indistinguishable for all major-element concentrations, with the exception of (i) biotite grains in Meguma Group country rocks of the distant contact aureole of the SMB which are low in Ti (<0.2 apfu) and low in X_{Mg} (<0.35), and (ii) biotite grains from one Grt-rich magmatic enclave which have a low-X_{Mg} composition (Fig. 5.7A; Table 5.3). Biotite from Meguma Group country rocks of the distant contact aureole of the SMB has a Ti concentration of ca. <0.2 apfu, Mn concentrations of <0.02 apfu, and X_{Mg} values of ca. 0.20-0.50. Country-rock biotite from Meguma Group rocks along the immediate contact with the SMB has higher Ti (~0.18-0.33 apfu), Mn (~0.02-0.04 apfu), and X_{Mg} concentrations (~0.38-0.45) than country-rock biotite of the distant contact aureole, but compositionally overlaps with biotite from the SMB rocks. Texturally orthoxenocrystic, xenolithic, and primary magmatic biotite have Ti concentrations between 0.16 and 0.41 apfu, Mn concentrations of 0.01 to 0.07 apfu, and an X_{Mg} between 0.47 and 0.68, where X_{Mg} varies more between samples than between different textural types in one sample. Biotite from the garnet-rich enclave has low X_{Mg} values of 0.21 to 0.38, but relative to the other biotite types, average concentrations of Ti (~0.27-0.42 apfu) and Mn (~0.01-0.05). Compositional zoning is not evident in any of the biotite crystals analyzed.

Concentrations of Li, V, Cr, Zn, Rb, Ba, and Cs are >100 ppm in the various biotite types, and Co, Ni, Ga, and Nb concentrations are on the order of several tens of ppm. Concentrations of all analyzed trace elements vary non-systematically with any of the major elements, and overlap largely for all biotite types studied, with the exception of country-rock biotite (Fig. 5.7B,C; Table 5.4). Country-rock biotite has on average higher Co and Ni concentrations, but lower average V, Nb, Ta, and Ba concentrations than all other biotite types. Concentrations of chromium are on average higher for country-rock biotite grains than for the primary magmatic biotite grains and overlap with the Cr concentration of xenolithic and texturally orthoxenocrystic biotite crystals (Fig. 5.7C). Xenolithic, texturally orthoxenocrystic, and primary magmatic biotite overlap compositionally for all trace elements, except that a large number of xenolithic and texturally orthoxenocrystic biotite grains show a higher Cr concentration than the texturally primary magmatic biotite grains with similar X_{Mg} compositions.

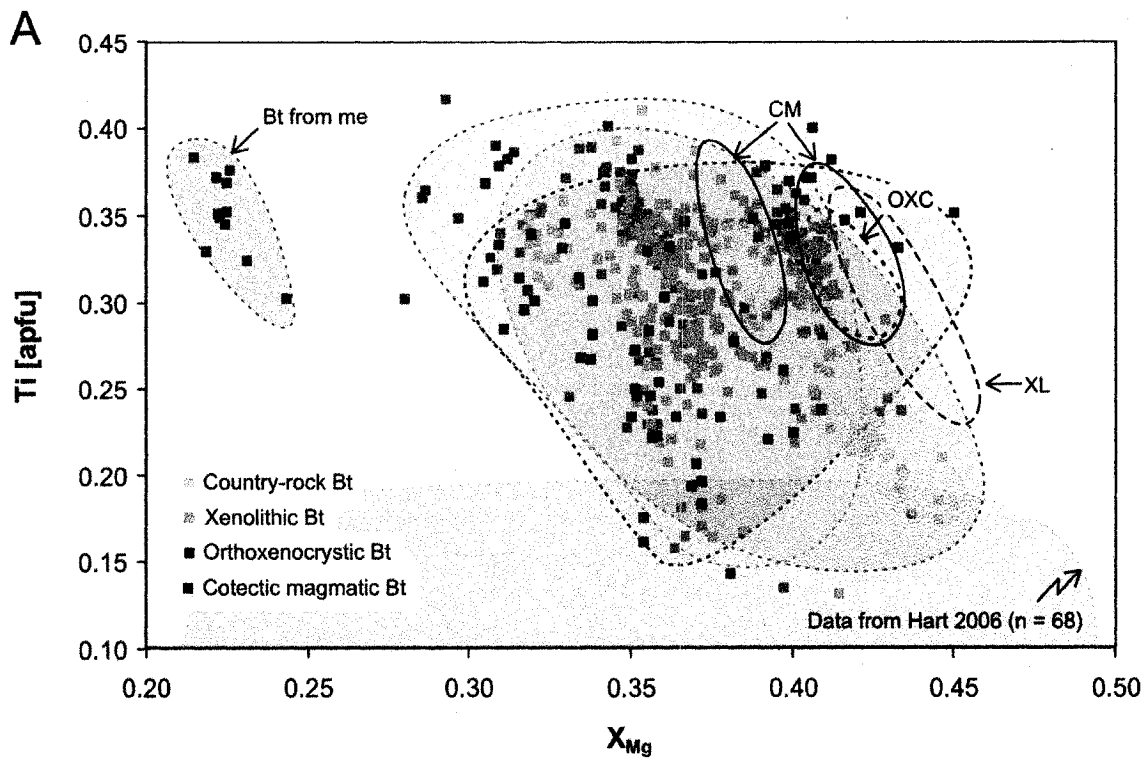
A
Ti [apfu]
0.45
0.40
0.35
0.30
0.25
0.20
0.15
0.10
0.20
0.25
0.30
0.35
0.40
0.45
0.50
X_{Mg}
Bt from me
CM
OXC
XL
Country-rock Bt
Xenolithic Bt
Orthoxenocrystic Bt
Cotectic magmatic Bt
Data from Hart 2006 (n = 68)

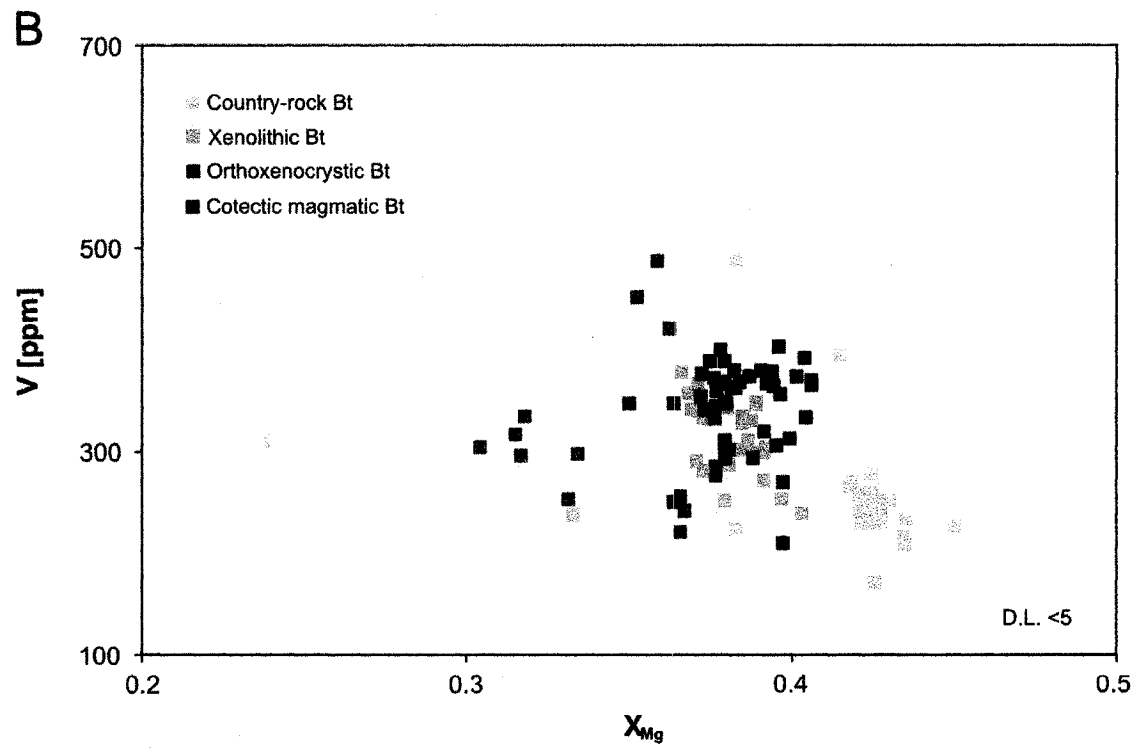
B
V [ppm]
700
500
300
100
0.2
0.3
0.4
0.5
X_{Mg}
Country-rock Bt
Xenolithic Bt
Orthoxenocrystic Bt
Cotectic magmatic Bt
D.L. <5

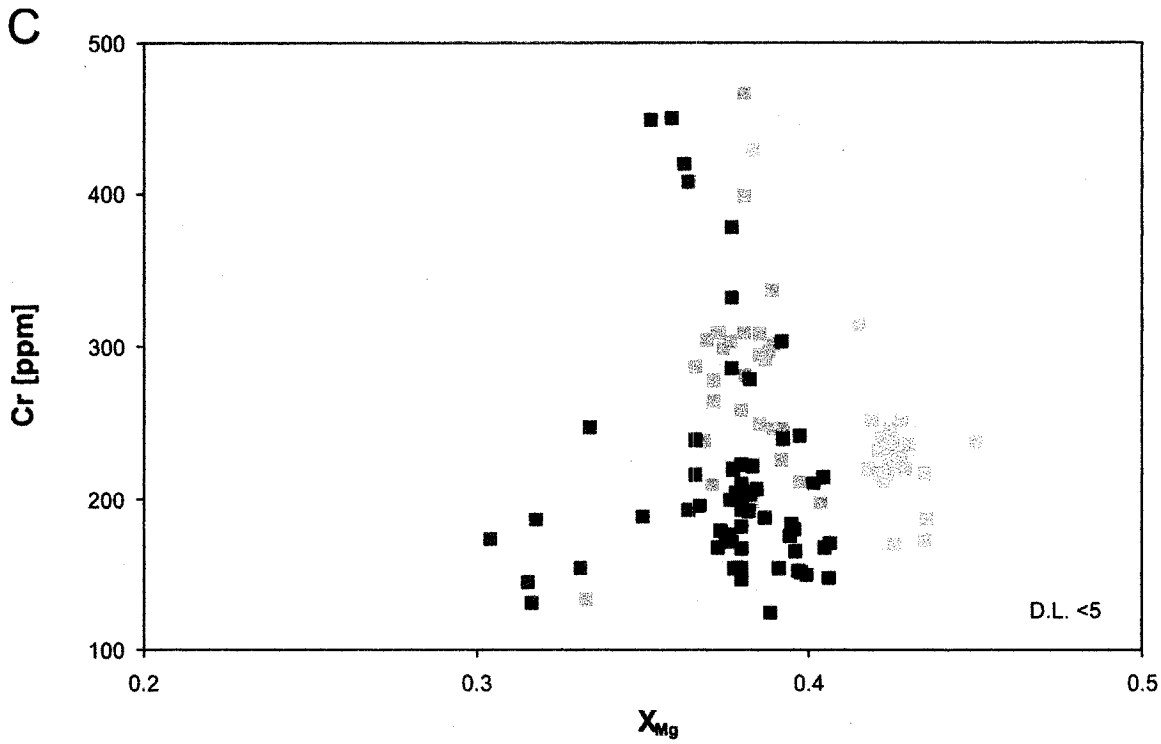

Figure 5.7: Compositions of the various textural biotite (Bt) types. A) Concentrations of Ti (apfu) versus X_{Mg} for country-rock, xenolithic, texturally orthoxenocrystic, primary magmatic biotite from the main SMB rocks, and primary magmatic biotite from a magmatic enclave (me). Colored fields outline the compositional fields for country-rock (yellow), xenolithic (orange), texturally orthoxenocrystic (red), primary magmatic biotite from the main SMB rocks (blue), and primary magmatic biotite from a magmatic enclave (grey). Open fields with solid black lines mark compositions for cognate magmatic biotite from two different samples; open fields with broken and stippled lines show the compositional range for xenolithic and texturally orthoxenocrystic biotite, overlapping with cognate magmatic biotite from the same sample. The yellow field without data points outlines the compositional field for country-rock biotite across the contact aureole of the SMB (Hart 2006). B) V (ppm) and C) Cr (ppm) concentrations of the various textural plagioclase types as a function of X_{Mg}.

Table 5.3: Biotite (Bt) major-element concentrations (determined by EMP) for the various textural groups.

	CR Bt			XLTH Bt			OXC Bt (pSMB)			PM Bt			ME Bt		
n	**38**			**265**			**58**			**160**					
	Av	Max	Min	Av	Max	Min	Av	Max	Min	Av	Max	Min	Av	Max	Min
SiO_2	34.77	37.44	34.12	34.71	38.71	26.41	34.00	37.84	30.00	34.15	37.26	30.50	33.44	33.96	32.73
TiO_2	2.51	3.54	1.95	3.14	4.30	0.12	2.77	4.07	0.50	3.32	4.31	1.40	3.62	4.26	3.04
Al_2O_3	18.89	20.01	17.00	18.77	22.39	17.02	18.02	19.91	17.45	18.55	21.38	16.90	17.58	18.28	16.38
FeO	20.69	21.76	19.01	21.18	28.08	18.82	20.68	27.94	18.77	21.09	24.97	19.42	26.09	27.01	25.08
MnO	0.30	0.36	0.19	0.48	12.64	0.02	0.37	0.65	0.15	0.37	0.58	0.13	0.36	0.42	0.11
MgO	8.52	9.23	6.95	7.22	13.55	1.66	6.80	11.00	4.84	7.08	8.77	5.23	4.44	5.84	4.05
CaO	0.01	0.21	0.00	0.03	1.09	0.00	0.02	0.81	0.00	0.01	0.56	0.00	0.00	0.02	0.00
Na_2O	0.15	0.69	0.06	0.18	0.77	0.02	0.19	0.45	0.09	0.18	0.38	0.07	0.18	0.44	0.14
K_2O	9.57	10.12	8.54	9.38	10.25	0.00	8.39	10.03	1.90	9.38	10.28	7.73	9.12	9.44	8.51
Cl	0.00	0.00	0.00	0.00	0.00	0.00	0.00	0.00	0.00	0.00	0.00	0.00	0.00	0.00	0.00
F	0.20	0.36	0.00	0.25	0.54	0.00	0.26	0.86	0.00	0.28	0.57	0.00	0.18	0.27	0.07
Cr_2O_3	0.13	0.23	0.05	0.06	0.21	0.00	0.06	0.20	0.00	0.06	0.20	0.00	0.00	0.00	0.00
BaO	0.00	0.00	0.00	0.02	0.22	0.00	0.01	0.12	0.00	0.03	0.33	0.00	0.01	0.02	0.00
Total	95.64	97.50	93.22	95.32	101.49	90.07	91.47	99.57	89.46	94.41	99.70	89.90	94.94	95.90	93.88
X_{Mg}	0.42	0.45	0.38	0.37	0.47	0.07	0.35	0.45	0.28	0.37	0.44	0.29	0.23	0.29	0.21

Complete data set available from authors upon request. CR = country-rock, XLTH =xenolithic, OXC = orthoxenocrystic, pSMB = from primitive SMB rocks, PM = primary magmatic, and ME = magmatic enclave. Av = average, Max = maximum, and Min = minimum.

Table 5.4: Biotite (Bt) trace-element concentrations (determined by LAM ICP-MS) for the various textural groups.

	D.L.	CR Bt			XLTH Bt			OXC Bt (pSMB)			OXC Bt (eSMB)			PM Bt (pSMB)		
n		27			30			7			11			42		
	Max	Av	Max	Min	Av	Max	Min	Av	Max	Min	Av	Max	Min	Av	Max	Min
Li	4	296	426	95	311	618	114	584	1398	113	243	503	144	215	227	192
Be	19	0	5	2	-	-	-	3	6	0	-	-	-	-	-	-
B	106	25	25	25	-	-	-	12	36	0	-	-	-	-	-	-
V	1	256	488	171	329	678	124	329	486	252	362	401	293	242	255	221
Cr	8	233	428	169	272	467	71	274	450	131	185	239	124	210	238	193
Co	0.1	52	59	35	41	52	30	-	-	-	44	51	32	-	-	-
Ni	0.4	122	158	83	78	119	46	-	-	-	60	140	37	-	-	-
Cu	0.3	9	20	3	10	23	3	-	-	-	9	61	1	-	-	-
Zn	5	295	375	180	271	533	124	389	482	271	363	594	137	294	337	216
Ga	1	38	48	21	47	60	23	51	80	31	52	76	41	34	36	31
Ge	2	10	19	2	12	30	1	2	6	1	9	45	2	4	6	2
Rb	0.4	405	531	233	448	618	188	789	1703	413	476	564	308	514	545	445
Sr	3	7	21	2	11	123	1	1	6	0	6	22	2	1	2	1
Y	0.2	1	1	0	1	14	0	1	60	0	1	6	0	5	17	1
Nb	0.2	32	61	22	52	61	37	70	144	29	56	65	45	35	37	30
Sn		6	8	4	7	9	6	-	-	-	8	11	5	-	-	-
Cs	0.1	22	42	7	18	51	4	42	207	8	17	89	6	31	45	13
Ba	1	927	1226	441	1364	2774	655	1103	2277	133	1852	3632	611	990	1439	711
La	0.1	0.2	0.3	0.0	0.2	2.2	0.0	0.1	0.5	0.0	0.1	0.3	0.0	0.4	1.2	0.1
Ce	0.1	0.2	0.8	0.0	0.4	4.2	0.0	0.2	1.7	0.0	0.2	1.0	0.0	1.5	4.5	0.3
Pr	0.0	0.1	0.3	0.0	0.1	0.5	0.0	0.0	0.3	0.0	0.0	0.2	0.0	0.2	0.6	0.0
Nd	0.2	0.6	1.6	0.1	0.4	1.8	0.0	0.2	1.2	0.0	0.2	0.8	0.0	0.8	2.3	0.1
Sm	0.2	0.6	1.3	0.0	0.6	4.9	0.0	0.1	0.5	0.0	0.2	0.7	0.1	0.3	0.8	0.0
Eu	0.1	0.2	0.5	0.0	0.1	1.2	0.0	0.0	0.1	0.0	0.1	0.2	0.0	0.0	0.0	0.0

Complete data set available from authors upon request. CR = country-rock, XLTH =xenolithic, OXC = orthoxenocrystic, pSMB = from primitive SMB rocks (biotite granodiorite and monzogranite), eSMB = from evolved SMB rocks (leucomonzogranites), and PM = primary magmatic. D.L. = detection limit, Av = average, Max = maximum, and Min = minimum.

5.5.1.3 Garnet

The texturally different garnet types are almandine-dominated, and relatively rich in X_{Py} and X_{Sps}; with the exception of some source-rock garnet crystals, their compositions mostly overlap (Fig. 5.8A; Table 5.5). Country-rock garnet is high in X_{Sps} (~0.20-0.25), and intermediate in X_{Alm} (~0.60-0.68). Xenolithic garnet analyzed has intermediate to high X_{Sps} (~0.08-0.26), and intermediate to high X_{Alm} concentrations between ca. 0.64 and 0.80, whereas paraxenocrystic garnet has X_{Sps} concentrations of ca. 0.03-0.23, and X_{Alm} concentrations between ca. 0.65 and 0.75. Both xenolithic and paraxenocrystic garnet have X_{Sps} and X_{Alm} compositions largely similar to those of primary magmatic garnet. Primary magmatic garnet from one garnet-rich magmatic enclave is intermediate in X_{Sps} (~0.15) and high in X_{Alm} (~0.76), and thus compositionally indistinct from paraxenocrystic and primary magmatic garnet. Source rock garnet is relatively low in X_{Alm}.

Country-rock, xenolithic, texturally orthoxenocrystic, paraxenocrystic, primary magmatic garnet, and garnet from the magmatic enclave have X_{Grs} concentrations of ca. 0.04. Source-rock garnet is distinct from all other garnet types analyzed, showing a higher X_{Grs} concentration of 0.10-0.27. The xenolithic and paraxenocrystic garnets show normal zoning, with a ≤400 μm but typically ≤50 μm wide low-X_{Py}, high-Mn rim (Fig. 5.9A,B). The primary magmatic garnet crystals have a ≤1000 μm wide inner zone, a ca. 300-700 μm wide intermediate zone, and a ≤1000 μm wide rim zone, where the core and rim zones are relatively rich in X_{Sps} and low in X_{Py} (Fig. 5.9C). Source-rock garnet shows reverse zoning with ≥500 μm wide high-X_{Py}, low-X_{Sps} rims (Fig. 5.9D). Zoning in X_{Grs} exhibits a low-X_{Grs} core, a ca. 500 μm wide high-X_{Grs} zone, and a ≥500 μm low- X_{Grs} rim.

Trace-element concentrations in all textural garnet types analyzed are high for V (~30-915 ppm; on average ~170 ppm) and Cr (~3-715 ppm; on average ~150 ppm), and on the order of 10 ppm or more for Zn, Ga, Ge, and Y (Fig. 5.8B,C; Table 5.6). For all garnet types, trace-element concentrations do not increase systematically with X_{Py}, X_{Alm}, X_{Grs}, or X_{Sps}. Xenolithic and texturally orthoxenocrystic garnet have on average a higher V, Cr, Nd, and Sm concentration, a similar Ge concentration, and a lower Zn and Y concentration than primary magmatic garnet. Paraxenocrystic garnet shows a higher Y concentration and similar Ge, Zn, Nd, and Sm concentrations as country-rock and xenolithic garnet, and V and Cr concentrations higher than primary magmatic garnet, but lower than country-rock and xenolithic garnet. Primary magmatic garnet from the garnet-

rich magmatic enclave has Ge and Y concentrations higher than, and Zn, Nd, and Sm concentrations similar to paraxenocrystic and primary magmatic garnet, and V and Cr concentrations lower than the paraxenocrystic garnets analyzed. Yttrium concentrations of garnet from the magmatic enclave are higher, Zn and Sm concentrations are similar, Cr and V concentrations are lower, and Ge concentrations are between those of country-rock and source rock garnet and similar to those of the primary magmatic garnet crystals analyzed. Source-rock garnet has a higher Ge and Zn concentration than paraxenocrystic and primary magmatic garnet, a higher V and Cr concentration than primary magmatic garnet, and a lower Nd and Sm concentration than paraxenocrystic and primary magmatic garnet. Compared to xenolithic garnet, source-rock garnet is low in Nd, Sm, V, and Cr, and high in Y and Eu. For source-rock garnet, V, Cr, and Ge decrease from core to rim, whereas for paraxenocrystic and primary magmatic, V and Cr concentrations tend to decrease from core to rim. The composition of the intermediate zone of the primary magmatic garnet relative to the core and rim zones is known for only one crystal, in which Sm, Eu, Nd, Cr, and V are higher and Ga is intermediate between the concentrations of the core and the rim zones.

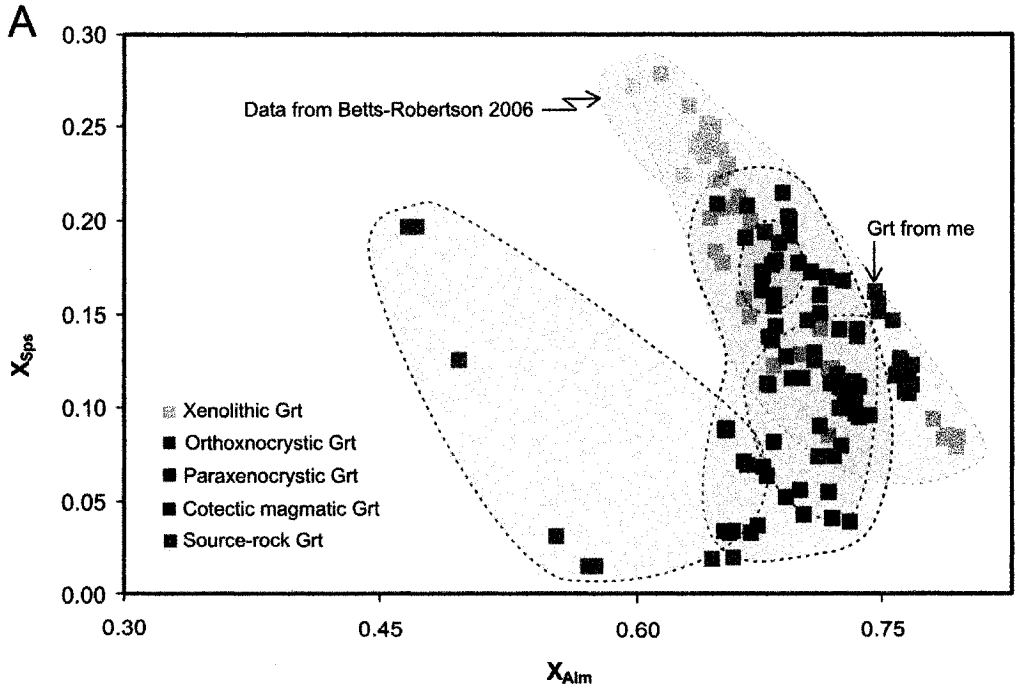

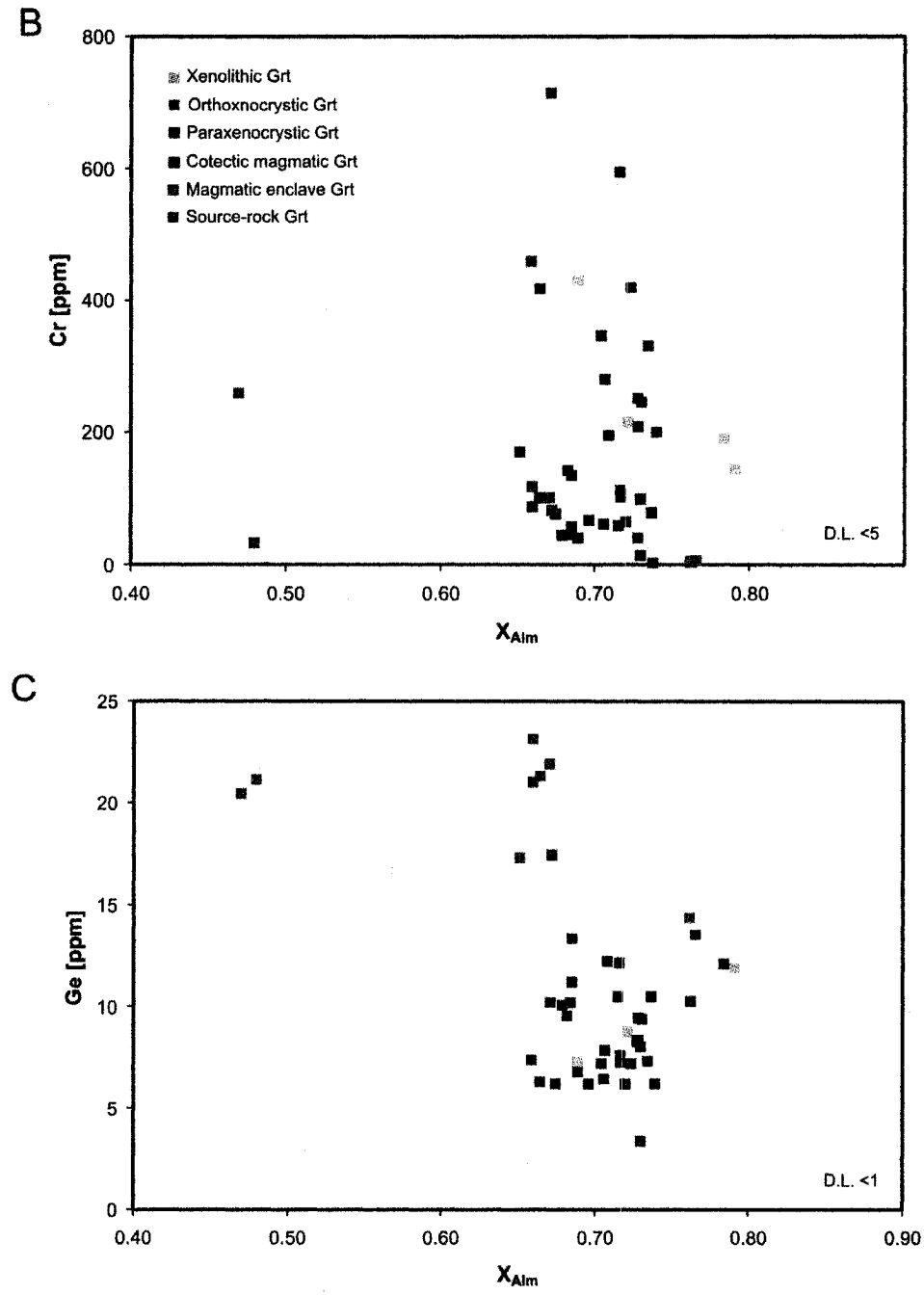

Figure 5.8: Compositions of the various textural garnet (Grt) types. A) Concentrations of Mn (apfu) versus X_{Mg} for country-rock, xenolithic, texturally orthoxenocrystic, paraxenocrystic, primary magmatic garnet from the main SMB rocks, magmatic garnet from a garnet-rich magmatic enclave (me), and source-rock garnet. Colored fields outline the compositional fields for country-rock (yellow), xenolithic (orange), texturally orthoxenocrystic (red), paraxenocrystic (purple), primary magmatic garnet from the main SMB muscovite-biotite monzogranites (blue), and primary magmatic garnet from a magmatic enclave (grey). Yellow fields without data points indicate compositional fields of country-rock garnet analyzed by Betts-Robertson (1998). B) Cr (ppm) and C) Ge (ppm) concentrations of the different textural plagioclase types versus X_{Mg}.

Table 5.5: Garnet (Grt) major-element concentrations (determined by EMP) for the various textural groups.

	XLTH Grt			OXC Grt			PXC Grt			ME Grt			PM Grt (eSMB)			SR Grt		
n	17			3			32			6			6			4		
	Av	Max	Min	Av	Max	Min	Av	Max	Min	Av	Max	Min	Av	Max	Min	Av	Max	Min
SiO_2	36.65	37.69	35.92	54.06	36.68	36.12	37.30	38.40	36.30	36.40	36.94	35.75	37.40	38.97	36.10	37.70	37.95	37.48
TiO_2	0.08	0.16	0.01	0.07	0.06	0.04	0.04	0.14	0.00	0.03	0.05	0.00	0.05	0.08	0.00	0.08	0.13	0.01
Al_2O_3	20.76	21.18	20.26	30.72	20.80	20.60	21.09	21.78	20.64	20.66	20.83	20.41	21.13	21.96	20.48	21.04	21.15	20.96
FeO	32.10	36.43	28.74	45.16	31.72	29.87	32.11	33.50	30.57	33.86	34.01	33.81	28.70	33.44	21.88	25.89	30.01	21.71
MnO	6.02	10.24	3.46	9.62	6.94	5.61	3.86	6.21	1.48	5.18	5.52	4.88	2.44	5.04	0.53	6.43	8.92	3.93
MgO	2.88	4.26	1.87	4.95	3.37	3.27	4.24	6.99	2.91	1.84	1.90	1.78	6.72	11.41	3.86	2.75	3.79	1.71
CaO	1.05	1.16	0.95	1.85	1.29	1.23	1.27	1.54	0.76	1.42	1.61	1.25	2.51	4.42	1.44	6.59	9.63	3.67
Na_2O	0.01	0.04	0.00	0.01	0.01	0.00	0.02	0.06	0.00	0.03	0.06	0.02	0.01	0.02	0.00	0.03	0.06	0.00
K_2O	0.00	0.00	0.00	0.00	0.00	0.00	0.00	0.03	0.00	0.00	0.00	0.00	0.00	0.00	0.00	0.00	0.00	0.00
Cl	0.00	0.00	0.00	0.00	0.00	0.00	0.00	0.00	0.00	0.00	0.00	0.00	0.00	0.00	0.00	0.00	0.00	0.00
F	0.00	0.00	0.00	0.00	0.00	0.00	0.01	0.32	0.00	0.00	0.00	0.00	0.00	0.00	0.00	0.00	0.00	0.00
Cr_2O_3	0.13	0.39	0.13	0.42	0.33	0.26	0.11	0.21	0.00	0.09	0.17	0.09	0.13	0.16	0.10	0.14	0.17	0.12
BaO	0.04	0.22	0.00	0.00	0.00	0.00	0.00	0.02	0.00	0.00	0.01	0.00	0.00	0.00	0.00	0.00	0.00	0.00
Total	99.72	101.64	98.02	146.61	99.19	98.50	100.06	101.61	98.72	99.52	100.23	98.39	99.09	99.59	98.49	100.63	101.14	100.20
X_{Mg}	0.12	0.17	0.08	0.21	0.14	0.14	0.17	0.28	0.11	0.08	0.08	0.07	0.16	0.20	0.13	0.13	0.17	0.09
Py	10.9	27.1	6.0	9.6	12.0	6.0	13.8	26.9	7.5	6.8	7.9	5.0	13.2	17.4	8.8	13.5	20.4	6.6
Alm	68.9	79.9	63.9	68.3	72.3	65.3	70.6	74.6	64.7	76.3	77.2	74.9	72.2	73.9	68.5	58.0	66.4	47.1
Gro	3.3	4.8	2.7	3.6	4.2	3.0	3.4	4.5	1.5	4.1	4.8	3.5	4.1	5.0	3.2	1.0	27.1	10.3
Sp	17.8	26.1	7.9	18.4	24.9	12.0	23.4	12.1	3.3	12.8	16.1	10.7	10.5	14.2	5.4	9.5	19.6	1.8

Complete data set available from authors upon request. XLTH =xenolithic, OXC = orthoxenocrystic, PXC = paraxenocrystic, ME = magmatic enclave, PM = primary magmatic, eSMB = from evolved SMB rocks, and SR = source-rock. Av = average, Max = maximum, and Min = minimum.

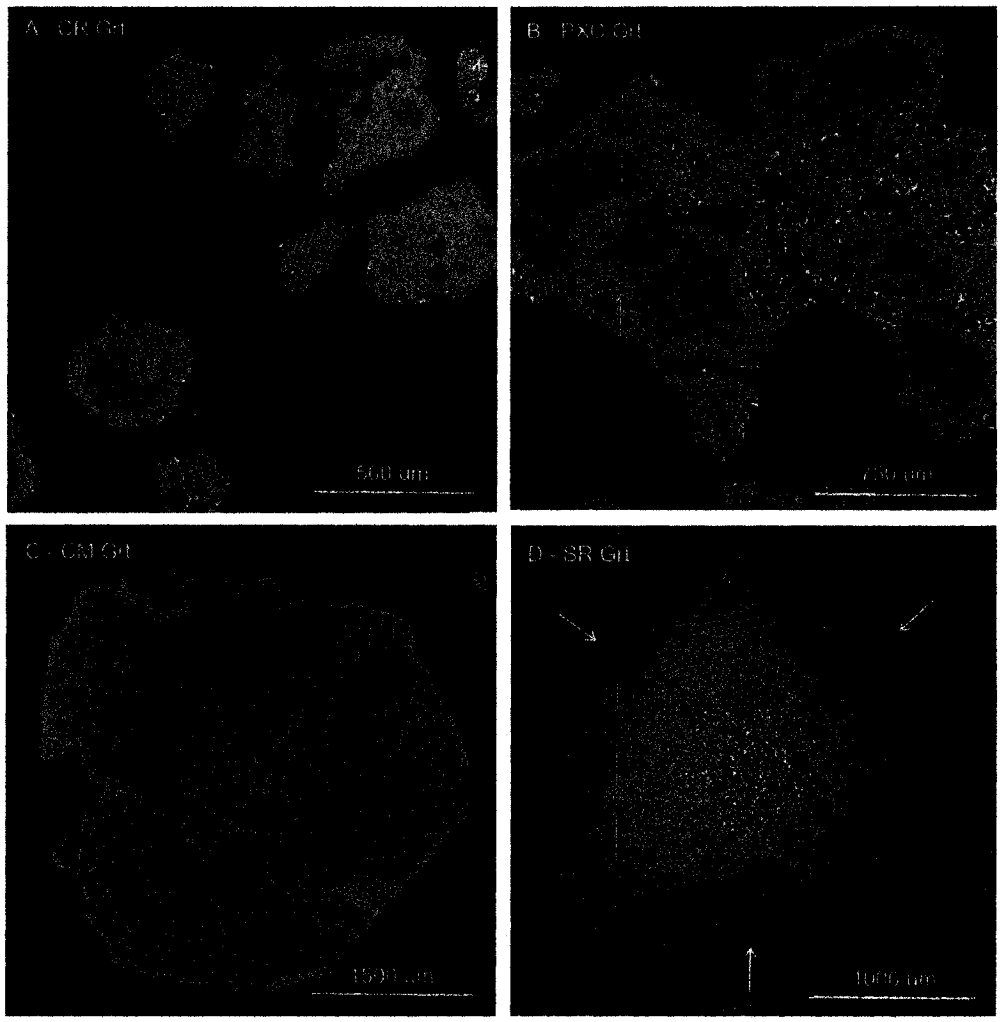

Figure 5.9: X-ray maps for garnet showing compositional zoning in Mn. Microprobe operating conditions were: 15 kV, 200 nA, 500 ms/pixel, 10 μm/pixel. Warm colours indicate higher Mn concentrations, but the colours are not standardized. A) CR Grt – country rock garnet, normal zoning. Sample E 430-Exp. B) PXC Grt – paraxenocrystic garnet, normal zoning, where Mn increases along grain boundaries and micro-cracks. Sample E 430B1. C) PM Grt – Primary magmatic garnet with core-intermediate-rim zoning. Sample BA-1. D) SR Grt – source rock garnet, reverse zoning. The rim of the garnet is partially resorbed as indicated by arrows. Sample TD-4.

Table 5.6: Garnet (Grt) trace-element concentrations (determined by LAM ICP-MS) for the various textural groups.

	D.L.	XLTH Grt			OXC Grt			PXC Grt			ME Grt			PM Grt (eSMB)			SR Grt		
n		4			3			22			5			3			4		
	Max	Av	Max	Min	Av	Max	Min	Av	Max	Min	Av	Max	Min	Av	Max	Min	Av	Max	Min
Li	4	26	35	11	19	28	10	16	30	6	37	48	24	27	47	15	20	32	3
V	1	491	915	318	444	467	404	134	270	33	38	43	34	55	55	54	202	286	112
Cr	8	245	431	144	551	716	345	177	458	13	4	5	3	45	77	1	98	169	33
Zn	5	64	75	54	53	62	40	71	99	49	83	94	71	61	89	1	94	121	57
Ga	1	13	16	10	13	13	12	11	14	10	15	16	14	11	14	10	12	15	9
Ge	2	10	12	7	10	12	7	8	13	6	13	14	10	11	11	10	20	23	17
Rb	0.4	0.3	0.6	0.0	1.1	1.1	1.1	0.2	0.9	0.0	0.2	0.3	0.1	0.1	0.2	0.0	0.06	0.10	0.03
Sr	3	-	-	-	0	0	0	0	1	0	1	1	0	1	1	1	0	0	0
Y	0.2	851	1412	97	115	186	75	1299	2684	120	3199	3408	2891	1089	1881	0	1178	2192	309
Nb	0.2	0.1	0.3	0.0	0.4	0.4	0.3	0.1	0.2	0.0	0.1	0.1	0.1	0.0	0.1	0.0	0.1	0.7	0.0
Cs	0.1	0.0	0.1	0.0	0.0	0.1	0.0	0.0	0.1	0.0	0.0	0.0	0.0	0.1	0.4	0.0	0.0	0.0	0.0
Ba	1	-	-	-	17	17	17	0	2	0	0	1	0	0	0	0	0	0	0
La	0.1	0.1	0.3	0.0	0.0	0.1	0.0	0.0	0.2	0.0	0.1	0.1	0.0	0.0	0.0	0.0	0.0	0.1	0.0
Ce	0.1	0.3	0.9	0.0	0.1	0.2	0.0	0.1	0.7	0.0	0.1	0.2	0.0	0.0	0.0	0.0	0.2	0.4	0.0
Pr	0.0	0.1	0.2	0.0	0.0	0.1	0.0	0.1	0.4	0.0	0.0	0.0	0.0	0.0	0.0	0.0	0.0	0.1	0.0
Nd	0.2	2.1	3.1	0.9	1.1	1.3	0.8	1.1	1.9	0.2	0.9	1.1	0.5	0.0	0.5	0.4	0.4	1.1	0.1
Sm	0.2	8.8	14.3	2.4	5.4	6.0	4.6	4.8	7.9	1.4	5.0	6.2	3.1	2.3	2.6	2.1	1.1	2.3	0.2
Eu	0.1	0.3	0.4	0.2	0.3	0.4	0.3	0.2	0.4	0.0	0.4	0.5	0.3	0.1	0.1	0.1	0.6	1.2	0.2

Complete data set available from authors upon request. XL =xenolithic, OXC = orthoxenocrystic, PXC = paraxenocrystic, ME = magmatic enclave, PM = primary magmatic, eSMB = from evolved SMB rocks (leucomonzogranites), and SR = source-rock. D.L. = detection limit, Av = average, Max = maximum, and Min = minimum.

5.5.1.4 Cordierite

Country-rock, paraxenocrystic, and primary magmatic cordierite from the SMB overlap largely in their X_{Mg} and Mn compositions, except for high-X_{Mg}, low-Mn paraxenocrystic, and low-X_{Mg}, high-Mn primary magmatic cordierite (Fig. 5.10A; Table 5.7). Sodium concentrations are low for country-rock cordierite (<0.11), but high for paraxenocrystic and primary magmatic cordierite (ca. 0.69-1.53). Country-rock cordierite shows X_{Mg} concentrations of ca. 0.35-0.67, Mn concentrations of 0.02-0.06 apfu, and Na concentrations of <0.11 apfu. The core of the paraxenocrystic cordierite analyzed has the highest X_{Mg} (~0.45-0.65), and the lowest Mn concentration (0.02 apfu), whereas the rim of the paraxenocrystic cordierite is compositionally similar to the primary magmatic cordierite crystals analyzed. Country-rock cordierite is largely unzoned, paraxenocrystic cordierite and some of the primary magmatic cordierite crystals show normal zoning, and some primary magmatic cordierite grains show large-scale (0.1-1.0 mm) oscillatory zoning in Mg-Mn-Fe (Erdmann et al. 2004) (Fig. 5.11). Normal and oscillatory zoned primary magmatic cordierites are compositionally similar.

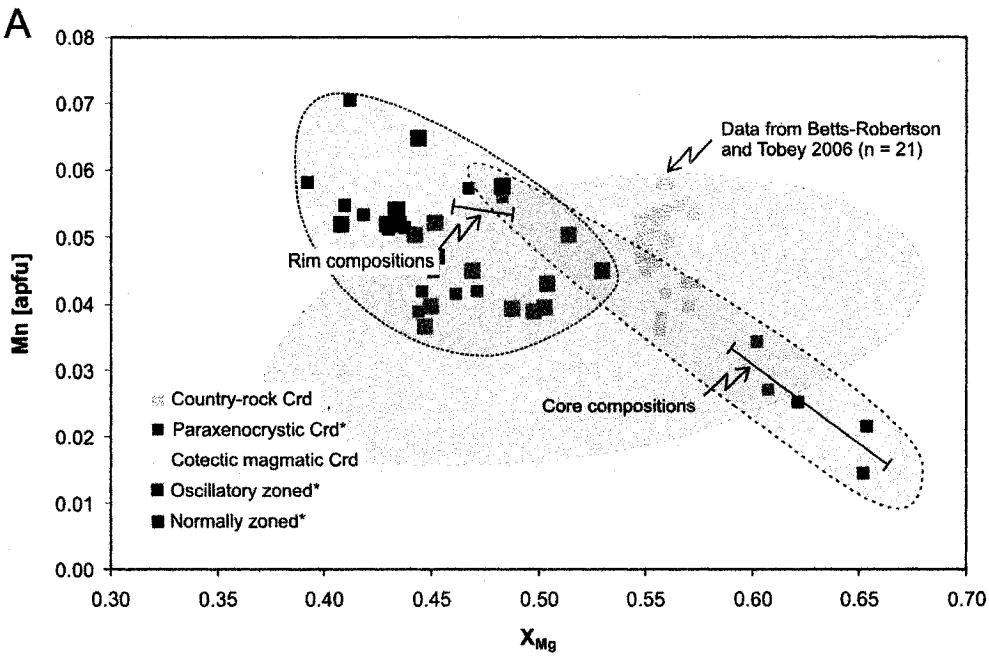

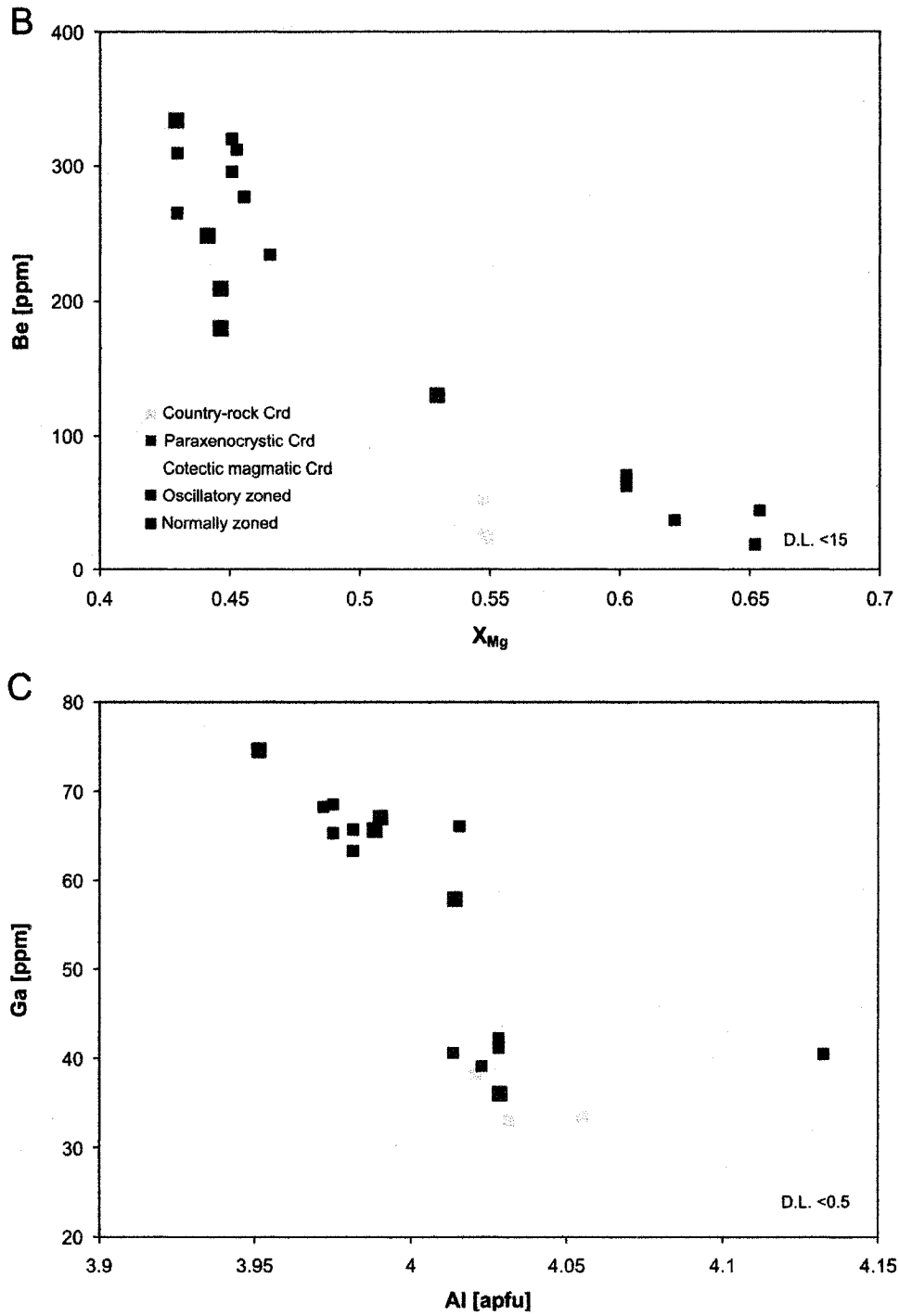

Figure 5.10: Compositions of the various textural cordierite (Crd) types. A) Concentrations of Mn (apfu) versus X_{Mg} for country-rock, paraxenocrystic, and normally and oscillatory zoned primary magmatic cordierite. Colored fields outline the compositional fields for country-rock (yellow), paraxenocrystic (purple), and primary magmatic plagioclase (blue). The yellow field encompasses compositional data from Tobey (2006); country-rock cordierite data points shown are from this study. * = Data from Erdmann et al. 2004. B) Be and concentrations of the various textural cordierite types as a function of X_{Mg}, and C) Ga concentrations as a function of Al (apfu).

Trace-element concentrations in paraxenocrystic and primary magmatic cordierite are high for Li and Cs, but low for country-rock cordierite, whereas all cordierite types have several tens of ppm or more of Be, B, and Ga (Table 5.8). Lithium, Be, and Ga vary non-systematically with Cs, X_{Mg}, Mn, or Ga, but are distinct for the various textural groups (Fig. 5.10B,C). Country-rock cordierite has lower concentrations for all trace elements than the primary magmatic cordierite, with the exception of one primary magmatic cordierite grain. Paraxenocrystic cordierite has higher Li and Cs concentrations, but similar Be and Ga concentrations than country-rock plagioclase, and lower Cs, Be, and Ga, as well as similar Li concentrations than the primary magmatic plagioclase crystals analyzed, except for one analysis from one primary magmatic grain. Characteristic variations in the trace-element concentration between the normal and oscillatory zoned primary magmatic cordierite crystals, or between core, intermediate, and rim zones are not evident from our data set.

Table 5.7: Cordierite (Crd) major-element concentrations (determined by EMP) for the various textural groups.

	CR Crd			**PXC Crd**			**PM Crd (eSMB)**		
n		**30**			**6**			**35**	
	Av	Max	Min	Av	Max	Min	Av	Max	Min
SiO_2	48.42	49.56	47.43	48.32	48.70	47.52	47.17	47.98	46.60
TiO_2	0.01	0.03	0.00	0.00	0.01	0.00	0.01	0.03	0.00
Al_2O_3	32.76	33.46	32.02	33.41	34.43	32.59	31.98	32.72	31.35
FeO	9.70	10.14	9.06	8.11	10.43	7.13	10.56	11.91	9.26
MnO	0.56	0.66	0.42	0.34	0.63	0.17	0.53	0.72	0.40
MgO	7.25	7.60	6.72	7.22	7.93	5.81	5.37	6.23	4.82
CaO	0.02	0.06	0.00	0.01	0.01	0.01	0.01	0.04	0.00
Na_2O	0.20	0.32	0.03	0.95	1.31	0.81	1.11	1.53	0.89
K_2O	0.01	0.09	0.00	0.00	0.01	0.00	0.01	0.11	0.00
Cl	0.00	0.01	0.00	0.00	0.00	0.00	0.00	0.01	0.00
F	0.03	0.15	0.00	0.00	0.00	0.00	0.00	0.00	0.00
Cr_2O_3	0.01	0.11	0.00	0.11	0.13	0.10	0.06	0.13	0.00
BaO	0.01	0.06	0.00	0.00	0.00	0.00	0.00	0.00	0.00
Total	98.98	99.74	97.60	98.47	99.77	97.52	96.92	98.14	95.59
X_{Mg}	0.56	0.57	0.55	0.60	0.65	0.48	0.46	0.53	0.41

Complete data set available from authors upon request. CR = country-rock, PXC = paraxenocrystic, PM = primary magmatic, and eSMB = from evolved SMB rocks. Av = average, Max = maximum, and Min = minimum.

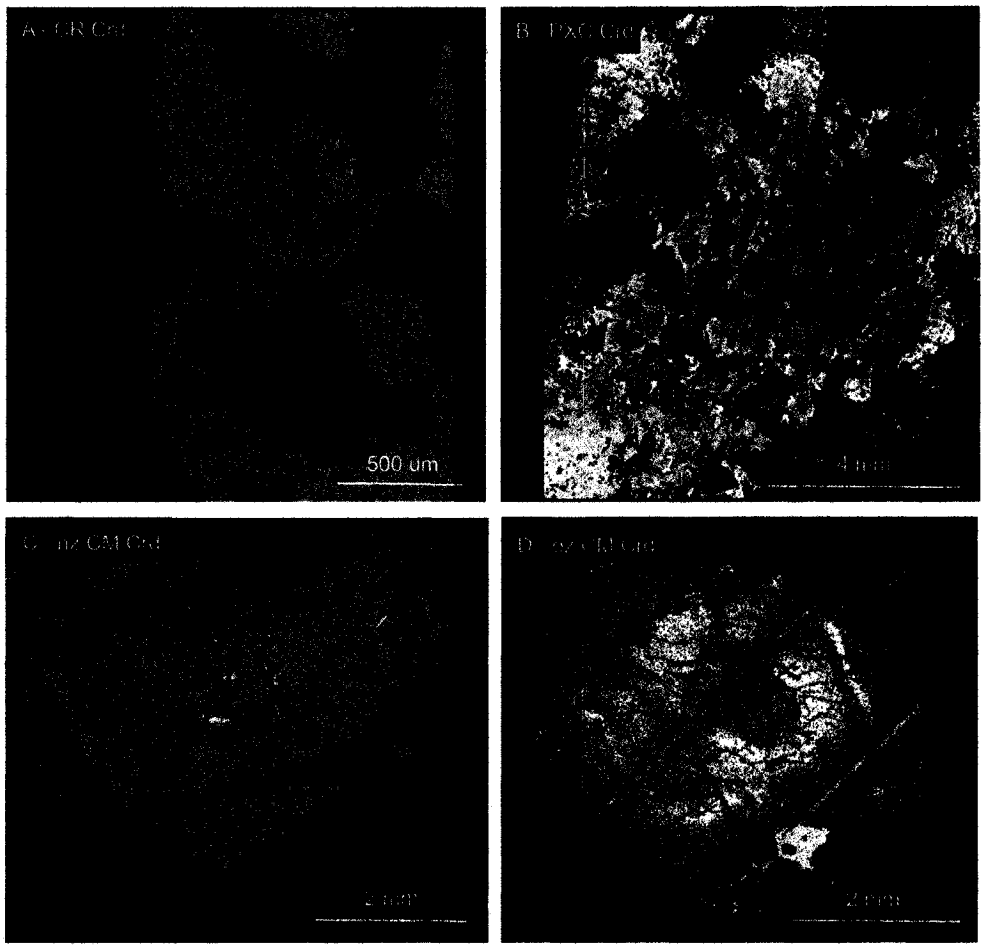

Figure 5.11: X-ray maps for cordierite with compositional zoning in Mg. Microprobe operating conditions were: 15 kV, 200 nA, 500 ms/pixel, 10 μm/pixel. Figures B-D from Erdmann et al. (2004). Warm colours mark higher Mg concentrations, but colours are not standardized. A) CR Crd – country-rock cordierite, largely unzoned. Sample H-03. B) PXC Crd – paraxenocrystic cordierite, patchy normal zoning. Note that the brightest red colours mark the distribution of biotite, and green and blue colours pinite. Sample 306-X. C) PM Crd – primary magmatic cordierite, normally zoned (nz). The dark blue colours mark pinite. Sample 304iii. D) PM Crd – primary magmatic cordierite, oscillatory zoned. The blue colours indicate pinite. Sample 304i.

Table 5.8: Cordierite (Crd) trace-element concentrations (determined by LAM ICP-MS) for the various textural groups.

	D.L.	CR Crd			PXC Crd			PM Crd (eSMB)		
n		3			5			12		
	Max	Av	Max	Min	Av	Max	Min	Av	Max	Min
Li	4	425	445	393	2208	2750	1738	2140	2485	1695
Be	19	33	51	23	46	70	18	259	335	131
B	106	26	33	21	20	36	11	46	292	3
V	1	1	1	1	1	2	0	1	2	0
Cr	8	1	1	1	1	1	1	1	4	0
Ga	1	35	38	33	41	42	39	64	75	36
Rb	0.4	1	1	0	4	10	1	12	20	3
Sr	3	2	3	1	1	2	0	0	1	0
Nb	0.2	0	0	0	0	0	0	0	0	0
Cs	0.1	1	1	1	103	128	88	143	174	68
Ba	1	1	2	0	4	18	0	0	2	0
La	0.1	0	0	0	0	0	0	0	0	0
Ce	0.1	0	0	0	0	0	0	0	1	0
Pr	0.0	0	0	0	0	0	0	0	0	0
Nd	0.2	0	0	0	0	1	0	0	0	0
Sm	0.2	0	0	0	0	0	0	0	0	0
Eu	0.1	0	0	0	0	0	0	0	0	0

Complete data set available from authors upon request. CR = country-rock, PXC = paraxenocrystic, PM = primary magmatic, and eSMB = from evolved SMB rocks (leucomonzogranites). D.L. = detection limit, Av = average, Max = maximum, and Min = minimum.

5.5.2 Cluster Analysis

5.5.2.1 Plagioclase

Using the concentrations of Sr, Ba, La, Ce, Pr, Nd, Eu, and Ga for the cluster analysis, we cannot unequivocally recognize the six texturally defined groups of plagioclase in an equivalent number of chemical clusters ($C1_{Pl}$-$C6_{Pl}$; Table 5.9). Only country-rock plagioclase is chemically largely distinct, whereas xenolithic, texturally orthoxenocrystic, and primary magmatic plagioclase from the SMB biotite granodiorites and monzogranites plot throughout clusters $C2_{Pl}$ to $C4_{Pl}$. Moreover, texturally orthoxenocrystic and magmatic crystals overlap compositionally in $C5_{Pl}$. Magmatic

plagioclase from the leucomonzogranites is mostly compositionally distinct, occurring in $C6_{Pl}$, with the exception of two core analysis plotting in cluster $C2_{Pl}$. The distribution of the various cases throughout the chemical clusters $C2_{Pl}$ to $C5_{Pl}$ are not related to samples or groups of samples (e.g., from the Five Mile Lake versus the Halifax pluton), the characteristic assemblage of the sample (e.g., the absence or presence of paraxenocrystic garnet), or the proximity to *in situ* country rocks or xenoliths. Core and rim analyses are chemically indistinct. Source rock plagioclase belongs to clusters $C3_{Pl}$ and $C4_{Pl}$, but the number of analyses is too low to be statistically relevant.

Table 5.9: Crosstabulation of chemical clusters ($C1_{Pl}$-$C6_{Pl}$) versus texturally defined origins for plagioclase. Chemical clusters are defined based on Sr, Ba, La, Ce, Pr, Nd, Eu, Ga, and Cs concentrations.

		Chemical cluster						
		$C1_{Pl}$	$C2_{Pl}$	$C3_{Pl}$	$C4_{Pl}$	$C5_{Pl}$	$C6_{Pl}$	Total
Textural type	CR	15	0	0	0	0	0	1
	XLTH	0	4	6	11	0	0	24
	OXC	0	16	5	8	5	0	30
	PM (p)	0	19	1	4	6	0	32
	PM (e)	0	2	0	0	0	9	11
	SR	0	0	2	1	0	0	3
	Total	20	9	14	25	11	9	115

CR = country rock, XLTH = xenolith, OXC = orthoxenocryst, PM = primary magmatic, p = more primitive SMB rocks (biotite granodiorite and monzogranite), e = more evolved SMB rocks (leucomonzo-granites), and SR = source-rock.

5.5.2.2 Biotite

Using the concentrations of V, Cr, and Nb in biotite for the cluster analysis, the analyzed country-rock biotite dominates $C1_{Bt}$, and xenolithic and texturally orthoxenocrystic biotite belongs mostly to $C2_{Bt}$ and $C3_{Bt}$ (Table 5.10). Magmatic biotite occurs mostly in $C4_{Bt}$, where magmatic biotite crystals that formed from a hybrid melt phase (e.g., occurring in garnet-rich schlieren) occurs in both $C1_{Bt}$ and $C4_{Bt}$ clusters. Various types of biotite crystals from the same sample tend to plot in the same chemical cluster.

Table 5.10: Crosstabulation of chemical clusters ($C1_{Bt}$-$C4_{Bt}$) versus texturally defined origins for biotite. Chemical clusters are chemical clusters determined for V, Cr, and Nb.

		Chemical cluster				
		$C1_{Bt}$	$C2_{Bt}$	$C3_{Bt}$	$C4_{Bt}$	Total
Textural type	CR	25	1	1	0	27
	XLTH	3	23	2	2	30
	OXC	1	11	3	3	18
	PM (p)	5	1	0	36	42
	Total	33	27	7	50	117

CR = country rock, XLTH = xenolith, OXC = ortho-xenocryst, PM = cotectic magmatic, and p = more primitive SMB rocks (biotite granodiorite and monzogranite).

5.5.2.3 Garnet

The six texturally identified garnet types do not correlate with the six chemical groups discriminated based on V, Cr, Zn, Y, Nd, and Sm ($C1_{Grt}$-$C6_{Grt}$; Table 5.11). If we consider core and rim analyses, all textural garnet types are distributed throughout more than one of the chemical clusters, except for texturally orthoxenocrystic garnet ($C1_{Grt}$) and garnet from the garnet-rich magmatic enclave ($C3_{Grt}$), both of which represent only one sample. Paraxenocrystic garnet forms part of the $C1_{Grt}$, $C3_{Grt}$, $C4_{Grt}$, and $C5_{Grt}$ clusters. The garnet analyses classified as $C1_{Grt}$ are core compositions only, whereas the $C3_{Grt}$ to $C5_{Grt}$ comprise core and rim compositions. Primary magmatic garnet belongs to the $C4_{Grt}$ and $C5_{Grt}$ chemical clusters, where the garnet analyses of $C4_{Grt}$ are from an intermediate, low-Mn, high-X_{Mg} zone, and garnet analyses that plot in $C5_{Grt}$ are core and rim compositions. If only core compositions and intermediate compositions of paraxenocrystic garnet, primary magmatic garnet, and source-rock garnet are considered, the cluster occupancy changes, but paraxenocrystic and primary magmatic garnet, as well as paraxenocrystic, orthoxenocrystic, and country-rock garnet, still overlap compositionally (Table 5.12).

Table 5.11: Crosstabulation of chemical clusters ($C1_{Grt}$-$C6_{Grt}$) versus texturally defined origins for garnet. Chemical clusters are defined based on V, Cr, Zn, Y, Nd, and Sm concentrations . Core, intermediate, and rim analyses are included.

		Chemical cluster						
		$C1_{Grt}$	$C2_{Grt}$	$C3_{Grt}$	$C4_{Grt}$	$C5_{Grt}$	$C6_{Grt}$	Total
Textural type	XLTH	3	2	0	0	0	0	5
	OXC	3	0	0	0	0	0	3
	PXC	5	0	6	13	5	0	29
	ME	0	0	6	0	0	0	6
	PM (e)	0	0	0	2	5	0	7
	SR	0	0	0	0	0	8	9
	Total	11	2	12	15	11	8	59

XLTH = xenolith, OXC = orthoxenocryst, PXC = paraxenocryst, PM = primary magmatic, e = more evolved SMB rocks (leucomonzogranites), and SR = source-rock.

Table 5.12: Crosstabulation of chemical clusters ($C1_{Grt}$-$C6_{Grt}$) versus texturally defined origins for garnet. Chemical clusters are defined based on V, Cr, Zn, Y, Nd, and Sm concentrations. Core, and intermediate analyses only.

		Chemical cluster						
		$C1_{Grt}$	$C2_{Grt}$	$C3_{Grt}$	$C4_{Grt}$	$C5_{Grt}$	$C6_{Grt}$	Total
Textural type	XLTH	1	1	2	0	0	0	4
	OXC	1	2	0	0	0	0	3
	PXC	5	0	0	8	9	0	22
	ME	0	0	0	3	0	0	3
	PM (e)	0	0	0	3	2	0	5
	SR	0	0	0	0	0	8	8
	Total	7	3	2	14	11	8	45

XLTH = xenolith, OXC = orthoxenocryst,
PM = primary magmatic, e = more evolved SMB rocks (leucomonzo-granites), and SR = source-rock.

5.5.2.4 Cordierite

Using Li, Cs, Ga, and Be as the independent variables, all three texturally variable cordierite types plot as three chemically distinct clusters ($C1_{Crd}$-$C3_{Crd}$; Table 5.13), with the exception of one primary magmatic cordierite grain that occupies the same chemical cluster ($C2_{Crd}$) as the paraxenocrystic cordierite analyzed. If four instead of three chemical clusters are predetermined, country-rock cordierite remains in a separate cluster ($C1^*_{Crd}$), and paraxenocrystic cordierite, as well as the one primary magmatic cordierite grain remain in another cluster ($C2^*_{Crd}$). The primary magmatic cordierites separate into two chemical clusters ($C3_{Crd}$* and $C4_{Crd}$*), with normal and oscillatory zoned cordierite crystals, distributed throughout both chemical clusters.

Table 5.13: Crosstabulation of chemical clusters ($C1_{Crd}$-$C4_{Crd}$) versus texturally defined origins for cordierite. Chemical clusters are determined for Li, Cs, Ga, and Be trace-element concentrations.

		Chemical cluster				
		$C1_{Crd}$	$C2_{Crd}$	$C3_{Crd}$	$C4_{Crd}$	Total
Textural type	CR	3	0	0	0	3
	PXC	0	5	0	0	5
	PM (e) nz	0	0	2	4	6
	PM (e) oz	0	1	3	2	6
	Total	3	6	5	6	20

CR = country rock, PXC = paraxenocryst, PM = primary magmatic, e = more evolved SMB rocks (leucomonzo-granites), nz = normal zoning, and oz = oscillatory zoning.

5.6 Discussion

5.6.1 Deciphering Petrogenetic Information from Mineral Chemical Data

Chemical groups evident from two-component concentration plots and multi-element cluster analysis for plagioclase, biotite, and garnet from Meguma Group country rocks, Tangier basement source rocks, and SMB rocks, do not match the texturally defined groups. Although it is possible that some of the analyzed crystals (e.g., some orthoxenocrysts) are texturally misclassified, this uncertainty cannot explain the

discrepancy between texturally and chemically defined groups, because several plagioclase, biotite, and garnet crystals of unquestionably different origins (e.g., country rock and source rock crystals, or obvious orthoxenocrysts and obvious primary magmatic crystals; Section 5.3; Figures 5.2, 5.4) plot in the same chemical clusters. Inspection of the plagioclase, biotite, and garnet clusters presented has not revealed any other meaningful groups, and cluster analysis using a higher or lower number or other independent variables (major- and trace-element concentrations), or a a higher or lower number of chemical clusters (not presented in this paper), showed similar results, although the distribution of the various cases throughout the clusters varied. We therefore suggest that the major- and trace- element concentrations we analyzed are not discriminating for the various plagioclase, biotite, and garnet crystal types of our sample set. On the other hand, for cordierite crystals from our samples set, paraxenocrystic and primary magmatic origin can be distinguished based on trace-element concentrations, but the chemical differences may disappear with the addition of further analyses.
Without a better alternative, we use the texturally grouped crystal types for further discussion, even though we acknowledge that our textural classification of the various crystal types may not be perfect.

5.6.2 Petrogenetic Information from the Rock-forming Minerals of the SMB

5.6.2.1 Plagioclase

The origin of orthoxenocrystic and magmatic plagioclase in the SMB may, with some uncertainty, be determined from textural criteria (Fig. 5.2, Chapter 4). On the other hand, major- and trace-element compositions, inspected in two-component concentration plots as well as multi-element cluster analysis, cannot unequivocally identify crystals of orthoxenocrystic or magmatic origin. Normal and oscillatory growth zoning in X_{An} shows that the original Na-Ca compositional characteristics of the magmatic plagioclase grains are largely preserved. However, zoning in X_{Or} is weak to absent, and country-rock plagioclase from the thermal aureole of the SMB, xenolithic, and orthoxenocrystic plagioclase are on average higher in X_{Or} than country-rock plagioclase distant from the SMB, indicating that K concentrations of plagioclase crystals in the vicinity of, or incorporated into, SMB magmas reequilibrated through ion exchange (K-Na interdiffusion is approximately three orders of magnitude faster than Ca-Na interdiffusion; Giletti and Shanahan 1997; Cherniak 2003).

The significant compositional overlap in X_{An} and X_{Or} between xenolithic plagioclase crystals and those crystals classified as orthoxenocrysts may indicate, but cannot unequivocally show, that the suspect phases are orthoxenocrysts derived from country rocks of the Meguma Group. That only few xenolithic and orthoxenocrystic plagioclase grains have X_{An} values of <0.2 may partly be a result of our sample selection, but may also reflect the increase of X_{An} in country-rock plagioclase towards the contact with the SMB, or the assimilation of low-X_{An} plagioclase in SMB magmas through partial melting (e.g., T_m of plagioclase with X_{An} ~ 0.2 is ca. 750 °C, whereas plagioclase with X_{An} ~ 0.4 is ca. 810 °C; Yoder et al. 1957).

Trace-element compositions of xenolithic plagioclase lie between those of country-rock plagioclase and primary magmatic plagioclase, except for Sr, whereas trace-element compositions of orthoxenocrystic plagioclase largely overlap with the compositions of primary magmatic plagioclase, except for some crystals that have signatures similar to the xenolithic crystals (Fig. 5.6). These compositional relations probably constitute further evidence for ion exchange between xenolithic minerals and the former SMB host magmas, with a higher degree of reequilibration between orthoxenocrysts and former host magma than between xenolithic crystals and former host magma. The exceptional compositional relation for Sr in the texturally variable plagioclase types, with high Sr concentrations for country-rock plagioclase, intermediate Sr concentrations for primary magmatic plagioclase, and low Sr concentrations for xenolithic and orthoxenocrystic plagioclase may seem contradictory to ion exchange reactions between country-rock-derived plagioclase and SMB host magmas. However, they can be explained by ion exchange reactions between country-rock-derived solids and SMB magmas fractionating plagioclase and other Sr-bearing phases. The explanation we suggest is that the cores of the primary magmatic plagioclase grains from the SMB biotite granodiorites and monzogranites crystallized during the early evolution of the magmas, coexisting with SMB melts relatively high in Sr, say on the order of 50 ppm Sr, if D_{Sr} was on the order of 10. Subsequent to their crystallization, the large cores of the primary magmatic crystals were not, or were only to a minor degree, affected by ion exchange reactions with the fractionating, increasingly Sr-depleted host SMB magma. On the other hand, for the smaller xenolithic, and even more so for orthoxenocrystic plagioclase grains, as well as for the rims of the primary magmatic plagioclase grains, partial to complete reequilibration of their compositions with the host magmas probably took place.

For the compositions of the plagioclase crystals studied, diffusive reequilibration of trace elements should have been efficient (Cherniak and Watson 1992, 1994; Giletti and Casserly 1994; Cherniak 1995, 2002, 2003). Over a length-scale of 100 μm, the Sr concentration, for example, may change by 10% in the center of the grain over ≤20,000 years at a temperature of 650 °C, and over ≤1000 years at a temperature of 800 °C. For slower diffusing cations, such as Nd, the original compositional signature of a 100 μm country-rock crystal may have resisted obliteration with a similar degree of change for ≥1 million years, even at temperatures of 800 °C, but even such a time-scale is not long for plutonic systems like the SMB, and it is therefore likely that efficient diffusive equilibration occurred.

Another possible explanation for the compositional variation in Sr for the various textural plagioclase types is that the high Sr concentration of the country-rock plagioclase crystals analyzed is not representative, and that the xenolithic and orthoxenocrystic plagioclase grains had originally lower Sr concentrations than the primary magmatic plagioclase grains, and reequilibrated towards higher Sr concentrations upon entrainment in the SMB magmas. Although we cannot completely rule out this possibility, we consider it unlikely, given that Meguma Group xenoliths from locations near the locations of *in situ* country-rock samples were studied, and that these xenoliths seem to have remained near their site of formation (Chapter 4). However, in both cases the result is similar, where the overlap in composition for the various crystal types permit no confident discrimination between country-rock-derived and cognate magmatic plagioclase grains in the SMB rocks.

The assimilation of country-rock material through partial melting or dissolution, as observed in field and textural studies, is not evident in the compositionally distinct zones in most of the analyzed primary magmatic plagioclase crystals, but may explain some of the detected compositional scatter (e.g., Fig. 5.6). Analyzed cores of primary magmatic plagioclase grains that crystallized from a melt with at least a contribution from Meguma Group country rocks (e.g., plagioclase of the garnet schlieren, Fig. 5.5: Chapter 4) are similar to plagioclase crystals that formed from apparently uncontaminated SMB rocks (which may be contaminated by Meguma Group country rocks, but likely with a lower amount of country-rock material present than in the garnet schlieren). Hence, both melt phases must have reequilibrated though diffusive exchange, given that the original melt compositions for SMB granodiorites and Meguma Group metasedimentary rocks were different, as determined in melting experiments (Chapter 3). Only some rim compositions

of primary magmatic plagioclase grains, which obviously crystallized at the immediate contact with Meguma Group xenoliths, are compositionally closer to xenolithic and orthoxenocrystic than to average primary magmatic plagioclase of the SMB. The reason for their country-rock-like compositional signature may be that the rims crystallized from the last increments of country-rock partial melt, which did not undergo vigorous diffusive reequilibration with the main magma, or diffusive reequilibration between country-rock solids and primary magmatic plagioclase crystals in contact. Zoning patterns of trace elements, which have not been determined, are most likely to reveal the assimilation of country-rock plagioclase through partial melting and/or dissolution (e.g., Edwards and Russell 1996; Weight et al. 2000; Tepley and Davidson 2003). However, with the relatively minor compositional variations between country rocks and SMB granites and their mineral phases, respectively, only the assimilation of large amounts of country-rock partial melt over a relatively short period of time may have resulted in a characteristic chemical signature in primary magmatic plagioclase and other primary magmatic of the SMB.

The difference in the plagioclase compositions between crystals from the biotite granodiorites and monzogranites and those from the leucomonzogranites may reflect fractional crystallization, magma recharge, or a combination (Fig. 5.6). In the case of fractional crystallization, the compositional variation between the primary magmatic plagioclase crystals from the SMB biotite granodiorites and monzogranites and those of the SMB leucomonzogranites may relate to the fractionation of a higher amount of K-feldspar, apatite, and other accessories, such as zircon and monazite, in the evolution of the leucomonzogranites relative to the SMB biotite granodiorites and monzogranites. For example, both K-feldspar and apatite would have fractionated Sr in addition to plagioclase (e.g., Bea et al. 1994), and thereby largely depleted the SMB melt phase in Sr, whereas lower Nd concentrations in plagioclase from the leucomonzogranites may reflect the fractionation of accessories, such as zircon and monazite, and the depletion of the SMB magmas in elements compatible in these phases. On the other hand, if magma recharge occurred, most of the primary magmatic plagioclase from the leucomonzogranites crystallized from a magma with a different composition than the primary magmatic plagioclase from the granodiorites and monzogranites. If so, only the two analyzed plagioclase phenocrysts with compositions similar to the primary magmatic crystals from the SMB biotite granodiorites and monzogranites may have crystallized

prior to magma recharge, or they may be the relics of mixing between granodiorite and leucomonzogranites magmas.

Source-rock plagioclase with initially low-X_{An} and high-X_{Or} compositions may form part of the plagioclase population classified as orthoxenocrysts (they are texturally similar), if ion exchange efficiently lowered the K and trace-element concentrations of the source-rock grains. However, the lack of plagioclase crystals in the SMB rocks with X_{An} trace-element compositions similar to those of Ca-rich source-rock plagioclase, which should have texturally and chemically survived the incorporation into the SMB magmas (given the refractory nature and low diffusivities in anorthite-rich plagioclase), suggests that source-rock plagioclase is absent, or at least rare in the SMB rocks studied. Most noticeable is that source-rock and primary magmatic plagioclase from the SMB biotite granodiorites and monzogranites have similar concentrations of Ga, Sr, Nb, Ba, and Eu, all of which are trace elements that largely reside in plagioclase or biotite (e.g., Bea et al. 1994). A hypothesis to explain the compositional similarity in Ga, Sr, Nb, Ba, and Eu between source rock and primary magmatic plagioclase is that the cores of the primary magmatic plagioclase crystallized from a melt phase that was largely derived from the Tangier basement source rocks as previously suggested based on whole-rock Sr-Nd isotopic data (Clarke and Chatterjee 1992; MacDonald 2001; Clarke et al. 2004; Clarke and Erdmann 2005; Chapter 4). The differences in the La, Ce, Pr, Nd concentrations between source-rock and primary magmatic plagioclase may indicate (local or global) disequilibrium between source-rock partial melts and refractory accessory minerals, and/or early fractional crystallization of trace minerals such as zircon or monazite prior to the crystallization of the cores of the analyzed SMB plagioclase phenocrysts.

5.6.2.2 Biotite

Textural criteria as well as major- and trace-element compositions cannot discriminate unequivocally between biotite of orthoxenocrystic and biotite of primary magmatic origin. The higher degree of compositional similarity for various biotite types within a single SMB sample than for a given biotite type between SMB samples shows that the major and trace- element compositions of xenolithic, orthoxenocrystic, and magmatic biotite are largely determined by the composition of the former SMB host magma. The larger compositional scatter for orthoxenocrystic biotite reflects a larger number of samples with a higher range in whole-rock composition than the samples from which our xenolithic and magmatic biotite crystals come. The higher average Cr concentration for

xenolithic and orthoxenocrystic biotite than for primary magmatic biotite from the SMB biotite granodiorites and monzogranites (X_{Mg} for all these biotites is ≥0.35) is the only chemical evidence for the country-rock origin of the analyzed biotite crystals. The high Cr concentration in xenolithic and orthoxenocrystic biotite may thereby reflect a higher Cr concentration in the biotite, or the presence of a microscopically invisible, exsolved chromium-rich phase. However, unequivocally identifying orthoxenocrystic biotite in the SMB based on a higher Cr concentration is not feasible, because the biotite orthoxenocrysts that potentially had a longer magma residence time (occurring in the more central parts of the batholith), compositionally overlap with biotite of primary magmatic origin. Moreover, primary magmatic biotite crystals, which certainly crystallized from a hybrid, country-rock-derived and cognate magmatic SMB melt phase, have compositions equivalent to cognate magmatic biotite grains that crystallized from a SMB melt phase with little or no contribution from country-rock-derived partial melt. Major-element as well as trace-element compositions are, therefore, incapable of deciphering the origin of texturally different biotite types in the SMB (e.g., biotite from biotite-rich schlieren which may be of cognate or foreign magmatic origin; Clarke and Erdmann 2005; Chapter 4). Similar conclusions, although based only on major element compositions, have been reached for biotite from biotite-rich schlieren and host diatextites of the St Malo migmatite terrane (Milord and Sawyer 2003), and for biotite from xenoliths, biotite-rich schlieren, and host tonalites of the Port Mouton pluton (McCuish 2001).

5.6.2.3 Garnet

The origin of orthoxenocrystic, paraxenocrystic, and primary magmatic garnet in the SMB may, with some uncertainty, be deciphered based on textural criteria (Allan and Clarke 1981; Chapter 4). Major- and trace-element compositions cannot discriminate between garnet crystals of orthoxenocrystic, paraxenocrystic and primary magmatic origin (Allan and Clarke 1981; this study), whereas major element compositions cannot, but trace-element compositions can, discriminate between source-rock garnet and the various other garnet types studied. Chemical zoning patterns are most useful to detect the origin of given garnet crystal and to decipher the condition of its formation in the SMB.

The large compositional scatter for the paraxenocrystic garnets probably reflects local conditions, with compositionally variable country-rock material and SMB magmas

involved in the garnet-forming reaction. Alternatively, the large compositional overlap between paraxenocrystic and primary magmatic garnet appears to suggest that the composition of the paraxenocrystic garnet grains is at least partly controlled by the composition of the SMB host melt.

The large-scale oscillatory zoning of the primary magmatic garnet grains probably reflects the crystallization from compositionally variable host magmas, given that core, intermediate, and rim zones have distinct major-element as well as trace-element compositions. Further analyses are needed to confirm the compositional relations, but the present data suggest that the intermediate zones have compositions more similar to the Meguma Group garnets (relatively high Sm, Eu, Nd, Cr, and V concentrations), whereas core and rim zones have chemical signatures more similar to the source rock garnets (relatively low Sm, Eu, Nd, Cr, and V concentrations). The zoning pattern of the garnets may thus relate to source variations and recharge of the SMB magma chamber, but another possibility is that the compositional zoning reflects the crystallization from a magma dominated by Tangier basement components during the early and late growth stages, and assimilation of Meguma Group country-rock material during the intermediate growth stage, without evidence for disrupted garnet growth or dissolution.

The origin of the primary magmatic garnet from the garnet-rich enclave remains unresolved, with major- and trace-element characteristics distinct from those of the analyzed paraxenocrystic, primary magmatic, and source-rock garnet crystals. Most probable is that the enclave resulted from the assimilation of partially melted country rocks of pelitic composition, given the unusual mineralogy and composition of the enclave with up to 20 vol% of garnet.

5.6.2.4 Cordierite

The origin of orthoxenocrystic, paraxenocrystic, and primary magmatic cordierite in the SMB may be determined from textural criteria (Erdmann et al. 2004), as well as from major- and trace-element characteristics (this study). The compositional differences between the one paraxenocrystic cordierite grain analyzed and the primary magmatic grains analyzed is striking, compared to the compositional variability of paraxenocrystic and primary magmatic garnet crystals. Further analyses are needed to verify that this relation does not relate to the small number of samples analyzed (one paraxenocrystic and five primary magmatic cordierite crystals), but even intense sampling for cordierite

was unsuccessful in obtaining more unaltered potential paraxenocrysts and primary magmatic cordierite than the crystals studied here.

If the compositional differences of the various cordierite types are characteristic, a previously deduced, partially foreign magmatic origin for the primary magmatic cordierites of the SMB (Erdmann et al. 2004; Clarke and Erdmann 2005; Chapter 3) is no longer tenable. The hypothesis was that the normally zoned cordierite grains may have grown from a hybrid melt with country-rock and SMB components, as a result of country-rock assimilation through partial melting of Meguma Group country-rock material (Chapter 3). Although this mechanism may in some cases explain the formation of primary magmatic cordierite in the SMB, field and textural observations indicate that the majority of primary magmatic cordierite crystals in the SMB formed from magmas with little contamination from Meguma Group rocks. With the support from distinct trace-element compositions for all but one of the primary magmatic cordierite analyses on one hand, and paraxenocrystic and country-rock cordierite on the other hand, a cognate magmatic origin for the cordierite grains is most convincing. Further support for such an interpretation may be one unusual analysis from one zone of one of the oscillatory zoned cordierite crystals, with trace-element compositions closer to the composition of the paraxenocrystic and country-rock cordierite crystals than to those of the primary magmatic cordierite grains (Fig. 5.10B,C). The analyzed zone of the cordierite crystal with unusual composition may reflect partial growth from a hybrid melt of country-rock and SMB components, and is thus possibly the only evidence country-rock contamination and assimilation recorded in cordierite in addition to the direct evidence from paraxenocrystic cordierite.

The origin of the oscillatory zoning in cordierite remains speculative, but in the light of the new trace-element data, the previously favoured process of magma recharge (Erdmann et al. 2004) appears less likely to explain the oscillatory zoning. Magma recharge should affect not only the major-element composition, but also the trace-element composition of the host magmas, and thus those of the growing cordierites., which does not seem to be the case. Most suitable to account for the observed oscillatory zoning may be eruption or degassing mechanisms (e.g., Shore and Fowler 1996 for a review; Erdmann et al. 2004 for cordierite). These mechanisms may have caused a change in the major-element composition, but not in the trace-element composition of the growing crystals by varying the stability field of cordierite and other Mg-Fe-Mn-bearing phases, and thus their compositions as a function of P_{fluid} (e.g.,

Clarke 1995). If so, oscillatory zoning in oscillatory zoning in micas (Clarke and Bogutyn 2003) and in cordierite suggest in combination that eruption of magmas or gases from the SMB occurred repeatedly, and as recorded in cordierite, also during an intermediate stage in the chemical evolution of the SMB.

5.6.3 Petrogenetic Information from Mineral Chemical Data in Plutonic Rocks

In plutonic systems other than the SMB, compositional differences between crystal types of various origins may be larger initially, and the chances of discriminating between foreign and cognate magmatic crystals may thus be higher. Moreover, depending on the composition of plagioclase, biotite, garnet, and other rock-forming minerals, elemental diffusivities may vary drastically (e.g., Sneeringer et al. 1984; Blundy and Wood 1991; Ganguly and Tirone 2001; Van Orman et al. 2002; Cherniak 2003). For example, anorthite-rich plagioclase may resist chemical obliteration for ten to several hundred times longer than plagioclase of oligoclase or labradorite composition (Cherniak 2003). Country-rock-derived plagioclase rich in the anorthite-component, may thus be chemically evident in igneous rocks, whereas chemical evidence for the presence of country-rock-derived oligoclase and labradorite may be readily lost.

A small grain size, such as small grain size of plagioclase and biotite of Meguma Group origin, is problematic for detecting the origin of crystals as well as magma chamber processes recorded in their composition, because the original composition of the crystals is more likely being blurred or lost over a geologically relatively short periods of time, or easily overlooked, if the analytical volume approaches or exceeds the volume of compositional zones (e.g., original composition in the core, reequilibrated composition along the rim).

5.7 Summary and Conclusions

Major- and trace-element compositions cannot unequivocally determine the origin of plagioclase, biotite, and garnet in the SMB. Obstacles for the identification of grains of various origins in the SMB using mineral chemical compositions are the negligible to small original compositional differences between the crystals of various origins, high elemental diffusivities in the rock-forming minerals, and the relatively small grain size of various crystal types.

In the light of this largely negative result, is there any potential for deciphering the origin of various crystal types, including the small crystals in granites and other plutonic rocks?

We believe that the answer is affirmative, even though there may not be an unequivocal answer for every single crystal under consideration. We suggest that the origin of the small crystals in the SMB and other igneous rocks is best determined on the basis of textural criteria and compositional zoning, and under consideration of the local mineral assemblage (e.g., if orthoxenocrystic cordierite is abundant, small quartz crystals are more likely to have an orthoxenocrystic origin than small quartz crystals in a rock that lacks clear evidence for foreign solids). Intimately linking the study of small crystals to the characterization of compositions and compositional zoning features of large crystals may give indirect evidence for the origin of the various crystal types in an igneous rock, and may reveal evidence for the significance and the relative timing of magma recharge, assimilation, and fractional crystallization processes, which field, textural, and whole-rock geochemical data alone cannot detect. Primary magmatic cordierite and garnet are two examples from this study, where combined major- and trace-element data provide evidence for phenomena of eruption and magma recharge, as well as country-rock assimilation, and a relative chronology of these events.

5.8 Acknowledgements

Saskia Erdmann acknowledges the support from a Killam Pre-doctoral Scholarship at Dalhousie University throughout this study, and D.B. Clarke acknowledges the support of an NSERC Discovery Grant that made this study possible. We thank Jiggs Diegor and Mike Tubrett for technical support, for carrying out a third of the trace-element analysis in our absence, and for reduction of the ICP-MS raw data. We thank Patricia Stoffyn for assistance at the Dalhousie Regional Electron Microprobe Laboratory, Gordon Brown for the polished thin sections, and Vaneeta Kaur Groover for her help with the cluster analysis.

CHAPTER 6

Energy-constrained Modelling of Country-rock Assimilation in the Granitic South Mountain Batholith, Nova Scotia, Canada

6.0 Preamble

This chapter is prepared as a manuscript for submission to the Canadian Journal of Earth Sciences by S. Erdmann. The study presented was motivated by discussions with D.B. Clarke and R.A. Jamieson, but I carried out all the modelling, did the interpretation, drafted the manuscript, as well as all Figures and Tables, and I am therefore solely responsible for the content of this chapter.

The incitement for modelling the energy-constrained assimilation of country rocks by SMB magmas arose from the limitation in the vertical exposure of the batholith with access only to the near-roof level. Modelling the significance of country-rock assimilation through partial melting at unexposed levels of the batholith is important in order to evaluate if the observed, near-roof degree of country-rock contamination and assimilation in the SMB is likely representative for the whole batholith, or if and to what degree country-rock contamination and assimilation may have been more significant at deeper levels of the SMB magma chamber.

6.1 Abstract

Energy-constrained modelling of open-system magmatic processes, including country-rock assimilation, provides a means to predict the relative and the absolute importance of various magma chamber processes in a given igneous system. In this contribution, I present energy-constrained models for the assimilation of country rocks in the South Mountain Batholith (SMB) through partial melting, simulating conditions for the near-roof level of the batholith, with a magma temperature of 800°C and an initial country-rock temperature of 350°C, as well as conditions for the unexposed, near-floor level of the batholith, with a magma temperature of 850°C and an initial country-rock temperature of 600°C. For magmas of granodiorite to leucogranite compositions, metapsammitic and metapelitic assimilants, and an equilibration temperature of 750 °C (the boundary temperature between country rocks and magma), the models compute no partial melting at the near-roof level of the batholith, but suggest that a country-rock mass of up to 8 % of the volume of the SMB may have partially melted at the near-floor level of the

batholith. Under natural conditions, assimilation of country rocks through partial melting at the near-roof level of the SMB occurred, and country-rock assimilation in the exposed part of the batholith was thus more efficient than modelled. On the other hand, assimilation of country rocks through partial melting at the near-floor level of the SMB may have been less efficient than modelled, as a result of a smaller magma chamber size than modelled, and less efficient melt extraction from country rocks than computed. Nevertheless, the assimilation of country rocks through partial melting at the near-floor level of the SMB may account for all detected former country-rock partial melt in the SMB, if selective contamination of the exposed SMB rocks by this partial melt occurred. If true, the evolution of the SMB has been dominated by processes of assimilation and fractional crystallization, but this hypothesis needs to be tested further by statistically relevant whole-rock geochemical analyses against an equally permissible petrogenetic model in which the country-rock partial melt was added to the SMB magmas as part of the source.

6.2 Introduction

Components derived from country rocks are recognized in most igneous rocks, but their quantification remains problematic and their relative and absolute significance controversial (e.g., Carter et al. 1978; Sparks 1986; Bédard 1991; Fitton et al. 1991; Maury and Didier 1991; Clemens 2003; Beard et al. 2005; Davidson et al. 2005). The major challenge in characterizing and quantifying the degree of country-rock contamination in an igneous system is to recognize the presence of all dispersed solid country-rock contaminants, and to estimate correctly the amount of assimilated former liquid country-rock contaminants.

The potentially most efficient mechanism of country-rock assimilation in magmas is the assimilation through melting and subsequent disaggregation and dispersal of the country-rock material (Fig. 6.1), resulting in the formation of orthoxenocrysts (xenocrysts of the original, subsolidus assemblage), paraxenocrysts (xenocrysts that formed in a peritectic melting reaction between contaminants and host magma), and variable amounts of partial melt mixed with the host magma (Fig. 6.1A,B). Once formed, xenoliths and xenocrysts may undergo ion exchange reactions or dissolution, and they may become dispersed and spatially separated from the country-rock-derived partial melt. The country-rock partial melt and the melt fraction of the main magma may mix to various degrees, forming hybrid melt at various degrees (Fig. 6.1C,D). In cases where

the foreign partial melt and solids mix only slightly with the main magma, it is relatively straightforward to recognize the contribution of foreign material (e.g., in the form of xenocryst-rich schlieren) (Fig. 6.1C); however, if mixing of the country-rock-derived and the cognate magmatic melt phases, and the dispersal of xenocrysts and peritectic reaction products is well advanced, the amount of foreign material present is difficult to determine, where small xenoliths and paraxenocrysts may be the most visible foreign constituents (Fig. 1.6E,F).

For the granitic South Mountain Batholith (SMB) of southern Nova Scotia, the presence and the amount of solid country-rock contaminants has been characterized with reasonable confidence (Clarke and Erdmann 2005; Erdmann and Clarke 2005; Chapter 4), and the relative significance of former country-rock partial melt has been constrained (Clarke et al. 2004). Field and textural data show a maximum of ca. 6 vol% of physically detectable country-rock material in a <200 metre wide zone near the external margin of the batholith, but ≤4 vol% of physically detectable country-rock material in the rest of the exposed SMB rocks (Chapter 4). Whole-rock Sr-Nd isotopic data, on the other hand, show the presence of up to ca. 36 % of additional country-rock material in the evolved and central rocks of the SMB, relative to the primitive and marginal rocks (Clarke et al. 2004). The higher amount of Meguma Group component in the more evolved and more central rocks of the SMB is physically invisible, and must be dominantly present as former country-rock partial melt (Chapter 4).

The question is which processes, or which combination of processes, best explain the scarcity of Meguma Group xenoliths and xenocrysts as well as the high amount of Meguma Group component in the central and more evolved rocks of the SMB. The most probable explanations are that: (i) progressive assimilation of physically visible xenoliths and xenocrysts from the marginal and more primitive to the more central and more evolved SMB rocks took place; (ii) bulk contamination of SMB rocks by Meguma Group rocks dominantly occurred near the margin of the batholith, and in addition selective contamination of the more evolved Meguma Group rocks by country-rock partial melt below the current level of exposure occurred; and (iii) contamination of the SMB dominantly affected the margin of the intrusion, whereas a source contribution of Meguma Group rocks to the evolving SMB underlies the whole-rock Sr-Nd isotopic variations. Progressive assimilation of Meguma Group rocks from the margin to the centre of the batholith alone cannot explain the detected isotopic variation, because the assimilation of Meguma Group rocks in the SMB magmas was only partial. The partial

assimilation resulted in the formation of physically detectable refractory solids which are largely absent in the isotopically highly contaminated rocks. The possibilities of selective contamination and a Meguma Group source contribution can equally explain field observations and isotopic data. To explore under which conditions assimilation at unexposed levels of the SMB, in combination with selective contamination of the exposed rocks, may account for the field and isotopic data, I model the assimilation of metapsammitic and metapelitic rocks in compositionally variable SMB magmas for the exposed, near-roof level, and the unexposed, near-floor of the batholith, using the *E*nergy-*C*onstrained *A*ssimilation and *F*ractional *C*rystallization (EC-AFC) numerical model of Spera and Bohrson (2001).

6.2.1 Geological Setting

The late-Devonian SMB is ca. 75,000 km^3 in volume, with an average intrusion thickness of 5 to 10 kilometres (Fig. 6.2; Clarke and Muecke 1985; Clarke and Chatterjee 1988; Benn et al. 1997). The exposed, near-roof, level of the batholith consists mostly of biotite granodiorite (10 %), biotite monzogranite (52 %), coarse-grained leucomonzogranite (21 %), fine-grained leucomonzogranite (7 %), and leucogranite (<1 %) (McKenzie and Clarke 1975; MacDonald et al. 1992; MacDonald 2001). Contacts between all rock types, except for contacts between the leucogranites and all other granitic facies, are gradational on a scale of metres to tens of metres.

The exposed country rocks of the SMB, dominantly metapsammitic and metapelitic rocks of the Meguma Group, have greenschist facies regional metamorphic grade (Keppie and Muecke 1979; MacDonald and Clarke 1985; Schenk 1971, 1995, 1997; Waldron et al. 1992; Mahoney 1996; Raeside and Mahoney 1996; Clarke et al. 1997; Hicks et al. 1999), overprinted by a typically 1-3 km wide contact metamorphic aureole. Temperatures in the metamorphic aureole are, with the exception of the immediate contact, between ca. 450 °C and ca. 600 °C; the characteristic mineral assemblage is characterized by the presence of cordierite, biotite, and aluminosilicates (Horne 1994; MacDonald et al. 1992; Raeside and Mahoney 1996; Hart 2006). At the immediate contact, evidence for partial melting of Meguma Group country rocks exists, where contact metamorphic peak temperatures reached ca. 750 °C (e.g., Bt + Als + Pl + Qtz → Grt/Crd + Kfs + L, Clarke and Erdmann 2005; Chapter 4; P-T grid of Thompson 1990).

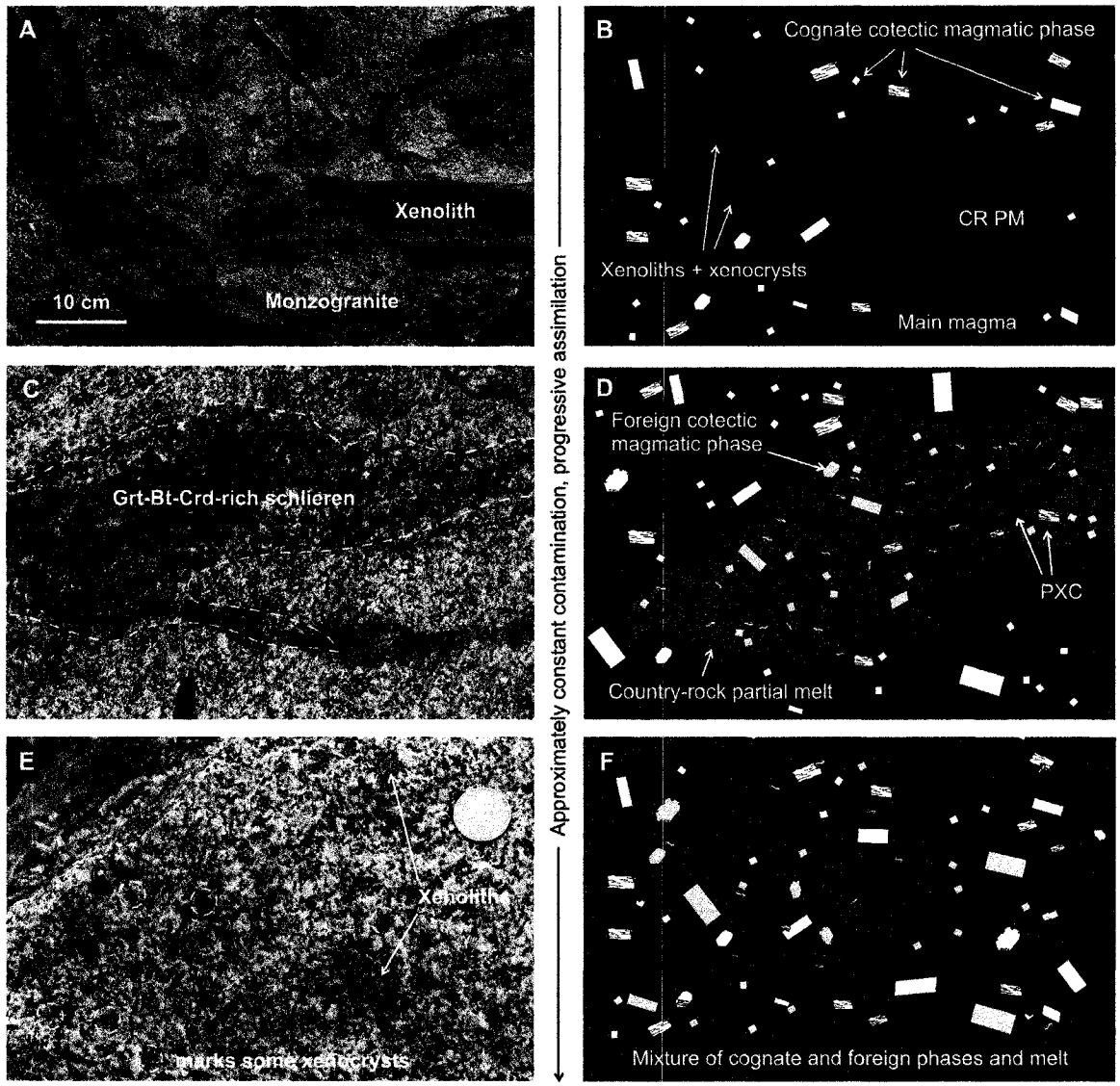

Figure 6.1: Country-rock contamination is the process of rendering a magma impure by country-rock material, where the nature of the contaminant may, or may not, be changed, whereas assimilation is the process of rendering a magma impure by country-rock material and changing the nature of the contaminant into the nature of the host magma (Clarke in press). Photographs from the South Mountain Batholith and comparable sketches showing approximately constant contamination of granites by country rocks, but progressive assimilation of the foreign material from A and B to E and F. A = Location Stop 1.7; C = Location E 430; E = Location E 465. Disintegration and assimilation of country-rock material may occur by partial melting and fracturing of xenoliths, as well as melting and dissolution of xenocrysts. The case made here considers disintegration and assimilation through partial melting. (A,B) ~30 vol% contamination, imperceptible assimilation; (C,D) ~30 vol% contamination, ~10 vol% assimilation; (E,F) ~30 vol% contamination, 25 vol% assimilation. Brown colours = xenoliths and orthoxenocrysts, red and green colours = paraxenocrysts, white colours = cognate primary magmatic crystals, and gray colours = primary magmatic crystals formed from country-rock partial melt. Different colours of cognate and foreign primary magmatic crystals may indicate possibly different compositions.

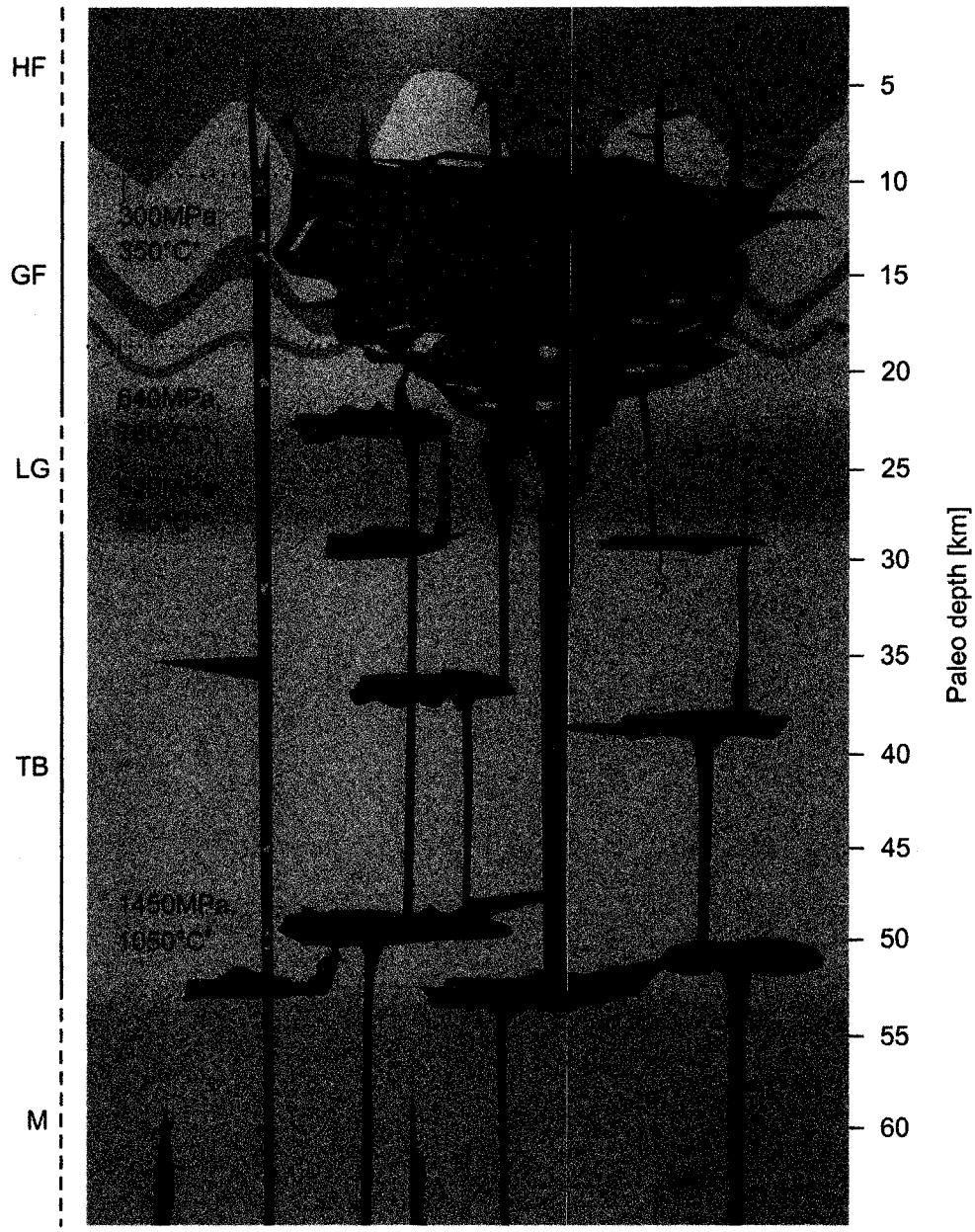

Figure 6.2: Simplified cross-section illustrating position and size of the South Mountain Batholith (SMB) at the time of its formation. Most of the SMB is surrounded by country rocks of the Meguma Group, consisting of the metapelite-dominated Halifax Formation (HF) and the metapsammite-dominated Goldenville Formation (GF) (Keen et al. 1991; Benn et al. 1999; Jackson et al. 2000; Culshaw and Lee 2006). The dark brown colour delineates metapelite-dominated strata, and the light brown colour metapsammite-dominated strata. Meguma Group and Liscomb Gneiss may have contributed to the source, but SMB magmas are dominantly generated in the Tangier Basement (TB), as a result of the injection of mafic magmas (MI) into a possibly previously thickened crust (MacDonald et al. 1992; Tate and Clarke 1995; Tate 1995; Clarke et al. 1997; Keppie and Krogh 1999; Murphy et al. 1999, 2004). M = Mantle. P-T estimates are from Raeside and Mahoney (1996) (*),Chatterjee unpublished data (**) and M.C. Corey unpublished data (#), both reported in MacDonald (2001). Stippled line marks the inferred present day surface.

The unexposed part of the SMB is also probably dominantly in contact with rocks of the Meguma Group (Keen et al. 1991; Benn et al. 1999; Jackson et al. 2000), but may locally be in contact with pelitic and metavolcanic gneisses of mid to upper amphibolite facies metamorphic grade, similar to those of the Liscomb Complex of central Nova Scotia (Fig. 6.2) (Clarke et al. 1993; Kontak and Reynolds 1994).

The late-Devonian, granitic intrusions of southern Nova Scotia, including the SMB, are probably the result of the injection of mafic magmas, possibly into a previously thickened crust (MacDonald et al. 1992; Tate and Clarke 1995; Tate 1995; Clarke et al. 1997; Keppie and Krogh 1999; Murphy et al. 1999, 2004). For the SMB, felsic rocks equivalent to those exposed as xenoliths in mafic dykes northeast of the SMB appear to be the volumetrically most important source (Eberz et al. 1991), but potential source-contributions from Liscomb gneisses as well as Meguma Group rocks may have occurred (Clarke et al. 1993; MacDonald 2001; Clarke et al. 2004; Chapter 4).

6.2.2 EC-AFC Model

6.2.2.1 Model Formulation

To characterize the potential amount of country-rock assimilation through partial melting in the SMB, I employed the numerical *E*nergy-*C*onstrained *A*ssimilation and *F*ractional *C*rystallization (EC-AFC) model of Spera and Bohrson (2001), available at http://magma.geol.ucsb.edu/. The basis of the model is that the heat absorbed by the country rocks is at all times equal to the heat liberated from the magma. The modelled boundary between magmas and country rocks is open and diathermal, allowing exchange of energy and partial melt, whereas the boundary between a defined country-rock mass and its surroundings is closed and adiabatic, allowing no exchange of energy or material (Fig. 6.3). The temperature of the country rocks is calculated to approach the temperature of the magma at a user-defined temperature, the so-called equilibration temperature T_{eq}. T_{eq} is the temperature that the boundary between magma and country rocks reaches, where a low boundary temperature implies that the heat transfer away from the magma is efficient, and vice versa.

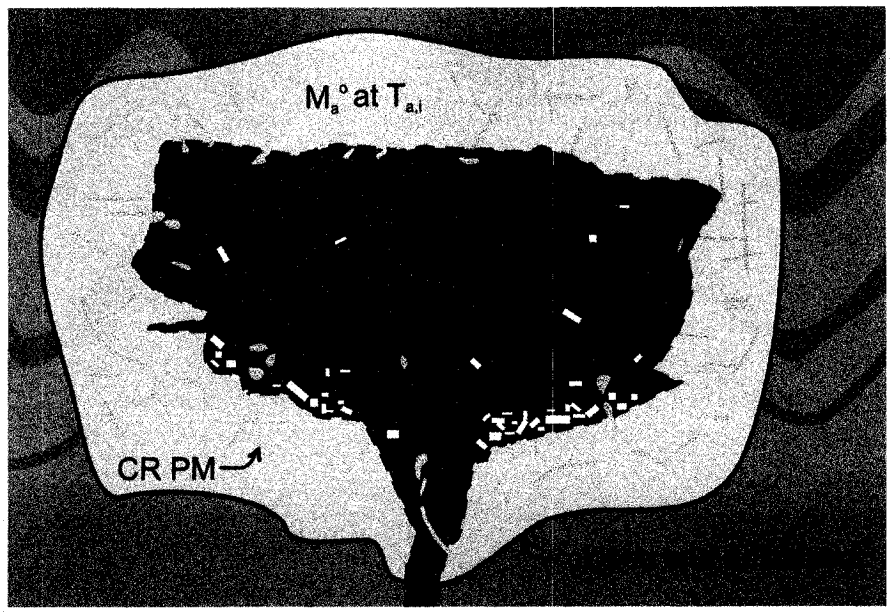

Figure 6.3: *E*nergy-Constrained *A*ssimilation and *F*ractional *C*rystallization (EC-AFC) model system (modified after Spera and Bohrson 2001). The country-rock subsystem ($M_a°$) is sealed off from its surroundings by a closed and adiabatic boundary, and separated from the magma subsystem by an open and diathermal boundary. Country rocks of a temperature $T_{a,i}$ and magma of a temperature $T_{m,i}$, relax toward thermal equilibrium, where the conservation of energy in the system incorporates heating and partial melting of country rocks, magma cooling, and the formation of cumulates. Country-rock partial melt (CR PM) forms within the $M_a°$ subsystem, and contaminates the magma as M_a*. The magma body (M_m) consists of melt, including M_a*, as well as cumulates (M_c).

Parameters required for the model calculations are the liquidus and the initial temperature of the magma ($T_{l,m}$, $T_m°$), the liquidus and the initial temperature of the assimilant ($T_{l,a}$, $T_a°$), the solidus temperature ($T_{s,m}=T_{s,a}$), the equilibration temperature of the system (T_{eq}), the crystallization enthalpy and the isobaric specific heat of the magma (Δh_{cry}, $C_{p,m}$), as well as the fusion enthalpy and the isobaric specific heat of the assimilant (Δh_{fus}, $C_{p,a}$). Table 6.1 defines all parameters. Parameters computed by the numerical model are the temperature of the magma (T_m), the temperature of the assimilant (T_a), the mass of the melt fraction in the system (M_m, including assimilated country-rock melt), the mass of cumulates (M_c), the mass of thermally affected country rocks ($M_a°$), as well as the mass of country-rock melt assimilated (M_a*). All masses calculated are normalized to the original mass of the magma body ($M_o=1$).

Table 6.1: Nomenclature.

Symbol	Definition	Unit
User-defined parameters (values in Table 6.3, 6.4, 6.5)		
$C_{p,a}$	Country-rock isobaric specific heat capacity	J/kg K
$C_{p,m}$	Magma isobaric specific heat capacity	J/kg K
T_a	Temperature of country rock	°C*
T_a^o	Initial country-rock temperature	°C*
$T_{l,a}$	Country-rock liquidus temperature	°C*
T_{eq}	Equilibration temperature	°C*
T_m	Magma temperature	°C*
$T_{l,m}$	Magma liquidus temperature	°C*
T_m^o	Initial magma temperature	°C*
Δh_{fus}	Enthalpy of fusion	J/kg
Δh_{cry}	Enthalpy of crystallization	J/kg
Computed parameters		
f_a	Melt productivity of country rocks	
f_m	Melt productivity of pristine magma	
h_{abs}	Heat absorbed by heating and partial melting of country rocks	J
h_{lib}	Heat liberated by cooling and crystallization of magma	J
M_a^o	Mass of thermally affected country rocks	kg
$\overline{M}_a^0 = \frac{M_a^0}{M_o}$	non-dimensional mass of assimilant	
M_a*	Mass of country-rock partial melt	kg
M_c	Mass of cumulates	kg
M_o	Mass of original magma (=1)	kg
M_m	Mass of melt in magma body	kg
$\overline{M}_m = \frac{M_m}{M_0}$	non-dimensional melt fraction in magma body	
$\overline{T}_a = \frac{T_a}{T_{l,m}}$	non-dimensional assimilant temperature	
$\overline{T}_{eq} = \frac{T_{eq}}{T_{l,m}}$	non-dimensional equilibration temperature	
$\overline{T}_m = \frac{T_m}{T_{l,m}}$	non-dimensional magma temperature	

Modified after Spera and Bohrson (2001). * Input in °C; calculation in K.

In a first step, the numerical model computes the total mass of thermally affected country rocks (M_a^o) for a set of thermal parameters and initial conditions (T_a^o, T_m^o) in the form of

$$\overline{M}_a^o = \frac{C_{p,m}T_{l,m}(\overline{T}_{l,m} - \overline{T}_{eq}) + \Delta h_{cry}[1 - f_m(\overline{T}_{eq})]}{C_{p,a}T_{l,m}(\overline{T}_{eq} - \overline{T}_a^o) + f_a(\overline{T}_{eq})\Delta h_{fus}} \quad \text{(E1)}$$

with

$$f_m(T_m) = (T - T_s)/(T_{l,m} - T_s) \text{ .and. } f_a(T_a) = (T - T_s)/(T_{l,a} - T_s), \quad \text{(E2)}$$

where dimensionless quantities are denoted by an overbar. The extent of country-rock partial melting (M_a^*) is a function of the mass of thermally affected country rocks that exceed their solidus temperature, calculated as

$$M_a^* = \frac{f_a(T_a)}{M_a^o}, \quad \text{(E3)}$$

where melt extraction from country rocks is assumed equal to unity. In a second step, the energy-constrained thermal path followed by magma and country rocks approaching T_{eq} is computed in the form

$$\frac{d\overline{T}_a}{d\overline{T}_m} = \frac{-1}{\overline{M}_a^o}\left\{\frac{T_{l,m}C_{p,m} + \Delta h_{cry}f'_m(\overline{T}_m) + T_{l,m}C_{p,a}\overline{M}_a^o f_a(\overline{T}_a)}{T_{l,m}C_{p,a}[1 - f_a(\overline{T}_a)] + \Delta h_{fus}f'_a(\overline{T}_a) + T_{l,m}C_{p,a}(\overline{T}_m - \overline{T}_a)f'_a(\overline{T}_a)}\right\} \quad \text{(E4)}$$

T_a is calculated on the basis that the heat from the magma and the heat absorbed by the country rocks is at all times equal (h_{lib}+h_{abs}=0), where the conservation of energy incorporates heating and partial melting of country rocks, magma cooling, and the formation of cumulates. The integral expression for the heat liberated and the heat absorbed are:

$$h_{lib} = M_0 f_m(T_{eq})C_{p,m}(T_m^0 - T_{eq}) + M_0[1 - f_m(T_{eq})]C_{p,m}(T_m^0 - T_{eq}) + \Delta h_{cry}] \quad \text{(E5)}$$

and

$$h_{abs} = M_a^0[1 - f_a(T_{eq})]C_{p,a}(T_{eq} - T_a^0) + f_a(T_{eq})M_a^0[C_{p,a}(T_{eq} - T_a^0) + \Delta h_{fus}] \quad \text{(E6)}$$

T_a is calculated as long as $T_a<T_{l,m}$. Mass conservation is solved for the magma temperature (T_m) according to

$$\frac{d\overline{M}_m}{d\overline{T}_m} = \overline{M}_a^o f'_a(\overline{T}_a)\frac{d\overline{T}_a}{d\overline{T}_m} + f'_m(\overline{T}_m). \qquad \text{(E7)}$$

Heat transfer mechanisms are unspecified, and the numerical model is zero dimensional in the sense that spatial and temporal fields are not taken into consideration.

6.2.2.2 SMB System Components

Table 6.2 summarizes the system components employed. The EC-AFC models were run for the three compositionally different SMB magmas given (GD_{corr}, LG_{corr}, and SMB_{corr}), as well as for metapsammitic (PSA) and metapelitic (PEL) country rocks, to explore if, and how, the potential for country-rock assimilation through partial melting may have varied for metapsammitic and metapelitic country-rock contaminants, and between primitive (GD), evolved (LG), and unfractionated (SMB) magmas. The initial SMB magma composition is unknown (MacDonald 2001; Clarke et al. 2004), and without a better alternative, I therefore used compositions of SMB granodiorites, leucogranites, and average SMB rocks (GD, LG, SMB), corrected for the inferred amount of bulk Meguma Group contaminants present (GD_{corr}, LG_{corr}, and SMB_{corr}) (Chapter 4). To correct for the presence of physically visible country-rock contamination and complementary partial melt in the SMB rocks, I subtracted 4% and 10%, 4% and 6%, and 4% and 2% of metapsammitic and metapelitic country-rock contaminants from SMB granodiorites, leucogranites, and average SMB rocks, respectively. The concentration of H_2O during the magmatic evolution of the SMB magmas is unknown, and I therefore selected "typical" H_2O concentrations of 3 and 5 wt% for the SMB magmas, whereas H_2O contents for the metapsammitic and metapelitic assimilants are set to 2 and 4 wt%, accounting for the relative abundance of hydrated minerals in their assemblages.

6.2.2.3 Model Parameters

Table 6.3 summarizes the model parameters employed. The isobaric specific heat of the magmas and the assimilants, as well as crystallization and fusion enthalpies, were calculated using data reported by Spera (2000). Liquidus temperatures of granodiorite magmas, average SMB magmas, and assimilants, are calculated from whole-rock

compositions and their CIPW modal mineralogies using the PELE software (Boudreau 1999), which employs the thermodynamic database and algorithms presented in Ghiorso (1985) and Ghiorso and Sack (1995). Liquidus temperatures for the leucogranite magmas are calculated using the CIPW software of Kurt Hollocher (http://faculty.fortlewis.edu/ COLLIER_J/Geol210/ norm4.xls), which approximates the liquidus temperature using the linear equation T_l (°C) = (-18.33 * SiO_2 wt%) + 2130.

Initial magma temperatures were set to 800 °C in the near-roof models, accounting for the absence of orthopyroxene (e.g., McKenzie and Clarke 1975), and to 850 °C in the near-floor models. Initial temperatures of the assimilants are set at 350 °C in the near-roof models, accounting for the inferred regional metamorphic temperatures at this level of the batholith (Schenk 1971, 1991, 1995; Keppie and Muecke 1979; Waldron et al. 1992, Hicks et al. 1999), and 600 °C in the near-floor models, assuming a geothermal gradient of ca. 35 °C/km. The solidus temperature is set at 650 °C, in agreement with solidus temperatures of metapelitic and metapsammitic rocks of the Meguma Group inferred from melting experiments at 200 MPa (Chapter 3), corrected for P and H_2O-saturation. The equilibration temperature inferred for the contacts between Meguma Group rocks and former SMB magmas varies between ca. 670 °C (defined by the reaction Ms + Pl + Qtz → Als + Kfs + L; Chapter 4; P-T grid of Thompson 1990; abbreviations after Kretz 1983), and ca. 750 °C (defined by the reaction Bt + Als + Pl + Qtz → Grt/Crd + Kfs + L; Clarke and Erdmann 2005, Chapter 4; P-T grid of Thompson 1990), at 400 to 820 MPa, between the exposed and the inferred floor-level of the SMB. The lower equilibration temperatures record a late-stage boundary condition in the evolution of the SMB, when country-rock contamination and assimilation most likely occurred only locally, with little or no dispersal of the country-rock contaminants. The higher equilibration temperatures record an early-stage boundary condition in the evolution of the SMB, when country-rock contamination and assimilation were efficient, with the products of these assimilation reactions, such as peritectic garnet or cordierite, occurring throughout the SMB. An equilibration temperature of 750 °C seems thus most appropriate to model country-rock assimilation through partial melting in the SMB, implying that the transfer of heat into the country rocks is only moderately efficient, heating the boundary to a temperature closer to the temperature of the magma than to temperature of the country rocks.

Table 6.2: Compositions of SMB and Meguma Group rocks, inferred magmas, and Meguma Group derived partial melts.

	GD	LG	SMB	GD_{corr}	LG_{corr}	SMB_{corr}	PSA	PEL	PSA_m	PEL_m
n	82	49	675	82	49	675	11	27	12	15
SiO_2	67.42	74.22	71.46	68.69	74.69	72.44	75.20	57.66	73.26	71.22
TiO_2	0.67	0.08	0.34	0.63	0.04	0.28	0.55	1.08	0.16	0.24
Al_2O_3	15.30	14.15	14.50	14.60	14.09	14.05	11.54	23.80	12.13	12.09
FeO_T	3.98	1.29	2.39	3.85	1.11	2.14	3.26	5.61	0.88	1.31
MnO	0.09	0.05	0.06	0.09	0.04	0.06	0.06	0.12	0.03	0.03
MgO	1.71	0.62	1.14	1.70	0.56	1.07	1.27	2.09	0.52	0.13
CaO	1.94	0.38	0.99	2.16	0.34	1.02	1.24	0.47	1.34	0.33
Na_2O	3.42	3.55	3.42	3.72	3.65	3.61	2.55	1.45	3.32	1.58
K_2O	3.72	4.15	4.40	3.77	4.26	4.53	2.03	4.13	2.23	5.24
P_2O_5	0.20	0.33	0.21	0.21	0.35	0.22	0.11	0.11	0.07	0.1
F	0.07	0.20	0.07	0.08	0.21	0.08	-	-	0.16	0.13
LOI	0.70	0.88	0.64	0.82	0.93	0.71	0.74	4.74	5.96	7.65
TOTAL	99.21	99.90	99.62	100.00	100.00	100.00	98.39	98.32	100.07	100.05
A/CNK	1.16	1.28	1.19	1.03	1.25	1.11	1.33	3.09	1.18	1.38

GD=granodiorite, LG=leucogranite, and SMB=average SMB granites. GD and LG compositions are average whole-rock compositions (Ham et al. 1989, 1990); the SMB composition accounts for all rock types and their estimated volumetric abundances in the batholith (MacDonald 2001). GD_{corr}, LG_{corr}, and SMB_{corr} are inferred magma compositions, corrected for physically detectable metapsammitic (PSA) and metapelitic (PEL) country-rock contaminants, using estimates of Chapter 4. For GDcorr, LGcorr, and SMBcorr, respectively, 4% PSA and 10% PEL, 4% PSA and 2% PEL, and 4% PSA, 6% PEL are subtracted from the whole-rock compositions (GD, LG, SMB). PSA_m=metapsammitic Meguma Group partial melt, PEL_m=metapelitic Meguma Group partial melt. PSA_m is PSA-7, and PEL_m is PEL-14 of Erdmann et al. (in press). n = No of analyses.

Table 6.3: EC-AFC model input parameters.

Component	H_2O (wt%)	T_l (°C*)	Δh (J/kg)	C_p (J/kg K)
GD_{corr}	3	1072	283765	1337
LG_{corr}	3	1008	240471	1319
SMB_{corr}	3	1016	253885	1326
GD_{corr}	5	1035	277915	1310
LG_{corr}	5	894	235513	1292
SMB_{corr}	5	979	248651	1299
PSA	2	1070	269855	1341
PEL	4	1066	399588	1330

T_l=liquidus temperature; Δh=crystallization and fusion enthalpies; Cp=isobaric specific heat. Parameters calculated using data of Table 6.2. * Input in °C; calculation in K.

In addition to the models computed for the above, and geologically most probable thermal parameters (results presented in Sections 6.3.1 and 6.3.2), the assimilation of metapsammitic rocks of the Meguma Group rocks in average SMB magmas at the near-roof level has been calculated for variable T_a, T_m, T_{eq}, T_s, Δh_{cry}, and Δh_{fus}, as well as $C_{p,m}$ and $C_{p,a}$ to constrain the sensitivity of the various input parameters (results presented in Section 6.3.3). All temperatures were arbitrarily changed by ±50°C, and the isobaric specific heat of magmas and assimilants, as well as crystallization and fusion enthalpies

were arbitrarily modified by 5 % and 50 %, respectively (the modification of Δh_{cry} and Δh_{fus} corresponds approximately to the variation in properties between a magma of granite and granodiorite composition; Spera 2000).

6.3 Results

6.3.1 Country-rock Assimilation at the Near-roof Level of the SMB

Table 6.4 summarizes the EC-AFC model results for the assimilation of Meguma Group country rocks near the roof of the SMB magma chamber for an equilibration temperature of 750 °C ($T_{a,i}$=350 °C; $T_{m,i}$=800 °C). For the conditions simulated, the country rocks reach temperatures of ca. 510-610 °C, and the calculated amount of country-rock assimilation through partial melting is therefore zero ($T_a<T_s$). The mass of thermally affected country rocks varies between ca. 33 and 47 % of the mass of the magma, with a maximum mass of thermally affected country rocks for a granodiorite-metapsammite contact relationship. At any given temperature, the leucogranite magmas have the lowest, the SMB magmas intermediate, and the granodiorite magmas the highest crystallinities, with melt fractions ranging between ca. 24 and 48 % of the mass of the magma. With increasing H_2O content of the system, but otherwise similar conditions, the final temperatures of the assimilants and the mass of magma increase, whereas the mass of cumulates and the mass of thermally affected country-rocks decrease.

6.3.2 Country-rock assimilation at the Near-floor Level of the SMB

Table 6.5 gives the EC-AFC model results for the assimilation of Meguma Group country rocks near the floor of the SMB magma chamber for an equilibration temperature of 750 °C ($T_{a,i}$ = 600 °C; $T_{m,i}$=850 °C). For the conditions simulated, the mass of thermally altered country-rocks is significantly higher, and the temperature of the country-rock assimilants is on average 150 °C higher than in the near-roof EC-AFC models. Also, country-rock temperatures reach ca. 690-730 °C, and the mass of country-rock material heated by the SMB magmas is similar, i.e. up to 31% larger than the mass of the original magma. The degree of country-rock partial melting ranges between 9 and 18 %, with the highest degrees of partial melting for metapsammitic rocks in contact with the leucogranite magmas. The mass of partial melt generated is equivalent to 4 to 8 % of the mass of the magma, and equivalent to 8 to 23 % of all melt remaining in the model system at 750 °C.

Table 6.4: EC-AFC model results for the near-roof level of the SMB.

T_{eq}=750 °C; $T_{m,i}$=850 °C, $T_{a,i}$=350 °C; 3 wt% H_2O

Magma	GD_{corr}		LG_{corr}		SMB_{corr}	
Assimilant	PSA	PEL	PSA	PEL	PSA	PEL
T_a	509	517	541	546	531	541
M_m	0.238	0.238	0.272	0.272	0.269	0.269
M_a*	0.000	0.000	0.000	0.000	0.000	0.000
M_c	0.762	0.762	0.724	0.724	0.731	0.731
M_a^o	0.471	0.450	0.398	0.381	0.419	0.401
T_{eq}	750	750	750	750	750	750

T_{eq}=750 °C; $T_{m,i}$=850 °C, $T_{a,i}$=350 °C; 5 wt% H_2O

Magma	GD_{corr}		LG_{corr}		SMB_{corr}	
Assimilant	PSA	PEL	PSA	PEL	PSA	PEL
T_a	517	531	596	612	544	554
M_m	0.260	0.260	0.419	0.481	0.304	0.304
M_a*	0.000	0.000	0.000	0.000	0.000	0.000
M_c	0.740	0.740	0.581	0.591	0.696	0.696
M_a^o	0.450	0.431	0.334	0.325	0.397	0.379
T_{eq}	750	750	751	750	750	750

T_a=temperature of the assimilant, M_m=mass of melt fraction in the system, including the assimilated country-rock melt M_a*; M_c=mass of cumulates, M_a^o=mass of thermally affected country rocks; and T_{eq}=equilibration temperature of the system and final temperature of the magma. All other abbreviations are explained in Table 6.2.

Table 6.5: EC-AFC model results for the near-floor level of the SMB.

T_{eq}=750 °C; $T_{m,i}$=850 °C, $T_{a,i}$=600°C; 3 wt% H_2O

Magma	GD_{corr}		LG_{corr}		SMB_{corr}	
Assimilant	PSA	PEL	PSA	PEL	PSA	PEL
T_a	690	692	699	703	698	700
M_m	0.361	0.356	0.415	0.408	0.409	0.402
M_a*	0.123	0.118	0.135	0.128	0.134	0.127
M_c	0.762	0.762	0.720	0.720	0.725	0.725
M_a°	1.312	1.178	1.149	1.032	1.183	1.062
T_{eq}	751	751	750	750	751	751

T_{eq}=750 °C; $T_{m,i}$= 850°C, $T_{a,i}$= 600°C; 5 wt% H_2O

Magma	GD_{corr}		LG_{corr}		SMB_{corr}	
Assimilant	PSA	PEL	PSA	PEL	PSA	PEL
T_a	693	696	727	727	703	705
M_m	0.390	0.385	0.591	0.577	0.447	0.458
M_a*	0.129	0.124	0.183	0.169	0.144	0.137
M_c	0.739	0.739	0.592	0.592	0.697	0.679
M_a°	1.259	1.130	1.017	0.913	1.145	1.028
T_{eq}	751	751	750	750	750	750

Abbreviations are similar to those of Tables 6.1-6.3.

6.3.3 Effects of Variable Thermal Conditions on Country-rock Assimilation in the SMB

Table 6.6 summarizes the EC-AFC model results for the assimilation of metapsammitic Meguma Group country rocks near the roof and the floor of the SMB magma chamber for variable thermal conditions. For assimilation at the near-roof level of the SMB, a higher initial magma temperature and a lower solidus temperature increase the country-rock temperature most significantly (~635 °C instead of 531°C), whereas the variation of all other thermal parameters considered has only a minor effect on the final country-rock temperature. Country-rock partial melting and assimilation occurs only, if the assumed solidus temperature of country rocks and magmas is 600°C, where country-rock temperatures reach ca. 633°C. The mass of country rocks that are thermally involved in the computed AFC event increases most significantly for a higher

Table 6.6: EC-AFC model results for the assimilation of metapsammitic rocks (PSA) in average SMB magmas (SMB_{corr}) at variable conditions.

Near-roof level assimilation

	T_a		T_m		T_{eq}		T_s		Δh_{cry}		Δh_{fus}		$C_{p,m}$		$C_{p,a}$	
	300 °C	400 °C	750 °C	850 °C	700 °C	800 °C	600 °C	700 °C	126943	380827	134923	404782	1260	1392	1274	1408
T_a	506	565	-	635	565	-	633	613	593	509	545	532	539	536	536	535
M_a*	0.000	0.000	-	0.000	0.000	-	0.033	0.000	0.000	0.000	0.000	0.000	0.000	0.000	0.000	0.000
M_a^o	0.377	0.472	-	0.531	0.705	-	0.476	0.608	0.265	0.537	0.443	0.398	0.413	0.424	0.439	0.401

Near-floor level assimilation

	T_a		T_m		T_{eq}		T_s		Δh_{cry}		Δh_{fus}		$C_{p,m}$		$C_{p,a}$	
	550 °C	650 °C	800 °C	900 °C	700 °C	800 °C	600 °C	700 °C	126943	380827	134923	404782	1260	1392	1274	1408
T_a	685	710	669	720	677	698	691	705	712	690	694	700	696	698	698	697
M_a*	0.081	0.230	0.043	0.239	0.159	0.067	0.199	0.021	0.126	0.147	0.144	0.127	0.130	0.142	0.142	0.132
M_a^o	0.960	1.613	0.949	1.436	2.496	0.595	1.034	1.470	0.854	1.554	1.370	1.074	1.180	1.229	1.251	1.140

Abbreviations as in Table 6.1.

initial magma temperature, a lower equilibration temperature, a higher solidus temperature, and a higher crystallization enthalpy, but decreases most considerably for a lower crystallization enthalpy.

For assimilation at the near-floor level of the SMB, the variation of the thermal parameters causes little or no variation in the calculated final country rock temperatures. However, the mass of thermally affected country-rocks and the amount of partial melting and country-rock assimilation do change, particularly with the variation of the various input temperatures. The mass of thermally affected country rocks significantly decreases for a higher equilibration temperature, and increases significantly for a lower equilibration temperature. The mass of partially molten country rocks decreases for a lower initial magma temperature and a higher solidus temperature, and increases for a higher initial country-rock temperature as well as a higher initial magma temperature.

6.4 Discussion

6.4.1 EC-AFC Model Results

The most significant thermal input parameters of the numerical model governing the computed amount of partial melting are the initial country-rock and magma temperatures, the equilibration temperature, as well as the solidus temperature of country rocks and magmas, whereas fusion and crystallization enthalpies as well as heat capacities have only a minor effect on the model results. For the interpretation of the results, the highest uncertainty introduced by my choice of model parameters arises from the assumed initial magma temperatures, as well as the assumed initial country-rock temperature at the near-floor level of the batholith, and the assumed solidus temperature. The initial temperatures of the SMB magmas are so far unconstrained, and I acknowledge that the estimates may have an uncertainty on the order of ±50°C, where it is more likely that I overestimated than underestimated the initial magma temperatures. Under natural conditions, particularly the temperature of the leucogranites may have been lower than assumed, and the amount of country-rocks assimilated in contact with the leucogranites may have been on the order of 30 % lower than estimated, if the magma temperature was 50°C lower. The initial temperature of the country rocks at depth can only be estimated, where uncertainties may be as high as ±100°C or more, where initial temperatures were more likely higher and not lower than assumed, and the possible degree of country-rock partial melting may therefore be underestimated. The selected solidus temperature is more likely too low than too high, and thus, higher degrees of

partial melting may have been computed than may have formed under natural conditions.

The EC-AFC model results are different for the various magma compositions employed (Tables 6.4, 6.5), but given the uncertainties for the input parameters, the differences are not significant. The result that metapsammitic and metapelitic rocks melt to a higher degree in contact with the leucogranite magmas than in contact with average SMB and granodiorite magmas is a consequence of the relatively low computed mass of thermally affected country rocks (E1; Table 6.1), and an accordingly relatively large mass of country rocks that is heated to temperatures above the solidus (E3; Table 6.1). Under natural conditions, this relation may be different, with higher degrees of partial melting occurring in country rocks in contact with the more primitive SMB magmas, where the higher degrees of partial melting are a consequence of a higher initial and/or emplacement level magma temperature for the more primitive than for the more evolved SMB magmas.

Unrealistic are the calculated higher mass fractions of partial melt generated from metapsammitic versus metapelitic contaminants, in contrast to field evidence and experimental data (Jamieson 1974; Clarke and Erdmann 2005; Chapter 2; Erdmann and Clarke 2005; Chapter 4). The reasons for the discrepancy are that the fusion enthalpy calculated for the metapelitic rocks is too high compared to the fusion enthalpy of the metapsammitic rocks (as a result of using modal instead of natural assemblages for the calculation), and that the melting functions of the numerical model are linearly solved, therefore not accounting for different stages of melting, and/or reactions with different melt productivities (e.g., Ms + Bt + Pl + Qtz = Crd + Kfs + L or Pl + Kfs + Qtz = L).

In addition to these limitations, the simulated system is zero-dimensional, and therefore lacks the consideration of thermal gradients, or the time-scales of heat liberation and absorption. As a result of the absence of thermal gradients, the calculations for country-rock assimilation at the near-roof level of the SMB magma chamber (T_a = 350°C), suggest that country rocks remain below their solidus temperatures (T_s = 650 °C, T_{eq} = 509-596 °C), and that the computed mass of country rock assimilated is therefore zero, whereas under natural conditions, with a thermal gradient developed, at least minor assimilation of country-rock material through partial melting occurred (Jamieson 1974; Clarke and Erdmann 2005; Chapter 4). The modelled significance of country-rock partial melting and assimilation at the near-roof level of the SMB is therefore a minimum estimate, and underlines the importance to interpret the model results only semi-

quantitatively. On the other hand, in the calculations for country-rock assimilation at the near-floor levels of the SMB magma chamber (T_a=600 °C, T_{eq} = 690-727°C), the country rocks reach temperatures above the solidus, and country-rock assimilation through partial melting is thus computed, with minor partial melting throughout the defined country-rock mass. In this case, the modelled mass of country-rock partial melting is also a minimum estimate for the amount of country-rock partial melt generated under natural conditions, given the lack of a thermal gradient, but probably a maximum estimate for the amount of country-rock partial melt assimilated in the SMB magmas, because not all country-rock partial melt generated would have been incorporated into the SMB.

Most importantly, given that the SMB was intruded in several pulses, and a magma chamber of the size of the entire batholith probably never existed at one time (MacDonald 2001), the computed mass fraction of country-rock assimilation through partial melting is certainly a maximum estimate for the amount of country rocks melted and assimilated by the SMB magmas under natural conditions. The enthalpy derived from the SMB magmas must have been partly lost to heat up older parts of the intrusion, and possibly Meguma Group country rocks without inducing partial melting. Most relevant for the efficiency of country-rock partial melting, but not considered in the EC-AFC model applied, are the country-rock-magma contact relations, the time-scale of diffusion for individual intrusions, and the time-scale of diffusion for the broader thermal anomaly (e.g., Spera and Bohrson 2001; Dufek and Bergantz 2005). All three factors are unknown for the SMB at depth, and only partly constrained for the exposed parts of the batholith. The exposed part of the intrusion shows that the SMB intruded in several magma pulses, but contacts between the different pulses are mostly, with the exception of the leucogranites, gradational on a scale of several metres to tens of metres, suggesting that later magma pulses intruded into only partly solidified magmas. However, the loss of enthalpy to heat up the older magma pulses is unconstrained, and will have to be estimated in a more sophisticated model. The importance of energy lost at depth is, in any case, only speculative, given the lack of exposure. If younger SMB magmas intruded dominantly older SMB magmas, if only a relatively small magma chamber existed at a time, and if the period of time between successive intrusions was long, the efficiency of country-rock partial melting will have been low, and much lower than calculated. On the other hand, if younger SMB magmas intruded dominantly Meguma Group country rocks, if a relatively large magma chamber existed at a time (e.g., in a vertically evolving system), or if the period of time between successive

intrusions was short, the efficiency of country-rock partial melting will have been high, and much not much lower than calculated.

6.4.2 Heat Budget of the SMB Magmas

The model calculations for the near-roof levels of the SMB magma chamber predict that a mass of Meguma Group rocks between 32 and 47 % of the mass of the SMB reached temperatures of ≥510 °C, whereas the exposed thermal aureole of the SMB, with Meguma Group rocks characterized by an average metamorphic temperature of >500 °C, is equivalent to <5 % of the SMB area, or an SMB mass on the same order. In addition to the condition that the SMB magma chamber probably never had the size of the batholith, and country-rock heating was thus not completely efficient, probable explanations for this contradiction are that under natural conditions, efficient removal of heat along fractures or shear zones occurred (e.g., Clarke and Bogutyn 2003), and/or that partial removal of the thermal aureole by stoping took place (e.g., Mahoney 1996; Clarke et al. 1998; Culshaw and Bhatnagar 2001; MacDonald 2001). The mass of thermally affected *in situ* or incorporated country rocks at the near-floor level of the SMB may also be overestimated, but may be closer to the calculated mass of thermally affected country rocks, given that both removal of heat along fractures or shear zones and stoping should have been less significant than at the upper-crustal, near-roof levels of the batholith. However, the thermal aureole at the near-floor level of the SMB may be smaller than the computed mass of thermally affected country rocks, if large xenoliths that originated from higher levels of the SMB magma chamber, and that only partly, but not completely thermally reequilibrated during their descent through the magma chamber, accumulated in this part of the batholith, and acted as heat sinks.

6.4.3 Significance of Country-rock Assimilation in the SMB

6.4.3.1 Country-rock Assimilation at the Near-roof Level of the SMB

The mass of country-rock partial melt assimilated at the near-roof of the SMB is zero in the model calculations, but field evidence indicates at least minor partial melting of *in situ* Meguma Group country rocks along the contact with the SMB (Jamieson 1974; Clarke and Erdmann 2005; Chapter 4). Thus, the question is not whether the temperature of the SMB magmas was high enough to cause partial melting of Meguma Group country-rocks at the near-roof level of the batholith, but whether enough heat was available to cause

the observed degree of country-rock partial melting. Estimates of country-rock contamination, based on field, textural, and experimental data, suggest that at most ca. 16 vol% of Meguma Group country rocks, including a maximum of 10 vol% of complementary country-rock partial melt, was assimilated at the exposed level of the SMB, in a < 200 m wide zone along the external contact of the batholith (Chapter 4). A mass of ≤10 % of country-rock partial melt (equivalent to 10 vol% of country-rock derived partial melt; melt and magma densities are unknown, but the density of the country-rock partial melt should have been lower than the density of the SMB magmas; Table 6.1) in a <200 metre wide zone of at the exposed margin of the batholith is small compared to a mass of the ca. 50x150 kilometre wide batholith. It seems thus possible that the heat of the SMB magmas was sufficient to have assimilated an equivalent mass of Meguma Group material through partial melting, if country-rock contaminants with a large surface-to-volume ratio were present, as field observations suggest (Jamieson 1974; Tate 1996; Clarke and Erdmann 2005; Chapter 4).

6.4.3.2 Country-rock Assimilation at the Near-floor Level of the SMB

The calculated mass of country-rock partial melt generated at the near-floor level of the SMB makes up 4-8 % of the mass of the SMB, and a maximum of 7-18 % of all melt in the system at a temperature of 750°C. Although the calculated degree of 9-18 % of country-rock partial melting contains uncertainties, and the degree of country-rock partial melting under natural conditions was likely lower, a large volume of Meguma Group country rocks may have been assimilated through partial melting at the near-floor level of the batholith, in contrast to the near-roof level of the batholith, if conditions of heat transfer from the SMB magmas into Meguma Group rocks was efficient.

6.4.3.3 Country-rock Assimilation at ≤750°C

At temperatures of ≤750°C and melt fractions of ≤24-48 % for SMB magmas at the near-roof and ≤36-51 % for SMB magmas at the near-floor level of the batholith, country-rock contamination and assimilation could have continued, but would have been less and less efficient. Melt production in the Meguma Group rocks would have decreased drastically (Chapters 2 and 4), thus limiting the contamination of SMB magmas by country-rock partial melt, whereas magma viscosities would have increased, limiting the large-scale dispersal of at least the solid country-rock contaminants. On the other hand, mixing of liquid country-rock contaminants and SMB melt, may have continued efficiently at

temperatures of ≤750 °C, particularly, if the remaining country rock and SMB melt fractions were concentrated and mixed in large-scale melt bodies.

6.4.4 Compositional Effects of Country-rock Assimilation in the SMB

The compositional effects of country-rock assimilation in the SMB depend on the nature of the contaminants, and on the relative timing of assimilation and fractional crystallization (Table 6.7). For the whole batholith, bulk contamination was probably the dominant style of contamination. However, certain parts or units of the batholith may have been selectively contaminated by either solid or the liquid contaminants derived from the metapsammitic and metapelitic country rocks, if the various contaminating components were spatially separated by gravity settling and/or flow fractionation (Clarke 2004; Clarke and Erdmann 2005; Chapter 4).

The peraluminosity, Sr and Nd trace-element, isotopic, and other compositional characteristics of partial melts generated from Meguma Group rocks under natural conditions are unknown, but I assume that A/CNK compositions are similar to the A/CNK values of partial melts from Meguma Group rocks determined in 800 °C melting experiments (Table 6.2, 6.7; Chapter 3). I estimated the Sr concentrations of the partial melts by assuming that all Sr resides in plagioclase, using the whole-rock Sr concentration of the metapsammitic and metapelitic rocks, and a Sr distribution coefficient of 11 (Table 6.7). The Sr distribution coefficient was calculated after Blundy and Wood (1999), assuming equilibrium conditions, and employing the average composition of plagioclase stable in the 800 °C melting experiments of Erdmann et al. (in press). Given that not all Sr of the Meguma Group rocks resides in plagioclase, the estimated Sr concentration for the partial melt derived from the Meguma Group rocks is not accurate, but nevertheless gives an idea of the compositional contrast between Meguma Group rocks and their partial melts. Neodymium concentrations for the partial melts of the metapsammitic and metapelitic rocks have not been calculated, given that equilibrium between Nd-rich accessory phases and the melt unlikely prevailed, and given that modal abundances for various Nd-rich phases are not accurately known. Strontium and Nd isotopic compositions of the country-rock partial melts are assumed to be similar to the isotopic compositions of the country rocks, which is a tenuous but necessary assumption. The compositions of the solid country-rock contaminants were estimated using compositional data from Meguma Group rocks and Meguma-Group-derived partial melts, as well as ratios for solid to liquid contaminants of 1:1 for the metapsammitic

rocks, and 1:2.3 for the metapelitic rocks, determined in 800°C melting experiments (Erdmann et al. in press). The assumption for the following calculations is that country-rock contamination and assimilation in the SMB occurred largely subsequent to the fractionation of the granodiorites, as isotopic signatures suggest (Clarke et al. 2004), and that the inferred compositions of the various system components are representative (Table 6.7).

Table 6.7: Compositions of SMB and Meguma Group rocks, inferred magmas, and Meguma Group derived partial melts.

	n	A/CNK	Sr	Nd	$^{87}Sr/^{86}Sr_i$	$^{143}Nd/^{144}Nd_i$
GD	82	1.16	164	31	0.70823	0.512047
LG	49	1.28	16	6	0.71020	0.511899
SMB	675	1.19	-	-	-	-
GD_{corr}	-	1.03	156	29	0.70706	0.512112
LG_{corr}	-	1.25	5	4	0.70998	0.511915
SMB_{corr}	-	1.11	-	-	-	-
PSA	11	1.33	188	26	0.71226	0.511634
PEL	27	3.09	210	47	0.71665	0.511654
PSA_m	12	1.38	17	-	0.71226	0.511634
PEL_m	15	1.18	19	-	0.71665	0.511654
PSA_{XC}	-	1.29	376	-	0.71226	0.511634
PEL_{XC}	-	7.56	654	-	0.71665	0.511654
$LG_{corr}2$ (PSA)	-	1.09	-	-	-	-
$LG_{corr}2$ (PEL)	-	1.35	-	-	-	-

Abbreviations as in previous Tables. $LG_{corr}2$ is the inferred initial magma composition of the leucogranites, corrected for all physically detectable contaminants and complementary partial melt (LG_{corr}), and corrected for the isotopically detected presence of 56 % former country-rock partial melt. The calculated difference in the isotopic signature of GD_{corr} and LG_{corr} indicates that ≥56% of former Meguma Group partial melt may be present in the leucogranites. $LG_{corr}2$ (PSA) = PSA_m assumed as the contaminant, $LG_{corr}2$ (PEL) = PEL_m assumed as the contaminant. n = No of analyses. Sr concentrations of PSAm and PEL_m are calculated for D_{Sr} = 11 (see text for details); $^{87}Sr/^{86}Sr_i$ and $^{143}Nd/^{144}Nd_i$ of PSAm and PEL_m are assumed to be similar to those of PSA and PEL. Sr, Nd, $^{87}Sr/^{86}Sr_i$ and $^{143}Nd/^{144}Nd_i$ compositions for $LG_{corr}2$ are not calculated, because uncertainties of the calculations are too high, given the large number of assumptions that had to be made.

The selective contamination of SMB magmas by xenocrysts or partial melt derived from the metapsammitic and metapelitic Meguma Group rocks, particularly from the metapelitic rocks, may have affected the peraluminosity, the Sr concentration, as well as

other compositional characteristics of the magmas differently than bulk contamination (Table 6.7). The addition of metapelite-derived partial melt may have increased the peraluminosity of all SMB magmas, whereas the addition of metapsammite-derived partial melt may have increased the peraluminosity of the granodiorite magmas, but decreased the peraluminosity of the leucogranite magmas. The addition of both metapelite- and metapsammite-derived partial melts may have decreased the Sr concentration of the granodiorite and the average SMB magmas, but may have had little or no effect on the Sr concentration of the leucogranite magmas. The addition of Meguma Group partial melts may have merely changed the Sr isotopic composition of the granodiorite and the average SMB magmas, even at high degrees of country-rock assimilation, but may have significantly affected the Sr isotopic composition of the leucogranite magmas, even at relatively low degrees of country-rock assimilation.

The contamination of SMB magmas by both metapelite- and metapsammite-derived solid contaminants may have increased the Sr concentration of the of SMB magmas significantly. The selective contamination of the SMB magmas by the solid contaminants derived from the metapsammitic Meguma Group rocks may have increased the A/CNK of the granodiorite magmas, but may have had little or no effect on the A/CNK compositions of the leucogranite magmas. On the other hand, the selective contamination of the SMB magmas by the solid contaminants derived from the metapelitic Meguma Group rocks may have largely increased the A/CNK of granodiorite, leucogranite, as well as average SMB magmas.

6.4.5 AFC Model for the SMB

A possible petrogenetic model for country-rock contamination and assimilation in the SMB is that xenoliths formed dominantly at the roof of the evolving magma chamber, but that the assimilation of these xenoliths and *in situ* country rocks mostly occurred at deeper levels of the magma chamber (Fig. 6.4). Xenoliths of various sizes and xenocrysts incorporated during the early AFC evolution of the SMB may have mostly sunk to deeper levels of the SMB, whereas small xenoliths and xenoliths incorporated during the late AFC evolution would have probably remained close to their site of formation (Fig. 6.4A). If large volumes of xenoliths formed during the early evolution of a large SMB magma chamber, they may have been efficiently heated, and a mass of country rocks similar, or close to the modelled maximum may have thus been assimilated. If so, most of the xenoliths and their solid reaction products must have

formed cumulates at unexposed, deeper parts of the batholith (Fig. 6.4B,C). The country-rock partial melt generated from xenoliths and/or *in situ* country rocks at the near-floor level of the SMB may have been mobilized, as a consequence of filter pressing, and migrated with evolved SMB magmas, forming part of the exposed leucogranites and possibly other evolved rocks of the batholith (Fig. 6.4C). Partially assimilated country-rock contaminants dispersed throughout the SMB may have originated from the disintegration and assimilation of sinking (Fig. 6.4A,B), or ascending contaminants (Fig. 6.4C), and the country-rock contaminants observed near the exposed external margin of the batholith may thus be the only country rock material that was incorporated and partly assimilated at the level of exposure.

6.4.6 Importance of Country-rock Contamination in the SMB

If the amount of country-rock contaminants in the exposed rocks of the SMB is representative for the average country-rock contamination in the SMB, then most of the space for the batholith may have been created by floor-down (Culshaw and Bhatnagar 2001) or roof-up displacement (Benn et al. 1997). However, given that most of the SMB is unexposed, the maximum vertical exposure is a few tens of metres (compared to an intrusion thickness of ca. 5 to 10 km), the importance of stoping and country-rock contamination for creating the space of the SMB magma chamber cannot be reliably constrained by observations from the exposure. But the proposed AFC model for the SMB applies no matter if the SMB magma chamber had a size similar to the whole batholith, or if the magma chamber of the SMB was significantly smaller at a time (e.g., discussions by Coleman et al. 2004; Glazner et al. 2004; Zak and Paterson 2005), although for a magma chamber with a smaller size at a time than the whole batholith, the assimilation of country-rock material through partial melting may have been less important, depending on the contact relationships between magmas and country rocks. If magmas during the late-stage magmatic evolution of the SMB rose through an insulated plumbing system, and/or intruded older, partly or largely crystallized magmas instead of Meguma Group country rocks, little or no country-rock contamination and assimilation may have occurred, and source variations would have to explain most of the isotopic variation in the SMB.

Given the lack of isotopic data for large parts of the batholith (Clarke and Halliday 1980, 1985; Clarke et al. 1988), and thus insufficient data on the distribution and abundance of former country-rock partial melt throughout the SMB, the overall amount of country-rock

contamination in the exposed parts of the batholith can with our current knowledge only be guessed. Considering only the physically detectable country-rock contaminants, the minimum amount of country-rock material present in the exposed SMB is ≤3 vol%, with ≤6 vol% of country-rock contaminants in a ca. 200 metre wide zone along the external margin of the batholith, and ≤3 vol% of country-rock contaminants in the rest of the batholith (Chapter 4). Considering the physically detectable country-rock contaminants and a maximum of 10 and 4 vol% of complementary partial melt in the marginal and the more central rocks of the SMB, respectively, the amount of country-rock material present in the SMB is ≤7 vol% (Chapters 3 and 4). Considering the physically detectable country-rock contaminants, the complementary partial melt, and assuming that the leucogranites, which make up ≤1 % of the exposed rocks of the SMB (MacDonald 2001), were selectively contaminated by a maximum of 56 vol% of Meguma Group partial melt (Clarke et al. 2004), the amount of Meguma Group country-rock material present in the SMB may be up to 8 vol%. Considering the physically detectable country-rock contaminants, the complementary partial melt, and assuming that an average of up to ca. 8 vol% of country-rock partial melt (assuming that mass% calculated in this study approximately equal vol%) was assimilated by the SMB magmas and contaminated the exposed rocks, a maximum amount of up to 16 vol% of Meguma Group material may be present in the exposed SMB rocks. Most likely, neither a minimum estimate of 3 vol% nor a maximum estimate of 16 vol% of country-rock material is accurate. If only the leucogranites were selectively contaminated by assimilated country-rock partial melt, the amount of former country-rock partial melt derived from unexposed levels of the would make up <0.6 % of the exposed mass of the batholith, given that the leucogranites make up 1 vol% of the exposed granites and that the maximum amount of Meguma-Group-derived partial melt present is 56 vol% (if the granodiorites are uncontaminated; abundance of leucogranites after MacDonald 2001). If so, country-rock assimilation through partial melting may account for the isotopic signature of the leucogranites, even if country-rock assimilation through partial melting under natural conditions was less efficient than the modelled maximum of 10 vol%. If, however, further whole-rock and mineral isotopic analyses reveal that large amounts of physically undetectable partial melt also occur in the granodiorites, monzogranites, and leucomonzogranites of the SMB, say, on the order of >10 vol%, country-rock contamination and assimilation cannot account for the presence of all the former country-rock partial melt. In such as case,

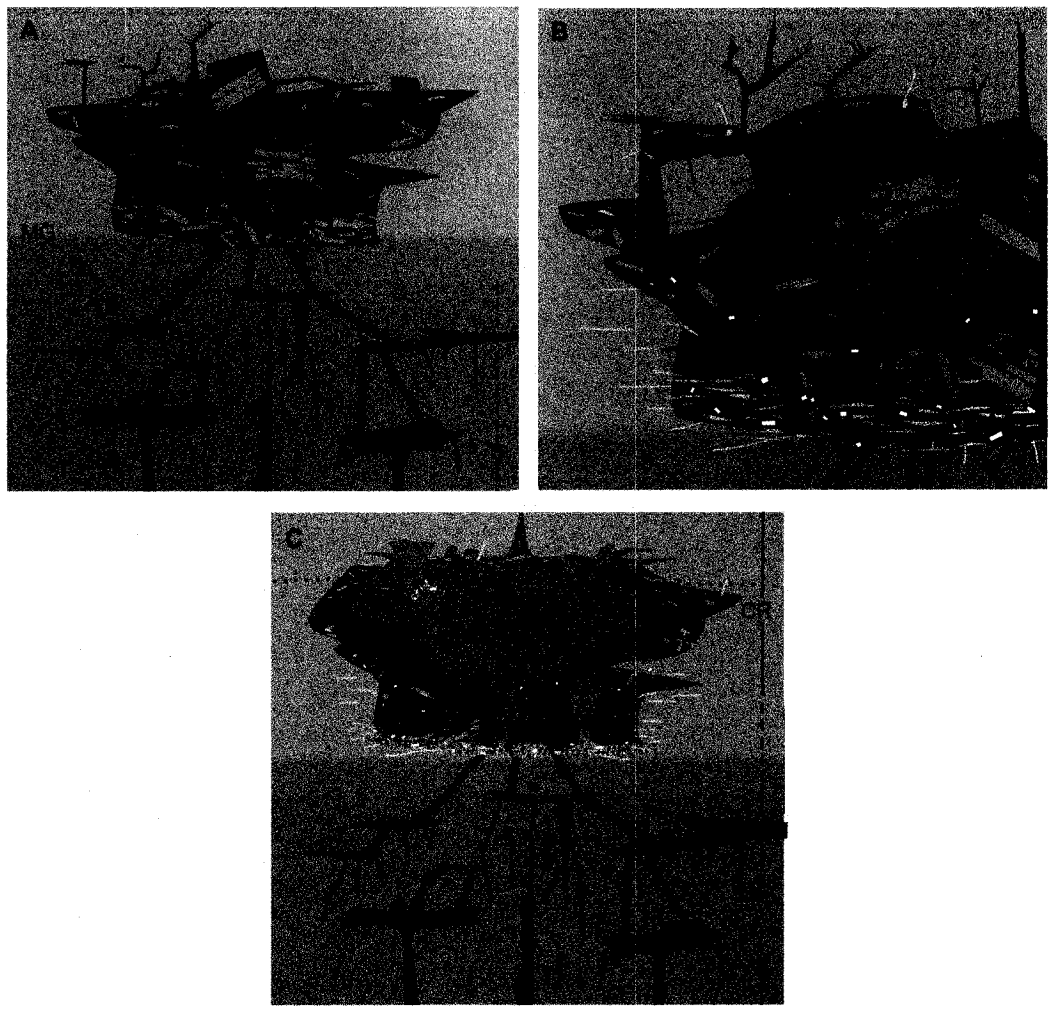

Figure 6.4: Possible AFC evolution of the South Mountain Batholith (SMB). A) SMB magmas are generated from felsic rocks of the Tangier basement (TB), emplaced dominantly within rocks of the Meguma Group (MG). Xenoliths that formed at various levels of the batholith sink through the magma column, accumulating at the floor of the magma chamber, possibly forming ("elephant's") graveyards. LG=Liscomb Gneisses; MI=Mafic intrusions; S=source. B) The SMB magmas fractionate. Xenoliths and *in situ* country-rocks partially melt where the mass of country-rock material and the degree of partial melting is significantly higher at deeper, near-floor levels of the SMB chamber. As a result, a compositionally distinct magma layer forms at the bottom of the batholith (yellow), characterized by a high amount of country-rock partial melt (CR PM), solid reaction products of partial melting (PXC), refractory xenocrysts, as well as xenoliths. MNG = monzogranite. C) During the late-stage AFC evolution, the SMB magmas are highly fractionated. LG = leucogranite; MP = mafic porphyry. Magmas derived from the Tangier basement, or fractionated SMB melts, mix with the bottom magma layer. These magmas, rich in country-rock-derived partial melt, are mobilized as isolated melt bodies, and represented by the late-stage leucogranites of the SMB. The stippled line marks the inferred present day surface.

source variations must have caused the addition of at least some of the Meguma-Group-derived melt (Fig. 6.5). In a scenario where only the exposed leucogranites were contaminated by Meguma Group partial melt, the composition of the uncontaminated granodiorite magmas may have been similar to the inferred magma composition Gd_{corr} (Table 6.1, 6.7). Compared to the exposed rocks, the uncontaminated magmas would have been only slightly peraluminous with an A/CNK of ca. 1.03. On the other hand, the composition of the uncontaminated leucogranite magmas ($LG_{corr}2$) would have been different from the composition of the inferred leucogranite magmas (LG_{corr}) and the exposed leucogranites (LG)(Table 6.7). If all Meguma Group partial melt added to the leucogranite magmas was derived from metapsammitic country rocks ($LG_{corr}2$(PSA)), the uncontaminated leucogranite magmas may have had an initial A/CNK of 1.09, and thus a peraluminosity similar to the granodiorite magmas. If all Meguma Group partial melt added to the leucogranite magmas was derived from metapelitic country rocks ($LG_{corr}2$(PEL)), the uncontaminated leucogranite magmas may have had an initial A/CNK of 1.35, and thus a peraluminosity significantly higher than the granodiorite magmas. In the case that contamination of the leucogranite magmas occurred dominantly by partial melt derived from metapelitic rocks, the higher peraluminosity of the leucogranites compared to the granodiorites of the SMB may dominantly be the result of country-rock contamination, or source variations. In the more probable case that contamination of the leucogranite magmas occurred largely by partial melt derived from metapsammitic rocks, given that the unexposed, deeper crustal Meguma Group rocks belong to the metapsammite-dominated Goldenville Formation (Figure 6.2), the higher peraluminosity of the leucogranites compared to the granodiorites may dominantly be the result of fractional crystallization.

6.5 Conclusions

The results of this study underscore the potential of EC-AFC models to estimate the significance of country-rock assimilation and contamination in a poorly exposed batholith. For the SMB, the model results suggest that assimilation of metapsammitic and metapsammitic rocks of the Meguma Group may be much more significant at the unexposed, near-floor level of the SMB than at the exposed, near-roof level of the batholith. The calculations show that all observed and estimated Meguma Group material in the SMB may be the result of country-rock contamination, but cannot

unequivocally decipher the origin of the former country-rock partial melt in the SMB. A possible AFC evolution for the SMB is that xenoliths incorporated at the near-roof level of the batholith sank to the near-floor level of the SMB magma chamber. With time, these xenoliths and in situ country rocks may have been assimilated through partial melting by SMB magmas. Subsequently, selective contamination of evolving SMB magmas, exposed in the form of leucogranites and possibly other SMB rocks, may have occurred. If mostly the leucogranites of the SMB were selectively contaminated by assimilated partial melt, all isotopically detectable Meguma Group material present in the SMB rocks may be explained by country-rock contamination and assimilation, but source variations have to be equally considered until current mineral and whole-rock trace element and isotopic studies permit further evaluation. However, if currently undetected former Meguma Group partial melt is furthermore volumetrically important in other rocks than the leucogranites of the SMB, a Meguma Group source contribution would have to account for at least some of the Meguma Group material present in the SMB.

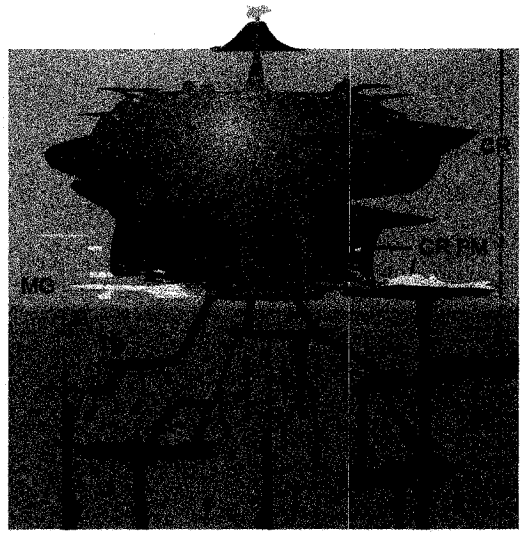

Figure 6.5: Alternative model for the evolution of the South Mountain Batholith (SMB), in which the Meguma Group is part of the source of the SMB magmas. The main difference between such an evolution and the assimilation of Meguma Group rocks by SMB magmas is that only partial melt and possibly minor solid phases become part of the SMB, whereas refractory and peritectic phases dominantly remain in the source region (Wall et al. 1987; Clemens 2003; Vernon in press).

6.6 Acknowledgements

I gratefully acknowledge the support from a Izaak Walton Killam Pre-Doctoral scholarship at Dalhousie, as well as support from an NSERC Discovery grant through Barrie Clarke. I am thankful for discussions with D.B. Clarke, R.A. Jamieson, and R.H. Vernon and their and comments on an earlier draft of this manuscript.

CHAPTER 7

Conclusion

7.0 Main Conclusions

The main conclusions from my thesis are:

(i) Country-rock contamination and assimilation played a role in the evolution of the SMB, where the assimilation of country-rock material occurred through a combination of fracturing, dispersal, partial melting, dissolution, and ion exchange reactions. Country-rock contaminants in the SMB occur dominantly in the form of xenoliths, orthoxenocrysts, paraxenocrysts, and former silicate and sulphide melt derived from metapsammitic to metapelitic rocks of the Meguma Group. Physically detectable country-rock contaminants are most abundant in a ≤200 m wide zone near the margin of the SMB (~6 vol%), and become less abundant towards the centre (≤4 vol%). *(Chapters 4 and 5)*

(ii) The assimilation of metapsammitic Meguma Group rocks through partial melting at ca. 800 °C may have resulted in the formation of ~19 vol% orthoxenocrysts (quartz, plagioclase, biotite, cordierite, garnet, and accessory minerals), ~75 vol% partial melt, and ~6 vol% paraxenocrysts (cordierite). The assimilation of metapelitic Meguma Group rocks through partial melting at ca. 800 °C may result in the formation a maximum of ~20 vol% paraxenocrysts (cordierite, garnet), ~70 vol% partial melt, and ~5 vol% orthoxenocrysts. Given these ratios, the physically detectable xenocrysts in the SMB rocks suggest that we may overlook a maximum of up to 10 vol% of complementary partial melt. Bulk contamination of the exposed SMB rocks by Meguma Group material may thus account for ≤16 vol% and ≤8 vol% of the marginal and the more central SMB rocks, respectively. *(Chapter 3 and 4)*

(iii) Country-rock-derived and small primary magmatic quartz are texturally and chemically largely indistinct, and their unequivocal discrimination if they occur as single quartz crystals in rocks of the SMB is therefore difficult. Orthoxenocrystic plagioclase and biotite are texturally similar to small primary magmatic crystals, and they lost their characteristic chemical signature as a result of ion exchange reactions with the SMB magmas, hampering a confident identification of single plagioclase and biotite orthoxenocrysts in any given rock. Garnet of various origins (e.g., paraxenocrystic and cognate magmatic garnet) is texturally distinct, but chemically indistinct, whereas all

present data suggest that cordierite of different origins is texturally as well as chemically characteristic. *(Chapters 2 and 5)*

(iv) Numerical modelling suggests that up to 8 vol% of Meguma Group material may have been assimilated through partial melting by SMB magmas. Thus, chemically recognizable but physically undetectable Meguma Group material in the leucogranites of the SMB may originate from the assimilation of Meguma Group country rocks through partial melting at the near-floor level of the batholith, and may reflect selective contamination. *(Chapter 6)*

7.1 Quantifying Country-rock Contamination in Igneous Rocks

A combined approach using field, textural, mineral chemical, experimental data, and numerical modelling, as carried out in this study, provides insights into the interaction between country rocks and magmas at a great level of detail, and appears, with our current knowledge, the best way of characterizing and quantifying the importance of country-rock components in a given igneous rock. Although innumerable studies on crust-magma interactions in magmatic systems of various compositions exist, the level of understanding the role, the nature, and the mechanisms of country-rock contamination in this case study on the SMB is, to the best of my knowledge, unprecedented for any other granite complexes (Clemens 2003). The importance of a multi-method approach in assessing country rock contamination in igneous rocks, instead of relying mostly on whole-rock geochemical data, or any other single-method approach, has been pointed out by numerous recent studies, but the approach I employed is advanced in a way that permits a semi-quantitative, and not just a qualitative, characterization of all components of country-rock contamination and assimilation (e.g., Simonetti and Bell 1993; Dungan and Davidson 2004; Beard et al. 2005; Costa and Dungan 2005; Ramos et al. 2005).

For the SMB, the characterization of the major country-rock contaminants is relatively straightforward, given that the system components, namely source rocks, granitic magmas, and country rocks are mineralogically and compositionally well characterized and relatively narrowly confined. However, the more complex the geological setting, particularly the more heterogeneous source and country rocks are, the more difficult it is to identify and quantify all source-rock versus country-rock-derived components in a given igneous complex. Moreover, if assimilation is advanced, refractory minerals, such as zircon and possibly monazite may record some of the only direct evidence for the contamination of magmas by rock types fertile for partial melting. If so, a search for

evidence for country-rock contaminants should first focus on the identification of refractory foreign crystals and the characterization of, for example, the various zircon populations present based on textures and/or chemical characteristics, and possibly ages (e.g., Schaltegger 2002). Once the important contaminants are identified and quantified, melting experiments employing different contaminant rock types may elucidate the relative and the absolute significance of assimilation of compositionally variable country rocks through partial melting. Then, knowing the composition of the country-rock-derived partial melt(s), one may decipher crystals that may have partly or dominantly crystallized from a country-rock-derived partial melt, or interpret the origin of zoning patterns in magmatic crystals (e.g., Davidson et al. 1990; Davidson and Tepley 1997; Cox et al. 1996; Knesel et al. 1999; Waight et al. 2000; Tepley and Davidson 2003; Gagnevin et al. 2005).

The two major uncertainties of the approach employed are to recognize unequivocally all solid country-rock contaminants, and to estimate correctly the amount of former liquid country-rock contaminants (Chapter 4; Clarke and Erdmann 2005; Clarke in press). Textural criteria may not have the potential to discriminate between every single crystal of xenocrystic, restitic, or cognate and foreign magmatic origin, for example, they cannot discriminate between small, single quartz crystals of potentially orthoxenocrystic and primary magmatic origin in the SMB. Original chemical compositions may be preserved for crystals of various origins, if magma residence times are short compared to time-scales of diffusive equilibration between foreign and cognate magmatic materials (e.g., in volcanic systems; e.g., Green 1994; Zellmer et al. 1999; Spell et al. 2001; Gardner et al. 2002; Hawkesworth 2004; Costa and Dungan 2005). My major- and trace-element study on rock-forming minerals of the SMB has shown that chemical discrimination among small crystals of various origins, even of those that once resided in relatively cold, granitic magmas with thermally limited ion exchange potential, is unlikely to be successful, unless the crystals have high effective closure temperatures (e.g., zircon). Most useful to recognize the origin of even small xenocrysts and restitic crystals may be the analysis of trace-element or isotopic zoning patterns by LAM ICP-MS or SIMS, circumventing the limitations of quantitative trace-element or isotopic analysis that may readily overlook the original chemical signatures or zoning patterns, given the currently required, relatively large analytical spot size (e.g., Müller et al. 2003; Davidson et al. 1998).

Reliably estimating the amount of former liquid country-rock contaminants is hampered by: (i) the problem of not knowing the exact bulk composition of the various country-rock contaminants (e.g., the compositional variation of metapelitic rocks assimilated in the SMB magmas); (ii) the simultaneous or subsequent operation of various processes of assimilation, such as physical disintegration and partial melting of xenoliths, and the resultant variable ratios of solid to liquid contaminants (e.g., physical disintegration results in 100% orthoxenocrysts, whereas partial melting of the same material may produce 20% orthoxenocrysts, 20% paraxenocrysts, and 60% partial melt); and (iii) the difficulty of unravelling the degree of selective contamination of a particular magma by solid or liquid country-rock contaminants. Nevertheless, keeping these limitations in mind, the approach I applied, or any other combination of textural, mineral chemical, and experimental analysis, is currently the most promising way to identify and to quantify all vestiges of country-rock contamination in a given igneous rock. In addition, whole-rock geochemical or isotopic data may help to constrain the presence and the amount of former liquid contaminants that do not occur in spatial association with their complementary solid contaminants, provided that the analyzed materials are well characterized (e.g., that source magma contributions and magma contributions from country rocks are distinguished and characterized). Numerical modelling can then help to constrain the possible maximum significance of country-rock assimilation through partial melting or relative to source variations or other magma chamber processes.

7.2 Country-rock Contamination in the SMB

Field and textural relations reveal evidence for the contamination of SMB magmas by xenoliths, xenocrysts, and former silicate and sulphide partial melt, dominantly derived from metapsammitic and metapelitic rocks of the of the Meguma Group (this study; Jamieson 1974; Allan and Clarke 1981; Poulson et al. 1991; Tate 1995; MacDonald 2001; Pelrine 2003; Clarke and Erdmann 2005; Samson 2005; Samson and Clarke 2005; Carruzzo et al. in press; Clarke and Carruzzo in press). These contaminants were incorporated into, and assimilated by, the SMB magmas through a combination of fracturing, dispersal, partial melting, dissolution, and ion exchange reactions (Chapter 3 and 4; Clarke and Erdmann 2005; Samson 2005; Carruzzo et al. in press; Clarke in press; Clarke and Carruzzo in press). The metapelitic rocks of the Meguma Group in contact with, or entrained in, the SMB magmas partially melted to a high degree, releasing dominantly paraxenocrystic garnet or cordierite, and a large fraction of partial

melt. The metapsammitic rocks of the Meguma Group in contact with, or entrained in, the SMB magmas partially melted to a low degree, releasing dominantly orthoxenocrysts of quartz, biotite, and plagioclase, and only a minor fraction of partial melt. Xenocrysts of ilmenite and rutile, Fe-sulphide xenocrysts and/or partial melt, as well as other country-rock minerals were also released into the SMB magmas (Pelrine 2003; Clarke and Erdmann 2005; Samson 2005; Samson and Clarke 2005; Carruzzo et al. in press; Clarke in press; Clarke and Carruzzo in press), but on average play a minor volumetric role in the SMB.

In SMB rocks remote from contacts with the Meguma Group rocks, textural relations, major- and trace-element compositions, as well as zoning patterns permit the identification of paraxenocrystic garnet and cordierite with confidence, but the detection of foreign quartz, biotite, and plagioclase xenocrysts is uncertain, and former partial melt is physically largely undetectable. New textural and chemical data on subhedral to euhedral, inclusion-poor cordierite crystals from large-scale, cordierite-rich zones of the SMB, which were previously interpreted to have a foreign paraxenocrystic origin (Chapter 2; Erdmann et al. 2004; Clarke and Erdmann 2005), show that the cordierite crystals are of primary magmatic origin (Chapter 4). Small-scale garnet-rich zones are partially assimilated metapelitic rocks, whereas small-scale biotite-rich zones represent most likely accumulated primary magmatic crystals, and not *in situ* assimilated bulk country-rock contaminants (Chapter 4).

The higher concentrations of xenoliths and xenocrysts in the marginal units of the batholith suggest that the late, and more central magmas had less opportunity to interact and become contaminated by bulk country-rock material. However the more evolved and typically more central SMB rocks comprise more Meguma-Group-derived partial melt, either as a result of country-rock contamination and assimilation or as a result of source variations (Chapter 6). The preferential addition of Meguma-Group-derived partial melt to the more evolved SMB magmas may have affected not only the chemical and isotopic composition of these rocks (Clarke et al. 1993; Clarke et al. 1998; MacDonald 2001; Clarke et al. 2004), but may have also contributed components to some of the magmatic (as opposed to external hydrothermal) mineral deposits of the batholith. Particularly Au, Mn, Pb, and Sn, occurring in relatively high concentrations in some of the rocks of the Meguma Group (e.g., Chatterjee et al. 1992; Cameron and Zentilli 1997), may have been added to the SMB magmas by assimilation of Meguma Group rocks though partial melting (e.g., MacDonald 2001; Carruzzo 2003; Carruzzo et al. 2004). However, with a

maximum of 8 vol% of assimilated country-rock partial melt, the contribution was limited, and more Meguma Group components may have added to the SMB magmas or SMB hosted mineral deposits as a result of the influx of Meguma Group-sourced hydrothermal fluids (e.g., Carruzzo 2003; Carruzzo et al. 2004).

7.3 Estimating the Significance of Country-rock Contamination in the SMB

Existing $\delta^{34}S$ data from SMB whole-rocks indicate locally a mixture of up to 70% Meguma-Group-derived sulfur and 30% cognate magmatic sulfur for some of the marginal granodiorites of the SMB (Poulson et al. 1991). Such a ratio for Meguma-Group-derived and cognate magmatic sulphur seems high, but tenable, if selective contamination of SMB magmas by country-rock sulphur, either through partial melting or through desulfidation reactions involving a fluid phase occurred (Poulson and Ohmoto 1989; Whitney 1989; Poulson et al. 1991; Clarke and Erdmann 2005; Samson 2005; Samson and Clarke 2005). Locally, similarly high concentrations of partially assimilated country-rock material occur in the SMB in the form of garnet-rich and rare orthoxenocryst-rich schlieren, and may occur in the form of physically invisible former Meguma-Group-derived silicate partial melt. Previous estimates for the degree of country-rock contamination throughout the SMB (Chapter 1) based on whole-rock Sr-Nd isotopic data suggested that the leucogranites of the SMB comprise up to ~36 % more Meguma Group country-rock contaminants than the granodiorites of the SMB, if bulk assimilation of metapelitic and metapsammitic Meguma Group rocks occurred (Clarke et al. 2004). The numerical models computed for country-rock assimilation through partial melting in the SMB (Chapter 6) suggest and permit the conclusion that 36% or more Meguma Group material may be present in the exposed leucogranites as a result of country-rock contamination and assimilation in combination with selective contamination. However, the previously suggested hypothesis that largely assimilated Meguma Group country rocks may explain up to ~36 % more Meguma Group material in the evolved and more central rocks of the SMB seems invalid to explain the isotopic characteristics of the SMB leucogranites, given that the assimilation of Meguma Group country-rock material in the SMB magmas was only partial. If the hypothesis were correct, physical evidence for the contamination by Meguma Group rocks should be abundant, but this is not the case (Chapter 4).

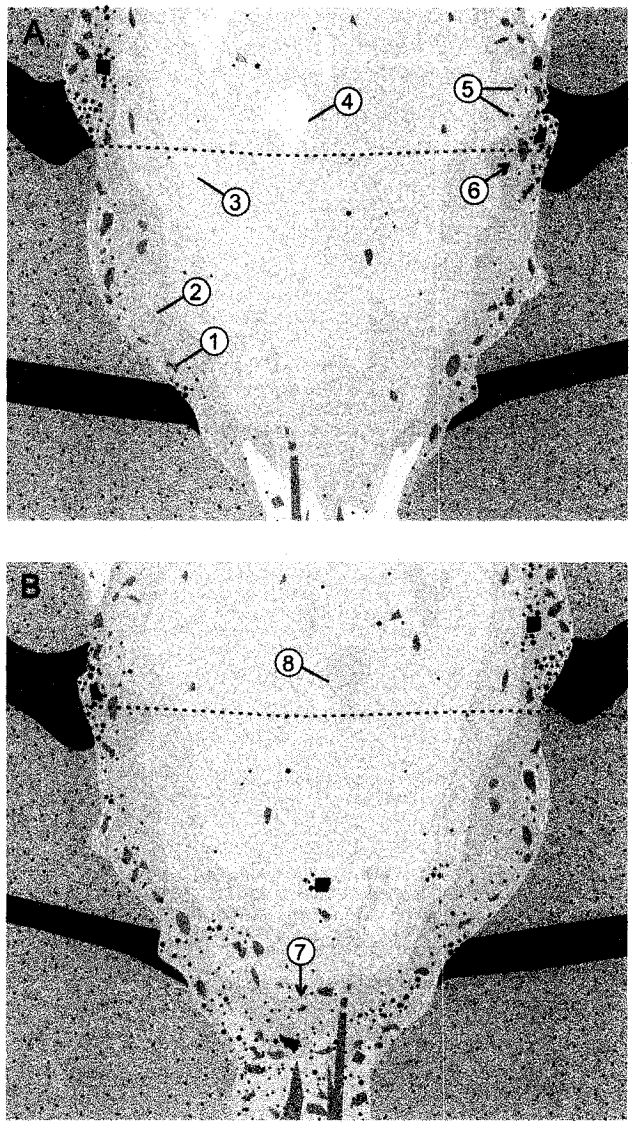

Figure 7.1: Sketches of two possible petrogenetic models to explain the observed mineralogical, textural, and chemical variations in the SMB. Gray colors indicate cognate SMB material. Different gray shades delineate compositionally variable SMB magmas. Contacts are diffuse to sharp. Yellow, orange (metapsammitic rocks), and red colors (metapelitic rocks) indicate country-rock material. Black stippled line marks the currently exposed section of the SMB. A) Material derived from country-rock contamination and assimilation occurs dominantly near the external margins of the batholith, including xenoliths, garnet-rich schlieren, and single paraxenocrysts and orthoxenocrysts. 1 = xenolith, 2 = biotite-rich zone, 3 = cordierite-rich zone, 4 = leucogranites, 5 = orthoxenocrysts (yellow) and paraxenocrysts, 6 = in light orange color, partial melt complementary to the physically evident xenoliths and xenocrysts. B) Country-rock assimilation by SMB magmas is much more significant near the floor of the SMB. 7 = highly contaminated zone, 8 = leucogranites with a significant proportion of Meguma-Group-derived partial melt, generated and mobilized from the highly contaminated near-floor zone of the SMB.

Data and observations presented in my thesis suggest that ~4 vol% and <2 vol% of xenocrysts occur in the in the marginal rocks and in the more central rocks of the exposed SMB, respectively (Fig. 7.1), if the biotite-rich and cordierite-rich zones of the SMB represent accumulated cognate magmatic material, if the garnet-rich zones are partly digested metapelitic xenoliths of Meguma Group origin, if all potential xenocrysts of the SMB rocks are true xenocrysts, and if all xenocrysts present in a given rock are detectable with the methods used. Using the ratios of xenocrysts to partial melt determined in melting experiments employing metapelitic and metapsammitic rocks of the Meguma Group (Chapter 3), the abundance of orthoxenocrysts and paraxenocrysts may suggest that ≤10 vol% of complementary former country-rock partial melt is present in the exposed SMB rocks with ≤2 vol% partial melt derived from metapsammitic and ≤8 vol% partial melt from metapelitic country-rock contaminants. Together, xenoliths, xenocrysts, and complementary partial melt make up ca. 16 vol% of Meguma Group country-rock material in the marginal (<200 metres) and ca. 8 vol% in the more central rocks of the exposed parts of the batholith (Fig. 7.1A; Chapter 4). However, if a maximum of 8 vol% of country-rock contamination occurred at unexposed levels of the SMB, and the selective contamination of the exposed SMB rocks by country-rock-derived partial melt played a significant role, country-rock assimilation through partial melting may moreover account for the presence of chemically detectable, but physically undetectable, former Meguma Group partial melt in the leucogranites and possibly other evolved rocks of the SMB (Fig. 7.1B; Chapter 6).

In both scenarios, crustal recycling by SMB magmas and country-rock contamination has played a role in the evolution of the SMB. If the selective addition of up to 56 vol% of Meguma Group derived partial melt through contamination and assimilation to the more evolved SMB rocks occurred (Chapter 6), country-rock contamination and assimilation significantly affected the composition and the mineralogy of these SMB rocks. However, effects from the source, fractional crystallization, and/or fluid interaction are overall more important to explain the mineralogical, textural, and chemical variations observed in and between most rock types of the exposed batholith, even if a maximum of 8 vol% of Meguma Group material may have been assimilated though partial melting. If the abundance of country-rock contaminants in the exposed SMB rocks is representative for the average country-rock contamination in the SMB, then most of the space for the batholith may have been created by floor-down (Culshaw and Bhatnagar 2001) or roof-up displacement (Benn et al. 1997). However, given that most of the SMB is unexposed,

the importance of stoping versus other mechanisms for creating the space of the SMB magma chamber cannot be reliably constrained.

7.4 Proposed Future Work

To further improve understanding of the role, nature, and timing of country-rock contamination in the SMB, I suggest three major lines of research: (i) enlarge the data set of whole-rock isotopic analyses for the various rock types of the batholith; (ii) continue the mineral chemical and isotopic characterization of large garnet, cordierite, and plagioclase crystals in the SMB, and tackle the mineral chemical and isotopic characterization of K-feldspar and zircon; and (iii) gather mineral chemical and isotopic data for various rock forming minerals from various samples of the SMB source rocks.

(i) Isotopic analyses of SMB rocks. The existing isotopic analyses show that the leucogranites of the SMB have a larger component of Meguma-Group-derived material than the granodiorites of the SMB (Chapters 4 and 5 this study), but the number of analyses is not sufficient to constrain the overall contribution of Meguma-Group-derived partial melt to the SMB rocks. Particularly for the volumetrically most important muscovite-biotite monzogranites and leucomonzogranites, further isotopic data are needed. With further whole-rock isotopic data, it should be possible to determine if the former Meguma Group partial melt manifested in the SMB rocks is largely derived from country-rock contamination at unexposed levels of the batholith, or if Meguma Group material became part of the SMB magma source, contributing country-rock partial melt, but little or no restitic material to the SMB magmas. If the former Meguma Group partial melt present in the exposed SMB rocks is largely derived from country-rock contamination at unexposed levels of the batholith, the overall amount of former Meguma Group partial melt in the SMB should be <8 %. If the former Meguma Group-derived partial melt present in the exposed SMB rocks is largely a result of source variations, the amount of former country-rock partial melt in the SMB may be >8 vol%. If the Meguma Group partial melt was added to the SMB magmas as a result of source variations, the presence of the former country-rock partial melt may be inextricably linked to fractionation trends and single plutons, whereas the addition of Meguma Group partial melt through country-rock contamination may have resulted in a more inhomogeneous distribution throughout the SMB, reflecting local interaction between country rocks and magmas.

Whole-rock isotopic analyses of cordierite-, garnet-, and biotite-rich zones, and adjacent rocks that are currently underway are a first contribution to this attempt to constrain further country-rock contamination in the SMB. The primary intention of these analyses is to eliminate uncertainties in the interpretation of the origin of the biotite-rich zones, and to characterize the composition of the SMB rocks that host up to 5 modal% magmatic cordierite crystals, but they may also provide a better idea of the degree of isotopic variation within the various units of the SMB.

(ii) *SMB mineral chemical and isotopic analyses.* Major- and trace-element analyses of large cordierite, garnet, and plagioclase crystals have revealed evidence not only for the origin of these minerals, but also details about magma recharge and magma or fluid degassing. However, a larger number of analyses is required to permit a more confident interpretation of the magma chamber processes recorded. The addition of quantitative mineral isotope analysis and qualitative mineral trace-element and isotope stratigraphy, using LAM ICP-MS or TIMS, will potentially offer more detailed insights into magmatic processes, and residence as well as growth times of the various rock constituents.

First $\delta^{18}O$ analyses of garnet by, and in collaboration with, J.S. Lackey (College of Wooster), J.W. Valley (University of Wisconsin), and D.B. Clarke, have revealed that orthoxenocrystic, paraxenocrystic, and cognate magmatic garnets have distinct isotopic fingerprints (Lackey et al. submitted), but further examples will be studied, and tested for oxygen isotopic zoning. I would focus on the study of crystals from some of the mafic porphyries of the SMB, which are characterized by tonalitic to granodioritic compositions, and have abundant garnet and andalusite (MacDonald 2001). The origin of these relatively mafic rocks in the SMB is poorly understood, but they appear to be zones in which partially assimilated country-rock and cognate magmatic material accumulated. Another focus I would set is the study of newly discovered garnet cumulates (personal communication A.M. Ryan, Dalhousie University, 2006), and other exposed cumulates of the SMB (e.g., plagioclase-rich zones). In both cases, the analytical results should permit a better characterization of country-rock contamination, assimilation, and other magma chamber processes during the early evolution of the batholith.

Trace-element and isotopic characterization of K-feldspar and zircon were not attempted in this study. However, the study of trace-element and isotopic zoning in K-feldspar megacrysts from various units of the SMB may be powerful way to further trace indirect evidence for country-rock contamination and other magma chamber processes. Zircon may be useful to identify largely assimilated country-rock material, and may, for example,

help to decipher, if all, some, or none of the biotite-rich zones in the SMB reflect highly digested country-rock material.

An investigation of the stable isotope composition of Fe±Cu-sulphides from Meguma and SMB rocks, carried out in collaboration between S. Erdmann, D.B. Clarke, and B.E. Taylor (Geological Survey of Canada, Ottawa), is also underway, and will further complete our understanding of the origin of isotopic heterogeneities in the SMB.

(iii) *Source-rock mineral chemical and isotopic analyses.* The analysis of trace-element and isotopic compositions of the rock-forming minerals from the SMB source rocks of the Tangier basement is important to better constrain the trace-element and isotopic compositions of the source-rock-derived partial melts (by calculating trace-element distributions among restitic crystals and coexisting melts; e.g., Bédard 1994; Blundy and Wood 2003). Studying a larger number of samples will help determine if isotopic compositions of the source-rock crystals are variable or relatively homogeneous, and also help to evaluate if isotopic variations in the SMB may partly be the consequence of source-rock inhomogeneities, or disequilibrium during the protracted generation of the SMB magmas.

References

Acosta-Vigil, A., London, D., Dewers, T.A., and Morgan VI, G.B. (2002): Dissolution of corundum and andalusite in H_2O-saturated haplogranitic melts at 800 °C and 200 MPa: Constraints on diffusivities and the generation of peraluminous melts. Journal of Petrology 43, 1885-1908.

Acosta-Vigil, A., London, D., Morgan VI, G.B., and Dewers, T.A. (2003): Solubility of excess alumina in hydrous granitic melts in equilibrium with peraluminous minerals at 700-800 °C and 200 MPa, and applications of the aluminum saturation index. Contributions to Mineralogy and Petrology 146, 100-119.

Aitcheson, S.J., and Forrest, A.H. (1994): Quantification of crustal contamination in open magmatic systems. Journal of Petrology 35, 461-488.

Aldendorfer M.S., and Blashfield R.K. (1984): Cluster Analysis. Beverly Hills, Sage Publications.

Allan, B.D., and Clarke, D.B. (1981): Occurrence and origin of garnets in the South Mountain Batholith, Nova Scotia. The Canadian Mineralogist 19, 19-24.

Ashworth, J.R., and Chinner, G.A. (1978): Coexisting garnet and cordierite in migmatites from the Scottish Caledonides. Contributions to Mineralogy and Petrology 65, 379-394.

Barbarin, B., and Didier, J. (1991): Macroscopic features of mafic microgranular enclaves. In: Enclaves and granite petrology. Editors: Didier, J., and Barbarin, B. Developments in Petrology 13, 253-262.

Barbey, P., Marignac, C., Montel, J.M., Macaudière, J., Gasquet, D., and Jabbori, J. (1999). Cordierite growth textures and the conditions of genesis and emplacement of crustal granitic magmas: the Velay granite complex (Massif Central, France). Journal of Petrology 40, 1425-1441.

Barboza, S.A., and Bergantz, G.W. (1997): Melt productivity and rheology; complementary influences on crustal melting following underplating. Eos, Transactions, American Geophysical Union 78, 797.

Barboza, S.A., and Bergantz, G.W. (1998): Rheological transitions and the progress of melting of crustal rocks. Earth and Planetary Science Letters 158, 19-29.

Bea, F., Pereira, M.D., and Stroh, A. (1994): Mineral/leucosome trace-element partitioning in a peraluminous migmatite (a laser ablation-ICP-MS study). Chemical Geology 117, 291-312.

Beard, J.S., Abitz, R.J., and Lofgren, G.E. (1993): Experimental melting of crustal xenoliths from Kilbourne Hole, New Mexico and implications for the contamination and genesis of magmas. Contributions to Mineralogy and Petrology 115, 88-102.

Beard, J.S., Ragland, P.C., and Crawford, M.L. (2005): Reactive bulk assimilation: A model for crust-mantle mixing in silicic magmas. Geology 33, 681-684.

Beard, J.S., Ragland, P.C., and Rushmer, T. (2004): Hydration crystallization reactions between anhydrous minerals and hydrous melt to yield amphibole and biotite in igneous rocks: Description and implications. Journal of Geology 112, 617-621.

Bédard, J.H. (1991): Cumulate recycling and crustal evolution in the Bay of Islands Ophiolite. Journal of Geology 99, 225-249.

Bédard, J.H. (1994): A procedure for calculating the equilibrium distribution of trace elements among the minerals of cumulate rocks, and the concentration of trace elements in the coexisting liquids. Chemical Geology 118, 143-153.

Benn, K., Horne, R.J., Kontak, D.J., Pignotta, G.S., and Evans, N.G. (1997): Syn-Acadian emplacement model for the South Mountain Batholith, Meguma Terrane, Nova Scotia; magnetic fabric and structural analyses. Geological Society of America Bulletin 109, 1279-1293.

Benn, K., Roest, W.R., Rochette, P., Evans, N.G., and Pignotta, G.S. (1999): Geophysical and structural signatures of syntectonic batholith construction; the South Mountain Batholith, Meguma Terrane, Nova Scotia. Geophysical Journal International 136, 144-158.

Bergantz, G.W. (1992): Conjugate solidification and melting in open and closed multi-component systems. The IMA Volumes in Mathematics and its Applications 41, 314-315.

Betts-Robertson, B.L. (1998): Silicate and sulphide mineral assembalges and metamorphic fabrics from pelites in the contact aureoloe of the South Mountain Batholith, Halifax area, Nova Scotia. Unpublished BSc thesis, Dalhousie University, Nova Scotia, 52 pp.

Bindeman, I.N., and Valley, J.W. (2003): Rapid generation of both high- and low-$\delta^{18}O$, large-volume silicic magmas at the Timber Mountain/Oasis Valley caldera complex, Nevada. Geological Society of America Bulletin 115, 581-595.

Birch, W.D., and Gleadow, A.J.W. (1974): The genesis of garnet and cordierite in acid volcanic rocks: evidence from the Cerberean cauldron, central Victoria, Australia. Contributions to Mineralogy and Petrology 45, 1-13.

Blundy, J.D., and Shimizu, N. (1991): Trace element evidence for plagioclase recycling in calc-alkaline magmas. Earth and Planetary Science Letters 102, 178-197.

Blundy, J.D., and Wood, B.J. (1991): Crystal-chemical controls on the partitioning of Sr and Ba between plagioclase feldspar, silicate melts, and hydrothermal solutions. Geochimica et Cosmochimica Acta 55, 193-209.

Blundy, J., and Wood, B. (2003):Partitioning of trace elements between crystals and melts. Earth and Planetary Science Letters 210, 383-397.

Bohrson, W.A., and Spera, F.J. (2001): Energy-constrained open-system magmatic processes; II, Application of energy-constrained assimilation-fractional crystallization (EC-AFC) model to magmatic systems. Journal of Petrology 42, 1019-1041.

Bohrson, W.A., and Spera, F.J. (2003): Energy-constrained open-system magmatic processes; IV, Geochemical, thermal and mass consequences of energy-constrained recharge, assimilation and fractional crystallization (EC-RAFC). G^3 4, DOI 10.1029/2002GC000316.

Boudreau, A.E. (1999): PELE; a version of the MELTS software program for the PC platform. Computers & Geosciences 25, 201-203.

Bouloton, J. (1992) : Mise en évidence de cordiérite des terrains traversés dans le pluton granitique des Oulad Ouaslam (Jebilet, Maroc). Canadian Journal of Earth Sciences 29, 658-668.

Bowen, N.L. (1922a): The reaction principle in petrogenesis. Journal of Geology 30, 177-198.

Bowen, N.L. (1922b): The behaviour of inclusions in igneous magmas. Journal of Geology 30, 513-570.

Bowen, N.L. (1928): The Evolution of Igneous Rocks. New Jersey, Princeton University Press.

Cameron, B.I., and Zentilli, M. (1997): Geochemical characterization of the mineralized transition between the Goldenville and Halifax formations and the interaction with adjacent granitoid intrusions of the Liscomb Complex, Nova Scotia. Atlantic Geology, 33, 143-155.

Campbell, I.H., and Turner, J.S. (1987): A laboratory investigation of assimilation at the top of a basaltic magma chamber. Journal of Geology 95, 155-172.

Carruzzo, S. (2003): Granite-hosted mineral deposits of the New Ross area, South Mountain Batholith, Nova Scotia, Canada. Unpublished PhD thesis, Dalhousie University, Nova Scotia, 571 pp.

Carruzzo, S., and Clarke, D.B. (2005): Assimilation of country-rock ilmenite and rutile in the South Mountain Batholith, Nova Scotia, Canada. GAC - MAC Annual Meeting Abstracts with Program, 25.

Carruzzo, S., Clarke, D.B., Pelrine, K., and MacDonald, M.A. (2006): Texture, composition, and origin of rutile in the South Mountain Batholith, Nova Scotia. The Canadian Mineralogist, 44, 715-729.

Carruzzo, S., Kontak, D.J., Clarke, D.B., and Kyser, T.K. (2004): An integrated fluid-mineral stable-isotope study of the granite-hosted mineral deposits of the New Ross area, South Mountain Batholith, Nova Scotia, Canada; evidence for multiple reservoirs. The Canadian Mineralogist 42, 1425-1441.

Carter, S.R., Evensen, N.M., Hamilton, P.J., and O'Nions, R.K. (1978): Neodymium and strontium isotope evidence for crustal contamination of continental volcanics. Science 202, 743-747.

Castro, A. (1987): On granitoid emplacement and related structures; a review. Geologische Rundschau 76, 101-124.

Castro, A. (2001): Plagioclase morphologies in assimilation experiments; implications for disequilibrium melting in the generation of granodiorite rocks. Mineralogy and Petrology 71, 31-49.

Cenki, B., Kriegsman, L.M., and Braun, I. (2002): Melt-producing and melt-consuming reactions in the Achankovil cordierite gneisses, South India. Journal of Metamorphic Geology 20, 543-561.

Chatterjee, A.K., Kontak, D.J., Smith, P.K., Thalhammer, O.A.R., Gibson, J.H., Seccombe, P.K., Zhao, R., Halls, C., Shine, C., Harrington, K., and Foster, R.P. (1992): Gold metallogenesis. Institution of Mining and Metallurgy 101, 166-168.

Cherniak, D.J. (1995): Diffusion of lead in plagioclase and K-feldspar; an investigation using Rutherford backscattering and resonant nuclear reaction analysis. Contributions to Mineralogy and Petrology 120, 358-371.

Cherniak, D.J. (2002): Ba diffusion in feldspar. Geochimica et Cosmochimica Acta 66, 1641-1650.

Cherniak, D.J. (2003): REE diffusion in feldspar. Chemical Geology 193, 25-41.

Cherniak, D.J., and Watson, E.B. (1992): A study of strontium diffusion in K-feldspar, Na-K feldspar and anorthite using Rutherford backscattering spectroscopy. Earth and Planetary Science Letters 113, 411-425.

Cherniak, D.J., and Watson, E.B. (1994): A study of strontium diffusion in plagioclase using Rutherford backscattering spectroscopy. Geochimica et Cosmochimica Acta 58, 5179-5190.

Christiansen, E.H. (2005): Contrasting processes in silicic magma chambers; evidence from very large volume ignimbrites. Geological Magazine 142, 669-681.

Clarke, D.B. (in press): Assimilation of xenocrysts in granitic magmas: principles, processes, proxies, and problems. The Canadian Mineralogist.

Clarke, D.B. (1995): Cordierite in felsic igneous rocks: a synthesis. Mineralogical Magazine 59, 311-325.

Clarke, D.B. (1981):The mineralogy of peraluminous granites; a review. The Canadian Mineralogist 19, 3-17.

Clarke, D.B., and Bogutyn, P.A. (2003): Oscillatory epitactic-growth zoning in biotite and muscovite from the Lake Lewis Leucogranite, South Mountain Batholith, Nova Scotia, Canada. The Canadian Mineralogist 41, 1027-1047.

Clarke, D.B., and Carruzzo, S. (in press). Assimilation of country-rock ilmenite and rutile in the South Mountain Batholith, Nova Scotia, Canada. The Canadian Mineralogist.

Clarke, D.B., and Chatterjee, A.K. (1988): Physical and chemical processes in the South Mountain Batholith. Special Volume - Canadian Institute of Mineralogy and Metallurgy 39, 223-233.

Clarke, D.B., Dorais, M., Barbarin, B., Barker, D., Cesare, B., Clarke, G., El Baghdadi, M., Erdmann, S., Förster, H.-J., Gaeta, M., Gottesmann, B., Jamieson, R.A., Kontak, D., Koller, F., Gomes, C.L., London, D., Morgan, G.B. VI., Neves, L.J.P.F., Pattison, D.R.M., Pereira, A.J.S.C., Pichavant, M., Rapela, C., Renno, A., Richards, S., Roberts, M., Rottura, A., Saavedra, J., Sial, A.N., Toselli, A.J., Ugidos, J.M., Uher, P., Villaseca, C., Visona, D., Whitney, D., Williamson, B., and Woodad, H.H. (2005): Occurrence and origin of andalusite in peraluminous felsic igneous rocks. Journal of Petrology 46, 441-472.

Clarke, D.B., and Erdmann, S. (2005): Contamination in the South Mountain Batholith and Port Mouton Pluton, southern Nova Scotia. Atlantic Geological Society Special Publication 21, 45 pp.

Clarke, D.B., and Halliday, A.N. (1980): Strontium isotope geology of the South Mountain Batholith, Nova Scotia. Geochimica and Cosmochimica Acta 44, 1045-1058.

Clarke, D.B., and Halliday, A.N. (1985): Sm/Nd isotopic investigation of the age and origin of the Meguma Zone metasedimentary rocks. Canadian Journal of Earth Sciences 22, 102-107.

Clarke, D.B, Halliday, A.N., and Hamilton, P.J. (1988): Neodymium and strontium isotopic constraints on the origin of the peraluminous granitoids of the South Mountain Batholith, Nova Scotia, Canada. Chemical Geology 73, 15-24.

Clarke, D.B., Henry, A.S., and White, M.A. (1998): Exploding xenoliths and the absence of "elephants' graveyards" in granite batholiths. Journal of Structural Geology 20, 1325-1343.

Clarke, D.B., Fallon, R., Heaman, L.M. (2000). Interaction among upper crustal, lower crustal, and mantle materials in the Port Mouton Pluton, Meguma lithotectonic zone, Southwest Nova Scotia. Canadian Journal of Earth Sciences 37, 579-600.

Clarke, D.B., MacDonald, M.A., and Erdmann, S. (2004): Chemical variation in Al_2O_3-CaO-Na_2O-K_2O space: controls on the peraluminosity of the South Mountain Batholith. Canadian Journal of Earth Sciences 41, 785-798.

Clarke, D.B., MacDonald, M.A., Reynolds, P.H., Longstaffe, F.J. (1993). Leucogranites from the eastern part of the South Mountain Batholith, Nova Scotia. Journal of Petrology 34, 653-679.

Clarke, D.B., MacDonald, M.A., and Tate, M.C. (1997): Late Devonian mafic-felsic magmatism in the Meguma Zone, Nova Scotia. Memoir - Geological Society of America 191, 107-127.

Clarke, D.B., and Muecke, G.K. (1985): Review of the petrochemistry and origin of the South Mountain Batholith and associated plutons, Nova Scotia, Canada. Institute of Mineralogy and Metallurgy, London, United Kingdom (GBR), 41-54.

Clemens, J.D. (1984): Water contents of silicic to intermediate magmas. Lithos 17, 272-287.

Clemens, J.D. (2003): S-type granitic magmas; petrogenetic issues, models and evidence. Earth-Science Reviews 61, 1-18.

Coleman, D.S., Gray, W., and Glazner, A.F. (2004): Rethinking the emplacement and evolution of zoned plutons; geochronologic evidence for incremental assembly of the Tuolumne Intrusive Suite, California. Geology 32, 433-436.

Connolly, J.A.D., Holness, M.B., Rubie, D.C., and Rushmer, T. (2000): Reaction-induced microcracking; an experimental investigation of a mechanism for enhancing anatectic melt extraction. Geology 25, 591-594.

Corey, M.C., and Chatterjee, A.K. (1990): Characteristics of REE and other trace elements in response to successive and superimposed metasomatism within a portion of the South Mountain Batholith, Nova Scotia, Canada. Chemical Geology 85, 265-285.

Cormier, R.F., and Smith, T.E. (1973): Radiometric Ages of Granitic Rocks, Southwestern Nova Scotia. Canadian Journal of Earth Sciences 10, 1201-1210.

Costa, F., Dungan, M.A. (2005): Short time scales of magmatic assimilation from diffusion modeling of multiple elements in olivine. Geology 33, 837-840.

Costa, F., Scaillet, B., and Pichavant, M. (2004): Petrological and experimental constraints on the pre-eruption conditions of Holocene dacite from Volcan San Pedro (36 °S, Chilean Andes) and the importance of sulphur in silicic subduction-related magmas. Journal of Petrology 45, 855-881.

Costa, F., Scaillet, B., and Pichavant, M. (2002): Experimental simulation of interactions between evolved hydrous liquids and gabbroic minerals at 200-400 MPa. Geochimica et Cosmochimica Acta 66, 855-881.

Cox, R.A., Dempster, T.J., Bell, B.R., and Rogers, G. (1996): Crystallization of the Shap Granite; evidence from zoned K-feldspar megacrysts. Journal of the Geological Society of London 153, 625-635.

Culshaw, N., and Bhatnagar, P. (2001): The interplay of regional structure and emplacement mechanisms at the contact of the South Mountain Batholith, Nova Scotia; floor-down or wall-up? Canadian Journal of Earth Sciences 8, 1285-1299.

Culshaw, N., and Lee, S.K.Y (2006): The Acadian fold belt in the Meguma Terrane, Nova Scotia: Cross sections, fold mechanisms, and tectonic implications. Tectonics 25, doi:10.1029/2004TC001752.

Currie, K.L., Whalen, J.B., Davis, W.J., Longstaffe, F.J., and Cousens, B.L. (1998): Geochemical evolution of peraluminous plutons in southern Nova Scotia, Canada; a pegmatite-poor suite. Lithos 44, 117-140.

Czmanske, G.K., and Wones, D.R. (1973): Oxidation during magmatic differentiation, Finmarka Complex, Oslo area, Norway: Part 2 the mafic silicates. Journal of Petrology 14, 349-380.

Daly, R.A. (1903): The mechanics of igneous intrusion. American Journal of Science 15, 269-298.

Daly, R. A. (1933): Igneous rocks and the depths of the Earth. McGraw-Hill Book Company, New York, London.

Davidson, J.P., de Silva, S.L., Holden, P., and Halliday, A.N. (1990): Small-scale disequilibrium in a magmatic inclusion and its more silicic host. Journal of Geophysical Research, Solid Earth and Planets 95, 17,661-17,675.

Davidson, J.P., Hora, J.M., Garrison, J.M., and Dungan, M.A. (2005): Crustal forensics in arc magmas. Journal of Volcanology and Geothermal Research140, 157-170.

Davidson, J.P, and Tepley III, F.J. (1997): Recharge in volcanic systems: Evidence from isotope profiles of phenocrysts. Science 275, 826-829.

Davidson, J.P., Tepley III, F.J., and Knesel, K.M. (1998): Isotopic fingerprinting may provide insights into evolution of magmatic systems. Eos, Transactions, American Geophysical Union 79, 185.

Davidson, J., Tepley, III F., Palacz, Z., and Meffan-Main, S. (2001): Magma recharge, contamination and residence times revealed by in situ laser ablation isotopic analysis of feldspar in volcanic rocks. Earth and Planetary Science Letters 184, 427-442.

Deer, W.A., Howie, R.A., and Zussman, J. (1997): Disilicates and Ring Silicates. Rock-forming Minerals. London, The Geological Society.

DePaolo D.J. (1981): Trace element and isotopic effects of combined wallrock assimilation and fractional crystallization. Earth Planetary Sciences Letters 53, 189-202.

DePaolo, D.J. (1985): Isotopic studies of processes in mafic magma chambers; I, The Kiglapait Intrusion, Labrador. Journal of Petrology 26, 925-951.

Ding, Y. (1995): AFM minerals in the Halifax Pluton. Unpublished MSc thesis, Dalhousie University, Nova Scotia, Canada.

Doe, B.R. (1967): The bearing of lead isotopes on the source of granitic magma. Journal of Petrology 8, 51-83.

Douma, M. (1978): Gravitational interpretation and modelling of the South Mountain Batholith, southern Nova Scotia. Unpublished BSc thesis, Dalhousie University, Nova Scotia, Canada.

Dufek, J., and Bergantz, G.W. (2005): Lower crustal magma genesis and preservation; a stochastic framework for the evaluation of basalt-crust interaction. Journal of Petrology 46, 2167-2195.

Dumond, G., Yoshinobu, A.S., and Barnes, C.G. (2005): Midcrustal emplacement of the Sausfjellet Pluton, central Norway; ductile flow, stoping, and in situ assimilation. Geological Society of America Bulletin 117, 383-395.

Dungan, M.A., and Davidson, J. (2004): Partial assimilative recycling of the mafic plutonic roots of arc volcanoes; an example from the Chilean Andes. Geology 32, 773-776.

Dungan, M.A., and Davidson, J. (2004): Partial assimilative recycling of the mafic plutonic roots of arc volcanoes; an example from the Chilean Andes. Geology 32, 773-776.

Dungan, M.A., Wulff, A., and Thompson, R.A. (2001): Eruptive stratigraphy of the Tatara-San Pedro Complex, 36 °S, southern volcanic zone, Chilean Andes; reconstruction method and implications for magma evolution at long-lived arc volcanic centers. Journal of Petrology 42, 555-626.

Eberz, G.W., Clarke, D.B., Chatterjee, A.K., Giles, P.S. (1991): Chemical and isotopic composition of the lower crust beneath the Meguma lithotectonic zone, Nova Scotia; evidence from granulite facies xenoliths. Contributions to Mineralogy and Petrology 109, 69-88.

Edwards, B.R., and Russell, J.K. (1996): Influence of magmatic assimilation on mineral growth and zoning. The Canadian Mineralogist 34, 1149-1162.

Erdmann, S., and Clarke, D.B. (submitted): Nature and significance of metapsammitic and metapelitic contaminants in the peraluminous South Mountain Batholith. Lithos.

Erdmann, S., and Clarke, D.B. (2005): The South Mountain Batholith – a country-rock contaminated granite. "Sheared magmas in nature and experiment: bridging the brittle and ductile fields", An international conference in honour of Ron H. Vernon, Abstracts with Programs.

Erdmann, S., Clarke, D.B., and MacDonald, M.A. (2004): Origin of chemically zoned and unzoned cordierites from the South Mountain and Musquodoboit batholiths. Transaction of the Royal Society of Edinburgh, Earth Sciences 95, 99-110.

Erdmann, S., London, D., Morgan VI, G.B., and Clarke, D.B. (in press). Contamination of granitic magma by metasedimentary country-rock material: an experimental study. The Canadian Mineralogist.

Evensen, J. M., and London, D. (2003): Experimental partitioning of Be, Cs, and other trace elements between cordierite and felsic melt, and the chemical signature of S-type granite. Contributions to Mineralogy and Petrology 144, 739-757.

Everitt, B. (1993): Cluster analysis. Edward Arnold, London, 3rd edition.

Fitton, J.G., James, D., and Leeman, W.P. (1991): Basic magmatism associated with late Cenozoic extension in the Western United States; compositional variations in space and time. Journal of Geophysical Research, Solid Earth and Planets 96, 13,693-13,711.

Flood, R.H., and Shaw, S.E. (1975): A cordierite-bearing granite suite from the New England batholith, NSW, Australia. Contributions to Mineralogy and Petrology 52, 157-164.

Fournet, J. (1846): Geologie lyonnaise. De Barret, Lyon, France, 744 pp.

Fowler, S.J., Bohrson, W.A., and Spera, F.J. (2004): Magmatic evolution of the Skye igneous centre, western Scotland; modelling of assimilation, recharge and fractional crystallization. Journal of Petrology 45, 2481-2505.

Furlong, K.P., and Myers, J.D. (1985): Thermal-mechanical modeling of the role of thermal stresses and stoping in magma contamination. Journal of Volcanology and Geothermal Research 24, 179-191.

Gagnevin, D., Daly, J.S., Waight, T.E., Morgan, D., and Poli, G. (2005): Pb isotopic zoning of K-feldspar megacrysts determined by laser ablation multi-collector ICP-MS; insights into granite petrogenesis. Geochimica et Cosmochimica Acta 69, 1899-1915.

Ganguly, J., and Saxena, S.K. (1984): Mixing properties of alumosilicate garnets: constraints from natural and experimental data, and applications to geothermo-barometry. American mineralogist 69, 88-97.

Ganguly, J., and Tirone, M. (2001): Relationship between cooling rate and cooling age of a mineral; theory and applications to meteorites. Meteoritics & Planetary Science 36, 167-175.

Gardner, J.E., Layer, P. W., and Rutherford, M.J. (2002): Phenocrysts versus xenocrysts in the youngest Toba Tuff; implications for the petrogenesis of 2800 km^3 of magma. Geology 30, 347-350.

Ghiorso, M.S. (1985): Chemical mass transfer in magmatic processes; 1, Termodynamic relations and numerical algorithms. Contributions to Mineralogy and Petrology 90, 107-120.

Ghiorso, M.S., and Kelemen, P.B. (1987): Evaluating reaction stoichiometry in magmatic systems evolving under generalized thermodynamic constraints; examples comparing isothermal and isenthalpic assimilation. Special Publication - Geochemical Society 1, 319-336.

Ghiorso, M.S., and Sack, R.O. (1995): Chemical mass transfer in magmatic processes; IV, A revised and internally consistent thermodynamic model for the interpolation and extrapolation of liquid-solid equilibria in magmatic systems at elevated temperatures and pressures. Contributions to Mineralogy and Petrology 119, 197-212.

Giletti, B.J., and Casserly, J.E.D. (1994): Strontium diffusion kinetics in plagioclase feldspars. Geochimica et Cosmochimica Acta 58, 3785-3793.

Giletti, B.J., and Shanahan, T.M. (1997): Alkali diffusion in plagioclase feldspar. Chemical Geology 139, 3-20.

Ginibre, C., Kronz, A., and Woerner, G. (2002): High-resolution quantitative imaging of plagioclase composition using accumulated backscattered electron images; new constraints on oscillatory zoning. Contributions to Mineralogy and Petrology 142, 436-448.

Glazner, A.F., Bartley, J.M., Coleman, D.S., Gray, W., and Taylor, R.Z. (2004): Are plutons assembled over millions of years by amalgamation from small magma chambers? GSA Today 14, 4-11.

Glenn, L.A., and Chudnovsky, A. (1986): Strain-energy effects on dynamic fragmentation. Journal of Applied Physics 59, 1379-1380.

Goodchild, J.G. (1892): Note on granite junction in the Ross of Mull. Geological Magazine 9, 447-451.

Gottesmann, B., and Förster, H.-J. (2004): Sekaninaite from the Satzung Granite (Erzgebirge, Germany); magmatic or xenolithic? European Journal of Mineralogy 16, 483-491.

Grady, D.E., and Kipp, M.E. (1987): Dynamic rock fragmentation. Editor: Atkinson, B.K. Academic Press, London, United Kingdom (GBR), 429-475.

Green, N.L. (1994): Mechanism for middle to upper crustal contamination; evidence from continental-margin magmas. Geology 22, 231-234.

Greenough, J.D., Krogh, T.E., Kamo, S.L., Owen, J.V., and Ruffman, A. (1999): Precise U-Pb dating of Meguma basement xenoliths; new evidence for Avalonian underthrusting. Canadian Journal of Earth Sciences 36, 15-22.

Grove, T.L., and Kinzler, R.J. (1986): Petrogenesis of andesites. Annual Review of Earth and Planetary Sciences 14, 417-454.

Halter, W.E., Williams-Jones, A.E., and Kontak, D.J. (1994): Geometry and distribution of tin mineralization at East Kemptville, Yarmouth, Nova Scotia. Department of Natural Resources, Report 93-2, 20 pp.

Ham, L.J., Corey, M.C., Horne, R.J., and MacDonald, M.A. (1990): Lithogeochemistry of the western portion of the South Mountain Batholith, Nova Scotia. Nova Scotia Department of Mines and Energy, Open File Report 90-007.

Ham, L.J., Marsh, S.W., Corey, M.C., Horne, R.J., and MacDonald, M.A. (1989): Lithogeochemistry of the eastern portion of the South Mountain Batholith, Nova Scotia. Nova Scotia Department of Mines and Energy, Open File Report 89-001.

Ham, L.J. (1999): Geological map of the Musquodoboit batholith. Nova Scotia Department of Natural Resources Minerals and Energy Branch. QFM ME 1999-2.

Harker, A. (1904): The Tertiary rocks of Skye. Memoir of the Geological Society of Scotland, 481 pp.

Harley, S.L., Thompson, P., Hensen, B.J., and Buick, I.S. (2002): Cordierite as a sensor of fluid conditions in high-grade metamorphism and crustal anatexis. Journal of Metamorphic Geology 20, 71-86.

Hart, G.G. (2006): Andalusite in the South Mountain Batholith contact aureole, Halifax NS: A tale of two isograds. Unpublished BSc thesis, Dalhousie University, Nova Scotia, Canada, 66 pp.

Hawkesworth, C., George, R., Turner, S., and Zellmer, G. (2004): Time scales of magmatic processes. Earth and Planetary Science Letters 218, 1-16.

Hawkins, D.P., and Wiebe, R.A. (2004): Discrete stoping events in granite plutons; a signature of eruptions from silicic magma chambers? Geology 32, 1021-1024.

Hibbard, M.J. (1991): Textural anatomy of twelve magma-mixed granitoid systems. In: Enclaves and granite petrology. Editors: Didier, J., and Barbarin, B. Developments in Petrology 13, 431-444.

Hicks, R.J., Jamieson, R.A., and Reynolds, P.H. (1999): Detrital and metamorphic $^{40}Ar/^{39}Ar$ ages from muscovite and whole-rock samples, Meguma Supergroup, southern Nova Scotia. Candian Journalof Earth Sciences 36, 23-32.

Hill, J.D. (1991): Petrology, tectonic setting, and economic potential of Devonian peraluminous granitoid plutons in the Canso and Forest Hill areas, eastern Meguma Terrane, Nova Scotia. Bulletin - Geological Survey of Canada, Report: 383, 96.

Hiroi, Y., Grew, E.S., Motoyoshi, Y., Peacor, D.R., Rouse, R.C., Matsubara, S., Yokoyama, K., Miyawaki, R., McGee, J.J., Su, S-C., Hokada, T., Furukawa, N., and Shibasaki, H. (2002): Ominelite, $(Fe,Mg)Al_3BSiO_9$ (Fe^{2+} analogue of grandidierite), a new mineral from porphyritic granite in Japan. American Mineralogist 87, 160-170.

Hoefs, J. Faure, G., and Elliot, D.H. (1981): Correlation of $\delta^{18}O$ and initial $^{87}Sr/^{86}Sr$ ratios in Kirkpatrick basalt on Mt. Falla, transantarctic mountains. Contibutions to Minralogy and Petrology 75, 199-203.

Holtz, F., and Johannes, W. (1991): Genesis of peralumnious granites I. Experimental investigation of melt compositions at 3 and 5 kbar and various H_2O activities. Journal of Petrology 32, 935-958.

Horne, R.J., Corey, M.C., Ham, L.J., and MacDonald, M.A. (1989): Lithogeochemical variation in the granodiorite and biotite monzogranite of the South Mountain Batholith, Nova Scotia. Atlantic Geology 25, 161.

Huppert, H.E., and Sparks, R.S.J. (1988): The generation of granitic magmas by intrusion of basalt into continental crust. Journal of Petrology 29, 599-624.

Hutton, D.H.W. (1996): The "space problem" in the emplacement of granite. Episodes 19, 114-119.

Jackson, H.R.D., Chian, M.S., and Shimeld, J. (2000): Preliminary crustal structure from the Scotian margin to the Maritimes Basin from wide angle reflection/refraction profiles. GeoCanada 2000, GAC Annual meeting, Abstracts with Program.

Jamieson, R.A. (1974): The contact of the South Mountain Batholith near Mount Uniacke, Nova Scotia. Unpublished BSc thesis, Dalhousie University, Nova Scotia, Canada, 52 pp.

Johannes, W. (1989): Melting of plagioclase-quartz assemblages of 2 kbar water pressure. Contributions to Mineralogy and Petrology 103, 270-276.

Johannes, W., and Koppke, J. (2001): Incomplete reaction of plagioclase in experimental dehydration melting of amphibolite. Australian Journal of Earth Sciences 48, 581-590.

Johannes, W., and Schreyer, W. (1981): Experimental introduction of CO_2 and H_2O into Mg-cordierite. American Journal of Science 281, 299-317.

Kaczor, S.M., Hanson, G.N., and Peterman, Z.E. (1988): Disequilibrium melting of granite at the contact with a basic plug; a geochemical and petrographic study. Journal of Geology 96, 61-78.

Keen, C.E., Kay, W.A., Keppie, D., Marillier, F., Pe-Piper, G., and Waldron, J.W.F. (1991): Deep seismic reflection data from the Bay of Fundy and Gulf of Maine; tectonic implications for the Northern Appalachians. Canadian Journal of Earth Sciences 28, 1096-1111.

Kelemen, P.B. (1990): Reaction between ultramafic rock and fractionating basaltic magma; I, Phase relations, the origin of calc-alkaline magma series, and the formation of discordant dunite. Journal of Petrology 31, 51-98.

Keppie, J.D., Dallmeyer, R.D., Krogh, T.E., and Aftalion, M. (1993): Dating mineralization using several isotopic methods; an example from the South Mountain Batholith, Nova Scotia, Canada. Chemical Geology 103, 251-270.

Keppie, J.D., and Krogh, T.E. (1999): U-Pb geochronology of Devonian granites in the Meguma Terrane of Nova Scotia, Canada; evidence for hotspot melting of a Neoproterozoic source. Journal of Geology 107, 555-568.

Keppie, J.D., and Muecke, G.K. (1979): Metamorphic map of Nova Scotia. Department of Mines and Energy, Halifax, Canada.

Knesel, K.M., Davidson, J.P., and Duffield, W.A. (1999): Evolution of silicic magma through assimilation and subsequent recharge; evidence from Sr isotopes in sanidine phenocrysts, Taylor Creek Rhyolite, NM. Journal of Petrology 40, 773-786.

Kontak, D.J. (1990): A sulfur isotope study of main-stage tin and base metal mineralization at the East Kemptville tin deposit, Yarmouth County, Nova Scotia, Canada; evidence for magmatic orgin of metals and sulfur. Economic Geology and the Bulletin of the Society of Economic Geologists 85, 399-407.

Kontak, D.J. (1993): ^{34}S enrichment in late-stage veins, East Kemptville tin and base metal deposit, Nova Scotia, Canada; evidence for late incursion of metasedimentary processed sulfur in a magmatic system. Economic Geology and the Bulletin of the Society of Economic Geologists 88, 203-207.

Kontak, D.J., and Reynolds, P.H. (1994): $^{40}Ar/^{39}Ar$ dating of metamorphic and igneous rocks of the Liscomb Complex, Meguma Terrane, southern Nova Scotia, Canada. Canadian Journal of Earth Sciences 31, 1643-1653.

Kontak, D.J., Strong, D.F., and Kerrich, R. (1988): Crystal-melt±fluid phase equilibria versus late-stage fluid-rock interaction in granitoid rocks of the South Mountain Batholith, Nova Scotia; whole rock geochemistry and oxygen isotope evidence. Maritime Sediments and Atlantic Geology 24, 97-110.

Kretz, R. (1983): Symbols for rock-forming minerals. American Mineralogist 68, 277-279.

Krogh, T.E., and Keppie, J.D. (1990): Age of detrital zircon and titanite in the Meguma Group, southern Nova Scotia, Canada; clues to the origin of the Meguma Terrane. Tectonophysics 177, 307-323.

Kubilius, W.P. (1983): Sulfur isotopic evidence for country rock contamination of granitoids in southwestern Nova Scotia. Unpublished MSc thesis, Pennsylvania State University, Pennsylvania, United States, 103 pp.

Kuno, H. (1950): Petrology of Hakone volcano and the adjacent areas, Japan. Geological Society of America Bulletin 61, 957-1014.

Lackey, J.S., Erdmann, S., Clarke, D.B., Fellah, K.L., Nowak, R.M., Spicuzza, M.J., and Valley, J.W. (in press): Oxygen isotope evidence for the origin of garnet in the peraluminous South Mountain Batholith, Nova Scotia. GSA Abstracts with Programs.

Lalonde, A.E., and Martin, R.F. (1983): The Baie-des-Moutons syenitic complex, La Tabatière, Québec. II. The ferromagnesian minerals. The Canadian Mineralogist 21, 81-91.

L'Heureux, I.L., and Fowler, A.D. (1996): Isothermal constitutive undercooling as a model for oscillatory zoning in plagioclase. The Canadian Mineralogist 34, 1137-1147.

Lukacs, R., Harangi, S., Ntaflos, T., and Mason, P.R.D. (2005): Silicate melt inclusions in the phenocrysts of the Szomolya Ignimbrite, Bukkalja volcanic field (northern Hungary); implications for magma chamber processes. Chemical Geology 223, 46-67.

MacDonald, M.A. (2001): Geology of the South Mountain Batholith, Southwestern Nova Scotia. Nova Scotia Department of Natural Resources, Open File Report ME2001-2.

MacDonald, M.A., and Clarke, D.B. (1985): The petrology, geochemistry, and economic potential of the Musquodoboit batholith, Nova Scotia. Canadian Journal of Earth Sciences 22, 1633-1642.

MacDonald, M.A., Corey, M.C., Ham, L.J., and Horne, R.J. (1988): South Mountain batholith project: a progress report on bedrock mapping. Nova Scotia Department of Mines and Energy Report 88-3, 109-116.

MacDonald, M.A., Corey, M.C., Ham, L.J., and Horne, R.J. (1992): An overview of recent bedrock mapping and follow-up petrological studies of the South Mountain Batholith, southwestern Nova Scotia, Canada. Atlantic Geology 28, 7-28.

MacDonald, M.A., Horne, R.J., Corey, M.C. and Ham, L.J. (1992): An overview of recent bedrock mapping and follow-up petrological studies of the South Mountain Batholith, southwestern Nova Scotia, Canada. Maritime Sediments and Atlantic Geology 28, 7-28

MacDonald, M.A., and Horne, R.J. (1988): Petrology of the zoned, peraluminous Halifax Pluton, South-Central Nova Scotia. Atlantic Geology 24, 33-45.

Mahoney, K.L. (1996): The contact metamorphic aureole of the South Mountain Batholith, Nova Scotia. Unpublished MSc thesis, Acadia University, Nova Scotia, Canada, 163 pp.

Maillet, L.A., and Clarke, D.B. (1985): Cordierite in the peraluminous granites of the Meguma Zone, Nova Scotia. Canadian Mineralogical Magazine 49, 695-702.

Marchildon, N., and Brown, M. (2002): Grain-scale melt distribution in two contact aureole rocks; implications for controls on melt localization and deformation. Journal of Metamorphic Geology 20, 381-396.

Marsh, J.S. (1989): Geochemical constraints on coupled assimilation and fractional crystallization involving upper crustal compositions and continental tholeiitic magma. Earth and Planetary Science Letters 92, 70-80.

Maury, R.C., Didier, J. (1991): Xenoliths and the role of assimilation. In: Enclaves and granite petrology. Editors: Didier, J., and Barbarin, B. Developments in Petrology 13, 529-542.

McKenzie, B. (1976): Gravitational interpretation and modelling of the Meguma and intrusive granite in the Halifax area. Unpublished BSc thesis, Dalhousie University, Nova Scotia, Canada.

McCuish, K.L. (2001): Schlieren in the South Mountain Batholith and Port Mouton Pluton, Meguma Zone, Nova Scotia. Unpublished BSc thesis, Dalhousie University, Nova Scotia, Canada, 101 pp.

McKenzie, B., and Clarke, D.B. (1975): Petrology of the South Mountain Batholith, Nova Scotia. Canadian Journal of Earth Sciences 12, 1209-1218.

McNulty, B.A., Tong, W., and Tobisch, O.T. (1996): Assembly of a dike-fed magma chamber; the Jackass Lakes Pluton, central Sierra Nevada, California. Geological Society of America Bulletin 108, 926-940.

Miller, R.B., and Paterson, S.R. (1999): In defense of magmatic diapirs. Journal of Structural Geology 21, 1161-1173.

Milord, I., and Sawyer, E.W. (2001): Schlieren formation in diatexite migmatite; examples from the St. Malo migmatite terrane, France. Journal of Metamorphic Geology 21, 347-362.

Morgan VI, G.B., and London, D. (1996): Optimizing the electron microprobe analysis of hydrous alkali aluminosilicate glasses. American Mineralogist 81, 1176-1185.

Morgan VI, G.B., and London, D. (2005): Effect of current density on the electron microprobe analysis of alkali aluminosilicate glasses. American Mineralogist 90, 1131-1138.

Muecke, G.K., and Clarke, D.B. (1981): Geochemical evolution of the South Mountain Batholith, Nova Scotia; rare-earth-element evidence. The Canadian Mineralogist 19, 133-145.

Müller, A., Wiedenbeck, M., van den Kerkhof, A.M., Kronz, A., and Simon, K. (2003): Trace elements in quartz; a combined electron microprobe, secondary ion mass spectrometry, laser-ablation ICP-MS, and cathodoluminescence study. European Journal of Mineralogy 15, 747-763.

Murphy, J.B., Fernandez-Suarez, J., Keppie, J.D., and Jeffries, T.E. (2004): Contiguous rather than discrete Paleozoic histories for the Avalon and Meguma Terranes based on detrital zircon data. Geology 32, 585-588.

Murphy, J.B., van Staal, C.R., and Keppie, J.D. (1999): Middle to late Paleozoic Acadian Orogeny in the Northern Appalachians; a Laramide-style plume-modified orogeny? Geology 27, 653-656.

Myers, J.S. (1975): Cauldron subsidence and fluidization; mechanisms of intrusion of the Coastal Batholith of Peru into its own volcanic ejecta. Geological Society of America Bulletin 86, 1209-1220.

Nelson, D.R., Robinson, B.W., and Myers, J.S. (2000): Complex geological histories extending for ≥4.0 Ga deciphered from xenocryst zircon microstructures. Earth and Planetary Science Letters 181, 89-102.

O'Hara, M.J. (1995): Trace element geochemical effects of integrated melt extraction and "shaped" melting regimes. Journal of Petrology 36, 1111-1132.

O'Hara, M.J. (1998): Volcanic plumbing and the space problem-thermal and geochemical consequences of large-scale assimilation in ocean island development. Journal of Petrology 39, 1077-1089.

Okubo, C.H., and Martel, S.J. (1998): Pit crater formation on Kilauea Volcano, Hawaii. Journal of Volcanology and Geothermal Research 86, 1-18.

O'Reilly, C.T. (1975) : Gravitational interpretation and modelling of the South Mountain Batholith utilising two and three dimensional computer programming. Unpublished BSc thesis, Dalhousie University, Nova Scotia, Canada.

Owen, J.V., Greenough, J.D., Hy, C., Ruffman, A. (1988): Xenoliths in a mafic dyke at Popes Harbour, Nova Scotia; implications for the basement to the Meguma Group. Canadian Journal of Earth Sciences 25, 1464-1471.

Paterson, S.R., Fowler, T.K., and Miller, R.B. (1996): Pluton emplacement in arcs; a crustal-scale exchange process. Special Paper - Geological Society of America 315, 115-123.

Patiño Douce, A.E. (1995): Experimental generation of hybrid silicic melts by reaction of high-Al basalt with metamorphic rocks. Journal of Geophysical Research, Solid Earth and Planets 100, 15,623-15,639.

Pelrine, K.M. (2003): Ilmenite-pyrophanite and niobian rutile in the South Mountain Batholith, Nova Scotia. Unpublished BSc theis, Dalhousie University, Nova Scotia.

Perchuck, L.L., Aranovich, L.Y., Podlessskii, K.K., Lavrent'eva, I.V., Gerasimov, V.Y., Fed'kin V.V., Kitsul, V I., Karasakov, L.P., and Berdnikov, N.V. (1985): Precambrian granulites of the Aldan shield, eastern Siberia, USSR. Journal of Metamorphic Geology 3, 265-310.

Perry, F.V., DePaolo, D.J., Baldridge, W.S. (1993): Neodymium isotopic evidence for decreasing crustal contributions to Cenozoic ignimbrites of the Western United States; implications for the thermal evolution of the Cordilleran crust. Geological Society of America Bulletin105, 872-882.

Phillips, G.N., Wall, W.J., and Clemens, J.D. (1981): Petrology of the Strathbogie batholith: a cordierite-bearing granite. The Canadian Mineralogist 19, 47-63.

Pouchou J.L., and Pichoir F. (1985): "PAP" $\varphi(\rho Z)$ procedure for improved quantitative microanalysis. In: Microbeam Analysis. Editor: Armstrong, J.T., 104-106.

Poulson, S.R., Kubilius, W.P., and Ohmoto, H. (1991): Geochemical behavior of sulfur in granitoids during intrusion of the South Mountain Batholith, Nova Scotia, Canada. Geochimica et Cosmochimica Acta 55, 3809-3830.

Poulson, S.R., and Ohmoto, H. (1989): Devolatilization equilibria in graphite-pyrite-pyrrhotite bearing pelites with application to magma-pelite interaction. Contributions to Mineralogy and Petrology 101, 418-425.

Pressley, R.A., and Brown, M. (1999): The Phillips Pluton, Maine, USA; evidence of heterogeneous crustal sources and implications for granite ascent and emplacement mechanisms in convergent orogens. Lithos 46, 335-366.

Raia, F., and Spera, F.J. (1997): Simulations of crustal anatexis; implications for the growth and differentiation of continental crust. Journal of Geophysical Research, Solid Earth and Planets 102, 22,629-22,648.

Raeside, R.P., and Mahoney, K.M. (1996): The contact metamorphic aureole of the South Mountain Batholith, southern Nova Scotia. GAC-MAC, Annual Meeting, Abstracts with Program, 77.

Ramos, F.C., Wolff, J.A., and Tollstrup, D.L. (2005): Sr isotope disequilibrium in Columbia River flood basalts; evidence for rapid shallow-level open-system processes. Geology 33, 457-460.

Reiners, P.W., Nelson, B.K., and Ghiorso, M.S. (1995): Assimilation of felsic crust by basaltic magma: Thermal limits and extents of crustal contamination of mantle-derived magmas. Geology 23, 563-566.

Richardson, S.E. (2000): Balanced structural cross-sections of the Meguma Group, Halifax, LaHave, Mahone Bay and Ecum Secum areas, Nova Scotia. Unpublished BSc thesis, Dalhousie University, Nova Scotia, Canada, 80 pp.

Rosenberg, C.L., Riller, U. (2000): Partial-melt topology in statically and dynamically recrystallized granite. Geology 28, 7-10.

Rubin, A.M. (1993): Dikes vs. diapirs in viscoelastic rock. Earth and Planetary Science Letters 119, 641-659.

Rushmer, T. (2001): Volume change during partial melting reactions; implications for melt extraction, melt geochemistry and crustal rheology. Tectonophysics 342, 389-405.

Samson, H.R. (2005): Origin of sulfides in the contact granodiorites of the South Mountain Batholith, Nova Scotia. Unpublished BSc thesis, Dalhousie University, Nova Scotia, Canada, 69 pp.

Samson, H., and Clarke, D.B. (2005): Assimilation of country-rock sulphide minerals in the South Mountain Batholith, Nova Scotia, Canada. GAC-MAC, Annual Meeting, Abstracts with Program, 170.

Sparks, R.S.J. (1986): The role of crustal contamination in magma evolution through geological time. Earth and Planetary Science Letters 78, 211-223.

Sawyer, E.W. (2001): Melt segregation in the continental crust; distribution and movement of melt in anatectic rocks. Journal of Metamorphic Geology 19, 291-309.

Schaltegger, U., Zeilinger, G., Frank, M., and Burg, J.-P. (2002): Multiple mantle sources during island arc magmatism; U-Pb and Hf isotopic evidence from the Kohistan arc complex, Pakistan. Terra Nova 14, 461-468.

Schenk, P.E. (1970): Regional variation of the flysch-like Meguma group (lower Paleozoic) of Nova Scotia, compared to the recent sedimentation off the Scotian shelf. Special Paper - Geological Association of Canada 7, 127-153.

Schenk, P.E (1991): Events and sea-level changes on Gondwana's margin: The Meguma Zone (Cambrian to Devonian) of Nova Scotia. Geological Society of America Bulletin 103, 512-521.

Schenk, P.E (1995): Meguma zone. In: Geology of the Appalachian-Caledonian Orogen in Canada and Greenland. Editor: Williams, H. Geological Survey of Canada, Geology of Canada 6, 261-277.

Schenk, P.E. (1997): Sequence stratigraphy and provenance on Gondwana's margin; the Meguma Zone (Cambrian to Devonian) of Nova Scotia, Canada. Geological Society of America Bulletin 109, 395-409.

Simonetti, A., and Bell, K. (1993): Isotopic disequilibrium in clinopyroxenes from nephelinitic lavas, Napak Volcano, eastern Uganda. Geology 21, 243-246.

Sparks, R.,J.S. (1986): The role of crustal contamination in magma evolution through geological time. Earth and Planetary Science Letters 78, 211-223.

Spell, T.L., Smith, E.I., Sanford, A., and Zanetti, K.A. (2001): Systematics of xenocrystic contamination; preservation of discrete feldspar populations at McCullough Pass Caldera revealed by $^{40}Ar/^{39}Ar$ dating. Earth and Planetary Science Letters 190, 153-165.

Spence, D.A., and Turcotte, D.L. (1985): Magma-driven propagation of cracks. Journal of Geophysical Research, Solid Earth and Planets 90, 575-580.

Spera, F.J. (2000): Physical properties of magmas. In: Encyclopedia of volcanoes. Editors: Sigurdsson, H., Houghton, B.F., McNutt, S.R., Rymer, H., and Stix, J., Academic Press, San Diego, CA, United States, 171-190.

Spera, F.J., Yuen, D.A., and Kirschvink, S.J. (1982): Thermal boundary layer convection in silicic magma chambers; effects of temperature-dependent rheology and implications for thermogravitational chemical fractionation. Journal of Geophysical Research, Solid Earth and Planets 87, 8755-8767.

Spera, F.J., Oldenburg, C.M., Christensen, C., and Todesco, M. (1995): Simulations of convection with crystallization in the system $KalSi_2O_6$-$CaMgSi_2O_6$; implications for compositionally zoned magma bodies. American Mineralogist 80, 1188-1207.

Spera, F.J., and Bohrson, W.A. (2001): Energy-constrained open-system magmatic processes; I, General model and energy-constrained assimilation and fractional crystallization (EC-AFC) formulation. Journal of Petrology 42, 999-1018.

Spera, F.J., and Bohrson, W.A. (2004): Open-system magma chamber evolution; an energy-constrained geochemical model incorporating the effects of concurrent eruption, recharge, variable assimilation and fractional crystallization (EC-χRAFC). Journal of Petrology 45, 2459-2480.

Schreyer, W., and Yoder, H.S.Jr. (1964): The system Mg-cordierite-H_2O and related rocks. Neues Jahrbuch für Mineralogie, Geologie und Paläontologie. Monatshefte 101, 271-342.

Shore, M., and Fowler, A.D. (1996): Oscillatory zoning in minerals: a common phenomenon. The Canadian Mineralogist 34, 1111-1126.

Singer, B.S., Dungan, M.A., and Layne, G.D. (1995): Textures and Sr, Ba, Mg, Fe, K, and Ti compositional profiles in volcanic plagioclase: clues to the dynamics of calc-alkaline magma chambers. American Mineralogist 80, 776-798.

Sneeringer, M., Hart, S.R., and Shimizu, N. (1984): Strontium and samarium diffusion in diopside. Geochimica et Cosmochimica Acta 48, 1589-1608.

Tate, M.C. (1994): The nature and origin of enclaves in four peraluminous granitoid intrusions from the Meguma Zone, Nova Scotia. Atlantic Geology 30, 205-215.

Tate, M.C. (1995): The relationship between Late Devonian mafic intrusions and peraluminous granitoid generation in the Meguma Lithotectonic Zone, Nova Scotia, Canada. Unpublished PhD thesis, Dalhousie University, Nova Scotia, Canada, 528 pp.

Tate, M.C., and Clarke, D.B. (1995): Petrogenesis and regional tectonic significance of Late Devonian mafic intrusions in the Meguma Zone, Nova Scotia. Canadian Journal of Earth Sciences 32, 1883-1898.

Tate, M.C., and Clarke, D.B. (1997): Compositional diversity among Late Devonian peraluminous granitoid intrusions in the Meguma Zone of Nova Scotia, Canada. Lithos 39, 179-194.

Taylor, H.P.Jr. (1980): The effects of assimilation of country rocks by magmas on $^{18}O/^{16}O$ and $^{87}Sr/^{86}Sr$ systematics in igneous rocks. Earth and Planetary Science Letters 47, 243-254.

Taylor, H.P.Jr., Giannetti, B., and Turi, B. (1979): Oxygen isotope geochemistry of the potassic igneous rocks from the Roccamonfina Volcano, Roman comagmatic region, Italy. Earth and Planetary Science Letters 46, 81-106.

Thomas, L., Blake, S., Kelley, S., and Morgan, D. (2002): The evolution of the Youngest Toba Tuff; a crystal disequilibrium study. Geochimica et Cosmochimica Acta 66, 772.

Tobey, N. (2006): A geological description of Point Pleasant Park. Unpublished BSc thesis, Dalhousie University, Nova Scotia, Canada, 99 pp.

Waight, T.E., Maas, R., and Nicholls, I.A. (2000): Fingerprinting feldspar phenocrysts using crystal isotopic composition stratigraphy; implications for crystal transfer and magma mingling in S-type granites. Contributions to Mineralogy and Petrology 139, 227-239.

Villaseca, C., and Barbero, L. (1994): Chemical variability of Al-Ti-Fe-Mg minerals in peraluminous granitoid rocks from Central Spain. European Journal of Mineralogy 6, 691-710.

Tepley III, F.J., and Davidson, J.P. (2003): Mineral-scale Sr-isotope constraints on magma evolution and chamber dynamics in the Rum layered intrusion, Scotland. Contributions to Mineralogy and Petrology 145, 628-641.

Tepley III, F.J., Davidson, J.P., and Clynne, M.A. (1999): Magmatic interactions as recorded in plagioclase phenocrysts of Chaos Crags, Lassen volcanic center, California. Journal of Petrology 40, 787-806.

Tepley III., F., Davidson, J.P., Tilling, R.I., and Arth, J.G. (2000): Magma mixing, recharge and eruption histories recorded in plagioclase phenocrysts from El Chichon Volcano, Mexico. Journal of Petrology 41, 1397-1411.

Thompson, A.B. (1990): Heat, fluids, and melting in the granulite facies. Mathematical and Physical Sciences 311, 37-57.

Van Breeman, O., Peterson, T.D., and Sandeman, H.A. (2005): U-Pb zircon geochronology and Nd isotope geochemistry of Proterozoic granitoids in the western Churchill Province; intrusive age pattern and Archean source domains. Canadian Journal of Earth Sciences 42, 339-377.

Van Orman, J.A., Grove, T.L., Shimizu, N., and Layne, G.D. (2002): Rare earth element diffusion in a natural pyrope single crystal at 2.8 GPa. Contributions to Mineralogy and Petrology 142, 416-424.

Vernon, R.H. (1990): Crystallization and hybridism in microgranitoid enclave magmas; microstructural evidence. Journal of Geophysical Research, Solid Earth and Planets 95, 17,849-17,859.

Vernon, R.H. (1991): Interpretation of microstructures of microgranitoid enclaves. In: Enclaves and granite petrology. Editors: Didier, J., and Barbarin, B. Developments in Petrology 13, 277-291.

Vernon, R.H. (in press): Problem of identifying restite in S-type granites of SE Australia, with speculations on magma and enclave sources. The Canadian Mineralogist.

Vielzeuf, D., and Holloway, J.R. (1988): Experimental determination of the fluid-absent melting relations in the pelitic system; consequences for crustal differentiation. Contributions to Mineralogy and Petrology 98, 257-276.

Waldron, J.W.F., Donohoe, H.V.Jr., and Keith, D. (1992): The Appalachian story. Atlantic Geoscience Society Special Publication 11, 21 pp.

Waldron, J.W.F., and Jensen, L.R. (1985): Geometry of turbidite sand bodies in the Cambro-Ordovician Goldenville Formation, Nova Scotia. AGS Abstracts with Programs, 66.

Wall, V.J., Clemens, J.D., and Clarke, D.B. (1987): Models for granitoid evolution and source compositions. Journal of Geology 95, 731-749.

Whitney, J.A. (1989): Origin and evolution of silicic magmas. Reviews in Economic Geology 4, 183-201.

Wilcox, R.E. (1954): Petrology of Paricutin volcano, Mexico. US Geological Survey Bulletin 965-C, 281-353.

Williams, H., and Hatcher, R.D.Jr. (1982): Suspect terranes and accretionary history of the Appalachian Orogen. Geology 10, 530-536.

Woerner, G., Moorbath, S., Harmon, R.S. (1992): Andean Cenozoic volcanic centers reflect basement isotopic domains. Geology 20, 1103-1106.

Wolf, M.B., London, D., and Morgan VI, G.B., (1994): Effects of boron on the solubility of cassiterite and tantalite in granitic liquids. GSA, Abstracts with Program 26, 450.

Wolff, J.A., Olin, P.H., and Knaack, C.M. (2005): LA-ICPMS studies of microscale trace element variations in zoned minimum-melt magma systems. Geochimica et Cosmochimica Acta 69, 245.

Wood, B.J. (1973). Fe^{2+}-Mg^{2+} partitioning between coexisting cordierite and garnet; a discussion of the experimental data. Contributions to Mineralogy and Petrology 40, 253-258.

Yoder, H.S.J., Stewart, D.B., Smith, J.R. (1957): Felspars. Yearbook 56, Carnegie Institution of Washington, 206-214.

Zak, J., and Paterson, S.R. (2005): Characteristics of internal contacts in the Tuolumne Batholith, central Sierra Nevada, California (USA); implications for episodic emplacement and physical processes in a continental arc magma chamber. Geological Society of America Bulletin 117, 1242-1255.

Zellmer, G.F., Blake, S., Vance, D., Hawkesworth, C., and Turner, S. (1999): Plagioclase residence times at two island arc volcanoes (Kameni Islands, Santorini, and Soufriere, St. Vincent) determined by Sr diffusion systematics. Contributions to Mineralogy and Petrology 136, 345-357.

APPENDIX 1 – Electronic Supplements

CD in back pocket of thesis.

APPENDIX 2 – Outcrop Locations and Sample List

CD in back pocket of thesis.